DISSERTATION

# TREX-SMA: A MULTI-EVENT HYBRID HYDROLOGIC MODEL APPLIED AT CALIFORNIA GULCH, COLORADO

Submitted by

James Halgren

Department of Civil and Environmental Engineering

In partial fulfillment of the requirements

For the Degree of Doctor of Philosophy

Colorado State University

Fort Collins, Colorado

Fall 2012

Doctoral Committee:

Advisor: Pierre Y. Julien

Stephanie K. Kampf
Timothy K. Gates
S. Karan Venayagamoorthy

UMI Number: 3551617

All rights reserved

INFORMATION TO ALL USERS
The quality of this reproduction is dependent upon the quality of the copy submitted.

In the unlikely event that the author did not send a complete manuscript
and there are missing pages, these will be noted. Also, if material had to be removed,
a note will indicate the deletion.


UMI 3551617

Published by ProQuest LLC (2013). Copyright in the Dissertation held by the Author.

Microform Edition © ProQuest LLC.
All rights reserved. This work is protected against
unauthorized copying under Title 17, United States Code


ProQuest LLC.
789 East Eisenhower Parkway
P.O. Box 1346
Ann Arbor, MI 48106 - 1346

Copyright by James Scott Halgren 2012

All Rights Reserved

ABSTRACT

TREX-SMA: A MULTI-EVENT HYBRID HYDROLOGIC MODEL APPLIED AT CALIFORNIA GULCH, COLORADO

This dissertation describes a hydrologic model, Two-Dimensional Runoff Erosion and Export (TREX)-Soil Moisture Accounting (SMA), created from adding the Sacramento Soil Moisture Accounting model (SAC-SMA) to the TREX surface hydrology model. TREX-SMA combines the capabilities of TREX as a distributed physical surface hydrology model with a conceptual rendering of infiltration and return flow as found in SAC-SMA. In order to form the hybrid, infiltrated water (computed as a distributed function on the surface) is aggregated as an input to a system of soil moisture accounting zones, underlying the entire watershed.

In each model time step, TREX-SMA releases baseflow from the accumulated infiltrated water according to simple transfer functions. Evapotranspiration (ET) losses from the soil moisture zones are computed based on potential ET demand and available water. As baseflow and ET are released between precipitation events, TREX-SMA recovers capacity in the soil moisture zones. Based on the simulated recovery, the model then re-initializes the infiltration parameters of the surface model to prepare for the next event, allowing continuous simulation of multiple events.

The capabilities of the TREX-SMA model to continuously simulate soil moisture, infiltration, and rainfall-runoff are demonstrated with an application to multi-event modeling on the 30 $km^2$ California Gulch watershed, near Leadville, Colorado, United States. Precipitation inputs are derived from measurements at a system of six precipitation and stream flow gauges providing ten-minute data for the summer of 2006. Eight major events were recorded during this time with runoff produced at all gauges. One additional event with partial watershed response was also

evaluated for a total of 54 event hydrographs in the 50-day simulated series. Time steps in the simulation ranged between 2.0 and 4.0 seconds.

Parameters for the surface hydrology were obtained from a prior calibration of TREX and were distributed across 34,000 grid cells based on the 30-meter United States Geological Survey (USGS) Digital Elevation Model (DEM). Parameters for the soil moisture zones were obtained from *a-priori* estimates used by the Arkansas Basin River Forecast Center of the National Weather Service (NWS) of the National Oceanographic and Atmospheric Administration (NOAA) in their real-time operational flood forecasting model for the Arkansas River. Using conceptual soil moisture states to re-initialize distributed infiltration parameters, the simulation results with TREX-SMA improved relative to results from the unmodified TREX model with constant infiltration parameters.

Model results are processed using gnuplot to create real-time hydrograph plots as the simulation progresses. Gnu R scripts produce real-time plots of simulated minus observed residual and statistical analyses as the simulation progresses. Statistics generated for each gauge include Nash-Sutcliffe, percent bias, absolute percent bias, Pearson correlation and modified Pearson correlation, and mean-squared error. These statistics were generated both for the entire simulation series and for each individual storm event. The gnuplot and R plots are produced using web-based technology for instantaneous sharing via the Internet. Model results such as surface and channel water depth are processed with GRASS GIS and KML scripts to create 2.5 dimensional, browseable animations overlaid on a Google Earth terrain.

Statistical measures of the improvement of TREX-SMA over TREX are presented in this dissertation. The overall accuracy, measured by the Nash-Sutcliffe coefficient, improved in four out of six gauges. Peak over-estimation was corrected in a majority of the 54 peaks evaluated.

Implementation of the TREX-SMA soil moisture accounting algorithm to re-initialize the infiltration parameters reduces the total absolute peak error from 180% to 135% of the observed peak flow rates. The Nash-Sutcliffe model efficiency improved over standard TREX simulations by 43%, 11%, 5%, and 10% at CG-1, CG-4, CG-6, and SHG09A.

ACKNOWLEDGMENTS

Thanks to my advisor, Pierre Julien for his unflagging encouragement.

For their service and attention as a committee, thanks to Tim Gates, Karan Venayagamoorthy, Stefanie Kampf, Ted Yang, Paul Wilbur, and Ellen Wohl. Thanks also to many friends and colleagues who have contributed significantly with their expertise. Thanks to Kristen Martinez for excellent copy editing and proofreading services.

Thanks to Kato Dee and the students and faculty associated with Colorado Mountain College for working to collect the basic hydrologic data for the California Gulch watershed and to Ed Muller at Tetra Tech for providing a copy of those data. Many thanks to Bill Lyle of Newmont Mining for providing Yak Tunnel operations data and thanks to the staff of the Leadville Sanitation District for graciously allowing access to discharge records.

Funding and institutional support for this research have been generously provided by the CSU/DoD Center for Geosciences and Atmospheric Research (CG/AR), The Center for Integrated Research in the Atmosphere, Colorado Mountain College, AECOM Design+Planning, Riverside Technology, inc., and the Office of Hydrologic Development at NOAA.

I owe all my gratitude to Jesus Christ for the capacity and desire to learn about this earth.

This work is dedicated to my wife and children

who are unequaled in their patience for me.

I love them.

TABLE OF CONTENTS

LIST OF TABLES

LIST OF FIGURES

# 1.0 INTRODUCTION

The Two-Dimensional Runoff Erosion and Export (TREX) model is a recently released descendant of the CASC2D hydrologic model developed at Colorado State University (CSU). TREX is a spatially distributed, physically based watershed scale hydrology model with additional capability to simulate sediment transport and chemical transport and fate (M. L. Velleux, J. F. England, and P. Y. Julien 2008). Applications of TREX can be found all over the world, including El Salvador, China, Malaysia, Slovakia, South Korea, Switzerland, and Vietnam. In the United States, simulations have been performed for watersheds in California, Colorado, Florida, Idaho, Mississippi, North Carolina, and Oklahoma.

## 1.1 PROBLEM STATEMENT AND NEED

Prior to the current research, the robust physics-based TREX model simulated watershed runoff response during a single storm. TREX, which was designed for single-event simulation, only accounts for infiltrated water as an accumulated depth and does not perform any sub-surface simulation. Therefore, baseflow between events can only be represented as an explicit input. Infiltration in TREX is computed using the Green and Ampt equation which performs well during a single event. However, without some form of re-initialization of soil moisture parameters, multiple events cannot be simulated. England et al. (2007) note that TREX would be improved by adding a mechanism for "soil infiltration capacity recovery."

TREX has been consistently linked with Geographic Information Systems (GIS) techniques to create visualizations of model output. Recent advances in GIS technology allow for potential improvements of these techniques. Some of the GIS techniques previously implemented with TREX have become obsolete. For instance, the program is no longer available that adjusts the

color ranges for display of water depth on the surface for use with an animation, and alternative methods are needed.

Before this research, hydrographs and other model outputs from TREX have been analyzed by importing text outputs into standard spreadsheet tools, then producing graphs and computations that allow for visual and statistical evaluation of results. To share TREX results for evaluation or review, a researcher must capture the spreadsheet output and prepare a static document. Now, with application of modern computing tools in the current research, graphs and statistical outputs can be produced in real-time with simulation results as an integrated part of the modeling process. In addition, these real-time results can now be shared instantly with the entire Internet audience.

### 1.2 Research Objectives

There are four objectives of this research: 1) Prepare a hybrid hydrologic model which captures spatial variability in driving parameters and which accounts for soil moisture as an aggregate parameter; 2) Show that the soil moisture state in the hybrid model may be used to re-initialize the distributed infiltration parameters; 3) Demonstrate the hybrid model with an application to multi-event modeling on the California Gulch watershed; and 4) Apply state-of-the art techniques in web programming and GIS to illustrate results from the hybrid model and to provide integrated statistical analysis.

### 1.3 Approach and Methodology

To accomplish the first objective, this research proposes hybridization of the National Weather Service Sacramento Soil Moisture Accounting (SAC-SMA) conceptual soil moisture model beneath the TREX framework. The hybrid model will be called TREX-SMA and will retain the distributed surface capabilities of TREX. Using the SAC-SMA techniques TREX-SMA

will account for soil moisture volumes to simulate return of infiltrated water. Continuous multi-event simulation will be made possible by combining the soil moisture accounting process with the infiltration calculation in the surface model. The hybrid model code will be written in ANSI C programming language and be based primarily on the TREX code, incorporating elements of SAC-SMA modified to correlate different time scales in the TREX model and the NWS implementation of SAC-SMA.

For the second objective, a simple demonstration case will be constructed. The concept of infiltration parameter re-initialization will be demonstrated by comparing TREX and TREX-SMA simulations with and without re-initialization of the soil moisture parameters.

The third objective, multi-event modeling with the hybrid model, will be accomplished using an existing implementation of the TREX model modified to include soil moisture accounting. Ten-minute precipitation and stream gauge records for various points in California Gulch during summer 2006 provide input for model simulations and act as the observed "truth" for evaluating the simulation results to accomplish the third objective. These data are made available through cooperative agreements with public monitoring agencies and private firms.

The fourth objective requires development of graphical tools in the form of scripts that read and combine model results with observed data, then analyze and display these results using Internet technology. The programs utilized for this fourth objective include the Geographic Resources Analysis Support System (GRASS), GIS engine, Google Earth and Keyhole Markup Language (KML), R, gnuplot, php, and other scripting tools.

## 1.4 CONTENT OF THE DISSERTATION

This dissertation is divided into eight main chapters arranged as follows:

**Chapter 1:** Introduction—this chapter;

**Chapter 2:** Literature review of hydrological models including different classification systems of models and a justification for the hybrid approach used in this research. Chapter 2 finishes with a summary of the development history of the models combined to form TREX-SMA, the hybrid model herein described;

**Chapter 3:** A process description of TREX-SMA and information about the algorithm;

**Chapter 4:** Details about data used to perform and evaluate simulations with TREX-SMA;

**Chapter 5:** Several simple demonstrations of model function;

**Chapter 6:** A description of the 50-day, multi-event simulation of the California Gulch watershed near Leadville, Colorado. TREX-SMA performance is compared to performance of the unmodified TREX model using several innovative graphical and statistical techniques;

**Chapter 7:** Details on computational and data management improvements, as well as improvements to integrated statistical analysis and graphical display of results for TREX;

**Chapter 8:** Conclusions from this research.

# 2.0 LITERATURE REVIEW

Watershed models have proliferated for various reasons: the growing availability of data to drive and calibrate them, the ever increasing availability and capability of computational resources, and increasing regulatory demands requiring model applications. This literature review first briefly examines the reasons why an engineer might undertake hydrologic modeling. Then, a summary view is given of both the diverse field of models presently available as well as the wide range of systems of classifying and distinguishing models. A broad justification from literature is then presented for the combination of techniques implemented in the present effort.

## 2.1 THE HYDROLOGIC CYCLE IN CIVIL ENGINEERING

Computational models of hydrology attempt, in many different ways, to represent the operation of the physical hydrologic cycle. The processes of the hydrologic cycle occur and interact across the entire globe on a continuous basis. Though the cycle is continuous both spatially and temporally, the cycle may be diagrammed as water passing through various fluxes and storages with water existing in all three states (liquid, vapor, and solid). Descriptive scientific models are stretching further and further to represent all of the hydrologic cycle.

In order to simplify the modeling process, engineers isolate portions of the hydrologic cycle. Surrounding storages and fluxes are approximated as boundary conditions. Separating the cycle components (indeed, even distinguishing them as components) is possible and sometimes even required due to the very disparate time and spatial scales at which the processes occur (Aral and Gunduz 2003, 2006; Gunduz 2004).

Eagleson's (1970) diagram (Figure 2.1) schematically represents the fluxes and storages of the hydrologic cycle and shows the state (liquid, solid, or vapor) of water during each part of the cycle.

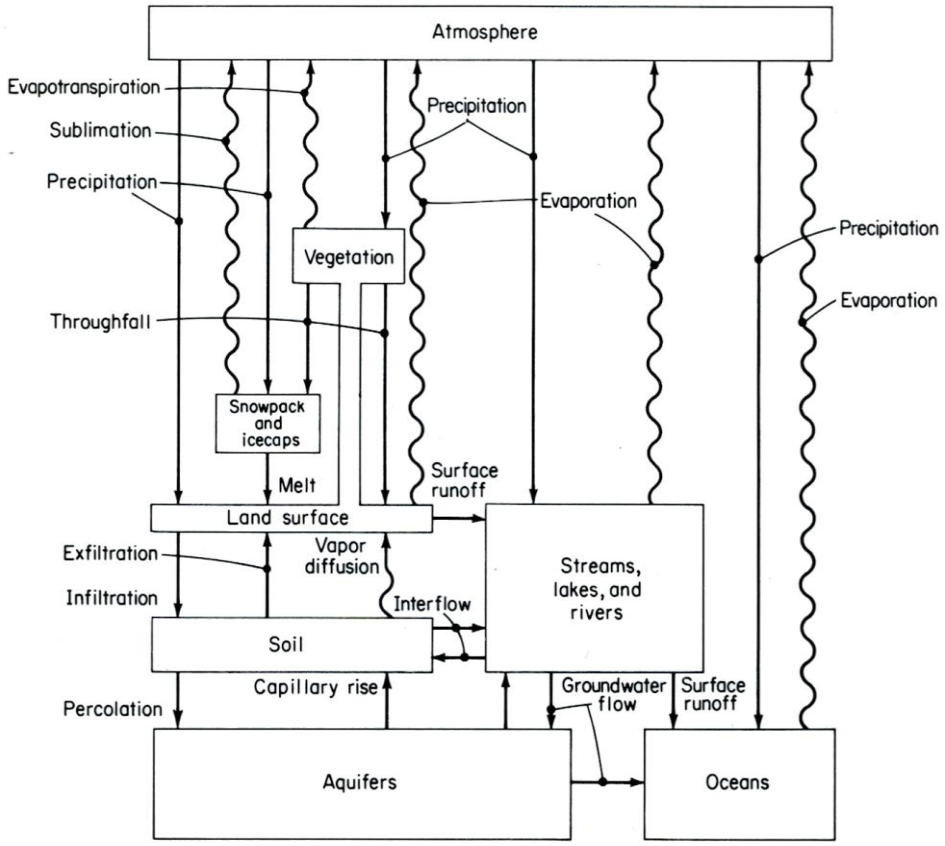


**Figure 2.1: The hydrologic cycle, diagrammed by Eagleson (1970). Storage of water shown as boxes; flux of liquid water as straight lines; water vapor flux is shown as wavy lines.**

Linsley et al. (1982) notes that hydrology in engineering is primarily used to support the services of hydraulic designers, i.e., to provide the design constraints to which their designs are suited. Other reasons for modeling include purely scientific objectives such as system description or theory testing. “However, the ultimate aim of prediction using models (especially in the discipline of engineering) must be to improve decision-making about a hydrological problem, whether that be in water resources planning, flood protection, mitigation of contamination, or licensing of abstractions, etc." (Beven 2000).

Rainfall-runoff modeling is performed because observations of runoff processes are limited. Models are most useful where observations cannot go—to predict watershed response in ungauged catchments, and in future events (Beven 2000).

The purposes of a hydrologic response model are as follows (Freeze and Harlan 1969):

1) to synthesize past hydrologic events;

2) to predict future hydrologic events and to evaluate, for design purposes, combinations of hydrologic events occurring rarely in nature;

3) to evaluate the effects of artificial changes imposed by man on the hydrologic regime;

4) to provide a means of research for improving our understanding of hydrology in general, and the runoff process in particular.

Hydrologic modeling is an answer for the task of an engineer: "*to do everything that is reasonably possible* to analyze the difficulties with which his or her client is confronted, and on this basis to design solutions and implement these in practice" (Abbott and Refsgaard 1996, emphasis in original).

## 2.2 CREATING A HYDROLOGIC MODEL

To create a hydrologic model, a hydrologist considers four types of input (Freeze and Harlan 1969):

1) model definitions (grid, time increments)
2) meteorological (precipitation and evapotranspiration)
3) flow parameters (roughness, permeability, hysteresis, moisture content, conductivity)
4) mathematical input (the model itself defined as equations)

A hydrologic model is conceived in a series of steps consisting of successively more concrete iterations (Beven 2000). A new hydrologic model first requires a human perception of the relative importance of the processes in the catchment and second, a determination (not necessarily constrained by mathematical theory) of which processes should be considered in the model. Following development of the "perceptual model," a "conceptual model" is created consisting of a mathematical reduction of the perceived processes, necessarily containing

assumptions and approximations. Next, boundary conditions are introduced to allow for a numerical or analytical solution to the mathematical equations that represent the continuous hydrologic processes. The "procedural model" comes next with the actual computer coding of the conceptual model. Finally, the model receives its first input. The procedures are run, debugged, and re-run until an acceptable output is produced. Figure 2.2 diagrams this process of model creation and shows that before the model is declared successful and useful for its intended purpose, some “validation” must occur.

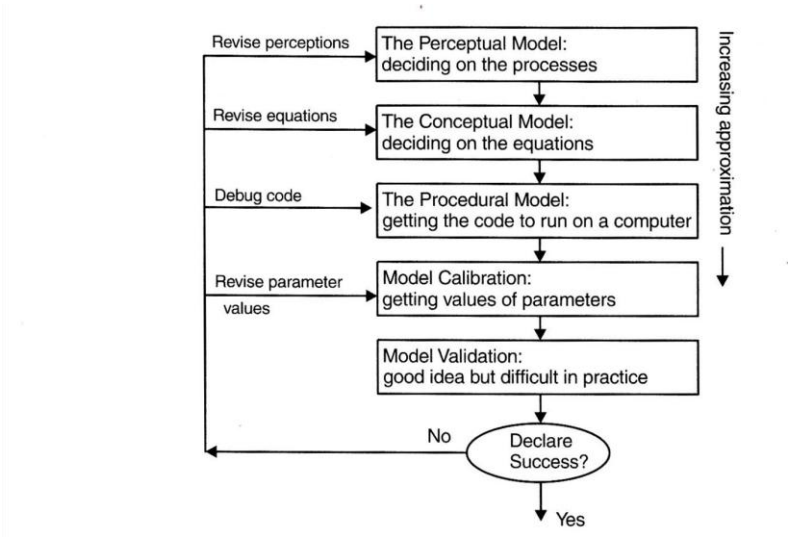


**Figure 2.2: A schematic outline of the different steps in the modeling process (Beven 2000).**

As a caution, Refsgaard and Storm (1996) point out that "a modelling system can, in principle, never be calibrated."

The term validation is now replacing the term verification in usage concerning the process of determining that a model is successful. Verification literally means "to make true." This is not completely possible with an approximate, incomplete representation of the hydrologic cycle. A model could not be entirely “true” until a complete representation is achieved and all assumptions have been replaced by correct computations of boundary processes.

Refsgaard (1996) explains that “validation” occurs after "applying the (procedural) model within the domain of applicability" and discovering that, indeed, the model performs with a "satisfactory range of accuracy consistent with the intended application of the model." Refsgaard and Storm (1996) suggest that the concept of validity is interchangeable with "the credibility of a given modelling system."

Abbott and Refsgaard (1996) develop a concept related to validation: practical model “qualification” that is the "adequacy of the conceptual model to provide an acceptable level of agreement of the domain of the intended application." They explain that the "domain of applicability" consists of the "prescribed conditions for which the computerised model has been tested, i.e. compared with reality to the extent that it is practically possible and judged suitable for use" (Abbott and Refsgaard 1996).

### 2.3 STATISTICS AND MODEL PERFORMANCE

A number of descriptive and comparative statistics are available to compare model outputs to reality and to characterize model performance in reproducing actual basin response.

Some of the most common:

- percent bias and absolute percent bias
- Nash-Sutcliffe efficiency
- Pearson and modified Pearson correlation coefficients
- root-mean-squared error

Model performance statistics must demonstrate mass error and bias, as well as overall goodness-of-fit when comparing simulated to observed values. These statistics provide the basis for a calibration algorithm.

### *2.3.1 Mass error statistics*

The percent bias is a measure of total volume difference between the observed and simulated time series and provides a view of the mass error. When combined with the absolute percent bias, the percent bias gives some estimate of the timing error in the peaks of the simulated series. If the percent bias is small but the absolute percent bias is large, then the timing of peaks is not very good (Smith et al. 2004).

$$\text{Percent Bias, } P.B. = \frac{\sum_{i=1}^{N} (S_i - O_i)}{\sum_{i=1}^{N} O_i} \times 100 \qquad \text{(Eq. 2.1)}$$

$$\text{Absolute Percent Bias, } A.P.B. = \frac{\sum_{i=1}^{N} |S_i - O_i|}{\sum_{i=1}^{N} O_i} \qquad \text{(Eq. 2.2)}$$

Where: $S_i$ = simulated flow

$O_i$ = observed flow

$N$ = number of observations

The series mean and standard deviation are used to normalize several of the other statistical measures in order to establish the relative size of error.

$$\text{Series Mean, } \bar{Y} = \frac{\sum_{i=1}^{N} Y_i}{N} \qquad \text{(Eq. 2.3)}$$

$$\text{Standard Deviation, } \sigma_Y = \sqrt{\frac{\sum_{i=1}^{N} Y_i - \bar{Y}^2}{N-1}} \qquad \text{(Eq. 2.4)}$$

Where: $Y_i$ = any series, observed or simulated

$N$ = number of observations (as above)

### *2.3.2 Goodness-of-fit statistics*

Goodness-of-fit is measured by the root mean squared error, which is the sum of the squared residuals.

$$\text{Root Mean Squared, } RMS\text{or}RMSE = \frac{\sqrt{\frac{1}{N}\sum_{i=1}^{N} S_i - O_i{}^2}}{\bar{O}} \qquad \text{(Eq. 2.5)}$$

Where: $S_i$, $O_i$, $N$ are defined as above and $\bar{O}$ is the observed mean.

The RMS error is made more useful by normalizing the observed mean to give the percent root mean squared error (NOAA 2004).

$$\text{Percent Root Mean Squared, } PRMS\text{or}\%RMSE = \frac{\text{RMS}(O,S)}{\bar{O}} \qquad \text{(Eq. 2.6)}$$

Where: RMS($O$ ,$S$) = Root Mean squared error (equation 2.5)

and $\bar{O}$ = mean of the observed series.

The RMS error may also be normalized by the observed standard deviation to produce a statistic that "incorporates the benefits of error index statistics and includes a scaling/normalization factor, so that the resulting statistic and reported values can apply to various constituents" (Moriasi et al. 2007).

$$\text{Root Mean Squared Ratio, } RSR = \frac{\text{RMS}(O,S)}{\sigma_O} \qquad \text{(Eq. 2.7)}$$

Where: $\sigma_O$ = standard deviation of the observed series

The lower the value of RSR, the lower the RMSE and the better the model simulation has conformed to observations. An RSR of zero indicates zero residual variation and therefore perfect model simulation.

Two other measures of goodness-of-fit demonstrate how well the model predicts the observed results relative to a random distribution: the correlation coefficient and the Nash-

Sutcliffe efficiency. The correlation coefficient varies between -1.0 and 1.0, a perfect prediction of observed values by the model indicated by a coefficient of 1.0 and a completely inverse prediction (i.e. when the model predicts high, the observation is low and vice versa) by a value of -1.0. McCuen and Snyder introduced a modified correlation coefficient which reduces the influence of outliers and diminishes the scaling effect of magnitude of the hydrograph to provide a more uniform measure of performance between watersheds (McCuen and Snyder 1975; Smith et al. 2004).

$$\text{Correlation Coeff.}, r = \frac{N\sum_{i=1}^{N} S_i O_i - \sum_{i=1}^{N} S_i \cdot \sum_{i=1}^{N} O_i}{\sqrt{\left[N\sum_{i=1}^{N} S_i^2 - \left(\sum_{i=1}^{N} S_i\right)^2\right] \cdot \left[N\sum_{i=1}^{N} O_i^2 - \left(\sum_{i=1}^{N} O_i\right)^2\right]}} \qquad \text{(Eq. 2.8)}$$

$$\text{Modified Correlation Coefficient}, r_{mod} = r \cdot \frac{min\{\sigma_{sim}, \sigma_{obs}\}}{max\{\sigma_{sim}, \sigma_{obs}\}} \qquad \text{(Eq. 2.9)}$$

The Nash-Sutcliffe efficiency (a type of coefficient of determination, $R^2$) compares the predictions of the model to the prediction of the mean of observations. When the efficiency is 1.0, the model perfectly predicts the observations. When the efficiency is zero, the model predicts observations no better than the mean of the observations; when less than zero, the model provides a less accurate prediction of outcomes than the mean alone (McCuen et al. 2006; Moriasi et al. 2007; Nash and Sutcliffe 1970).

$$\text{Nash-Sutcliffe Efficiency Coefficient}, NSE = 1.0 - \frac{\sum_{i=1}^{N} S_i - O_i^2}{\sum_{i=1}^{N} O_i - \bar{O}_i^2} \qquad \text{(Eq. 2.10)}$$

### *2.3.3 Overall performance measures*

Moriasi et al. (2007) gives a table of recommended values for several statistics used to compare simulated results to an observed mean. The Moriasi performance ratings are at least qualitatively useful, even though they are tabulated for models run on a monthly time step in

contrast to the much more refined time step of the TREX-SMA model. Most of the models analyzed by Moriasi had similar values when evaluated on a daily time-step as opposed to monthly.

**Table 2.1: General performance ratings for recommended statistics for a monthly time step (Moriasi et al. 2007).**

| Performance Rating | RSR | NSE | PBIAS |
|---|---|---|---|
| Very good | $0.00 \leq \text{RSR} \leq 0.50$ | $0.75 < \text{NSE} \leq 1.00$ | $\text{PBIAS} < \pm 10$ |
| Good | $0.50 < \text{RSR} \leq 0.60$ | $0.65 < \text{NSE} \leq 0.75$ | $\pm 25 \leq \text{PBIAS} < \pm 40$ |
| Satisfactory | $0.60 < \text{RSR} \leq 0.70$ | $0.50 < \text{NSE} \leq 0.65$ | $\pm 40 \leq \text{PBIAS} < \pm 70$ |
| Unsatisfactory | $\text{RSR} > 0.70$ | $\text{NSE} \leq 0.50$ | $\text{PBIAS} \geq \pm 70$ |

RSR: Root mean squared ratio (ratio of RMSE to standard deviation)
NSE: Nash-Sutcliffe efficiency
PBIAS: Percent Bias

Moriasi et al. (2007) gives additional qualitative guidance regarding more single-event models: "Accurate prediction of peak flow rate and time-to-peak is essential for flood estimation and forecasting." Time to peak and peak flow rate are affected by antecedent moisture conditions, soil infiltration properties, drainage network topology, channel roughness, and rainfall intensity (Moriasi et al. 2007; Ramírez 2000).

Error in peak flow rate may be quantified as a percentage by dividing the difference between simulated and observed by the observed value. For example, a simulated peak twice the value of the observed will have an error of 100%.

Although the Nash-Sutcliffe efficiency has become a very common measure of hydrologic model performance, an important shortcoming of the Nash-Sutcliffe statistic occurs in periods of low flow. If the flow approaches the average value, the value of the statistic becomes unstable and may show an extremely poor match (highly negative) with only minor model error (Watershed Management Committee, Irrigation and Drainage Division 1993). Jain and Sudheer

(2008) also gives several examples of specious Nash-Sutcliffe efficiency values which approach the optimal value of 1.0, even for a model showing poor performance relative to observed.

### *2.3.4 Graphical performance evaluation*

In some cases where very complex models are being evaluated (as is the case with nearly every hydrologic model), the graphical comparisons are more effective than the analytical statistics (Gelman 2004; Watershed Management Committee, Irrigation and Drainage Division 1993). Simple plots of observed values with simulation results, as well as a plot of residuals, can provide a very quick visual confirmation of model goodness-of-fit.

Very large peak values can easily obscure the smaller values in either flow or residual plots. A simple log transform or plotting in log scale allows for viewing of high and low values of flow. However, residual error values may be negative and cannot be plotted directly on logarithmic scale. By transforming the error with the inverse hyperbolic sine function, the extreme values become log-transformed and the inner values are approximately linear.

The inverse hyperbolic sine function is equivalent to the following:

$$arcsinh(x) = \ln x + \sqrt{(x^2 + 1)} \qquad \text{(Eq. 2.11)}$$

This type of transform (or plotting on a transformed scale of this type) allows for viewing of a dataset with both negative and positive values with both large peaks and significant variation closer to zero (Lupton et al. 1999; Parks et al. 2006).

## 2.4 SYSTEMS OF CLASSIFICATION

A number of researchers have attempted to classify the different watershed models according to various systems. As with nearly all systems of classification, there are exceptions which, if carried to an illogical limit, could eventually define each model as completely unique. Most

models fall within a spectrum, containing attributes germane to either extreme at some level of implementation. Even so, the systems of classification are helpful in determining the applicability and potential for future development of many models.

Part of the difficulty in creating a classification system for hydrologic models is that there does not seem to be a "generally agreed upon catchment classification system" (Wagener et al. 2007) for the watersheds which the models represent. The field of hydrology is similar to that of biology in the 1800s when the taxonomy of living organisms was finally becoming a scientific practice. A framework for the taxonomy of watersheds would be similar to the taxonomy for models.

> Such a classification framework should provide a mapping of landscape form and hydro-climatic conditions on catchment function (including partition, storage, and release of water), while explicitly accounting for uncertainty and for variability at multiple temporal and spatial scales. This framework would provide an organizing principle, create a common language, guide modeling and measurement efforts, and provide constraints on predictions in ungauged basins, as well as on estimates of environmental change impacts. (Wagener et al. 2007)

### *2.4.1 Lumped vs. distributed*

One of the most common systems of hydrologic model classification is lumped vs. distributed. According to Abbot and Refsgaard (1996), a *lumped model* is a model where the catchment is regarded as one unit and variables and parameters in the model represent average or effective values for the entire catchment. On the other hand, a *distributed model* takes into account the spatial variations in all variables and parameters (Abbott and Refsgaard 1996).

Aral and Gunduz (2006) define lumped parameter models as those in which the watershed is “a single unit behaving in accordance to a completely empirical or quasi-empirical response function with little or no dependence to the analytic description of physical processes and spatial heterogeneity.” In contrast, a distributed model treats the system “as a discretized set of small homogeneous units that address the spatial heterogeneity with full reference to the analytic

representation of physical processes that act on each unit" (Aral and Gunduz 2006). Kampf and Burges (2007) define lumped models as "effectively one-dimensional" because they average processes over some domain to produce an estimate of stream flow at the outlet. Distributed models, by comparison, attempt to represent the "water pathways in XY or XYZ space" (Kampf and Burges 2007).

Beven (2000) also classifies models as either "lumped" or "distributed." Lumped models, according to Beven, are "unashamedly empirical" and are really "data-based modelling, usually at the catchment scale, without making much physical argument or theory about process." Beven does not discount their utility in any way. He does caution that the empirical methods may yield a model which accurately predicts watershed behavior, but which gives a confusing picture of the mechanisms. The distributed models, Beven states, are almost all based on the "Freeze-Harlan 'blueprint' ," or are simplifications of the same (cf. Freeze and Harlan 1969).

Reggiani and Schellekens (2003) casts doubt on the validity of either approach (lumped or Freeze-Harlan/distributed) and proposes a semi-distributed approach based on a "representative elementary watershed" (REW) concept. The REW approach integrates the microscale equations representing mass and energy flux, with a time and space scale "characterizing hydrological flow processes" (Reggiani and Schellekens 2003). TOPMODEL (Beven and Kirkby 1979; Beven 1986) is another semi-distributed model with advantages over "traditional lumped conceptual systems" due to explicit accounting of the "spatial variability and direct use of spatial data such as topography and channel system together with semi-distributed calculations of hydrological variables" (Refsgaard 1996).

### *2.4.2 Runoff generation mechanism*

Kampf and Burges (2007) give a classification system which further subdivides distributed models based on different representations of processes in the 1) subsurface, 2) surface, 3) atmosphere, and 4) biosphere. For distributed rainfall-runoff models, the most important distinction is the surface runoff generation mechanism. Two primary types of runoff generation are described in the literature: Hortonian (Horton 1933) and Dunne (Dunne and Black 1970a, b).

Hortonian or "infiltration excess" runoff occurs when the rate of rainfall arriving at the soil interface exceeds the infiltration rate of the soil surface (Beven 2004). Dunne or "saturation excess" runoff will occur when "vertical flow of soil water from rain is impeded by a limiting layer of sufficiently low permeability that a saturated zone develops above it, which under continuing rainfall events may rise until the soil surface is reached, and a wet 'direct' contributing area is formed" (Smith and Hebbert 1983). The distinction between these two runoff types is most important for short, intense hydrologic events, since as a rainstorm progresses, the infiltration rate at the soil surface decreases and the Horton and Dunne mechanisms will eventually converge at saturation when the infiltration rate is zero.

### *2.4.3 Empirical, conceptual, or physical*

Abbot and Refsgaard (1996) further classify models according to the degree of transparency in the production of results:

> A *black box* or an *empirical model* is a model developed without any considerations of the physical processes that we otherwise associate with the catchment. The model is merely based on analyses of concurrent input and output time series.

> A *conceptual model* is one that is constructed on the basis of the physical processes that we "read" into our observations of the catchment. In a conceptual model, physically sound structures and equations are used together with semi-empirical ones. However, the physical significance is not usually so clear that the parameters can be assessed from direct measurements. Instead, it is necessary to estimate the parameters from calibrations, applying concurrent input and output time series. A conceptual model, which is usually a lumped-type model, is often called a *grey box model*.
>
> A *physically-based model* describes the natural system using the basic mathematical representations of the flow of mass, momentum and various forms of energy. For catchment models, a physically-based model in practice also has to be fully distributed. This type of model, also called a *white box model*, thus consists at its most basic "human-friendly" level of a set of linked partial differential, integral-differential, and integral equations together with parameters which, in principle, have direct physical significances and can be evaluated by independent measurements. (Refsgaard 1996)

Physically-based models represent flow using equations derived from equations of conservation of mass, momentum, and energy and will internally function using variables and parameters that, at least theoretically, directly represent physically-measurable quantities in the field (Kavvas et al. 2004). GSSHA, CASC2D for WMS, and TREX are all examples of physically-based distributed models. Flow between cells and in channels is described by the diffusive approximation of the St. Venant equations. Model states and input and output values are all distributed over the entire grid unless specified as a basin or domain average value.

Conceptual models, by comparison, operate on parameters that represent physical values indirectly through equations assembled to represent a conceptualization of hydrologic processes. Aral and Gunduz (2006) suggests that all lumped models are conceptual and non-physical, asserting that they contain no connection to physical processes except through a black-box empirical function. The Sacramento Soil Moisture Accounting model (most commonly implemented via the NWSRFS as SAC-SMA) is considered to be a conceptual lumped parameter model with inputs across whole watersheds. Parameters in the SAC-SMA model have

corollaries in the physical processes of water transfer, but they do not explicitly describe the flow dynamics that determine rates transfer and flux.

### *2.4.4 Deterministic and stochastic*

Deterministic models are those which, for a given input or series of inputs, will always produce the same result. This is as opposed to stochastic models that use assumed or computed variation in the input parameters to produce ensembles of potential model outcomes (Refsgaard 1996). The range of variation in the output ensembles is compared to a standard distribution to compute confidence intervals and probabilities of occurrence. The assumptions regarding the nature of these distributions both for the input parameters and output variables are subjects of debate and research, since a different underlying distribution will yield different probabilities and levels of confidence.

In any case, the distinction between deterministic and stochastic models is somewhat arbitrary, since a deterministic model may be made to function stochastically simply by comparing results from multiple simulations with a random or prescribed variation in the input parameters. Results from this type of modeling—deterministic modeling with a suite of possible input parameters—are also referred to as “ensembles.”

### *2.4.5 Technological classification*

Models may also be classified according to level of distribution and use. According to Refsgaard (1996), models go through a series of developmental “generations” beginning with a pioneering first generation that is a simple computerized formula using a computer as a "super slide rule." Second generation models, so-called “one-off” numerical models, are used purely in research applications. Third generation models are "generalised numerical modelling systems" with wide applicability and mature scientific code, but with few users. Finally, fourth generation

models have a well-developed user interface and are widely distributed and applied. Fourth generation status means a model is more widely available but cost is increased by increasing focus on application features which are superfluous to the actual model operation. A final, fifth technological level is identified: "smart models," which do not require expert operation.

## 2.5 Benefits and Disadvantages of Different Types

The aim of distributed hydrologic modeling is:

> …to make the fullest use of cartographic data, of geological data, of satellite data, of stream discharge measurements, of borehole data, of observations of crops and other vegetation, of historical records of floods and droughts, and indeed of everything else that has ever been recorded or remembered, and then to apply to this everything that is known about meteorology, plant physiology, soil physics, hydrogeology, sediment transport and everything else that is relevant within this context. (Refsgaard and Abbott 1996)

A physically-based three-dimensional hydrologic model can perform continuous multi-event simulations—even on large spatial domains—and can include all of the relevant processes noted above from Refsgaard and Abbot (1996). See for example, Ebel et al. (2008), Panday and Huyakorn (2004), and Storm and Refsgaard (1996). The fully coupled physics-based model becomes cumbersome though, both in terms of computational resources and in terms of the data required to construct, calibrate, and operate the model. Advances in the processing power of computers continue to remove the computational barriers to fully coupled models. Remote sensing provides increasingly greater volumes of data regarding surface hydrology. Still, the subsurface remains difficult to characterize without expensive and intensive monitoring programs.

Citing Refsgaard and Abbott (1996), Wagener states that the advantage of gridded models is the correlation between the spatial discretization of the model (grids, hillslopes, or other hydrologic response unit) and applications where therefore "a high level of spatial discretization

is important, e.g., to estimate local effects on soil erosion, or surface and groundwater pollution" (Wagener 2004). If the “main interest simply lies in the estimation of streamflow response at the catchment scale and if calibration data are available,” then parametric (conceptual) models perform “at least as well,” according to Wagener (2004). Wagener concludes that lumped conceptual models with relatively simple structures are preferable for continuous modeling.

Comparing the advantages of physics-based distributed modeling with conceptual lumped-parameter modeling, Ebel and Loague offer the following:

> A comprehensive physics-based model…would be a poor choice if the objective of a simulation effort was to estimate an integrated response (e.g. discharge from an ungauged catchment). On the other hand, if the objective of the simulation effort was to quantitatively estimate the spatial and temporal distributions of pore pressures within the variably saturated 3D subsurface (i.e. for understanding slope failure initiation at the hillslope/catchment scale), then a comprehensive physics-based model would be a good choice. (Ebel and Loague 2006)

Wagener (2004) warns that "No completely successful application of these simple continuous models to ungauged catchments has been reported yet." But Ebel and Loague (2006) suggest keeping an open mind: "Knowing that no hydrologic-response model works equally well for all situations, it is unproductive (at this time) to suggest the complete abandonment of any approach."

## 2.6 THE STATE-OF-THE-ART

The goal of modern hydrologic modeling is to both find a relationship of rainfall inputs to discharge outputs by understanding the flow pathways of water and then creating a "representation of theory [in the form of] quantitative predictive models" (Wagener 2004). The difficulties currently faced in hydrologic modeling are a result of a "lack of suitable measurement techniques" of these inputs and flows (Kieth Beven in preface to Wagener 2004). Flow pathways

such as river discharge may be measured with reasonable accuracy, but even when using radar rainfall estimates it is difficult to characterize the spatial and temporal variability of rainfall.

Abbot and Refsgaard (1996) tabulated (see Table 2.2) the areas of needed improvement in hydrologic modeling showing that many areas are lacking in examples of practical application. The areas of need noted in the table are due to difficulties with data availability; inadequate scientific basis for modeling; and cultural, administrative, and financial roadblocks. TREX SMA approaches some of these limitations in the state-of-the art by making available in long-term or multi-event mode the strengths of TREX in the areas of 1) soil erosion, 2) effects of land-use change on flows and water quality, and 3) aquatic ecology.

Ebel and Loague (2006) assert that current physics-based models are not suited for real-time flood forecasting. However, the TREX-SMA implementation at California Gulch is a beginning for continuous flash-flood guidance with the soil-moisture accounting allowing for continuous operation and TREX providing the surface runoff computations which primarily drive flash-flooding. NOAA researchers have been improving the techniques for providing continuous flash flood guidance across the nation on a 4-km gridded model (Reed et al. 2007) and TREX-SMA could participate in that improvement by adding finer scale surface computations.

**Table 2.2: "Status of application of hydrological modelling systems to various problem types" (after Abbott and Refsgaard 1996).**

| | STATUS OF APPLICATION | | | | |
|---|---|---|---|---|---|
| Field of Problem | Adequacy of Scientific Basis | Scientifically Well Tested | Validation on Pilot Schemes | Practical Applications | Major Constraint for Practical Application |
| Water resources assessment | | | | | |
| • Groundwater | Good | Good | Adequate | Standard/Part | Administrative |
| • Surface water | very good | Very good | Adequate | Standard/Part | Administrative |
| Irrigation | Good | Good | Partially | Very limited | Techno/Admin |
| Soil erosion | Fair | Fair | Very limited | Nil | Science |
| Surface water pollution | Good | Good | Adequate | Some cases | Administrative |
| Groundwater pollution | | | | | |
| • Point sources (landfills) | Good | Good | Partially | Standard/Part | Techno/Admin |
| • Non-point (agriculture) | Fair | Fair | Very limited | Very limited | |
| On-line forecasting | | | | | |
| • River flows/water levels | Very good | Very good | Adequate | Standard | Nil |
| • Surface water quality | Good | Good | Adequate | Standard/Part | Data/Admin |
| • Groundwater heads w/table | Very good | Very good | Partially | Very limited | Data-Techno |
| • Groundwater quality | Fair | Fair | Nil | Nil | Science |
| Effects of Land use change | | | | | |
| • Flows | Good | Fair | Fair | Very limited | Science |
| • Water quality | Fair | Fair | Fair | Nil | Science |
| Aquatic ecology | Fair | Fair | Very limited | Very limited | Science Techno |
| Effects of climate change | | | | | |
| • Flows | Good | Good | Fair | Very limited | Science |
| • Water quality | Fair | Fair | Nil | Nil | Science |

LEGEND

*Adequacy of scientific basis*

- Poor: Large and crucial needs for improvements in scientific basis
- Fair: Considerable need for improvements in scientific basis
- Good Some needs for improvements in scientific basis
- Very good: No present significant need for improvements in scientific basis

*Scientifically well tested ?*

- Poor: Large needs for fundamental tests of scientific methodologies
- Fair: Considerable needs for testing (some) of the scientific basis
- Good Some needs for testing of the scientific basis
- Very good: No present significant need for testing of the scientific basis

*Validation on pilot schemes?*

- Nil: No success validation on well controlled pilot schemes so far – urgent need for validation on pilot schemes
- Very limited: A few (a couple of) validation cases – considerable needs for more validation projects on pilot schemes
- Partially: Some cases with successful validation on pilot schemes – some needs for further validations
- Adequate: Many good validations – no further present needs

*Practical applications*

- Nil Practically no operation applications
- Very limited A few well proven cases of operational practical applications
- Some cases Some cases of well proven operation practical applications
- Standard/Part Standard professional tool in some regions
- Standard Standard professional tool in many regions of the world

*Major constraint for practical application*

- Data: Data availability a major constraint
- Science: Inadequate scientific basis is a major constraint
- Technology: A technology push is required in order to make well proven methods more widely applicable
- Administrative: Administrative tradition or mission economical motivation is a major constraint

Beven (2000) reiterates that the greatest uncertainty in studying (and modeling) hydrologic systems lies in our inability to understand *subsurface* processes and that the magnitude of the subsurface non-linearity and uncertainty is such that at a certain level, “rainfall-runoff modelling is an impossible problem!”

Under the ground surface, "our measurement techniques are even more inadequate in that they tend to give only very local information about water storage and potentials…but the heterogeneity of soils and rocks is such that quantitative prediction in any real catchment remains very difficult." In mountain areas, the presence of fracture flow adds significant complexity and in arid or semi-arid areas, there are often complex interactions between various hydrological processes " such as presence of snow, high solar radiation, intense evaporation, use of water for irrigation" (Millares et al. 2009).

Despite these limitations, "practical water management (an engineering problem), requiring estimates of water yields and river flows under *both high and low flow conditions* (emphasis added) is increasingly driving the use of model predictions despite the worries of academics about the difficulties of doing modelling properly” (Wagener 2004, preface).

## 2.7 HYBRID MODEL JUSTIFICATION

Wagener (2004) indicates that to model properly "means more than just relating rainfall inputs to discharge outputs, it means trying to understand the flow pathways of the water within a catchment." The different flow pathways—open channel flow, overland flow on the ground surface, and the unsaturated zone and saturated zone groundwater flow below the ground surface—experience entirely different time and space scales (Aral and Gunduz 2006). The consequence of these differences is a rather significant computational inefficiency if the various pathways are modeled, because of model formulation, on a similar grid space and time scales. In

2003, the idea of a "hybrid modeling concept was introduced in the literature" in order to "resolve some of the problems associated with the fully physics-based representation of all subsystem processes of a watershed while providing a much better and sophisticated interpretation that can be provided by an empirically based lumped parameter model." Aral's reasons are as follows:

> For large-scale applications such as catchment modeling, the small-scale requirements of overland and unsaturated zone flow domains exhibit severe limitations on efforts of fully integrating the system. *Consequently, a hybrid modeling approach is more suitable in which distributed- and lumped-parameter models are essentially linked and blended to obtain a semi distributed watershed model.* (Aral and Gunduz 2006, emphasis added)

Hybrid models have been proposed as a potential solution for the complexity imposed by solving fully coupled flow equations. Hybrid models can also overcome the problems caused by dissimilarities in the time and spatial scale of flow processes in the channel, overland plane, and subsurface by allowing these processes to occur uncoupled. "Semi-distributed" as used here is different than in most literature. Other literature refers to semi-distributed with a uniform spatial and temporal scale throughout the model, while here it is a portion of the spatial or temporal domain which is distributed while the rest is lumped, hence "semi distributed."

Kirchner (2006) states that modern physically based models are developed upon the premise that the well understood physics of the micro-scale may be applied via "up scaling" to the aggregated grid or lumped domains of modern hydrologic models and that at the model scale, the same governing equations will apply with averaged state variables and "effective" parameters (e.g., saturated conductivity, characteristic curves) that somehow subsume the heterogeneity of the subsurface." Kirchner further proposes that hybrid "gray box" models might be developed as a middle ground between distributed explicit process models and conceptual aggregations with

too many free parameters to be constrained by available data. Such an approach, he says, allows some latitude for unexpected physical processes (Kirchner 2003).

TREX and SAC-SMA differ in nearly all of the systems of classification: one is lumped, the other distributed; one is empirical and conceptual, the other physically-based. (Both are deterministic—though the tools coupled with SAC-SMA in the NWSRFS allow for stochastic ensembles to be evaluated) But the large range of differences is why coupling them creates a hybrid rather than a "semi-distributed" model. Although many elements of the TREX-SMA hybrid model have common elements found in other models, the nature of the coupling— particularly the variation in the spatial representation of the processes— is a unique concept.

TREX is limited because it does not allow for continuous temporal representation. SAC-SMA is limited because it does not allow for continuous spatial representation. But the TREX model does simulate distributed surface rainfall-runoff response and erosion, and the SAC-SMA model does simulate continuous hydrologic response. So if a hybrid can be made wherein the TREX surface veneer is placed on top of a SAC-SMA continuous soil moisture engine, this could be very useful for applications where the surface processes need to be highly discretized but subsurface processes are not as critical. Potential applications include continuous flood forecasting and continuous sediment delivery modeling. The TREX model is currently formulated with the diffusive wave approximation of the St. Venant equations for computation of flow.

TREX-SMA allows a model which has been shown to perform well in high-flow conditions (i.e. the TREX model) to now perform well under low flow conditions by means of hybridization with SAC-SMA procedure. The difficulties of representing the specific flow pathways in the subsurface "where the infiltrating rainfall goes" (Wagener 2004), are somewhat side-stepped by

the method of conceptually representing subsurface response in the Sacramento model. While this does not qualify as "proper" in the sense that it truly mimics (or models) the hydrologic cycle, it can certainly aid in the development of engineering estimates of high- and low-flow conditions. And, with the distributed chemical and sediment transport features of the TREX model made available on a long-term, continuous basis, the hybrid techniques in TREX-SMA can help answer the needs described above by Abbot and Refsgaard (1996) in Table 2.2 for improvement in modeling of soil erosion, impacts of land use change, and water quality.

## 2.8 TREX AND SAC-SMA

In order to understand the conceptual model of the hybrid model TREX-SMA, it is advantageous to discuss the conceptual models underlying the primary constituent models in the hybrid: The TREX surface hydrology model developed at CSU and the Sacramento Soil Moisture Accounting model (SAC-SMA) from the National Weather Service. Each of these models has strengths derived from their development history that lead to their selection for this effort. Each also has limitations, some of which are overcome to an extent and some that are still manifest in the hybrid model.

### *2.8.1 TREX model development history*

The TREX model is a descendant of the CASC2D surface hydrology model developed at CSU. The hydrologic model CASC2D originally began with a two-dimensional overland flow routing algorithm developed and written by P.Y. Julien at CSU in 1988 (Saghafian and Julien 1991). Successive modifications by Saghafian (1992), Ogden (1992), Johnson (1997), and Rojas-Sánchez (2002) improved the hydrologic and hydraulic computations and added a sediment transport algorithm. With the addition of the sediment transport algorithm, the code was renamed CASC2D-SED (Johnson et al. 2000; Rojas Sánchez et al. 2003).

Ogden and Saghafian (1997) pursued modifications to the hydrologic schema of CASC2D and incorporated their model into the USACE Watershed Modeling System (WMS). This code continued to be known as CASC2D until progressing to version 1.18. At that point, development efforts diverged and a version of CASC2D was moved to the Environmental Lab at the U.S. Army Corps of Engineers Engineering Research and Development Center (ERDC-EL) while the ERDC Coastal and Hydraulics Lab (ERDC-CHL) took up development on another branch.

Following significant reprogramming, the CHL version of the code was renamed GSSHA, Gridded Surface Subsurface Hydrologic Analysis. GSSHA is made available as an executable-only download from CHL or as a component of the WMS (Byrd et al. 2005; Downer et al. 2002). Presently, the ERDC-EL version is in limited distribution and is used for research purposes only and many of its capabilities have been incorporated into GSSHA (Johnson and Gerald 2006; Billy Johnson, personal communication, April 17, 2008).

Since the GSSHA model shares the TREX-SMA model presented in this dissertation, it is useful to observe its continued development, which is well summarized by Downer and Ogden (2004). Ogden and Saghafian (1997) developed the Green and Ampt with Redistribution (GAR) technique to account for dissipation of the wetting front pulse and consequent changes in Green and Ampt infiltration rates during short rainfall hiatuses within a single storm. The GAR technique was applied by Senarath et al. (2000) for continuous simulation. This simulation did not account for infiltrated water as a source of baseflow and the soil moisture recovery between events was only from evapotranspiration. At the beginning of the next storm, the quantity of soil water storage remaining after evapotranspiration was used to re-initialize the Green and Ampt infiltration antecedent moisture parameter (Senarath et al. 2000). Explicit modeling of the sub-surface flow may also be performed with GSSHA, though not fully coupled with the surface flow.

At CSU, simultaneous with the ERDC-led development, progress has been made with the transport aspects of the CASC2D-SED model. Velleux added a contaminant transport algorithm and with capability to model multi-phase transport and fate of metals (Velleux 2005). The new code, now called TREX, was demonstrated by computing transport of Zn, Cu and Cd from mining areas at California Gulch, Colorado. Velleux also added capabilities to use Gridded Radar Rainfall precipitation from the NEXRAD/WSR88D radar network (Velleux et al. 2008b). Prior to the current development, TREX and CASC2D did not account for any return flows and were not suitable for multi-event simulation. The capabilities of the CASC2D family of models are summarized in Table 2.2.

**Table 2.3: Hydrologic process models implemented in the CASC2D-SED derivative models.**

| Process/Model Component | CASC2D[†] | GSSHA | TREX |
|---|---|---|---|
| Precipitation Distribution | Theissen, inverse distance square weighted | Same + Radar rainfall, GIS rainfall via WMS. | Theissen, inverse distance square weighted, stochastic storms, gridded radar |
| Snowfall accumulation and melting | N/A | Energy balance | Degree days method |
| Precipitation interception | Two parameter | Same | Same |
| Overland water retention | Specified depth | Same | Same |
| Infiltration | G&A, multilayer G&A, GAR | G&A, multilayer G&A, GAR, RE | G&A, |
| Overland flow routing | 2D diffusive wave: Explicit | 2D diffusive wave: Explicit, ADE, and ADEPC | 2D diffusive wave: ADE |
| Channel routing | 1D diffusive wave: Upstream explicit<br>1D full dynamic: Preissmann | 1D up-gradient explicit diffusive wave | 1D diffusive wave: Upstream explicit<br>- |
| Evapotranspiration | Deardorff, Penman-Monteith | Deardorff, Penman-Monteith with seasonal canopy resistance | User entered PET[*] |
| Soil moisture in vadose zone[*] | Bucket | Bucket, RE | Bucket[*] |
| Lateral groundwater flow | N/A | 2D vertically averaged | Conceptual[*] |
| *Stream/groundwater interaction | N/A | Darcy's law | 1-way return from SMA zones[*] |
| Exfiltration | N/A | Darcy's law | N/A |

Note: Processes and approximation techniques in the CASC2D and GSSHA models G&A = Green and Ampt (1911); GAR=Green and Ampt with Redistribution (Ogden and Saghafian 1997); RE=Richard's equation (1931); ADE=alternating direction explicit; ADEPC=alternating directions explicit with prediction correction.
[†]CASC2D refers to version 1.18b, also known as CASC2D for WMS
[*]TREX model as TREX-SMA

The TREX code may be obtained freely from the project website www.engr.colostate.edu/trex, and developers with an interest in contributing to the project may do so by requesting permission to access the source code repository.

### *2.8.2 TREX Conceptual Model*

Watershed hydrology is "based on the analysis of flow pathways in the surface and subsurface domains" (Aral and Gunduz 2006). Flow pathways represented in TREX include: 1) precipitation/interception; 2) infiltration and transmission loss; 3) depression storage; and 4) overland and channel flow (see Figure 2.3).

The equations used to represent these pathways in TREX are described in section 3.2.

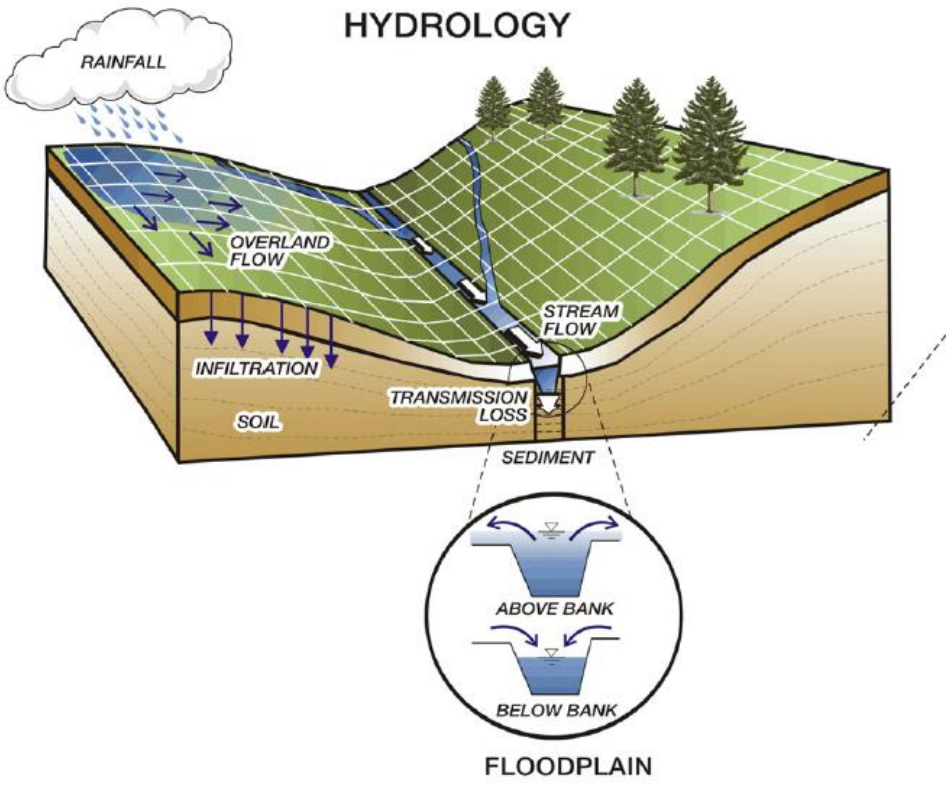


**Figure 2.3: Schematic of TREX hydrology processes (from Velleux et al. 2008a).**

### *2.8.3 SAC-SMA Development History*

The Sacramento Soil Moisture Accounting model (SAC-SMA) is part of the National Weather Service River Forecast System (NWSRFS), which is considered the standard in flood forecasting models for the United States (Singh and Woolhiser 2002). Although a number of rainfall-runoff models are available within the NWSRFS, SAC-SMA is the primary model used for river elevation and water supply forecasts. The SAC-SMA code is one of many descendants from the Stanford Watershed Model (Singh and Frevert 2006).

Research by the national weather service during recent years has focused on producing estimates of the SAC-SMA parameter values from known soil properties and remotely sensed data. These a priori estimates of the model parameters allow for uncalibrated simulation of watershed scale rainfall-runoff response with distributed versions of the SAC-SMA model (Anderson et al. 2006; Koren et al. 2003, 2004; Smith et al. 2004).

### *2.8.4 SAC-SMA conceptual model: bucket-style conceptual subterranean flow*

In contrast to the highly discretized process representation provided by the TREX model, the SAC-SMA model conceptualizes the watershed as an abstracted soil column divided vertically into two storage zones which are filled and emptied to simulate infiltration, percolation, baseflow, and interflow through the watershed. The upper and lower zones represent the infiltration capacity of shallow soils and the underlying aquifer, respectively.

Runoff is computed as the net excess volume remaining from precipitation after interception and infiltration have been satisfied. Rates of infiltration and water holding capacities of the zones are represented with conceptual parameters which, while not directly physical, correspond closely to physical values such as void space ratio and saturated hydraulic conductivities (Burnash and Ferral 2002).

An excerpt from Smith et al. (2003) describes the model process:

> Basically, the SAC-SMA is a two layer conceptual model of a soil column, with several modifications to account for the spatial variability of certain processes. Six types of runoff can be generated to form a complete runoff hydrograph. Each of the two layers in the SAC-SMA contains a tension water and free water component. Rain falling on the soil column first encounters the upper zone. Here, rain falling on any impervious areas generates impervious area runoff, while rain falling on the non-impervious areas of the basin first encounters the upper tension water storage. After filling this reservoir, excess soil water enters the upper zone free water. Water in this free water storage can percolate into the lower zone storages or flow out as interflow. If the upper zone free water fills completely, then excess soil water flows out as surface runoff. Most percolated water flows into the lower zone tension water storage, although some can go directly to free water storages in the lower zone. Upon filling the lower zone tension water storage, all soil water moves into the two lower zone free water storages. These two free water storages generate fast and slow responding base flow. The combination of these two base flows is designed to model a variety of hydrograph recessions.

The authors of the Sacramento model conceived it as "an attempt to parameterize soil moisture characteristics in a manner that would:

- logically distribute applied moisture in various depths and energy states in the soil
- have rational percolation characteristics
- allow an effective simulation of streamflow" (Burnash and Ferral 2002).

Figure 2.4 shows a schematic of processes represented by the SAC-SMA model.

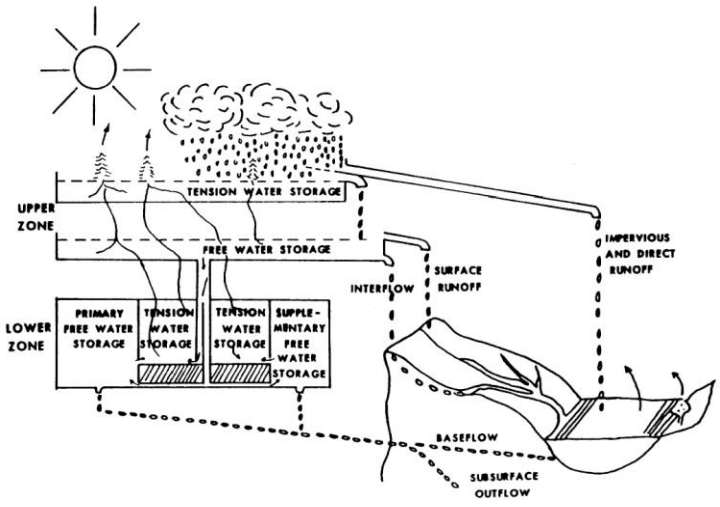


**Figure 2.4: Schematic of SAC-SMA model processes (Burnash and Ferral 2002).**

The conceptualization of finite volumes filling, draining, and spilling like a collection of interconnected buckets, gives rise to the SAC-SMA model's designation as a "bucket" model. Various parameters govern the rate of filling and spilling as well as the distribution of water in the various upper and lower zone buckets. Although not physical parameters themselves, the Sacramento model parameters can be estimated a priori using the assumption that plant extractable soil moisture is related to tension water, and that free water storages relate to gravitational soil water (Koren et al. 2000). Using the ranges of soil properties such as saturated moisture content $\theta_s$, field capacity $\theta_{fld}$, and wilting point $\theta_{wp}$ defined in the SSURGO dataset, and based on calibration experience, Anderson et al. (2006) developed a range of acceptable values for 11 of the SAC-SMA parameters as shown in Table 2.3.

**Table 2.4: SAC-SMA parameters and their feasible ranges (Anderson et al. 2006).**

| No. | Parameter | Description | Ranges |
|---|---|---|---|
| 1 | ***UZTWM*** | The upper layer tension water capacity, mm | 10–300 |
| 2 | ***UZFWM*** | The upper layer free water capacity, mm | 5–150 |
| 3 | ***UZK*** | Interflow depletion rate from the upper layer free water storage, $day^{-1}$ | 0.10–0.75 |
| 4 | ***ZPERC*** | Ratio of maximum and minimum percolation rates | 5–350 |
| 5 | ***REXP*** | Shape parameter of the percolation curve | 1–5 |
| 6 | ***LZTWM*** | The lower layer tension water capacity, mm | 10–500 |
| 7 | ***LZFSM*** | The lower layer supplemental free water capacity, mm | 5–400 |
| 8 | ***LZFPM*** | The lower layer primary free water capacity, mm | 10–1000 |
| 9 | ***LZSK*** | Depletion rate of the lower layer supplemental free water storage, $day^{-1}$ | 0.01–0.35 |
| 10 | ***LZPK*** | Depletion rate of the lower layer primary free water storage, $day^{-1}$ | 0.001–0.05 |
| 11 | ***PFREE*** | Percolation fraction that goes directly to the lower layer free water storages | 0.0–0.8 |
| 12 | *PCTIM* | Permanent impervious area fraction | Not estimated |
| 13 | ADIMP | Maximum fraction of an additional impervious area due to saturation | Not estimated |
| 14 | RIVA | Riparian vegetarian area fraction | Not estimated |
| 15 | SIDE | Ratio of deep percolation from lower layer free water storages | Not estimated |
| 16 | RSERV | Fraction of lower layer free water not transferable to lower layer tension water | Not estimated |

The model has a single outlet to which all water is routed, unless it is lost through evaporation or to deep groundwater. The SAC-SMA procedure is usually performed with a

number of cascading watersheds connected to form a larger river basin with routing between the watershed outlets performed using unit hydrograph or Muskingum routing techniques.

# 3.0 TREX-SMA: PROCESS AND ALGORITHM

With TREX hybridized to the SAC-SMA conceptual soil moisture accounting model, TREX-SMA has three primary layers: the TREX *surface*, the SAC-SMA *upper zone*, and the SAC-SMA *lower zone* (see Figure 3.1).

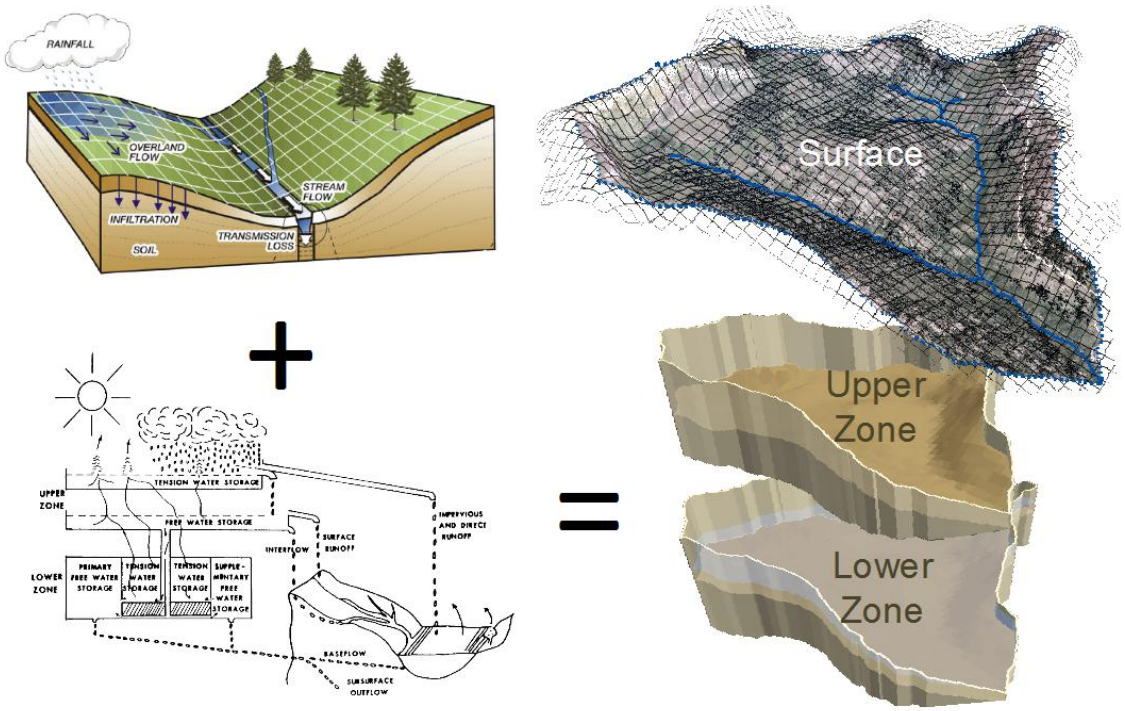


**Figure 3.1: TREX-SMA—Three-layer hybrid with TREX surface and SAC-SMA upper and lower zones.**

## 3.1 HYBRID MODEL APPROACH

The hybrid model essentially preserves the function of TREX model for simulation of surface processes—precipitation excess is routed across the surface as runoff and when it arrives at a channel, it is conducted to a domain outlet. Infiltration rates are computed according to the Green and Ampt equation and the infiltrated volume is removed from the surface domain. Once the Green and Ampt infiltration leaves the surface, it becomes input to the soil moisture accounting procedure.

Within the soil moisture accounting procedure, the volume (or depth) of water in the soil column is divided into several simple zones representing bound and free-flowing water in both the near-surface and deeper soil horizons. Evapotranspiration is extracted from the near surface zones and from the deep bound water. Free water moves to bound water zones when the latter is depleted. Free-flowing water in the upper horizon flows into the lower horizon according to a percolation function.

Since the TREX formulation uses the diffusive wave approximation for both overland and channel flow, the momentum of infiltrating and returning water is neglected. In order to prevent instability, the SMA return flows should be distributed across several cells to prevent artificial mounding.

At present, the TREX SMA model only allows one-way flow—down from the surface, into the SMA zones, and back into the channel. This is appropriate for high gradient watersheds where any saturation excess flow is localized and where the phreatic surface is not likely to intersect the ground surface. The TREX SMA model as presently constituted could simulate Dunne, or Saturation Excess runoff, with the addition of an approximation technique for disaggregating the soil moisture from a regional zone value to gridded values such as is described by Perry and Niemann (2007).

## 3.2 SURFACE PROCESSES

As already noted, the surface processes of TREX remain largely unchanged. In the TREX-SMA hybrid, the infiltration procedure provides the input to the SMA Upper Zone and channel inflow computations provide and outlet for the drainage for those zones. In the present formulation, a simple constant potential evapotranspiration rate is applied across the model.

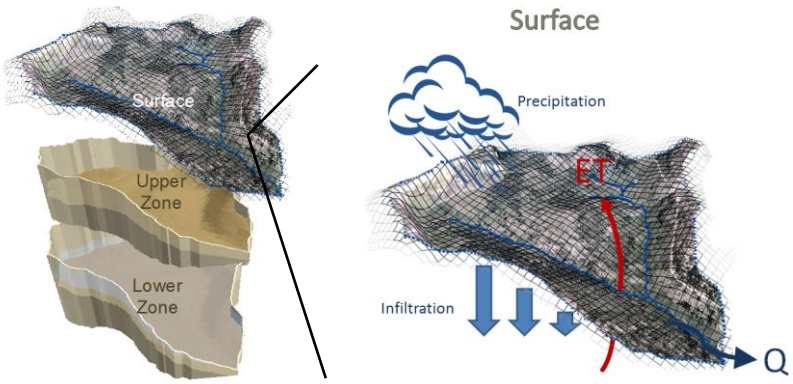


**Figure 3.2: TREX-SMA—TREX surface processes.**

### *3.2.1 Rainfall and interception*

The first pathway of the hydrologic cycle described in TREX is that of liquid precipitation reaching surface of the land or water. Interception is removed as a volume directly from the precipitation volume. The rate of water reaching the near surface is:

$$\frac{\partial V_g}{\partial t} = i_g A_s \qquad \text{(Eq. 3.1)}$$

Where: $V_g$ = gross precipitation water volume [$L^3$]

$i_g$ = gross precipitation rate [L/T]

$A_s$ = surface area over which precipitation occurs [$L^2$]

$t$ = time [T]

TREX uses a linearly interpolated precipitation function to represent point gauge intensities; and, if multiple gauges are available, an inverse distance weighted function is applied to compute rainfall intensities at points between the gauges. Precipitation reaching the ground surface is reduced by interception—capture of precipitation on the surfaces of plants, and other objects. The volume of interception is subtracted from the precipitation volume to obtain net precipitation volume. When interception capacity exceeds rainfall volume, the net precipitation is computed as zero.

$$V_i = S_i + E \cdot t_R A_s \quad \text{(Eq. 3.2)}$$

$$\begin{array}{ll} V_n = V_g - V_i & \text{for:} V_g > V_i \\ V_n = 0 & \text{for:} V_g \leq V_i \end{array} \quad \text{(Eq. 3.3)}$$

Where: $V_i$ = interception volume [$L^3$]

$S_i$ = interception capacity of projected canopy per unit area [$L^3/L^2$]

$E$ = evaporation rate [L/T]

$t_R$ = precipitation event duration [T]

$V_n$ = net precipitation volume reaching the surface [$L^3$]

In TREX, the net precipitation volume is expressed as a unit flow rate by multiplying by cell area and dividing by the time step length:

$$i_e = \frac{1}{A_s} \cdot \frac{V_n}{\Delta t} \quad \text{(Eq. 3.4)}$$

Where: $i_n$ = net (effective) rainfall rate at the surface [L/T]

$\Delta t$ = time step [T]

### *3.2.2 Green and Ampt infiltration*

The Green and Ampt (1911) equation models infiltration as a step or "piston" wetting front which penetrates downward into an infinite soil horizon according to soil moisture deficit, capillary suction head, and saturated hydraulic conductivity as diagrammed in Figure 3.3. As noted in the figure, runoff is computed as the excess volume after infiltration is removed from the net rainfall. The head due to depth of ponding is ignored in the Green and Ampt equation as formulated in TREX-SMA, as given by Julien et al. (1995):

$$f = K_h \cdot 1 + \frac{H_c \cdot M_d}{F} \quad \text{(Eq. 3.5)}$$

Where $f$ = infiltration rate [L/T]

$K_h$ = saturated hydraulic conductivity [L/T]

$H_c$ = capillary pressure head at the wetting front [L]

$M_d$ = soil moisture deficit [dimensionless]

$F$ = total infiltrated depth [L]

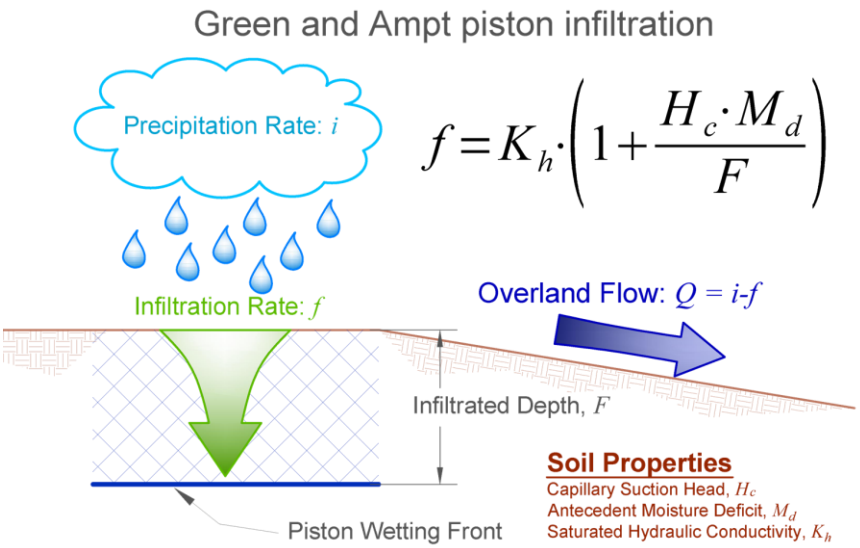


**Figure 3.3: Schematic of Green and Ampt piston wetting front. Note that total overland flow volume rate is the result of subtracting infiltration rate (and any other abstraction) from the rainfall rate multiplied by the area affected by the precipitation.**

Moisture deficit may be written in terms of porosity and saturation as:

$$\begin{aligned} M_d &= (\theta_e - \theta_i) \\ \theta_e &= (\varphi - \theta_r) \end{aligned} \qquad \text{(Eq. 3.6)}$$

$\theta_i$, $\theta_r$ = initial and residual saturation, respectively [dimensionless]

$\theta_e$, $\phi$ = effective and total soil porosity, respectively [dimensionless]

In the TREX-SMA model, the Moisture deficit is computed from the degree of initial saturation, $S_e$, given as the ratio of initial saturation and effective porosity:

$$\begin{aligned} M_d &= (1 - S_e) \cdot \theta_e \\ S_e &= \frac{\theta_i}{\theta_e} \end{aligned} \qquad \text{(Eq. 3.7)}$$

The Green and Ampt equation in CASC2D-TREX is solved for the middle of the time step, $\Delta t$, to produce the following equation.

$$f = \frac{p_1 + \sqrt{p_1{}^2 + 8 \cdot p_2 \cdot \Delta t}}{2.0 \cdot \Delta t} \qquad \text{(Eq. 3.8)}$$

Where $p_1$ and $p_2$ are solution parameters as given by Velleux (2005):

$$\begin{aligned} p_1 &= K_h \cdot \Delta t - 2.0 \cdot F \\ p_2 &= K_h \cdot (F + H_c \cdot M_d) \end{aligned} \qquad \text{(Eq. 3.9)}$$

With $F$, $K_h$, $\Delta t$, $M_d$, and $H_c$ defined as above with Equations 3.5 through 3.7.

Transmission loss in channels is modeled identically with the exception that infiltration head due to ponded depth is not neglected and is summed with the capillary suction head for a total driving head as given below (Abdulrazzak and Morel-Seytoux 1983; Freyberg 1983).

$$f = K_h \cdot 1 + \frac{(H_w + H_c) \cdot M_d}{T} \qquad \text{(Eq. 3.10)}$$

$H_w$ = hydrostatic pressure head of water [L]

$T$ = total depth of transmission losses [L]

The Green and Ampt equation determines the maximum rate of water entering the subsurface domain and gives a depth of new infiltration in each cell for each time step. Infiltration depths are summed across the cells belonging to a particular upper zone and an average is computed as the primary input for the soil moisture code. Flux between the surface water model and the TREX-SMA model requires unit conversion from units of meters depth to an average depth in millimeters across the upper zone.

### *3.2.3 Storage and point abstraction*

As runoff begins to occur, some of the precipitation excess will be retained in small discontinuous depressions in the land surface. A similar process can retain water in local low

areas in channels. The retained water volume is referred to as depression storage on the land surface and dead storage when it occurs in channels. Dead and depression storage is always subject to infiltration and evaporation, but the evaporation may be neglected for a single event. Depression storage acts functionally as a simple abstraction from the volume of water running off of the land surface. For multiple events, dead and depression storage remaining from previous events will contribute to more rapid runoff response in the watershed. Point abstractions from the surface and from channels are simulated as time dependent volumetric flow rates.

### *3.2.4 Diffusive wave overland and channel flow*

CASC2D set itself apart from other watershed models in 1980 by explicitly modeling the flow of water from cell to cell on a distributed DEM grid. The CASC2D model family (including TREX-SMA) uses a diffusive wave approximation of the Saint Venant equation to estimate the energy grade line or friction slope (Sf) for modeling both overland and channel flow. The diffusive wave approximation considers flow generated by differences in head due to depth, as well as slope, and so allows for flow on adverse slopes. Manning roughness derived from land cover and soil type is used to determine flow resistance and energy slope.

The diffusive wave approximation neglects the local and convective acceleration terms of the Saint-Venant equations. An error term describing the difference between the full dynamic solution and the diffusive approximation for channel flow is given by Lettenmaier and Wood (1993):

$$E \propto \frac{{q_p}^{0.4}}{T_r \cdot {S_0}^{0.7}} \qquad \text{(Eq. 3.11)}$$

Where $T_r$ = Time of rise

$S_0$ = channel bottom slope

And $q_p$ = unit width peak discharge

If the discharge is too great or if the time of rise and slope product is too small, then the error in the diffusive approximation becomes large. Otherwise, the approximation may be used with confidence. This approximation is appropriate as long as the neglected terms (convective acceleration and momentum change due to unsteady flow) are small relative to the remaining terms (bed slope, water surface slope). Lettenmaier and Wood (1993) identify four conditions where this may not be the case and where a dynamic wave solution would be necessary:

1) upstream wave propagation such as from tidal action or storm surges

2) backwater effects caused by downstream reservoirs or tributary flows

3) rivers with extremely flat bottom slopes, e.g., $S0 < 0.0005$

4) abrupt waves caused by rapid reservoir releases or dam failures

At California Gulch, none of these criteria are of concern except possibly the potential for a dam failure. With the average slope of 12.5%, the error term given as Eq. 3.11 can be expected to be no larger than 10%, even for the over-simulated flow of 120 cfs from the first storm in the multi-event simulation.

In addition to channel flow, Richardson and Julien (1994) use a similar derivation to confirm that neglected terms of the St. Venant equation are insignificant and that the diffusive approximation is appropriate for most cases of sub-critical overland flow.

Ogden and Julien (1993) and later Molnár and Julien (2000) point out that spatial and temporal distribution of rainfall and grid scale may be expected to affect the behavior of the hydrograph far more than effects of applying the diffusive wave approximation to compute flow. However, based on their conclusions, the 30m grid spacing used at California Gulch is adequate to prevent grid scale effects from influencing the results from this research.

The two-dimensional continuity equation in partial differential form is

$$\frac{\partial h}{\partial t} + \frac{\partial q_x}{\partial x} + \frac{\partial q_y}{\partial y} = i_e \qquad \text{(Eq. 3.12)}$$

Where: $i_e$ = net rainfall excess [L/T]

$\frac{\partial h}{\partial t}$ = change in depth with respect to time [L/T]

$\frac{\partial q_y}{\partial y}, \frac{\partial q_x}{\partial x}$ = partial derivatives of planar components of the unit flow (volumetric flow divided by width) with respect to their corresponding flow directions [L/T]

The solution scheme for overland and channel water depth in TREX is the second order modified Euler scheme (a.k.a. the midpoint method), which uses the current depth plus an approximate first derivative of the state derived from the prior time step to predict the next time step state. The method uses the unit flow computed from the Manning formulation to predict the depth of water in a model cell in the next time step as detailed in Julien et al. (1995).

$$h^{t+\Delta t}(j,k) = h^{t}(j,k) + \Delta t \cdot i_e - \left[\frac{q_x^t(k \rightarrow k+1) - q_x^t(k-1 \rightarrow k)}{W} + \frac{q_y^t(j \rightarrow j+1) - q_y^t(j-1 \rightarrow j)}{W}\right] \cdot \Delta t \qquad \text{(Eq. 3.13)}$$

Where $h^{t+\Delta t}(j,k)$ = Depth of at cell (j,k) in next time step

$h^t(j,k)$ = current time step water depth

$\Delta t$ = time step

$i_e$ = net rate of infiltration excess runoff production

$q_x^t(k \rightarrow k+1)$; $q_x^t(k-1 \rightarrow k)$ = unit outflow and inflow in x direction

$q_y^t(j \rightarrow j+1)$; $q_y^{tj}(j-1 \rightarrow j)$ = unit outflow and inflow in y direction

And W = cell width

The midpoint method is a common solution for solving simple Ordinary Differential Equations (O.D.E.s) and may be found in any numerical methods textbook (e.g., Cheney and

Kincaid 1999, p. 407) and it is known to be unconditionally stable as long as the forward step size satisfies the Friedrichs-Lewy (CFL) condition (Alexiades et al. 1996; Courant et al. 1928). The specific CFL function is dependent on approximated function; for TREX, the forward time step is limited by the following:

$$\Delta t < \frac{\Delta x}{V} \qquad \text{(Eq. 3.14)}$$

Where $\Delta t$ = time step

$\Delta x$ = grid cell size

And $V$ = flow velocity

For the 30-meter gridded domain used at California Gulch with time steps on the order of one second during the peak hydrograph periods, the maximum velocity which can be expected to be stably simulated is about 30 meters per second, well above any velocity encountered in the model.

Conservation of momentum is described in TREX by the diffusive wave approximation of the Saint Venant equations.

$$S_{fx} = S_{0x} - \frac{\partial h}{\partial x} \qquad \text{(Eq. 3.15)}$$

$$S_{fy} = S_{0y} - \frac{\partial h}{\partial y} \qquad \text{(Eq. 3.16)}$$

Where: $S_{fx}$, $S_{fy}$ = friction slope in each of x and y directions [dimensionless]

$S_{0x}$, $S_{0y}$ = change in depth with respect to time [dimensionless]

$\frac{\partial h}{\partial x}, \frac{\partial h}{\partial x}$ = partial derivatives of depth with respect to their corresponding flow directions [L/L]

Flow in two directions is defined using the Manning formulation:

$$q_x = \alpha_x h^{\beta} \qquad \text{(Eq. 3.17)}$$

$$q_y = \alpha_y h^{\beta} \quad \text{(Eq. 3.18)}$$

$$\alpha_x = \frac{{S_{fx}}^{1/2}}{n} \quad \text{(Eq. 3.19)}$$

$$\alpha_y = \frac{{S_{fy}}^{1/2}}{n} \quad \text{(Eq. 3.20)}$$

Where: $\alpha_x$, $\alpha_y$ = resistance coefficient in the x- or y-direction [$L^{1/3}/T$]

$\beta$ = resistance exponent = 5/3 [dimensionless]

$n$ = Manning roughness coefficient [$T/L^{1/3}$]

Channel flow is computed using one-dimensional formulations of the continuity equation and Manning equation along with the one-dimensional diffusive wave approximation of the Saint Venant equation. The one-dimensional (laterally and vertically integrated) continuity equation for gradually varied flow is:

$$\frac{\partial A_c}{\partial t} + \frac{\partial Q}{\partial x} = q_l \quad \text{(Eq. 3.21)}$$

Where: $A_c$ = cross sectional area of flow [$L^2$]

$Q$ = total discharge [$L^3/T$]

$q_l$ = unit lateral inflow [$L^2/T$]

Point inflows or extractions such as water treatment plant discharges, springs, or irrigation diversions may be normalized by width and added (or subtracted) from the unit lateral inflow source term.

### *3.2.5 Sediment and contaminant transport*

The TREX model has robust sediment and contaminant transport capabilities. Only advective sediment transport processes are computed for both the channel and overland plane; dispersion and diffusion are neglected. Chemicals may be transported, dissolved in water, or bound to a

sediment particle. Computations of erosion and deposition alter the elevation of a given cell and thereby affect the hydraulics. The sediment and contaminant transport features of TREX are not used in this study.

## 3.3 SMA UPPER ZONE

Infiltrated water enters the subsurface domain via the upper soil moisture zone. Water is distributed between the two divisions in the upper zone: the bound water portion (tension water) and the free-flowing portion (free water). Abstractions from the upper zone include evaporation, transpiration, percolation losses to the lower zone, and return flow releases to the surface, as shown in Figure 3.4.

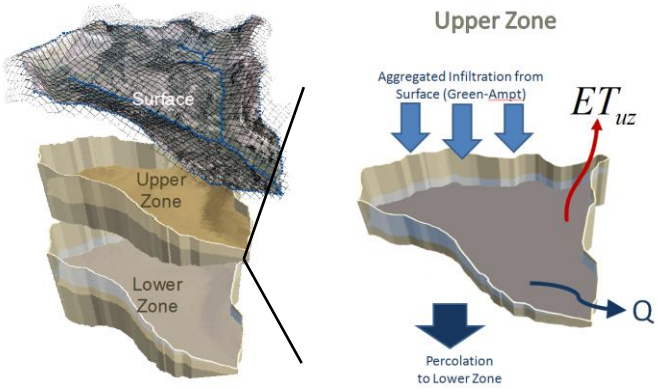


Figure 3.4: TREX-SMA—SAC-SMA upper zone.

### *3.3.1 Evaporation and Transpiration*

Central to the mass balance in the inter-storm periods, ET abstraction is removed first from the bound pore water volumes in the model. TREX-SMA currently uses a single constant ET demand for the entire simulation and uniform across the model domain. Any distribution of ET computed from any model could theoretically be used as input since the model aggregates the demand from all cells to compute a total ET for each upper zone.

ET is first removed from upper zone tension water according to the equation:

$$ET_{actual,uz} = ET_{demand} \cdot \frac{Fw_{c,uz}}{Fw_{m,uz}} \quad \text{(Eq. 3.22)}$$

Where: $ET_{demand}$ = accumulated ET demand for the upper zone for the time step [L]

$ET_{actual,\,uz}$ = amount of demand removed from the upper zone [L]

$Fw_{c,uz}$ = upper zone free water current storage [L]

$Fw_{m,uz}$ = upper zone free water capacity [L]

If the scaled demand is greater than the amount available in the upper zone tension water storage volume, the additional demand is subtracted from the lower zone tension water storage and upper zone free water storage. Lower zone free water is not consumed by evapotranspiration.

### *3.3.2 Redistribution*

In addition to gravity driven percolation, water in the physical soil column is influenced by capillary forces which drive water movement toward dry soils with a high capillary potential. The tension water zone represents this capillary soil storage and following the subtraction of evapotranspiration losses, a balancing equation transfers excess free water to the tension volume. The transfer occurs when the storage ratio of the tension water is less than the storage ratio of free water:

$$\frac{Tw_{c,uz}}{Tw_{m,uz}} < \frac{Fw_{c,uz}}{Fw_{m,uz}} \quad \text{(Eq. 3.23)}$$

The redistribution computation exchanges water between the free water and tension water storage until the free and tension water ratios (the current volume divided by maximum storage) are equal. A similar computation balances the water in the lower zone if evaporation demand is sufficiently high. For the lower zone, the redistribution occurs if the tension water storage ratio is less that the total lower zone storage ratio:

$$\frac{Tw_{c,lz}}{Tw_{m,lz}} < \frac{Fw_{c,lz}+Tw_{c,lz}}{Fw_{m,lz}+Tw_{m,lz}} \quad \text{(Eq. 3.24)}$$

The assumption is that if for any reason the free water storage contains significantly more volume than the tension water, then free water will resupply the tension water. This could happen if the tension water capacity is small relative to the free water capacity, and the evaporation is high. This assumption is consistent with the overarching assumption in the Sacramento model that tension water volumes are always satisfied first before any other volumes.

### *3.3.3 Interflow*

In each time step, upper zone free water storage volumes release to the surface a portion of their water as interflow[1]. Interflow is computed based on a simple rate equation.

$$V_{intf} = k_{uz,eff} \cdot Fw_{c,uz} \qquad \text{(Eq. 3.25)}$$

Where: $V_{intf}$ = baseflow unit volume for the time step (L)

$Fw_{c,uz}$ = current unit volume of upper zone free water (L)

$k_{uz,eff}$ = effective upper zone free water storage depletion coefficient (dimensionless)

The effective depletion coefficient is obtained by multiplying the standard depletion coefficient by the time step.

$$k_{uz,eff} = k_{uz} \cdot \Delta t \qquad \text{(Eq. 3.26)}$$

Where: $k_{uz}$ = standard upper zone free water storage depletion coefficient $\left[\frac{L}{L \cdot T}\right]$

$\Delta t$ = current model time step (T)

The upper zone storage depletion coefficient defines the flow released per volume of stored water in the zone, normalized by the area of the model contributing to the given zone. The

[1]Interflow is an upper zone process so it is described here, however, it is actually computed following satisfying demand for percolation from the lower zones.

internal units of the soil moisture accounting procedure are a one-dimensional-length, millimeters, so the outgoing flow is scaled by the upper zone area. As used in the Sacramento Model implemented in NWSRFS, the standard upper zone depletion coefficient is calibrated in units of millimeters released per millimeters stored per day. In order to use the same parameter ranges, the TREX-SMA model uses a conversion factor to account for different time steps, which gives an equation with units as follows:

$$V_{intf} = k_{uz} \cdot \Delta t \cdot Fw_{c,uz} \cdot Area \cdot conversionfactors \qquad \text{(Eq. 3.27)}$$

Or, written to emphasize the units:

$$V_{intf} = k_{uz,eff} \cdot \Delta t \cdot Fw_{c,uz} \cdot Area \cdot conversionfactors$$
$$[m^3] = \left[\frac{mm}{mm \cdot day}\right] \cdot [seconds] \cdot [mm] \cdot [m^2] \cdot \frac{meter}{1000mm} \cdot \left[\frac{1day}{86400seconds}\right] \text{(Eq. 3.28)}$$

Similar scaling is required to obtain an effective storage depletion coefficient for the lower zone free water storage depletion coefficients, taking into consideration the time step and also scaling from the NWSRFS parameter range to that used in TREX-SMA.

### *3.3.4 Saturation excess rejection*

If the upper zone tension and free water storage volumes are full, conceptually, this would mean that the TREX-SMA algorithm has several options that do not permit further entry of infiltrated water. Infiltration is set to zero, and excess water is distributed back into the overland flow domain, the total amount returned being scaled by the infiltration contribution of each cell.

## 3.4 SMA Lower Zone

Water drains into the lower zone via percolation. Losses from the lower zone include evapotranspiration and baseflow, as shown in Figure 3.5.

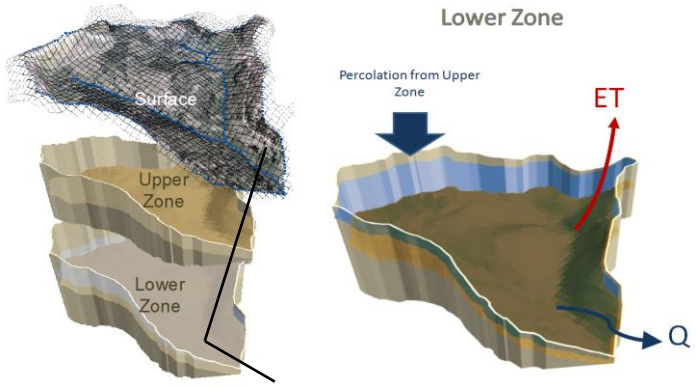


**Figure 3.5: TREX-SMA—SAC-SMA lower zone.**

### *3.4.1 Percolation*

Water is transferred from the upper zones to the lower zones via the percolation computation. The percolation demand is computed as a demand in millimeters per day. A conversion is applied to determine the effective demand for the relatively small time steps occurring in the TREX-SMA model. Lower zone percolation demand is computed using the equation

$$Perc_{demand} = Perc_{base} \cdot \left[1 + zperc \cdot \frac{a^{rexp}}{b}\right] \qquad \text{(Eq. 3.29)}$$

Where: $Perc_{demand}$ = percolation demand [L/T]

$Perc_{base}$ = base percolation rate [L/T]

*zperc* = percolation multiplier

*rexp* = wet vs. dry percolation differentiation exponent

and factors *a* and *b* define the aggregate lower zone deficiency ratio:

$$\frac{a}{b} = \frac{Tw_{m,lz} + \Sigma Fw_{m,lz} - Tw_{c,lz} + \Sigma Fw_{c,lz}}{Tw_{m,lz} + \Sigma Fw_{m,lz}} \qquad \text{(Eq. 3.30)}$$

Actual percolation is computed from the percolation demand based on the availability of upper zone free water. The percolation demand is scaled by the upper zone free water storage ratio and the total volume removed is limited by the amount in the upper zone free water current storage volume, to prevent mass balance errors.

$$Perc_{actual} = Perc_{demand,eff} \cdot \frac{Fw_{c,uz}}{Fw_{m,uz}} \leq Fw_{c,uz} \qquad \text{(Eq. 3.31)}$$

### *3.4.2 Baseflow*

Baseflow is modeled as water released to the surface from the lower zone free water storage based on a simple rate equation.

$$V_{basf} = k_{lz,eff} \cdot Fw_{c,lz} \qquad \text{(Eq. 3.32)}$$

Where: $V_{basft}$ = baseflow volume [L]

$k_{lz,\,eff}$ = Effective lower zone free water storage depletion coefficient [dimensionless]

= $k_{lz}\left[\frac{L}{L \cdot T}\right] \cdot \Delta t[T]$

The total baseflow from a particular lower zone is distributed to *n* interflow outlets using a simple user assigned partition coefficient; the sum of *n* partition coefficients must equal 1.0 to ensure mass balance.

The subterranean storage represented by the SAC-SMA zones interacts with *the* surface water model by the following: 1) receiving infiltrated water; 2) returning interflow and baseflow from the upper soil moisture zone; and 3) returning baseflow from the lower zone storage volumes. The SAC-SMA upper and lower soil moisture zones release water as point sources into the TREX channel. These volumes are treated in the channel model the same as if they were point sources from a treatment plant or spring. The rate of flow is added to the source term in the

1-D mass conservation equation (Equation 3.21) and the volume is then routed with the rest of the flow in the channel.

## 3.5 TREX-SMA ALGORITHM

The model operates once per time step in a purely explicit computation which depends only on the state of the zone storage volumes from the previous time step and evaporation and precipitation in the current time step. As the model passes through the TREX-SMA code, exchanges of water are computed between the surface and subsurface domains and internally within the subsurface domain (as described in sections 36–50, above).

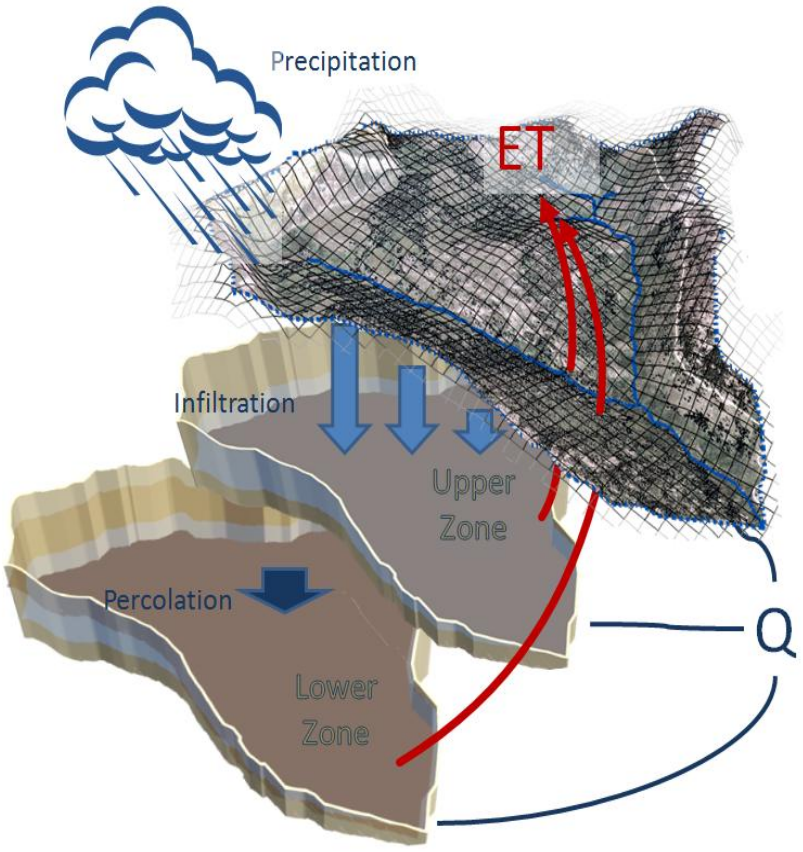


**Figure 3.6: Layer interactions in SMA-2 model.**

The following processes controlling these exchanges are listed below according to the order of computation:

- evapotranspiration—water lost due to ET processes is subtracted
- redistribution—free water storage replenishes tension water
- infiltration capture—upper zone tension water storage receives infiltration
- baseflow return—deep free water storage discharge to the surface grid
- percolation demand—lower zone free water deficiency creates percolation demand
- percolation—upper zone free water supply satisfies percolation demand
- interflow return—upper zone free water storage discharge to surface grid
- new water distribution—new volumes of precipitation, infiltration, and percolation are allocated and internally distributed
- saturation excess—rejects infiltrated water that exceeds maximum storage
- soil moisture redistribution—state of soil moisture storage volumes is used to reinitialize infiltration parameters

More details about the TREX-SMA code are found in Appendix B.

# 4.0 CALIFORNIA GULCH, COLORADO

The TREX-SMA model will be demonstrated using data from the California Gulch watershed near Leadville, Colorado. This chapter describes the data collected for the California Gulch model. During a site reconnaissance in June 2010, various photographs were taken that are reproduced in Appendix C.

## 4.1 LOCATION AND SITE DESCRIPTION

A general description of the California Gulch watershed is given by Velleux et al:

> California Gulch is part of a historical mining district located near Leadville, Colorado (USA). The site is in the headwaters of the Arkansas River basin and covers an area of 30 $km^2$…The watershed includes upper and lower reaches of California Gulch (CG), Stray Horse Gulch, Starr Ditch (SD), and several smaller drainages. (Velleux et al. 2008a)

Leadville is accessed via US Highway 24 from Copper Mountain

Due to the history of surface mine waste accumulation, the area of California Gulch was added to the USEPA National Priority List in 1983 (HDR Engineering 2002; US EPA Region 8 2010). The national priority list sites are designated as part of the Comprehensive Environmental Response, Compensation, and Liability Act (CERCLA) commonly known as Superfund (US EPA 2010).

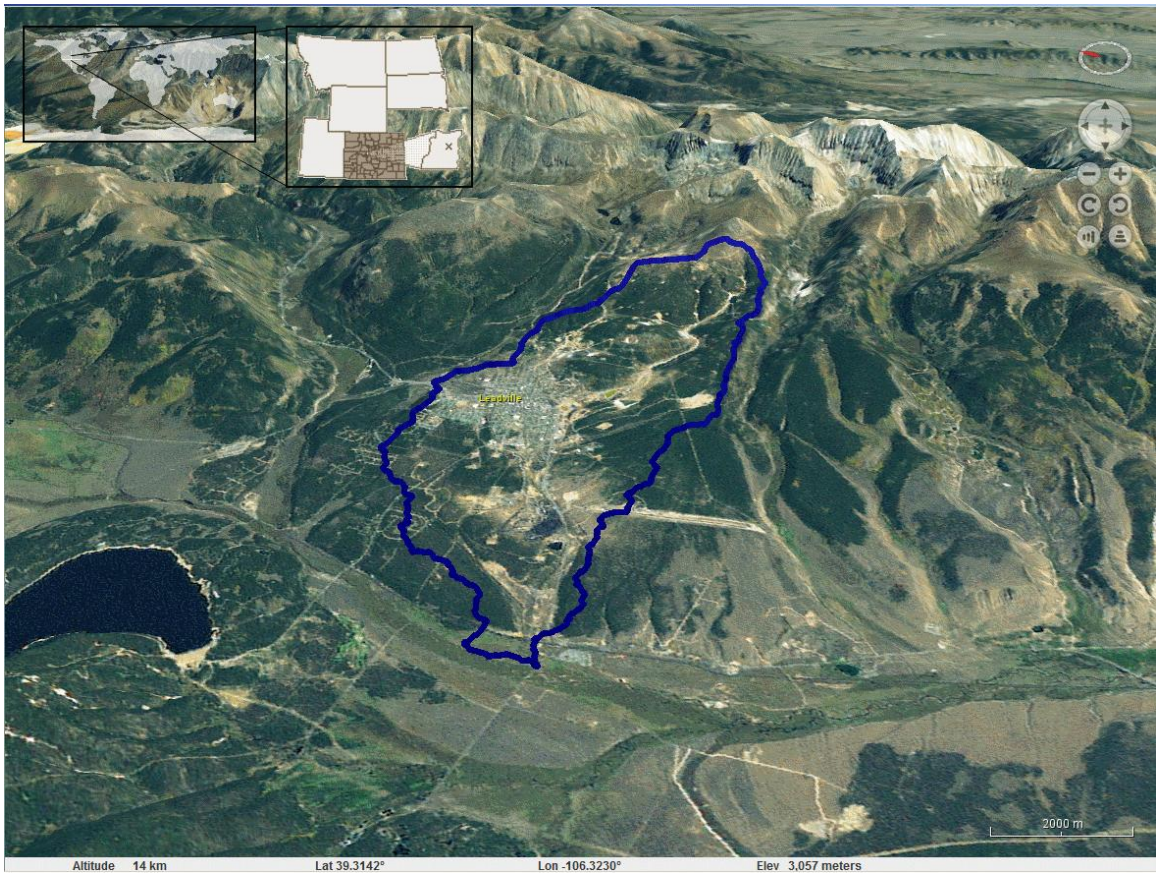


**Figure 4.1: Oblique view of the California Gulch watershed (outlined in blue) looking east by northeast. The Mosquito Range of the Continental Divide is seen in the background. The Arkansas River flows through the valley in the foreground from left to right. Images from NASA and USEPA. The vertical dimension exaggeration is 2x.**

## 4.2 ELEVATION AND TOPOGRAPHY

Elevations in the watershed range from 2900 m (9600 ft.) at the Arkansas River to 3650 m (12000 ft.) on top of Ball Mountain at the eastern boundary of the watershed. The average slope is 12.6 % (Velleux et al. 2008a). The city of Leadville, roughly in the center of the watershed, contains a small watershed divide between California Gulch and Malta Gulch with the majority of runoff from the city draining into California Gulch. The deep channel of California gulch dominates the general topography of the valley as it runs from the bedrock formations of the upper watershed down through the alluvium and glacial deposits in the lower watershed.

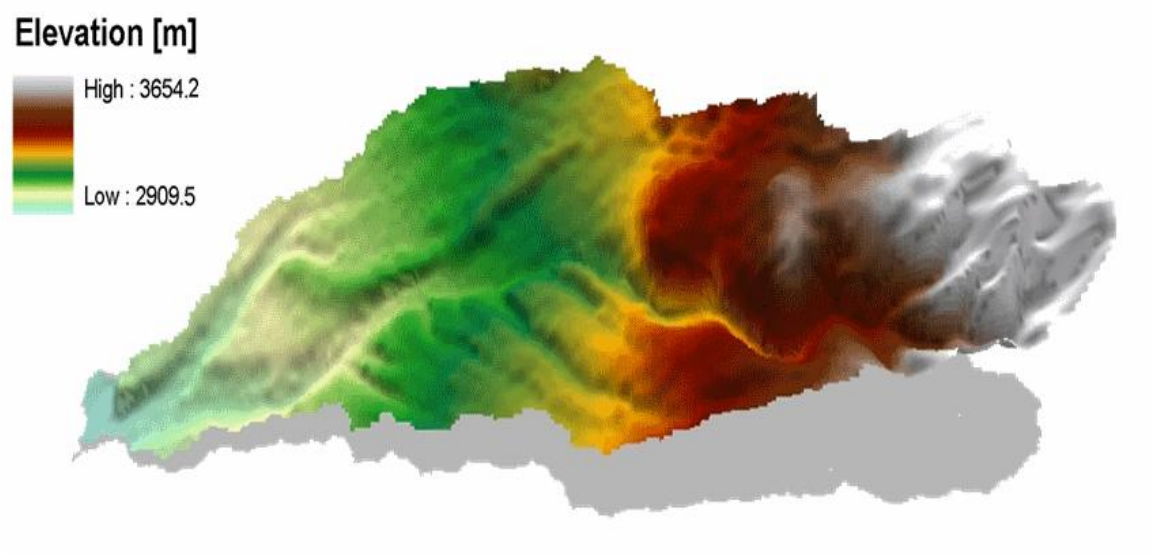


**Figure 4.2: Elevations in California Gulch watershed. Color shading indicates elevations derived from the USGS NED 30 meter resolution digital elevation model.**

The USGS 1/3rd Arc Second digital elevation model (DEM) from the National Elevation Dataset (NED) provides the basis for all topographic computations in the model. The Velleux et al. (2008a) model setup was replicated for use with the TREX-SMA simulations. The site was simulated on a 30-meter by 30-meter grid based on the nominal dimensions of the NED and the watershed area was delineated with 34,002 cells for the overland plane. All other distributed inputs were converted to the same spacing for purposes of calculation.

### 4.3 LAND USE

In the TREX-SMA model, land use classification is used to determine overland flow roughness and interception depth. The NLCD 2001 land use dataset from NASA and USGS distinguishes 13 different land use classes in the California Gulch watershed. Evergreen forest dominates the majority of the watershed except for the urban area of Leadville, and mined or otherwise industrially impacted lands which are classified as either Commercial or Bare Rock.

Figure 4.3 shows the spatial distribution of these classes and Table 4.1 presents the detailed description from the NLCD documentation.

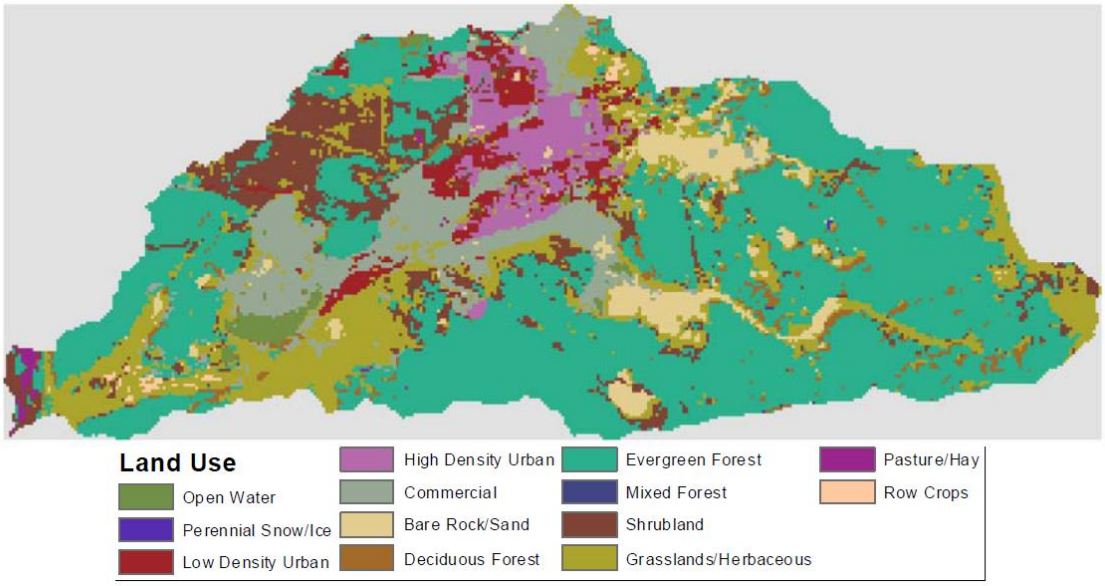


**Figure 4.3: Spatial distribution of land use classes from the NLCD 2001 dataset.**

**Table 4.1: Land use class descriptions from NLCD 2001 for California Gulch watershed.**

| Description (NLCD 2001 designation) | Manning n | Interception depth [mm] |
|---|---|---|
| Open Water (NLCD 11) (mostly misclassed: tailings ponds, treat as bare) | 0.15 | 0.00 |
| Perennial Ice/Snow (NLCD 12) | 0.15 | 0.25 |
| Low Intensity Residential (NLCD 21) | 0.08 | 0.10 |
| High Intensity Residential (NLCD 22) | 0.05 | 0.00 |
| Commercial/Industrial/Transportation (NLCD 23) | 0.15 | 0.10 |
| Bare Rock/Sand/Clay (NLCD 31) | 0.15 | 0.00 |
| Deciduous Forest (NLCD 41) | 0.45 | 0.50 |
| Evergreen Forest (NLCD 42) | 0.45 | 2.00 |
| Mixed Forest (NLCD 43) | 0.45 | 2.00 |
| Shrubland (NLCD 51) | 0.4 | 2.00 |
| Grasslands/Herbaceous (NLCD 71) | 0.3 | 1.00 |
| Pasture/Hay (NLCD 81) | 0.3 | 1.00 |
| Row Crops (NLCD 82) (misclassed in NLCD, treat as grassland) | 0.3 | 1.00 |

## 4.4 SOIL TYPE

Within the watershed, the USDA identifies 14 different soil associations. These were used along with a separate class for soils within the City of Leadville urbanized (subdivided by land use) to create a total of 17 soil classes for the model.

The characteristics ($K_h$, $H_c$, $K$, porosity, grain size distribution etc.) of each soil class were defined based on values reported in the NRCS SSURGO database as well as texture. Table 4.2 details the SSURGO soil types found in California Gulch.

# Table 4.2: Physical soil properties for soils surveyed near California Gulch

**Physical Soil Properties Chaffee-Lake Area, Colorado, Parts of Chaffee and Lake Counties**

[Entries under "Erosion Factors--T" apply to the entire profile. Entries under "Wind Erodibility Group" and "Wind Erodibility Index" apply only to the surface layer. Absence of an entry indicates that data were not estimated. This report shows only the major

| USDA map symbol and soil name | Depth | Sand | Silt | Clay | Moist bulk density | Saturated hydraulic conductivity | Available water capacity | Linear extensibility | Organic matter | Erosion factors | | | Wind erodibility group | Wind erodibility index |
|---|---|---|---|---|---|---|---|---|---|---|---|---|---|---|
| | | | | | | | | | | Kw | Kf | T | | |
| | In | Pct | Pct | Pct | g/cc | micro m/sec | In/In | Pct | Pct | | | | | |
| BrF: | | | | | | | | | | | | | | |
| Bross | 0-8 | --- | --- | 15-18 | 1.35-1.50 | 14.11-42.34 | 0.05-0.07 | 0.0-2.9 | 3.0-5.0 | .05 | .15 | 2 | 8 | 0 |
| | 8-17 | --- | --- | 7-18 | 1.35-1.50 | 14.11-42.34 | 0.05-0.07 | 0.0-2.9 | 0.5-1.0 | .10 | .28 | | | |
| | 17-24 | --- | --- | 7-18 | 1.35-1.50 | 14.11-42.34 | 0.07-0.08 | 0.0-2.9 | 0.0-0.5 | .10 | .32 | | | |
| | 24-60 | --- | --- | 7-18 | 1.35-1.50 | 14.11-42.34 | 0.03-0.04 | 0.0-2.9 | 0.0-0.5 | .05 | .32 | | | |
| GP: | | | | | | | | | | | | | | |
| Pits, gravel | 0-60 | --- | --- | 0-10 | --- | 14.11-705.00 | 0.02-0.03 | 0.0-2.9 | 0.0 | .02 | .15 | --- | 8 | 0 |
| MP: | | | | | | | | | | | | | | |
| Dumps | 0-60 | --- | --- | 0-1 | --- | 42.34-141.14 | 0.01-0.02 | 0.0-2.9 | 0.0-0.1 | --- | --- | --- | 8 | 0 |
| Mine pits | 0-60 | --- | --- | 0 | --- | --- | 0.00 | --- | --- | --- | --- | --- | 8 | 0 |
| MW: | | | | | | | | | | | | | | |
| Misc. water | --- | --- | --- | --- | --- | --- | --- | --- | --- | --- | --- | --- | --- | --- |
| NfB: | | | | | | | | | | | | | | |
| Newfork | 0-6 | --- | --- | 5-15 | 1.35-1.50 | 14.11-42.34 | 0.07-0.10 | 0.0-2.9 | 2.0-4.0 | .10 | .20 | 2 | 3 | 86 |
| | 6-12 | --- | --- | 5-15 | 1.35-1.50 | 14.11-42.34 | 0.05-0.07 | 0.0-2.9 | 0.0-1.0 | .10 | .28 | | | |
| | 12-60 | --- | --- | 0-5 | 1.45-1.60 | 141.14-705.00 | 0.03-0.04 | 0.0-2.9 | 0.0-0.5 | .05 | .20 | | | |
| PgD: | | | | | | | | | | | | | | |
| Pierian | 0-5 | --- | --- | 5-10 | 1.35-1.50 | 14.11-42.34 | 0.07-0.10 | 0.0-2.9 | 2.0-4.0 | .10 | .20 | 2 | 3 | 86 |
| | 5-9 | --- | --- | 5-10 | 1.35-1.50 | 14.11-42.34 | 0.07-0.10 | 0.0-2.9 | 0.0-1.0 | .15 | .28 | | | |
| | 9-60 | --- | --- | 0-5 | 1.45-1.60 | 141.14-705.00 | 0.03-0.04 | 0.0-2.9 | 0.0-0.5 | .05 | .20 | | | |
| PlF: | | | | | | | | | | | | | | |
| Pierian | 0-5 | --- | --- | 5-10 | 1.35-1.50 | 14.11-42.34 | 0.07-0.10 | 0.0-2.9 | 2.0-4.0 | .10 | .20 | 2 | 3 | 86 |
| | 5-9 | --- | --- | 5-10 | 1.35-1.50 | 14.11-42.34 | 0.07-0.10 | 0.0-2.9 | 0.0-1.0 | .15 | .28 | | | |
| | 9-60 | --- | --- | 0-5 | 1.45-1.60 | 141.14-705.00 | 0.03-0.04 | 0.0-2.9 | 0.0-0.5 | .05 | .20 | | | |
| Pn: | | | | | | | | | | | | | | |
| Placer diggings | 0-60 | --- | --- | 0-1 | --- | 42.34-141.14 | 0.01-0.02 | 0.0-2.9 | 0.0-0.1 | --- | --- | --- | 8 | 0 |
| Tailings | 0-60 | --- | --- | 0-1 | --- | 42.34-141.14 | 0.01-0.02 | 0.0-2.9 | 0.0-0.1 | --- | --- | --- | 8 | 0 |
| RtC: | | | | | | | | | | | | | | |
| Rosane | 0-6 | --- | --- | 10-18 | 1.25-1.40 | 14.11-42.34 | 0.14-0.18 | 0.0-2.9 | 3.0-5.0 | .20 | .20 | 3 | 8 | 0 |
| | 6-30 | --- | --- | 8-18 | 1.35-1.50 | 14.11-42.34 | 0.10-0.13 | 0.0-2.9 | 0.5-1.0 | .28 | .28 | | | |
| | 30-60 | --- | --- | 0-5 | 1.45-1.60 | 141.14-705.00 | 0.03-0.04 | 0.0-2.9 | 0.0-0.5 | .05 | .20 | | | |
| Sw: | | | | | | | | | | | | | | |
| Slickens | 0-10 | --- | --- | 0-10 | --- | 1.41-4.23 | 0.10-0.12 | 0.0-2.9 | 0.0-0.1 | .64 | --- | 5 | 2 | 134 |
| | 10-30 | --- | --- | 0-10 | --- | 1.41-4.23 | 0.10-0.12 | 0.0-2.9 | --- | .64 | --- | | | |
| | 30-60 | --- | --- | --- | --- | 0.01-4.23 | 0.00 | --- | --- | --- | --- | | | |
| ToE: | | | | | | | | | | | | | | |
| Tomichi | 0-7 | --- | --- | 5-10 | 1.35-1.50 | 14.11-42.34 | 0.09-0.12 | 0.0-2.9 | 1.0-3.0 | .24 | .24 | 2 | 3 | 86 |
| | 7-13 | --- | --- | 5-10 | 1.35-1.50 | 14.11-42.34 | 0.07-0.10 | 0.0-2.9 | 0.0-1.0 | .15 | .28 | | | |
| | 13-60 | --- | --- | 0-5 | 1.45-1.60 | 141.14-705.00 | 0.04-0.06 | 0.0-2.9 | 0.0-0.5 | .10 | .20 | | | |
| TrE: | | | | | | | | | | | | | | |
| Troutville | 0-14 | --- | --- | 5-15 | 1.35-1.50 | 14.11-42.34 | 0.07-0.10 | 0.0-2.9 | 0.5-1.0 | .15 | .28 | 4 | 3 | 86 |
| | 14-20 | --- | --- | 5-18 | 1.35-1.50 | 14.11-42.34 | 0.05-0.07 | 0.0-2.9 | 0.0-0.5 | .10 | .32 | | | |
| | 20-40 | --- | --- | 5-18 | 1.35-1.50 | 14.11-42.34 | 0.03-0.04 | 0.0-2.9 | 0.0-0.5 | .05 | .32 | | | |
| | 40-60 | --- | --- | 0-5 | 1.45-1.60 | 141.14-705.00 | 0.03-0.04 | 0.0-2.9 | 0.0-0.5 | .05 | .20 | | | |
| W: | | | | | | | | | | | | | | |
| Water | --- | --- | --- | --- | --- | --- | --- | --- | --- | --- | --- | --- | --- | --- |
| Wa: | | | | | | | | | | | | | | |
| Wet alluvial land | 0-10 | --- | --- | 5-40 | 1.20-1.60 | 1.41-42.34 | 0.06-0.18 | 3.0-5.9 | 0.5-1.0 | .20 | .24 | 3 | 3 | 86 |
| | 10-60 | --- | --- | 0-10 | 1.50-1.65 | 42.34-141.14 | 0.05-0.08 | 0.0-2.9 | 0.0-0.5 | .10 | .28 | | | |
| Wet alluvial land | 0-3 | --- | --- | --- | --- | 14.11-42.34 | 0.20-0.25 | 0.0-2.9 | 50-70 | .05 | .05 | 5 | 8 | 0 |
| | 3-60 | --- | --- | --- | --- | 1.41-42.33 | --- | --- | 0.5-1.0 | --- | --- | | | |
| Wet alluvial land | 0-6 | --- | --- | 0-1 | --- | 42.34-141.14 | 0.02-0.03 | 0.0-2.9 | 0.0-0.1 | --- | --- | --- | 8 | 0 |
| | 6-60 | --- | --- | 0-1 | --- | 42.34-141.14 | 0.02-0.03 | 0.0-2.9 | --- | --- | --- | | | |

Survey Area Version:
Survey Area Version Date: 01/30/2008

The parameters chosen for each of the soil zones in the California Gulch watershed as used in the simulations reported in this research are shown in Table 4.3. Spatial distribution of these classes is shown in Figure 4.4.

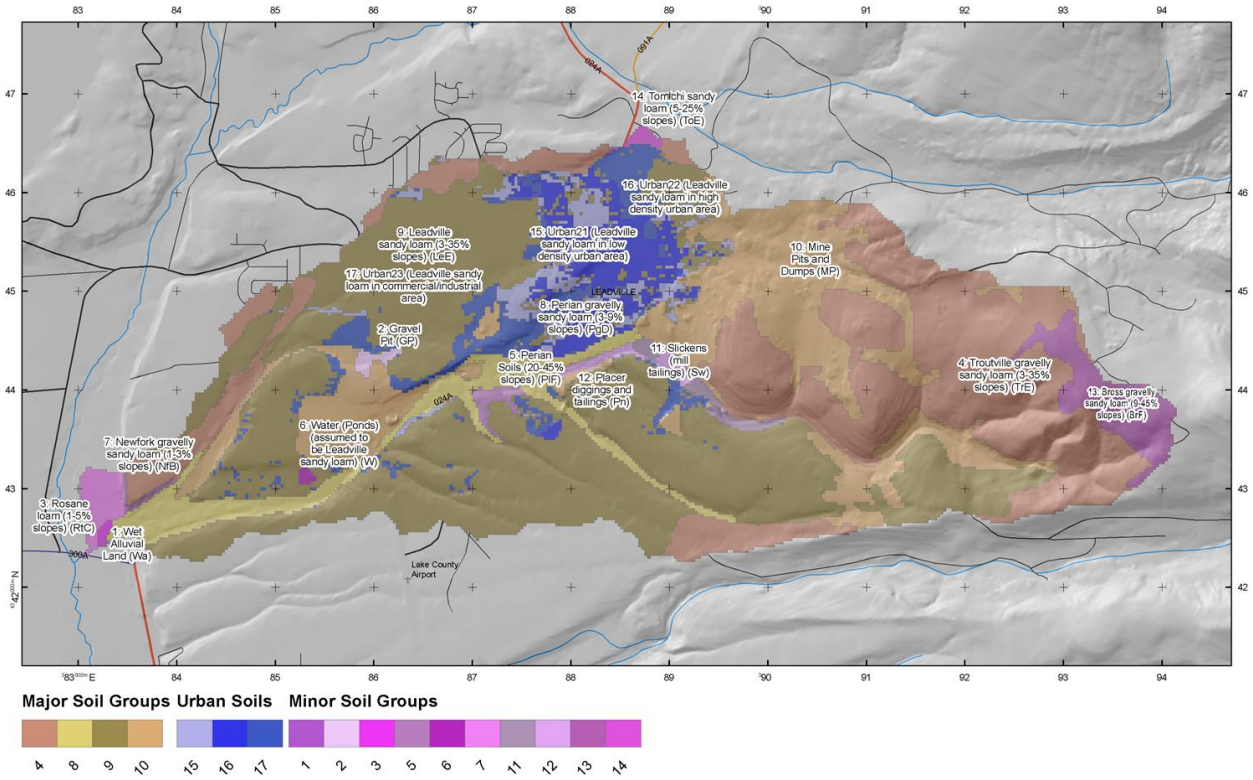


**Figure 4.4: Soil Groups defined in California Gulch according to SSURGO (NRCS n.d.).**

The method of Rawls et al. (1982, 1983) was used to generate initial values for the Green and Ampt parameters (saturated hydraulic conductivity and capillary suction head) for use in the model. $K_h$ values were adjusted by Velleux et al. (2008a) during calibration to achieve agreement between measured and simulated runoff.

**Table 4.3: Soil parameters used in the Green and Ampt equation.**

| Soil Description | Saturated Hydraulic Conductivity (TREX-SMA) | Capillary Suction Head | Initial Soil Moisture |
|---|---|---|---|
| Wet Alluvial Land (Wa) | 3.50E-06 | 0.0232 | 32.7% |
| Gravel Pit (GP) | 3.50E-06 | 0.0232 | 32.7% |
| Rosane loam (1-5% slopes) (RtC) | 3.50E-06 | 0.0091 | 32.9% |
| Troutville gravelly sandy loam (3-35% slopes) (TrE) | 3.70E-06 | 0.0035 | 32.7% |
| Perian Soils (20-45% slopes) (PIF) | 3.50E-10 | 0.0150 | 32.8% |
| Water (Ponds) (assumed to be Leadville sandy loam) (W) | 3.50E-10 | 0.0509 | 32.8% |
| Newfork gravelly sandy loam (1-3% slopes) (NfB) | 4.00E-06 | 0.0071 | 32.8% |
| Perian gravelly sandy loam (3-9% slopes) (PgD) | 3.00E-07 | 0.0071 | 32.8% |
| Leadville sandy loam (3-35% slopes) (LeE) | 3.50E-06 | 0.0509 | 32.8% |
| Mine Pits and Dumps (MP) | 9.80E-06 | 0.0001 | 32.6% |
| Slickens (mill tailings) (Sw) | 3.50E-06 | 0.0008 | 32.8% |
| Placer diggings and tailings (Pn) | 3.00E-06 | 0.0001 | 32.6% |
| Bross gravelly sandy loam (9-45% slopes) (BrF) | 3.50E-06 | 0.0016 | 32.7% |
| Tomichi sandy loam (5-25% slopes) (ToE) | 3.50E-06 | 0.0284 | 32.8% |
| Urban21 (Leadville sandy loam in low density urban area) | 3.25E-06 | 0.0509 | 32.8% |
| Urban22 (Leadville sandy loam in high density urban area) | 1.05E-06 | 0.0509 | 32.8% |
| Urban23 (Leadville sandy loam in commercial/industrial area) | 3.25E-06 | 0.0509 | 32.8% |

## 4.5 TEMPERATURE

Hourly air temperature data were obtained for the modeling period from the Western Regional Climate Center (WRCC) for the weather station at the Leadville airport 5 km (3.2 mi.) south of Leadville. The hourly instantaneous temperature and daily maximum and minimum temperatures are shown in Figure 4.5.

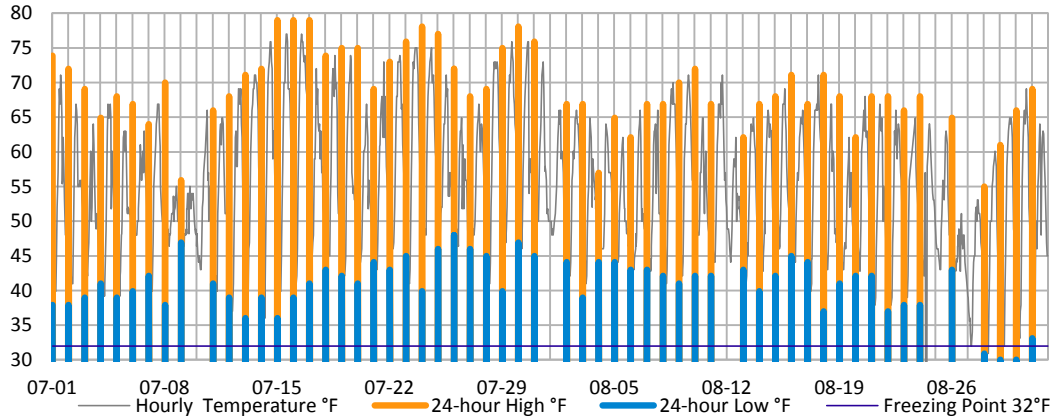


**Figure 4.5: Hourly and daily temperature extremes for July and August 2006 at Leadville Airport Weather Station (KLXV) from the Western Regional Climate Center http://www.wrcc.dri.edu/.**

The Leadville airport gauge is at 9938 feet above mean sea level. A normal adiabatic lapse rate of 3.6 ºF per 1000 feet would predict temperatures approximately 8 °F cooler at the top of Ball Mountain (elevation 12300'), and 1 °F warmer at the watershed outlet (elevation 9530 ft.) into the Arkansas River. The climate record shows that daily extremes stayed well above freezing for nearly all the simulated period eliminating concern about frozen ground effects. In the last week of the simulated period from August 27–30, temperatures at the airport gauge were low enough to indicate the possibility of frozen precipitation in the upper watershed. If the modeling period were to be extended into the cooler months later in the year, both frozen ground effects and frozen precipitation would have to be extensively considered.

## 4.6 EVAPOTRANSPIRATION (ET)

The inter-event recovery of infiltration capacity in the soil moisture zones of TREX-SMA is driven by release of water to the channel and by evapotranspiration (Senarath et al. 2000). Pan evaporation is measured at the Sugarloaf Reservoir weather station operated by the Bureau of Reclamation. A photo of the site is given in Figure 4.6 and descriptive data in Table 4.4.

**Figure 4.6: Climatological monitoring equipment at Sugarloaf Reservoir.**

**Table 4.4: Descriptive data for Sugarloaf Reservoir meteorological station.**

**Sugarloaf Reservoir Weather Station: NCDC data inventories**

<http://www4.ncdc.noaa.gov/cgi-win/wwcgi.dll?wwDI~StnSrch~StnID~20003674>

| | |
|---|---|
| In Service: | 01 Aug 1948 to Present |
| Elevation: | 2968.1m (9738') above sea level |
| Lat/Lon: | 39°15' North 106°22' West |
| Location: | Lake County, Colorado, United States |

The pan is located southeast of the dam approximately 7 km (4.4 mi.) west of the city of Leadville and 125 meters (410 ft.) lower in elevation. During summer months, when snow cover is largely absent, the values from the Sugarloaf Pan should be indicative of conditions in California Gulch (Henning and Henning 1981).

Monthly evaporation values are provided by the Western Regional Climate Center from data recorded at the pan. Values recorded during 2006 for the months of July and August were lower than the cumulative monthly averages for 1948–2005 as shown in Figure 4.7. The reduced evaporation indicates the occurrence of more precipitation that usual, one reason why this summer period was chosen for simulation.

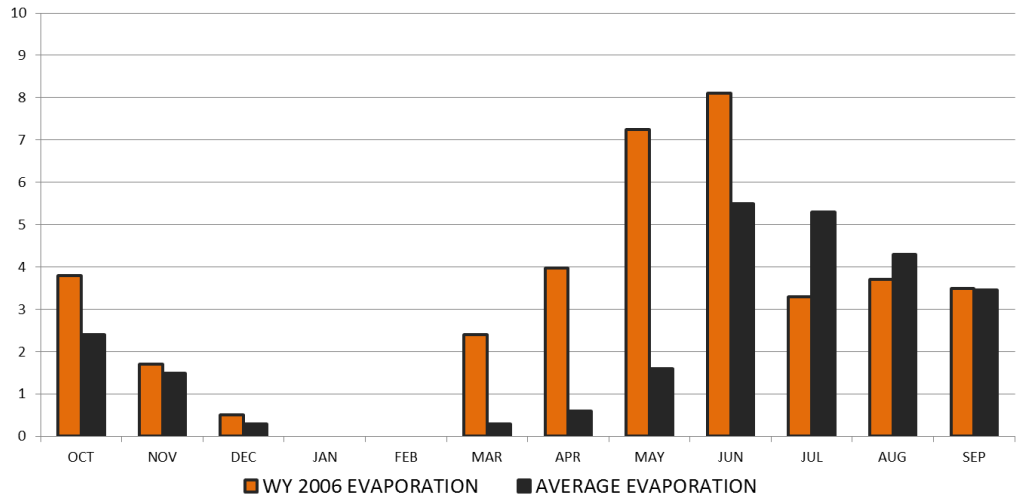


**Figure 4.7: Water year 2006 and average monthly evaporation at Sugarloaf Dam (Bureau of Reclamation 2006).**

Daily records (Figure 4.8) from the pan show fluctuations between nearly zero and 0.32 inches per day for July and August 2006.

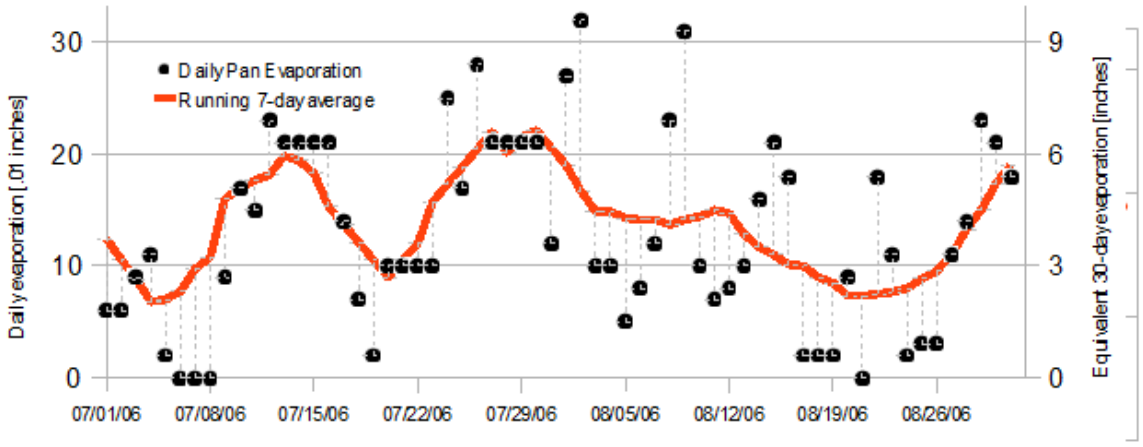


**Figure 4.8: Daily pan evaporation at Sugarloaf Dam (National Climatic Data Center 2010).**

For purposes of simulation, the 2006 monthly averages from the Western Regional Climate Center were used to compute an average potential ET rate of 5.6 inches per month. This value was applied as a constant demand during all simulations.

## 4.7 PRECIPITATION

Several weather stations in the vicinity of Leadville are operated in cooperation with the US National Weather Service including the Leadville airport gauge (see Table 4.5) and the Bureau of Reclamation meteorology station at the base of Sugarloaf Dam (a.k.a. Turquoise Lake).

**Table 4.5: Descriptive data for Leadville Airport meteorological station.**

**Leadville Lake County Airport Weather Station: NCDC data inventories**

<http://www4.ncdc.noaa.gov/cgi-win/wwcgi.dll?wwDI~StnSrch~StnID~20003673>

| | |
|---|---|
| ICAO Call Sign: | LXV / KLXV |
| In Service: | 18 Jun 1976 to 01 Jan 2009 |
| Elevation: | 3029.1m (9938') above sea level |
| Lat/Lon: | 39°13' North 106°19' West |
| Location: | Lake County, Colorado, United States |

The Bureau of Reclamation station has the longer period of record of these two but the data from the station are only reported as daily totals. Daily total precipitation is difficult to apply for modeling but does give a good picture of how the summer of 2006 compares with the historical average as seen in Figure 4.9:

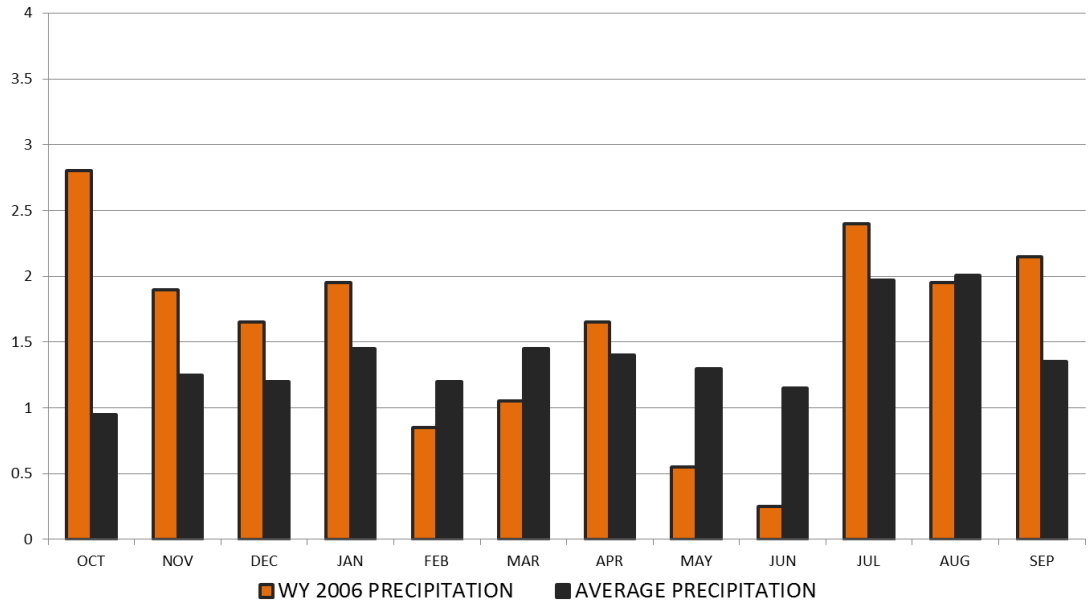


**Figure 4.9: Measured monthly average precipitation for 2006 and period of record at Sugarloaf Dam (Bureau of Reclamation 2006).**

The Leadville airport data were available for both hourly and daily intervals but inconsistencies in the hourly data over predicted total rainfall as tabulated by that twenty-four hour data, which had been quality checked by NOAA. So the KLXV intensity data were not used for modeling.

As part of the CERCLA/Superfund efforts in California Gulch, a program to monitor the impact of mine waste transport on Arkansas River ecology, a network of automated pluviographic and fluvial gauging stations (Figure 4.10, Table 4.6) was established by the EPA and maintained by Tetra Tech, inc. Data from these gauging stations for the summer of 2006 were obtained through an agreement with Tetra Tech.

The summer of 2006 included at least eight significant convective storms with measurable precipitation recorded at all four automated pluvial gauging stations. Figure 4.12 shows the timing of these storms. Cumulative rainfall shown for each gauge indicates the relative distribution of rainfall during the different storms.

In Figure 4.11, the intensity scale shows the 10 minute precipitation intensity as reported by the gauge. Several storms produced intense precipitation in the upper watershed but produced relatively little (or no) recorded additional flow at the watershed outlet (e.g. July 21, 24, August 6, and 21). One of these (August 6) was included in the series for analysis in Chapter 6.

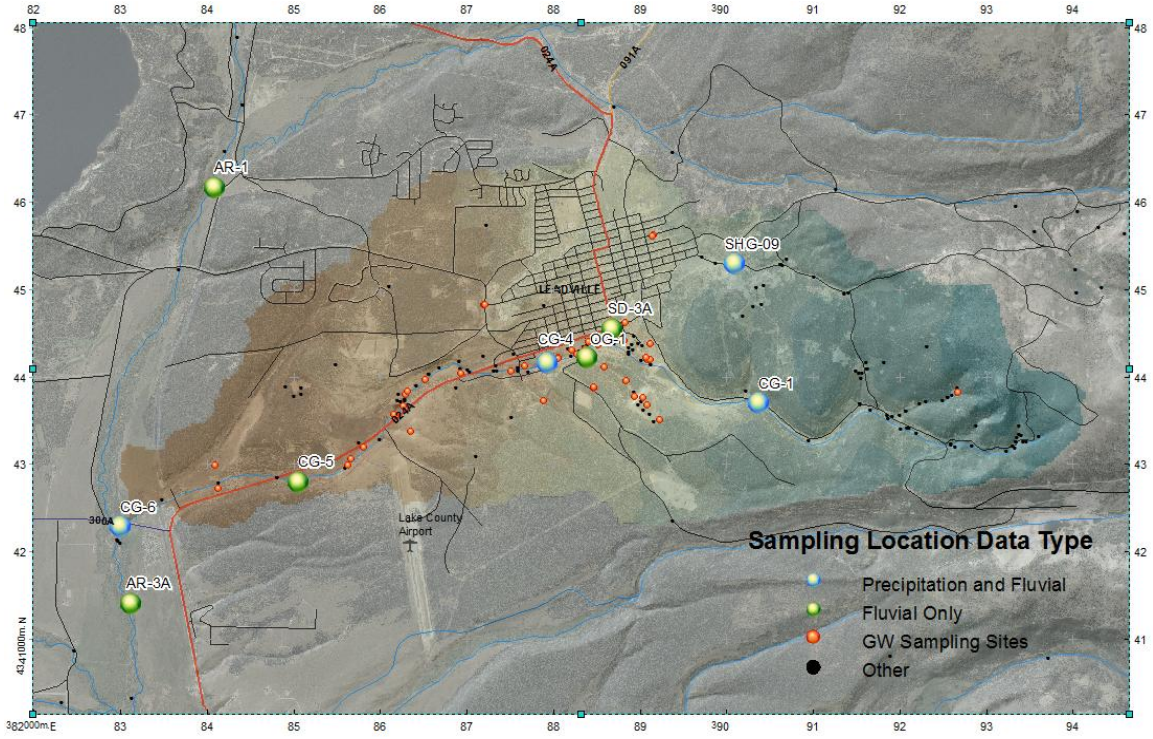


**Figure 4.10: Location of automated gauging stations at California Gulch. Other sampling sites from the CERCLA database are also shown. CG-6 is at the watershed outlet.**

## Table 4.6: Automated precipitation gauge locations and available data

| Gauge | Description | Available Data | Northing meters NAD83 UTM zone 13N | Easting meters NAD83 UTM zone 13N | Elevation meters NAVD88 |
|---|---|---|---|---|---|
| SHG-09 | 300 feet below Emmett retention pond | 1, 2, 3, 4, 5, 6 | 4,345,292 | 390,078 | 3,185 |
| SD-3A | Flume in Starr Ditch downstream of Monroe St. and upstream of drop | 1, 2, 3, 4, 5 | 4,344,564 | 388,670 | 3,074 |
| CG-1 | California Gulch immediately upstream of the Yak Tunnel portal | 1, 2, 3, 4, 5, 6 | 4,343,707 | 390,360 | 3,149 |
| OG-1 | Oregon Gulch immediately upstream of confluence with California | 1, 2, 3, 4, 5 | 4,344,236 | 388,376 | 3,059 |
| CG-4 | California Gulch downstream of confluence with Oregon Gulch | 1, 2, 3, 4, 5, 6 | 4,344,164 | 387,920 | 3,037 |
| CG-5 | California Gulch upstream of the Leadville Wastewater Treatment | 1, 2, 3, 4, 5 | 4,342,811 | 385,048 | 2,953 |
| CG-6 | California Gulch immediately upstream of confluence with Arkansas | 1, 2, 3, 4, 5, 6 | 4,342,289 | 382,991 | 2,904 |
| AR-1 | Arkansas River upstream of confluence with California Gulch, approximately 0.25 miles downstream of the confluence with | 1, 2, 3, 4, 5 | 4,346,176 | 384,082 | 2,963 |
| AR-3A | Arkansas River approximately 0.5 miles downstream of confluence with California Gulch | 1, 2, 3, 4, 5 | 4,341,426 | 383,112 | 2,894 |

1) Stage, 2) Discharge, 3) Temperature, 4) Conductivity, 5) pH, 6) Precipitation

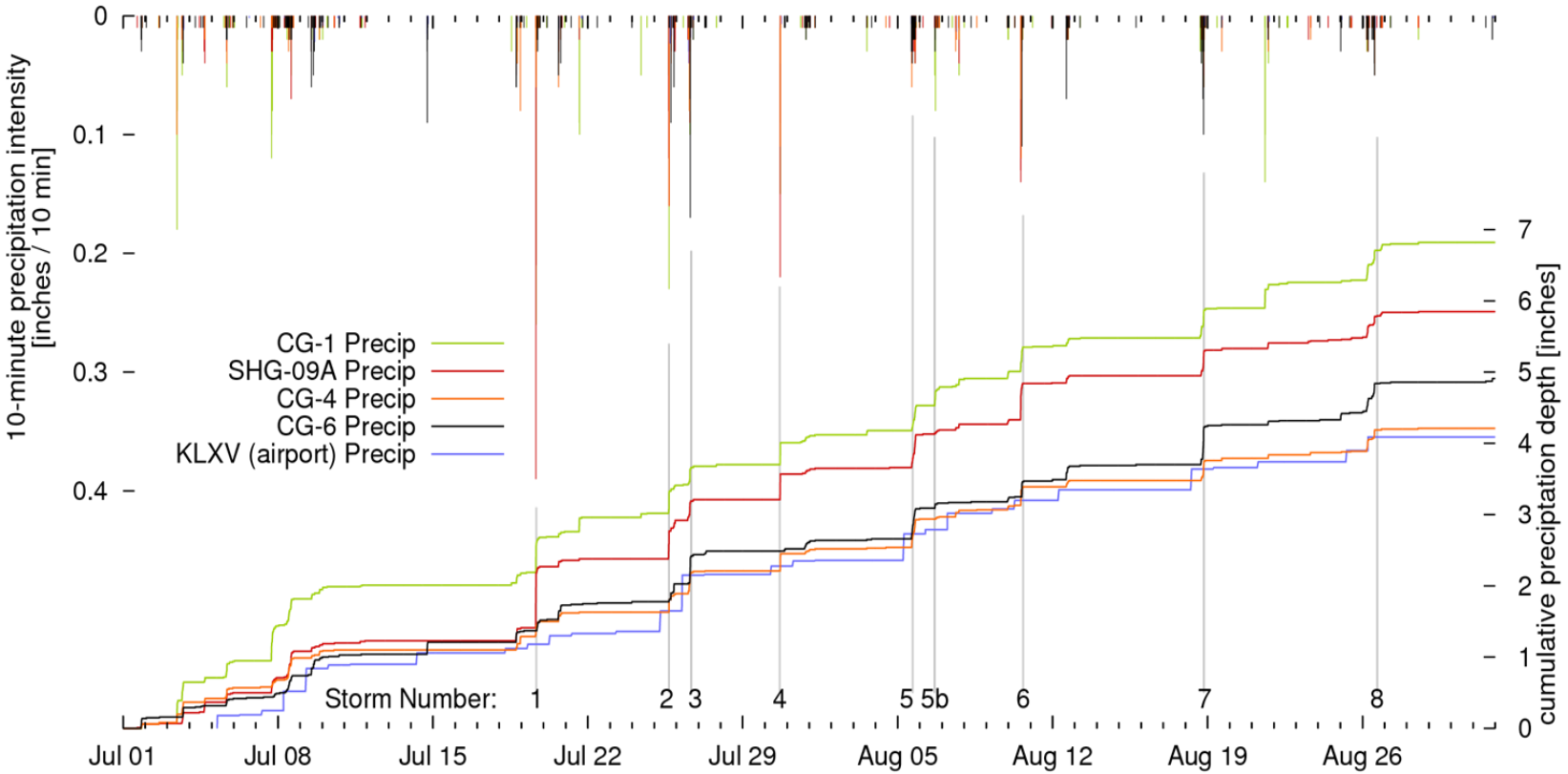


**Figure 4.11: Observed precipitation measurements in California Gulch and vicinity for summer 2006. Note that daily totals at the KLXV gauge are reported at the beginning of the day and so appear to slightly anticipate the other gauge values.**

## 4.8 STREAM FLOW

The stream through upper California Gulch is narrow, steep and ephemeral. The stream meanders through lower California Gulch with a milder slope and perennial flow from ephemeral drainages. The Yak Tunnel mine water treatment works and Leadville wastewater treatment plant (WWTP) also contribute to surface drainage. For the model, a DEM based stream network of twenty-five links (reaches) totaling 1395 nodes represented the channel network, defining a total stream length of approximately 42 km (including both perennial streams and intermittent drainages). The watershed outlet is the California Gulch confluence with the East Fork of the Arkansas River (Velleux et al. 2008a).

The Leadville wastewater treatment plant collects sanitary flows from the entire city of Leadville and performs simple primary clarification and sludge concentration. The primary clarifier supernatant is discharged to a finishing pond which overflows continuously but with varying discharge according to diurnal fluctuations in flow. Daily average discharge from the treatment plant was computed from the total daily discharge volume obtained from plant records included in Appendix C.

From June 1 to September 31, the WWTP average discharge was 0.55 cfs with fluctuations as high as 0.82 and as low as 0.24 cfs. The daily average discharge may be influenced by time of reading since it is computed from a total volume difference between daily readings of a flow meter so the three-day average is plotted in Figure 4.13 to highlight trends in the rate of discharge. A normal business workweek creates a clearly visible weekly fluctuation with WWTP discharge data shown.

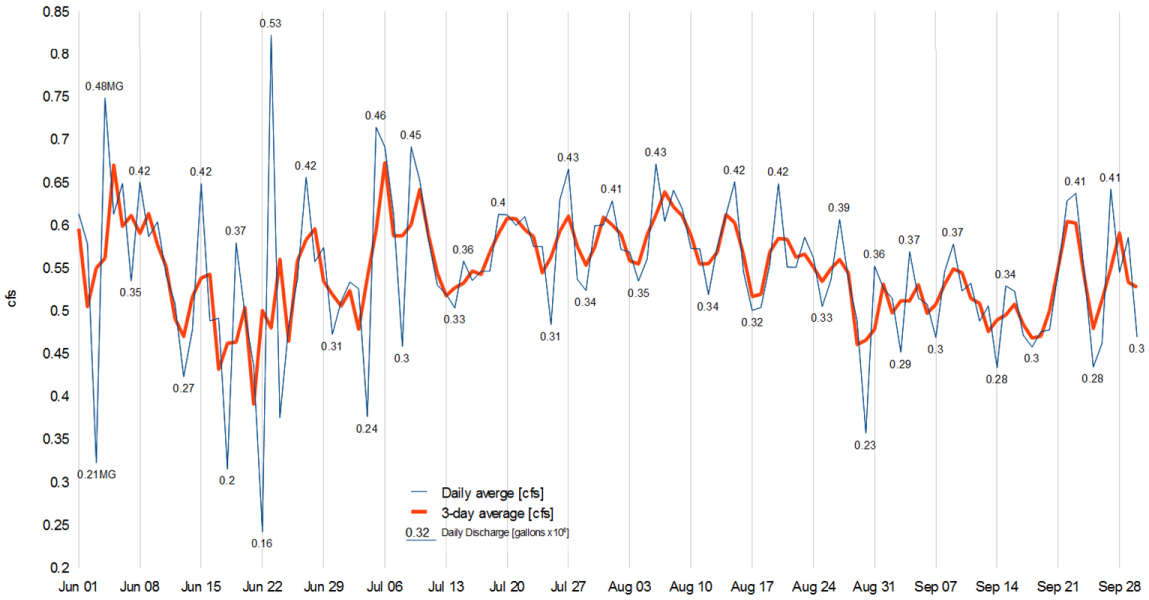


**Figure 4.12: Daily and three-day-average outflow for 2006 from Leadville wastewater treatment plant.**

When operating, the Yak Tunnel treatment plant has a relatively constant outlet flow approximately 1.83 cubic feet per second, but the plant is not operated continuously. Plant closures lasting approximately 72 hours occurred at intervals of about 10 days during July and August 2006 as seen in Figure 4.14.

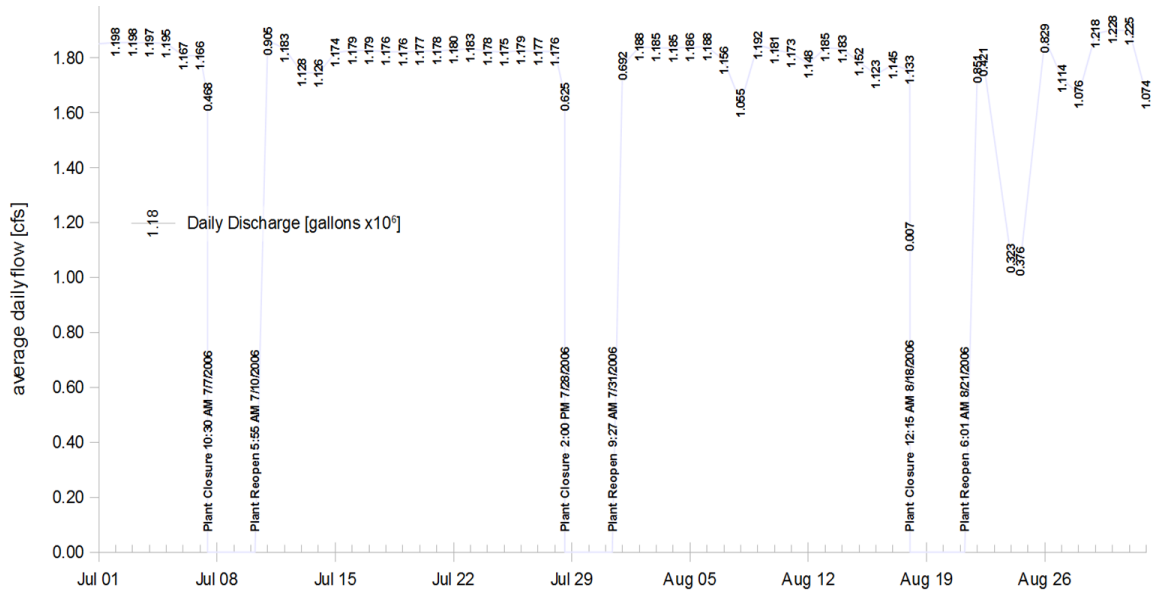


**Figure 4.13: Yak tunnel treatment plant outflows for 2006.**

The upper watershed is monitored in both Stray Horse Gulch and California Gulch by gauges SHG-09A and CG-1 on the north and south portions of the watershed, respectively. Runoff from the pavement area of Leadville is the primary influence at the Starr Ditch gauge (SD-3A) with additional input from the upper watershed through Stray Horse Gulch. Below CG-1, the Yak Tunnel treatment plant contributes mine drainage to the flow in the channel.

The CG-4 gauge measures the cumulative input of all these just below the confluence of upper California Gulch with Stray Horse Gulch in the center of the watershed. Flow from Oregon Gulch, measured by OG-1, also contributes to the flow at the CG-4 gauge. CG-5 follows CG-4, and several hundred meters downstream of CG-5, the WWTP outlet discharges into California Gulch. Malta Gulch contributes to the flow in the gulch and finally, CG-6 measures the flow just before the confluence with the Arkansas River.

Gauge locations in UTM NAD 1983 zone 12 N coordinates, along with the description provided in the EPA database are tabulated in Table 4.6 above. Precipitation and channel flow are recorded at ten-minute intervals for stations labeled as CG-1, SHG-09, CG-4, and CG-6 as

already shown in Figure 4.11 (above). Additional flow-only measurements are made at locations CG-5, SD-3A, OG-1, AR-1, AR-3A.

The automated sampling stations were installed each summer from 2003 to 2008 approximately from June through September. The automated sampling program was scaled back in 2009 and 2010 to include only the peak runoff season. Gauges consist of a Parshall flume installed across the channel with a bubbler in a stilling well to record stage. Photographs of a typical station (CG-5) are shown in Figures 4.15 and 4.16

**Figure 4.14: Stage indicator and bubbler at CG-5.**

**Figure 4.15: CG-5 with data-logger in case on left bank.**

Data from 2003–2007 were evaluated to find a suitable modeling period. Figure 4.17 shows the complete series, including data from the Arkansas River gauges, which are also part of the

EPA monitoring program. Snowmelt runoff effects are visible dominating the hydrograph from late April through July in most years.

For the initial tests with the TREX-SMA model as described in this chapter, a non-snowmelt period at the end of the summer of 2006 was selected. Several large peaks allow for significant runoff signatures to observe simulation quality during both high and low flows. Figure 4.18 shows the summer of 2006 with snowmelt tapering off in early July.

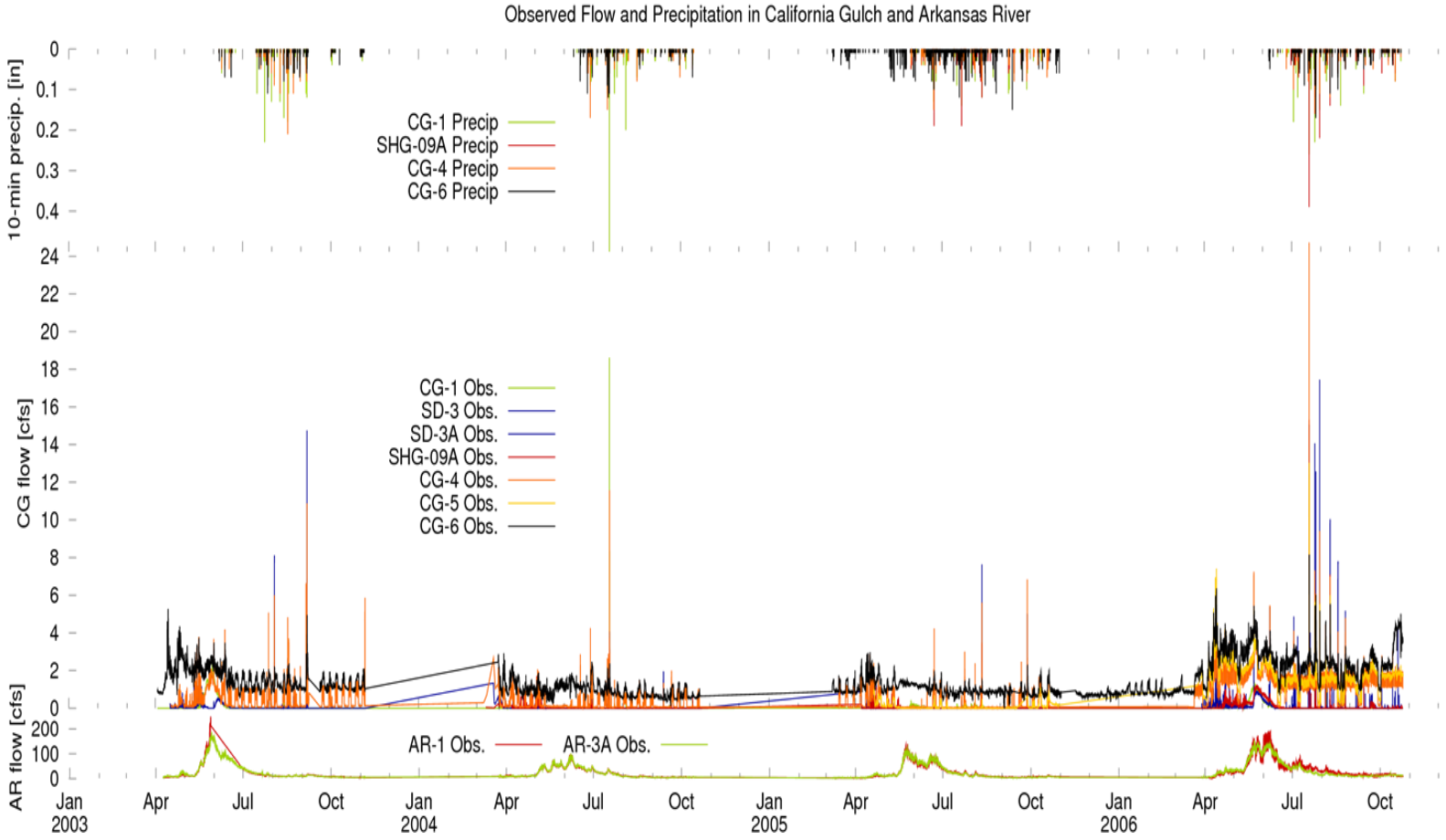


**Figure 4.16: Observed precipitation plotted with flow in both California Gulch and the Arkansas River for all data collected from EPA automated sampling stations from 2003–2006. Note that gauges were dismantled in winter months because of the difficulty measuring during frozen conditions. Also note that several additional gauges were added in 2006.**

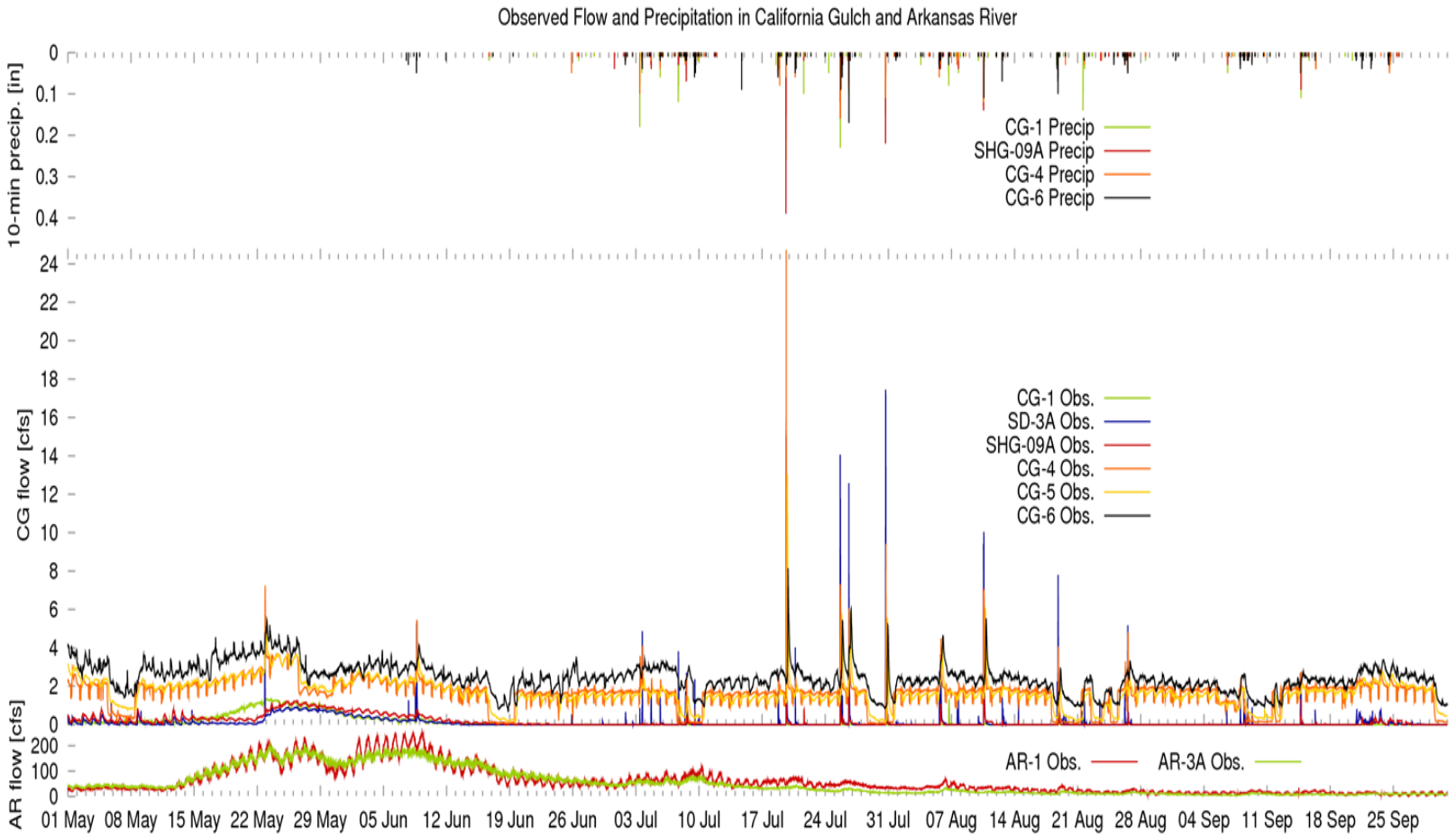


**Figure 4.18: Observed precipitation plotted with flow in both California Gulch and the Arkansas River for summer 2006.**

## 5.0 TREX-SMA APPLICATIONS AT CALIFORNIA GULCH (PART I)

Results from a series of simulations using TREX-SMA are presented in this chapter and in Chapter 6. Results from all TREX-SMA simulations are compared to the results of operating the TREX model without any soil moisture accounting procedure. Throughout this and the following chapter, references will be made to "SMA" and "no-SMA" cases, meaning the TREX-SMA model results with soil moisture accounting and the former TREX model results without. In the current chapter, hypothetical simulations are constructed to demonstrate capabilities of TREX-SMA for:

1) modeling baseflow by release of infiltrated water back to the channel
2) re-initializing Green and Ampt infiltration parameters using soil moisture zone states at the onset of a new precipitation event.

The simulations in Section 5.1 are not compared to actual watershed runoff volumes or flows. Chapter 5.3 presents a simulation concerning the ability of TREX-SMA for continuous multi-event modeling by bridging the gaps between precipitation events with the soil moisture accounting model.

The multi-event simulation results are compared to observed watershed response at four of the stream gauging stations.

For all simulations, values for surface hydrology model such as soil, channel, land-use, and topography were used as reported in Chapter 4 according to calibration by Velleux (2005) and Velleux et al. (2008a). Initial soil moisture was set at 33%. Precipitation data collected at the automated sampling stations during summer of 2006 provided driving model data. Where applicable, observations of stream flow from the automated sampling stations were used to evaluate model performance.

Two sets of parameters for the soil moisture zones were applied. For simulations described in this chapter, a set of parameters tuned to demonstrate the capabilities of the model for simulating baseflow and for GA parameter re-initialization was applied. A second set was used for multi-event models, as described in Chapter 6.

## 5.1 BASEFLOW (SINGLE-EVENT) SIMULATION

By simulating return flows from the Sacramento soil moisture storage zones, TREX-SMA has the capability to simulate baseflow recession following a single storm event. In fact, based on the sampling reports and model observations, California Gulch has little to no baseflow during the late summer months. Therefore, a hypothetical scenario was constructed to demonstrate the baseflow capabilities of the TREX-SMA model. Real precipitation inputs were used to drive the model, but no comparison is made to observed flows, since these do not contain any perceptible baseflow component.

### *5.1.1 Soil moisture zone parameters*

For the baseflow demonstration simulation, a single set of soil moisture zones is coupled with the surface domain, and all infiltrated water in the model is lumped together. A single set of Sacramento model parameters controls the behavior of these zones and a listing of these parameters is found in Table 5.1 Two outlet points are chosen in the channel to receive interflow and baseflow from the soil moisture zones. Distributing the return flow between two outlet points reduces the "mounding" in the channel from the point source returns, enhancing the numerical stability of the simulation. Figure 5.1 identifies the outlet points as "SMA Point #1" and "SMA Point #2."

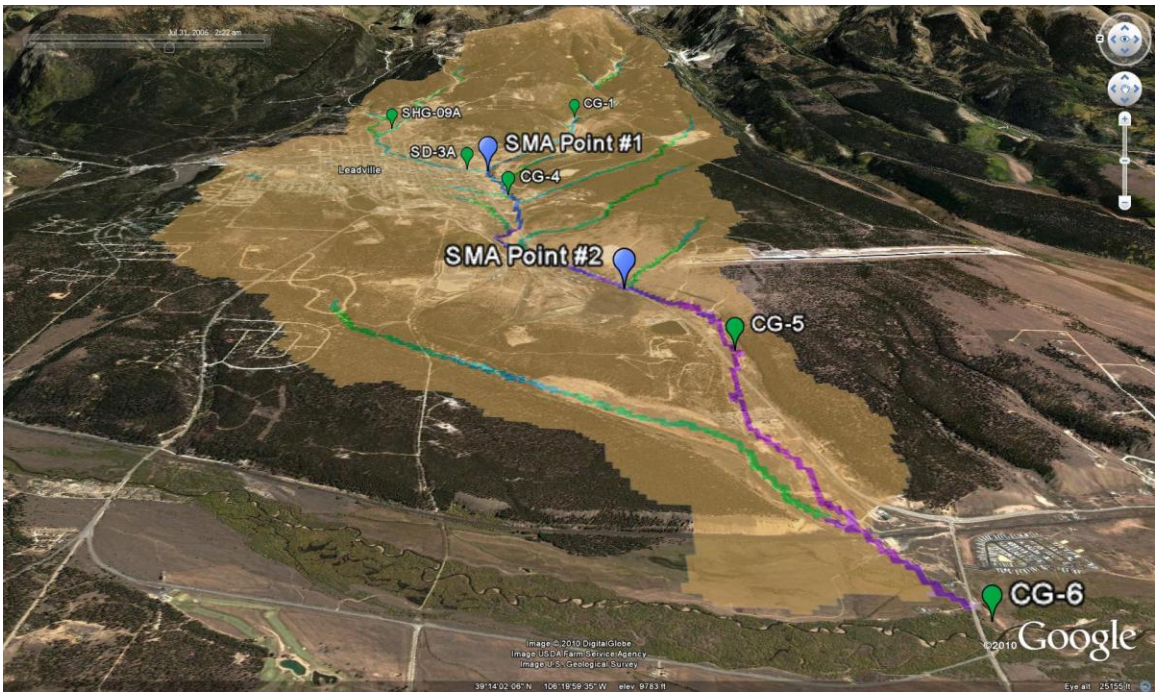


**Figure 5.1: SMA outlets in California Gulch above CG-4 and CG-5.**

**Table 5.1: Sacramento Soil Moisture Accounting model parameters used for re-initialization simulation.**

| No. | Parameter | Description | Used for Model | Acceptable Ranges |
|---|---|---|---|---|
| 1 | UZTWM | The upper layer tension water capacity, mm | 5 | 10–300 |
| 2 | UZFWM | The upper layer free water capacity, mm | 8.00 | 5–150 |
| 3 | UZK | Interflow depletion rate from the upper layer free water storage, $day^{-1}$ | 0.020 | 0.10–0.75 |
| 4 | ZPERC | Ratio of maximum and minimum percolation rates | 85.0 | 5–350 |
| 5 | REXP | Shape parameter of the percolation curve | 1.20 | 1–5 |
| 6 | LZTWM | The lower layer tension water capacity, mm | 40 | 10–500 |
| 7 | LZFSM | The lower layer supplemental free water capacity, mm | 5.0 | 5–400 |
| 8 | LZFPM | The lower layer primary free water capacity, mm | 10.0 | 10–1000 |
| 9 | LZSK | Depletion rate of the lower layer supplemental free water storage, $day^{-1}$ | 0.04 | 0.01–0.35 |
| 10 | LZPK | Depletion rate of the lower layer primary free water storage, $day^{-1}$ | 0.0020 | 0.001–0.05 |
| 11 | PFREE | Percolation fraction that goes directly to the lower layer free water storages | 0.30 | 0.0–0.8 |
| 15 | SIDE | Ratio of deep percolation from lower layer free water storages | 0.00 | Not Given |
| 16 | RSERV | Fraction of lower layer free water not transferable to lower layer tension water | Not Used | Not Given |

Although the lumped soil moisture accounting does not explicitly predict the locations of return flows, it was assumed that these returns would be most logically placed in the model where groundwater is observed to be interacting with the surface water. Observations of

phreatophytic plant species in the vicinity of the SMA outlets were made during the June 2010 site reconnaissance (see Figures 5.2, 5.3). These observations support the assumptions guiding the placement of the soil moisture zone outlets.

**Figure 5.2: Photographs showing phreatophyte plant species in vicinity of upper SMA outlet. (Top) View looking upstream toward the confluence of Starr Ditch and upper California gulch. (Bottom) Looking downstream toward CG-4 (about ¼ mile downstream).**

**Figure 5.3: Vegetation indicative of some groundwater connection near location of lower SMA outlet. Phreatophyte species are present but not as prevalent as at upper outlet.**

### *5.1.2 Precipitation*

Figure 5.4 shows the measured precipitation data obtained during the July 19, 2006 event and used for a testing the baseflow capability of TREX-SMA.

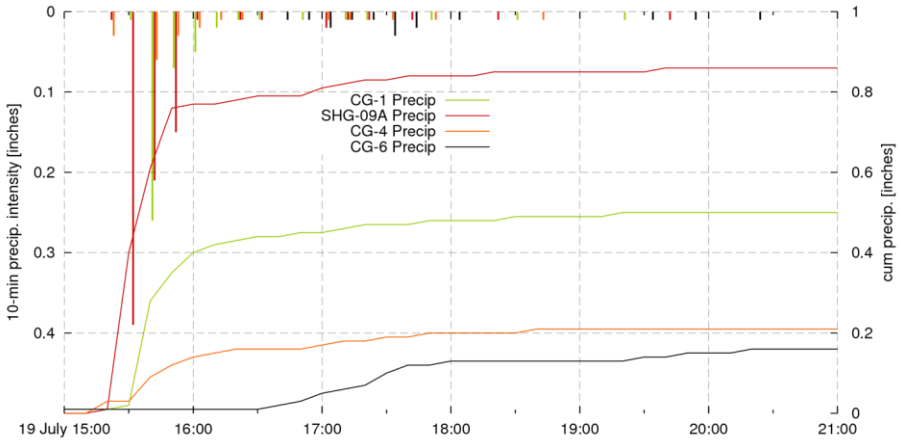


**Figure 5.4: Measured precipitation in California Gulch on July 19 and 20, 2006.**

### *5.1.3 Baseflow demonstration results*

The July 19, 2006 data were incorporated into a TREX-SMA model simulation run to evaluate the effectiveness of the hybrid model TREX-SMA to improve baseflow modeling. Figure 5.5 shows the slight baseflow curve added with the TREX-SMA sub-model active.

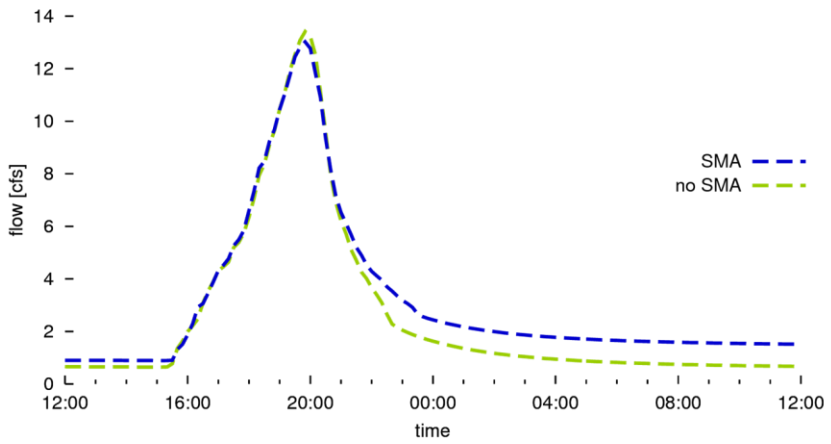


**Figure 5.5: Demonstration of TREX-SMA model effect on baseflow hydrograph at CG-5**

## 5.2 RE-INITIALIZATION (DOUBLE EVENT) SIMULATION

TREX-SMA uses the soil moisture zone states to reinitialize the Green and Ampt infiltration parameters for sequential events. By reinitializing the infiltration parameters, a more accurate estimate of runoff volume during multiple events may be obtained.

### *5.2.1 Infiltration parameter re-initialization*

In order to allow multi-event simulation with TREX-SMA, the saturation condition of the soil moisture is used to re-initialize the parameters of the Green and Ampt infiltration equation (see also Figure 3.3).

$$f = K_h \cdot 1 + \frac{H_c \cdot M_d}{F} \qquad \text{(See Eq. 3.5)}$$

Among parameters in the Green and Ampt equation, saturated hydraulic conductivity ($H_k$) and capillary suction head are considered to be constants—these represent soil properties at standard states (fully saturated and at field capacity, respectively). However, the moisture deficit and the infiltrated depth are variable parameters, the former given as an initial state of the ambient soil, scaling the effect of the capillary suction head; the latter increases as a storm progresses and asymptotically reduces the infiltration rate to zero. The infiltration parameter

adjustment algorithm allows TREX-SMA to continuously model a series of storm events by appropriately adjusting the two variable parameters of the Green and Ampt equation. The effect of this readjustment is shown schematically in Figure 5.6.

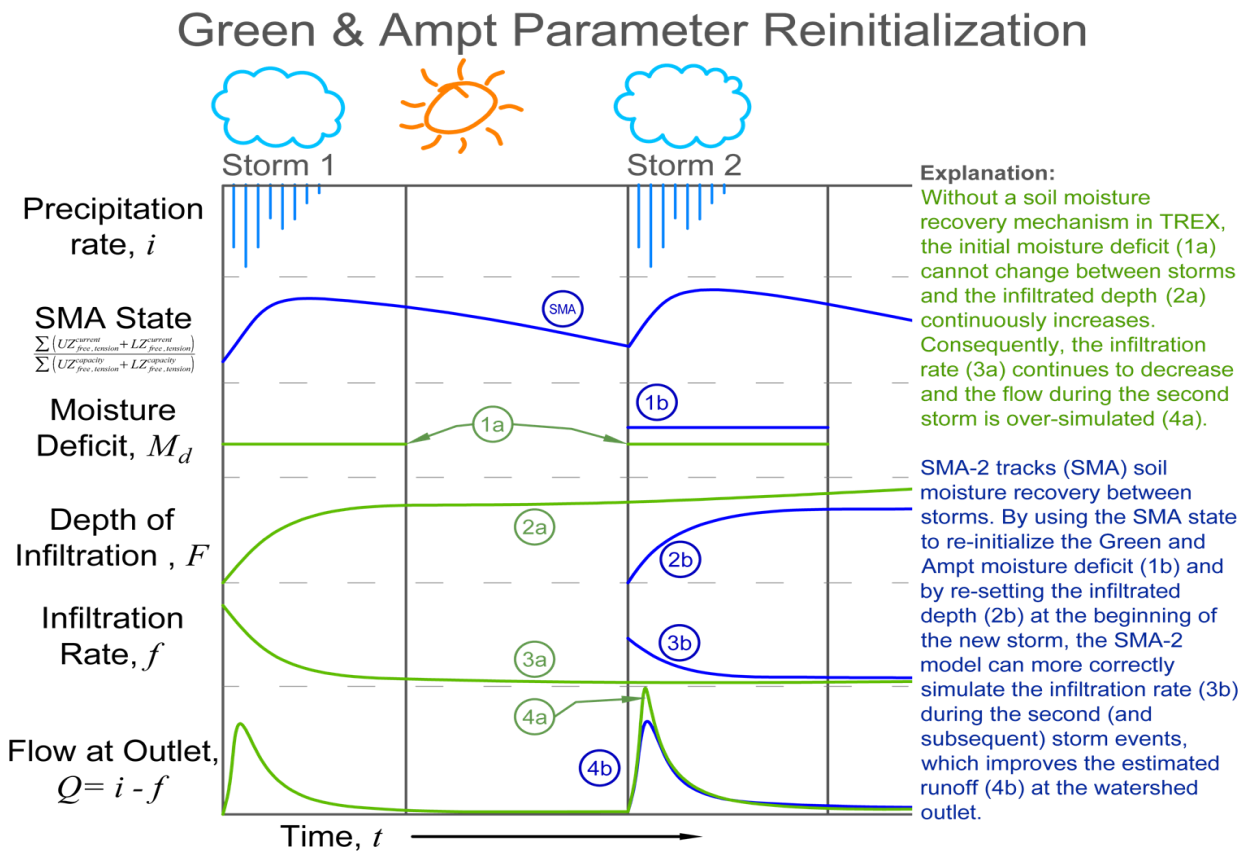


**Figure 5.6: Moisture deficit re-initialization using conceptual parameter states. Green indicates a note or parameter from TREX without soil moisture accounting. Blue indicates parameters or notes pertaining to TREX-SMA.**

Infiltration parameters remain fixed for the duration of a single storm. During the interval between the storms, infiltration patterns are allowed to recover according to the recovery of the soil moisture zones by evapotranspiration and drainage. In SMA2, a storm ends at cessation of rainfall, when the precipitated water falls below a user entered threshold value. The model does not change the infiltration parameters immediately upon cessation of rainfall, but continues to allow infiltration to occur using the Green and Ampt parameters as modified from the beginning

of the storm (during the first storm, boundary values for moisture deficit are defined in the input file; infiltrated depth is assumed to be zero). When precipitation depth in any cell in the SMA zone rises again above the threshold, the infiltrated depth is reset to zero (driving infiltration rate to a maximum) and the moisture deficit for the cells corresponding to the each SMA zone is modified to be equal to the SMA summary state:

$$\text{SMA Summary State} = \frac{\sum Tw_{c,uz}, Fw_{c,uz}, Tw_{c,lz}}{\sum Tw_{m,uz}, Fw_{m,uz}, Tw_{m,lz}} \qquad \text{(Eq. 5.1)}$$

This is consistent with the conceptual model that the water from the previous storm passes downward according to the parameters in the SMA2 model and that new water is received as a new storm.

The Green and Ampt equation models infiltration as a piston wetting front. Head to drive water into the soil matrix is a composite of the suction head of the dry soil matrix at the wetting front and the ponded head at the surface, acting across the distance $D_i$, the depth of infiltration. The rate of infiltration is moderated throughout a storm by the increase in depth. Capillary suction head and saturated hydraulic conductivity are properties of the soil under standard conditions and do not change. The initial moisture deficit, which scales the effect of the capillary suction head pulling down at the piston wetting front, is constant during a particular infiltration event.

When precipitation ceases in TREX-SMA, the wetting front and infiltration piston are assumed to dissolve so that at initiation of Storm 2, the depth of infiltration is again set to zero, and the moisture deficit re-initializes according to the soil moisture zone states.

### *5.2.2 Precipitation*

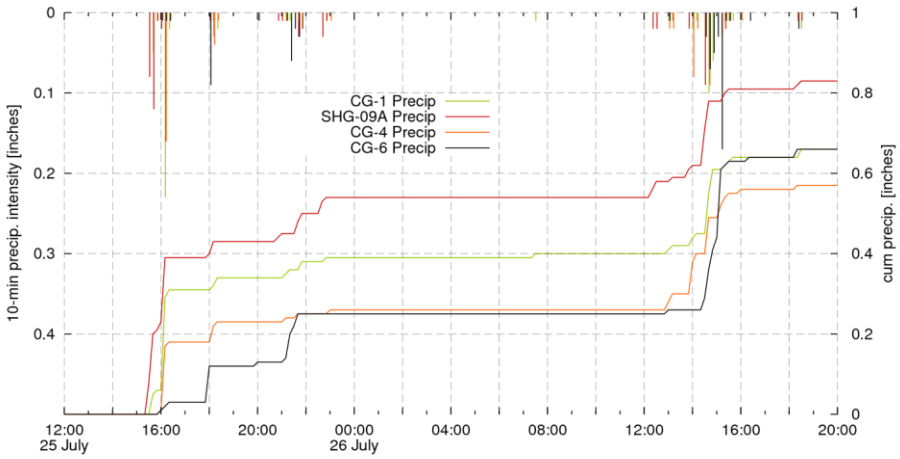


**Figure 5.7: Hydrographs in California Gulch during double-event period July 25–26, 2006.**

The double event features two storms with very similar hydrographs. Precipitation measured at CG-6, the outlet of the watershed, is greater during the second storm. The most intense precipitation during the first storm was measured in the upper watershed at Stray Horse Gulch in the SHG-09A gauge.

### *5.2.3 Re-initialization results*

The response of the subsurface is visible in the SMA zone volumes and release rates as shown in Figure 5.8. The upper zone tension water volume reaches capacity in the beginning of the first storm and twice during the second storm. Each sawtooth on the upper zone graph corresponds to a period of intense precipitation. Water begins to accumulate in the upper free water zone as soon as the tension water is full and a portion of the free water begins to recharge the slow-draining lower zones. The size of each zone in millimeters is indicated on the graphic.

The straight descending lines in the release rate curve on semi-log scale reveal the exponential decay behavior of the SMA zones releases back to the surface (see equations 3.22 and 3.29). Releases are distributed to the various outlets (in this case, an upper and lower outlet

as indicated on Figure 5.1) according to a user input factor. In this case, 25% was sent to the upper outlet and 75% to the lower outlet to demonstrate the possibility of using an uneven distribution.

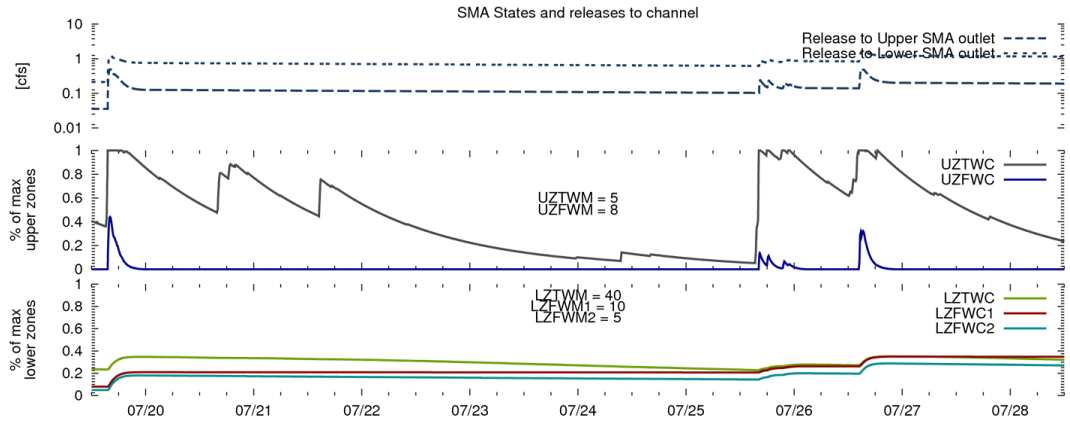


**Figure 5.8: SMA states during simulation of TREX-SMA showing infiltration re-initialization.**

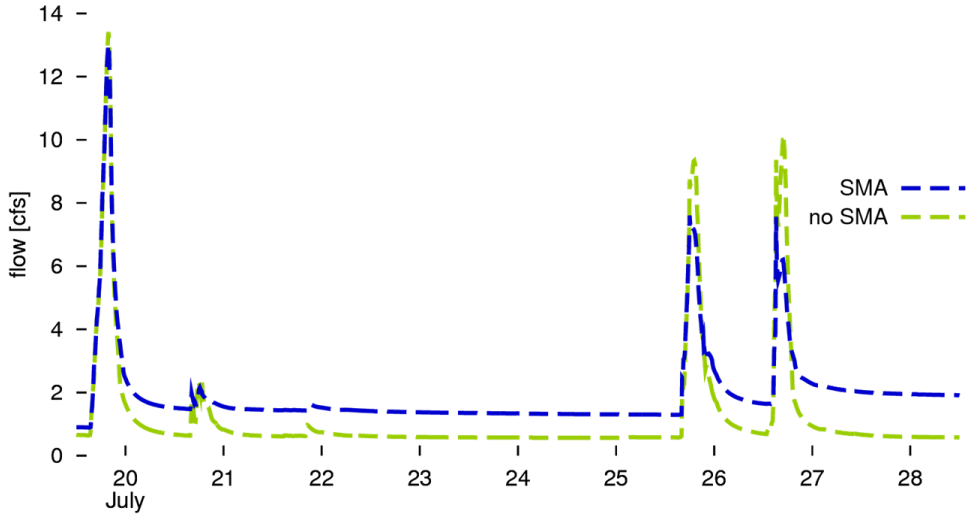


**Figure 5.9: Demonstration of TREX-SMA model effect with infiltration re-initialization.**

Figure 5.9 shows the ability of the model to modify the hydrograph as anticipated. The hydrograph peaks of the later storms are reduced due to the increased infiltration capacity. Using computations based on the soil moisture zone states water is received into the upper zone and

percolated into the lower zone. The figure demonstrates soil moisture recovery in the week-long gap between the two primary events. The inter-event recovery is driven by evapotranspiration and by baseflow and interflow returns back into the channel.

# 6.0 TREX-SMA APPLICATIONS AT CALIFORNIA GULCH (PART II)

TREX-SMA has various capabilities including continuous multi-event modeling. This section describes the application of the TREX-SMA model to a real case at California Gulch in which 50 days of precipitation inputs were used to drive a model simulation. Section 5.4 describes model results using output from a new suite of tools developed to visually analyze and share model results in real-time. Selected results from the model are presented as 3-D perspective inundation extents projected on aerial imagery using Google Earth™. The end of the section presents analysis of the improvements in accuracy of simulation due to the changes introduced in TREX-SMA and discusses some of the sources of uncertainty.

## 6.1 MULTI-EVENT SIMULATION

All surface model parameters for the multi-event simulation draw from model setup as explained in Chapters 4 and 5 as calibrated by Velleux (2005). These calibrated parameters have been used for several event-based simulations of contaminant transport as seen in two papers by Velleux et al. (2006, 2008a) and further discussed by Caruso et al. (2008). Related work in the same basin has also been published by Rojas-Sánchez et al. (2008) and England et al. (2007).

### *6.1.1 Soil moisture zone parameters*

For the hypothetical cases reported in Chapter 5 of the dissertation, the Sacramento model parameters were a hand-tuned set which demonstrated the ability of the model to return flow from the subsurface to the channel. These were within the “acceptable range” as given in table 2.3. The hypothetical cases were simulated using an arbitrarily selected time series of precipitation data as a forcing function and assumed that the Yak tunnel and Leadville WWTP contributed no flow to the channel.

For the multi-event simulation reported in this chapter, the anthropogenic sources of channel flow completely dominated the entire low-flow signature of the basin. Though the model is capable of returning water to the channel from the subsurface storages, it was apparent that very little subsurface return actually occurs at California Gulch—at least, outside of what is controlled directly by the Yak tunnel and any infiltration into the WWTP collection system. So parameters for the SMA zones for the multi-event simulation were drawn from the a-priori dataset described by Koren et al. (2003) and provided by the National Weather Service Arkansas Basin River Forecast Center (ABRFC). This dataset is used by scientists at ABRFC for regional forecasting of lateral inflows using the NWS Distributed Hydrological Model (DHM) (Koren et al. 2004). The purpose of not calibrating was to show that this model hybridization could be used in other watersheds in a similar fashion, e.g., by obtaining already-calibrated parameter sets for the independent models, then combining these into a single hybrid model. Research into different techniques for calibration (e.g., Gupta et al. 1998) is certainly valuable, but is not part of this dissertation.

The parameter values are determined a priori using soils and land use data. For this research, the parameters from the three 4km x 4km grid cells aligned east and west nearest to Leadville (those most nearly corresponding to the California Gulch watershed area) were averaged to provide values for use in modeling.

**Table 6.1: Soil moisture accounting parameters used for multi-event model simulation.**

| No. | Parameter | Description | Used for Model | Acceptable Ranges |
|---|---|---|---|---|
| 1 | UZTWM | The upper layer tension water capacity, mm | 52 | 10–300 |
| 2 | UZFWM | The upper layer free water capacity, mm | 43 | 5–150 |
| 3 | UZK | Interflow depletion rate from the upper layer free water storage, $day^{-1}$ | 0.51 | 0.10–0.75 |
| 4 | ZPERC | Ratio of maximum and minimum percolation rates | 45 | 5–350 |
| 5 | REXP | Shape parameter of the percolation curve | 1.54 | 1–5 |
| 6 | LZTWM | The lower layer tension water capacity, mm | 240 | 10–500 |
| 7 | LZFSM | The lower layer supplemental free water capacity, mm | 17.3 | 5–400 |
| 8 | LZFPM | The lower layer primary free water capacity, mm | 219 | 10–1000 |
| 9 | LZSK | Depletion rate of the lower layer supplemental free water storage, $day^{-1}$ | 0.180 | 0.01–0.35 |
| 10 | LZPK | Depletion rate of the lower layer primary free water storage, $day^{-1}$ | 0.0473 | 0.001–0.05 |
| 11 | PFREE | Percolation fraction that goes directly to the lower layer free water storages | 0.080 | 0.0–0.8 |
| 15 | SIDE | Ratio of deep percolation from lower layer free water storages | 0.99 | Not given |
| 16 | RSERV | Fraction of lower layer free water not transferable to lower layer tension water | Not used in TREX-SMA | |

### *6.1.2 Precipitation*

A series of nine storms from summer 2006 were used as input to test the multi-event simulation capabilities of the TREX-SMA model. The first and most intense storm in the series occurred on July 19 (the same used for the baseflow modeling simulation). The subsequent storms occurred on a roughly weekly basis following the first storm on: July 25/26, July 30/31, August 5/6, and August 10/11 as shown in Figure 6.2. All of these storms occurred when snowmelt influences on streamflow in California gulch had largely subsided for the summer.

During the July 19 storm, the most intense precipitation was measured in Stray Horse Gulch at the SHG-09A gauge, registering 0.4 inches in ten minutes, equivalent to an intensity of 2.4 inches per hour. For comparison, a 100-year, two-hour storm for the watershed would occur with approximately 0.87 inches per hour, distributed over the watershed (Simons and Associates, Inc. 1997).

The observations at the four different precipitation gauges show that the storms vary in geographic distribution. Throughout the summer, storms were recorded in which not all gauges received precipitation. Many of these were biased toward the upper watershed (near CG-1 and

SHG-09A). For instance, Storm 5b was an upper watershed storm which generated significant flow at CG-1 but at no other gauge (visible as a green spike near the axis of the graph on August 6). A simple weighting scheme placing the centroid of the total precipitation along the east-west axis of the watershed classified each storm as primarily upper or lower watershed. The precipitation totals and relative axial position are plotted in Figure 6.1.

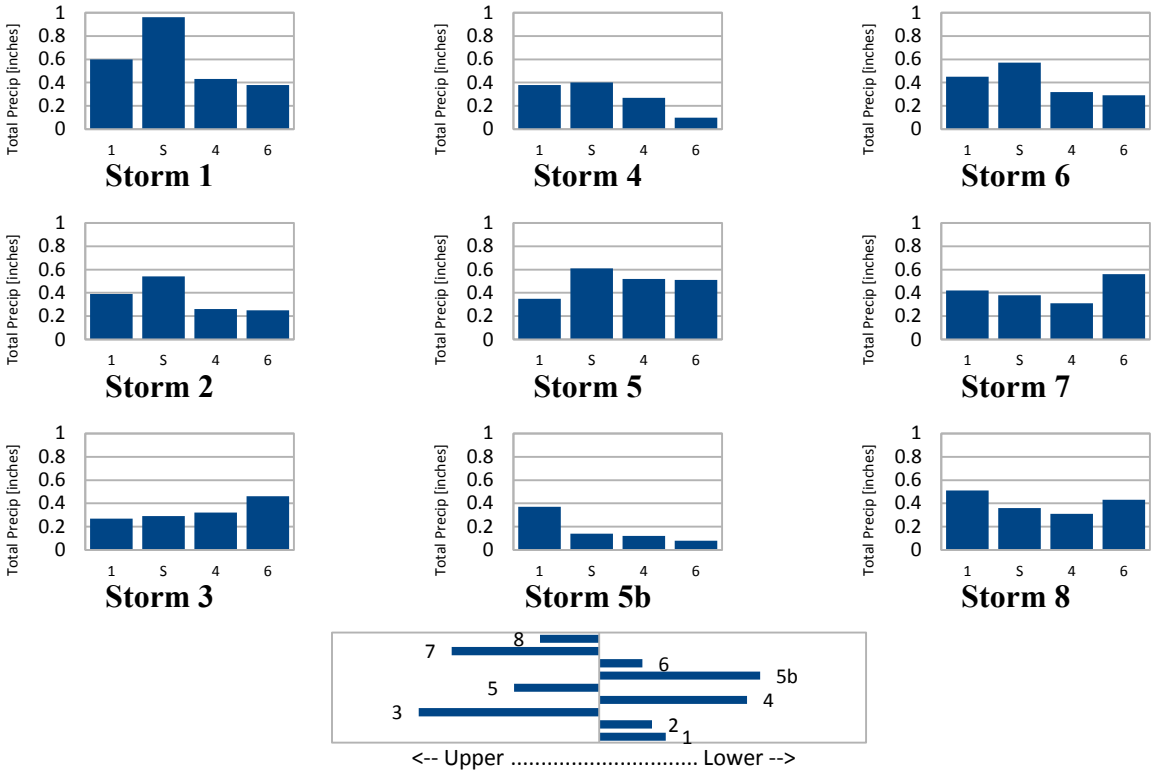


**Figure 6.1: Total precipitation during each of the identified storms and general classification as upper or lower watershed storms. Precipitation at CG-1, SHG-09A, CG-4, and CG-6 are indicated by "1," "S," "4," and "6," respectively.**

### *6.1.3 Flow Observations*

Observed flow rates in California Gulch vary widely at the different gauges. The largest recorded flow during the summer of 2006 at any gauge was 24 cfs at CG-4, associated with the July 19 storm. The upper watershed channels (measured at CG-1 and SHG-09A) are entirely ephemeral and only bear flow during precipitation events. The lower watershed exhibits

perennial flow. However, it was noted in the preparation of the simulation, that what is apparently baseflow at gauges CG-4 and CG-6 is actually composed almost entirely of discharge from the Yak tunnel treatment plant and the Leadville WWTP. In order to account for this, the SIDE parameter, which determines the percentage split of water between channel returns and deep groundwater losses, was adjusted to 99% so that only 1% of the infiltrated water in the SMA zones actually returned to the surface. The rest was lost to deep groundwater, presumably contributing to flow in the Arkansas River.

Regarding the variability of flow, it is interesting to note that while rainfall amounts were not hugely variable (Figure 6.1 shows Storms 2, 4, 5, 6, 7, and 8 with similar total amounts), the different peak rainfall intensities observed, produced large variation in the peak flow rate at each gauge indicating the dominant effect of direct surface runoff on the hydrographs.

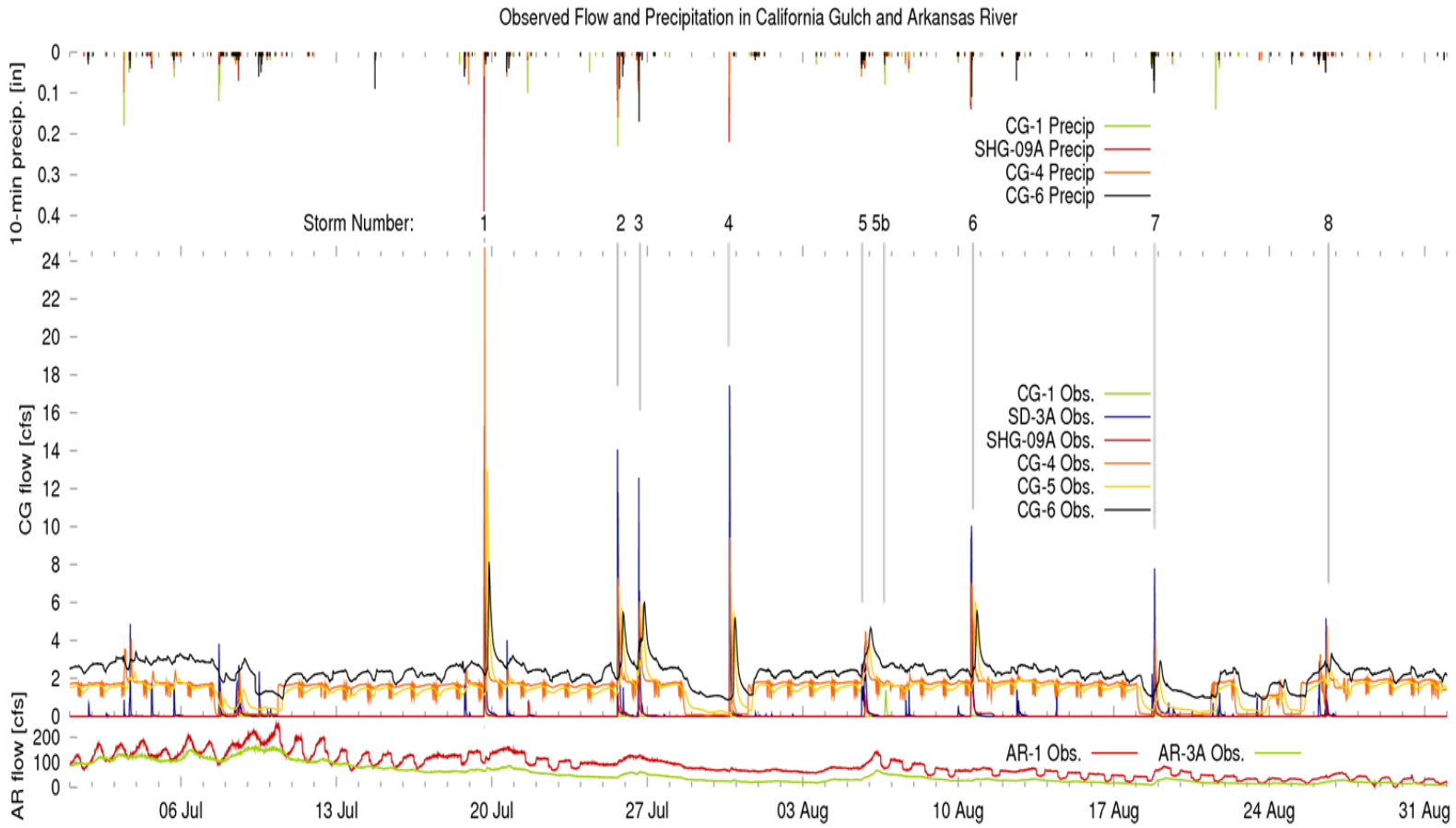


**Figure 6.2: Observed flow and precipitation at California Gulch and Arkansas River for multi-event simulation. Observed precipitation is the driving input for the model; simulated results are compared to streamflow observations.**

## 6.2 MULTI-EVENT SIMULATION RESULTS

The multi-event simulation was carried out twice: once with the SMA submodel active, resetting the infiltration parameters at appropriate times, and once again with no infiltration resetting. As previously, the simulations and their respective results are distinguished in the discussion of this section as "SMA" and no-"SMA."

### *6.2.1 Hydrographs*

The basin hydrologic response is captured most succinctly in the hydrographs showing the flow as a function of time through the simulated period. As expected, the TREX-SMA simulation reduces the simulated hydrograph peaks, especially for storms later in the series as the SMA zones dry out toward the end of summer. Figure 6.3 shows the aggregate basin response at CG-6 (the watershed outlet to the Arkansas River) for simulations with and without the SMA sub-model. Observed flows are also shown on the plot, for comparison to the simulated flow. The graphical evidence of the reduced peaks shown in these figures is the most convincing measure of the improvement brought with the SMA re-initialization procedure. For most storms, the green line (no-SMA) over-predicts the basin response while the reduced SMA peak corresponds more closely to the observed flow. Flows in the inter-storm periods are largely controlled by the YAK tunnel releases which are included in the model input.

Figures 6.4 a–c show the modeling results with and without the active as well as the observed streamflows as measured at the CG-1 and SHG09-A gauges in the upper watershed and at the CG-4 gauge in the middle watershed.

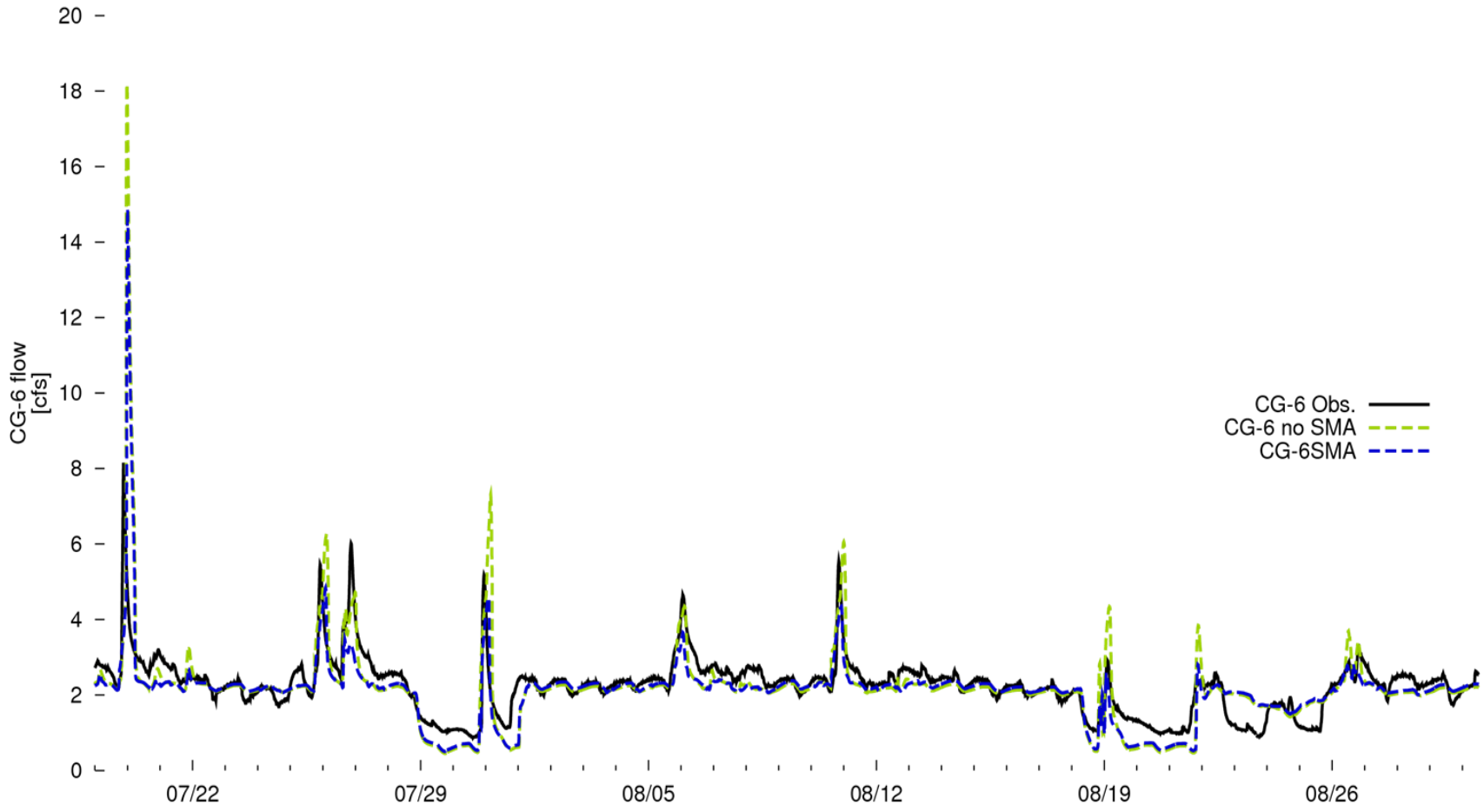


**Figure 6.3 Simulated TREX-SMA (blue), TREX without SMA (green), and observed hydrographs (black) for California Gulch model results at CG-6—just above the watershed outlet at the Arkansas river during multi-event simulation period, July 19–August 31, 2006. Flows at this gauge are not affected by Arkansas backwater.**

**Figure 6.4 a)**

**CG-1—Upper California Gulch**

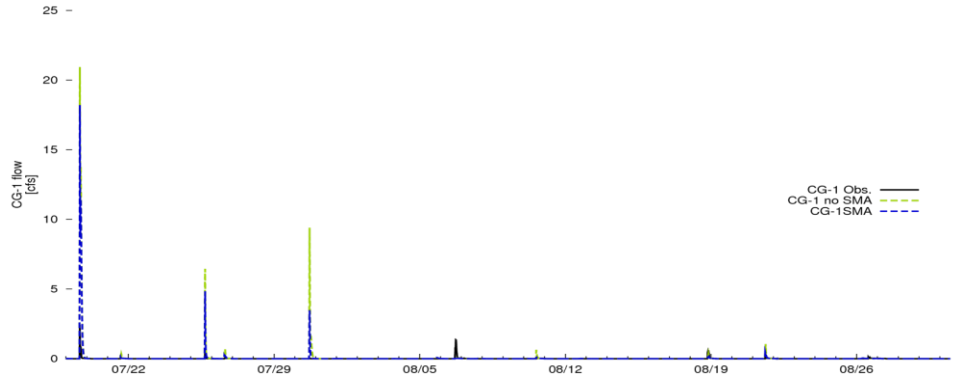


**b) SHG-09A —Stray Horse Gulch above Leadville**

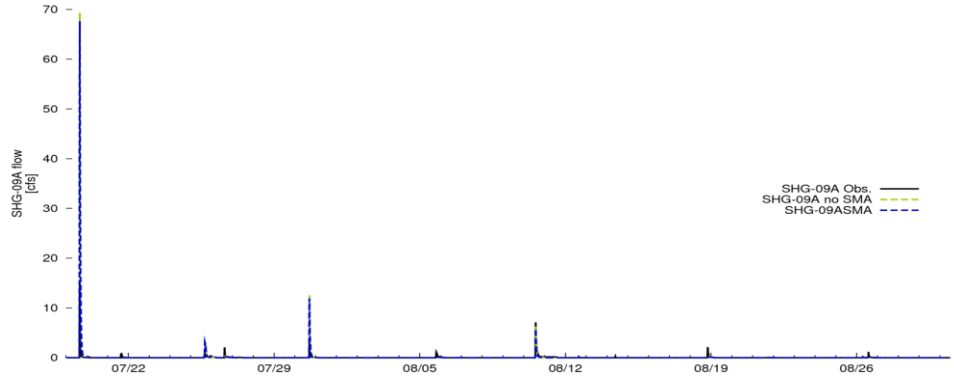


**c) CG-4—California Gulch below Starr Ditch where majority of Leadville urban runoff enters channel**

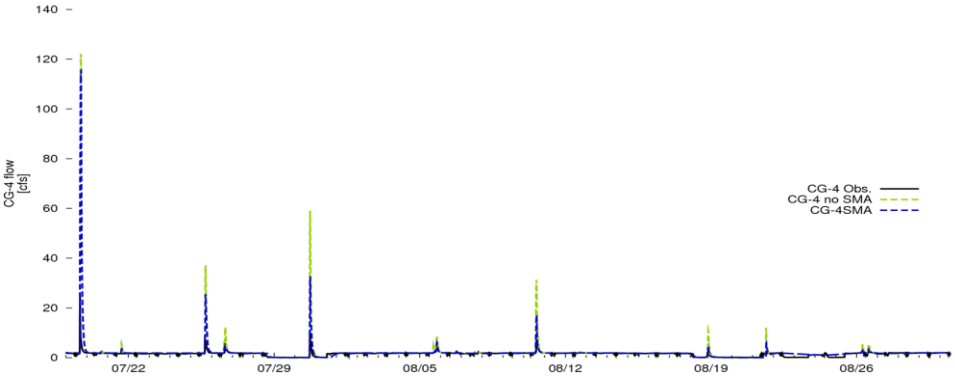


**Figure 6.4 a–c: Simulated TREX-SMA (blue), TREX without SMA (green), and observed hydrographs (black) for California Gulch sub-watershed areas during multi-event simulation period, July 19–August 31, 2006.**

Generally speaking, the hydrographs show that the TREX-SMA model has reduced the over-prediction of peaks. Only the SHG-09A hydrograph seems unmodified—the soil types in that portion of the watershed have such low infiltration rates that the differences in soil moisture do little to increase or decrease the infiltration.

At the CG-6 gauge, the second and third storms form a pair, which illustrate some of the idiosyncrasies of the model. Of the pair, both were reduced in magnitude by the re-initialization procedure; but the later storm was surprisingly reduced more, not less, than the earlier storm. (We would expect that the second storm would occur in more saturated conditions and produce more runoff.)

The inter-event periods show apparently very good fit to observed data for both SMA and no-SMA cases. The low-flows are strongly correlated to observed flows to the discharges from the Yak tunnel and Leadville waste water treatment plants, which were known and included as model inputs.

### *6.2.2 Real-time hydrograph output*

During the execution of this research, a technique was developed to allow model results to be displayed in real-time as the simulation progresses. A simple function was added to the code to compute and record the actual date and time where previously, only elapsed time from start was recorded. As the simulation progresses, a plotting program, gnuplot (Janert 2010), produces a hydrograph plot based on the output data file. Where observed data are available, these may be plotted as well. The plots generated with gnuplot may be viewed through a web page and can automatically be refreshed to show changes in output. Simple web tools juxtapose the plots for rapid evaluation of model progress. Figure 6.5 gives an example of such a plot. A grid containing all 108 plots from the multi-event simulation (nine events and six stations each with a

hydrograph and statistical summary) is found in Appendix D. The simulated hydrograph for the SMA case is reduced due to the re-initialized soil moisture state preceding the event.

The residual plot in Figure 6.5 shows much less deviation from zero for the SMA case than for no-SMA and the statistics on the super-imposed table are reasonable as well with all statistics for this storm showing significant improvement. The explanation requires that we recall the distribution of rainfall as shown in Figure 6.1 and Figure 5.7, and that we consider the conditions of calibration from the Rojas-Sánchez (2002) and Velleux (2005; also Velleux et al. 2008a). The September 2003 event used to validate the surface parameters was an upper watershed storm similar to Storm 4; we would expect that the surface parameters would predict the watershed response well in this case, similar to the calibration and validation.

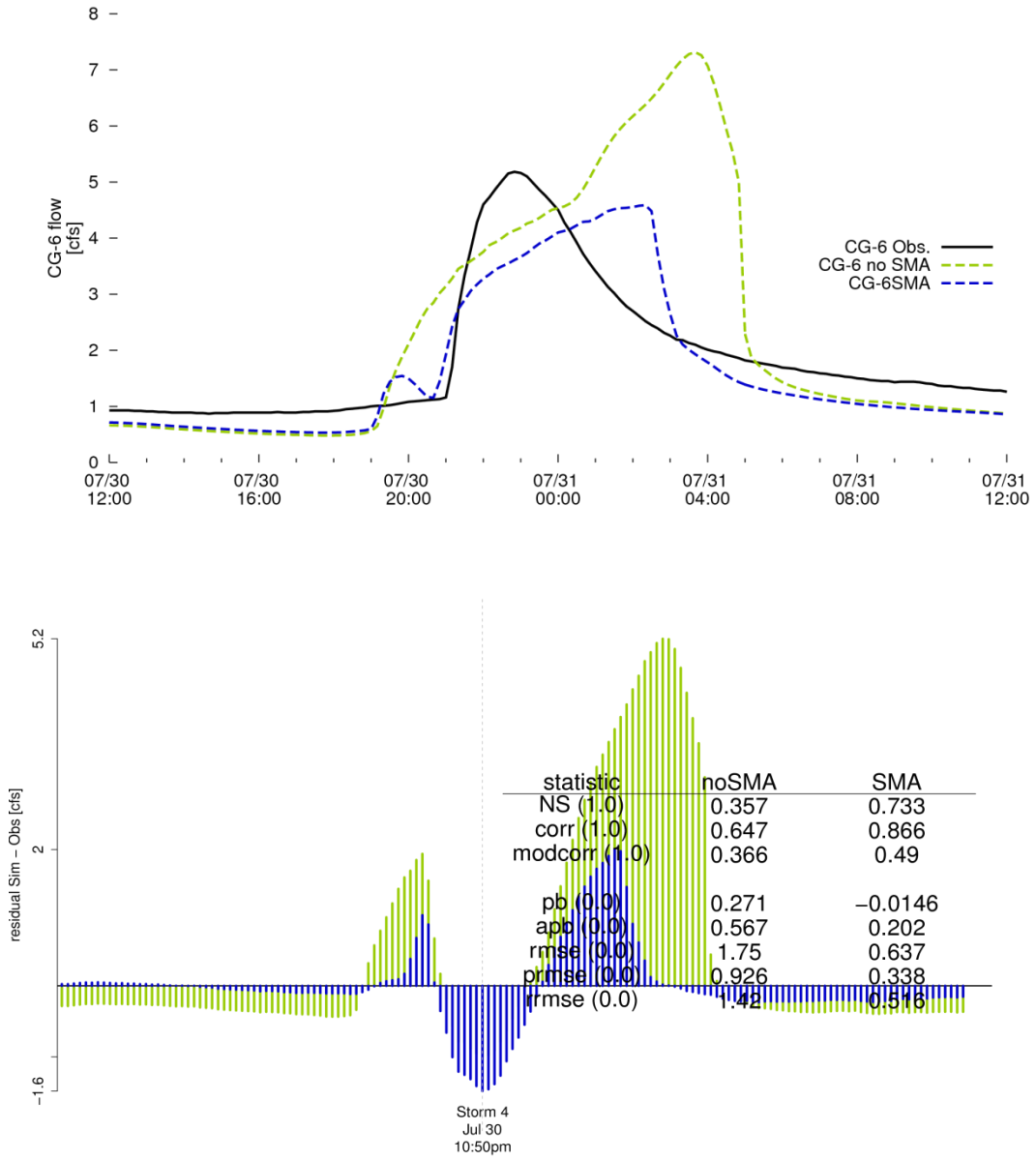


**Figure 6.5: Zoomed-in hydrograph from Storm 4 from the multi-event simulation.**

### *6.2.3 Results display Google Earth and KML*

In order to further evaluate the simulation results, three-dimensional interactive results display was implemented using Google Earth and the Keyhole Markup Language (KML). Google Earth ™ is a web-based "virtual globe" which shows a 3-D view of the earth's surface in varying resolutions based on various sources of aerial imagery and digital terrain models. The

Keyhole Markup Language is an xml-based scripting language designed to allow display of text and graphics on a virtual globe such as Google Earth (Whitmeyer et al. 2010).

To use Google Earth to display TREX-SMA results, grid cell values of the land surface and channel water depth were exported from the model simulation at given time intervals as raster images and these images were ingested into a GRASS GIS database (Neteler and Mitasova 2008). The maps were colorized according to the data values for each cell and then exported as a flat graphic which is referenced as a ground overlay in a simple KML file. The KML file specifies the spatial and temporal extent of the overlay (e.g. an overlay may represent the average model states from July 30, 2006 12:00 a.m. to 12:10 a.m. and have a north, south, east, and west maximum extent). The KML time points were specified along with an offset from GMT and positions using latitude and longitude. The appropriate KML tags were inserted to specify the transparency of each overlay to allow partial viewing of the standard Google Earth aerial image underneath the overlay showing the modeled value. The ground overlays were produced to show depth of flow (on the land surface and in channels) but could show any other distributed variable from the TREX-SMA output.

Viewing the model output in the context of the geography and other imagery is useful for at least two reasons. First, the visual comparison of topography and other geographic and spatial features allows for a rapid evaluation of the success of the simulation. Model output is visually compared to expectation similar to the visual comparison on observed and simulated hydrographs on a plot. Second, the primary consumers of the information from a hydrologic model will have questions with specific respect to location of effects such as overbank flow, points of maximum velocity, and scour problem areas. All of these effects may be evaluated with the TREX-SMA model.

The Google Earth viewer allows browsing of the series of overlays both in time and space. Any area may be highlighted for close viewing and the entire series may be animated or a particular time chosen using a time selector in the Google Earth interface. Other data such as gauge locations may be inserted for additional context.

Figure 6.6, shows the runoff being generated by the impermeable surfaces in the city of Leadville and in the upland areas where rainfall was most intense for a storm on July 30, 2006. The slider bar in the upper left corner of the graphic is the time selector. The flood wave can be seen developing in the various subwatershed channels below the city. Gauge locations may also be linked to the hydrograph and statistical plot images associated with different time spans as shown in Figure 6.7. This side-by-side view brings the detailed analysis directly into the picture of the entire watershed.

The Google Earth interface also allows for the series of individual frames to be animated showing evolution of model processes over time. Figure 6.8 displays a series of frames from such an animation generated from the simulation output for the storm occurring on July 30, 2006. The animation shows movement of the different flood waves and can help in analyzing the watershed flood generation mechanism. For instance, in Figure 6.8 and Figure 6.9, the lower permeability of the bare upland soils is evident in that ponded water is still present well into the simulation when only the impervious surfaces in Leadville city are still producing runoff. The concentration of impervious surfaces combined with the fact that the storm centered on the upper watershed to produce a sharp runoff peak.

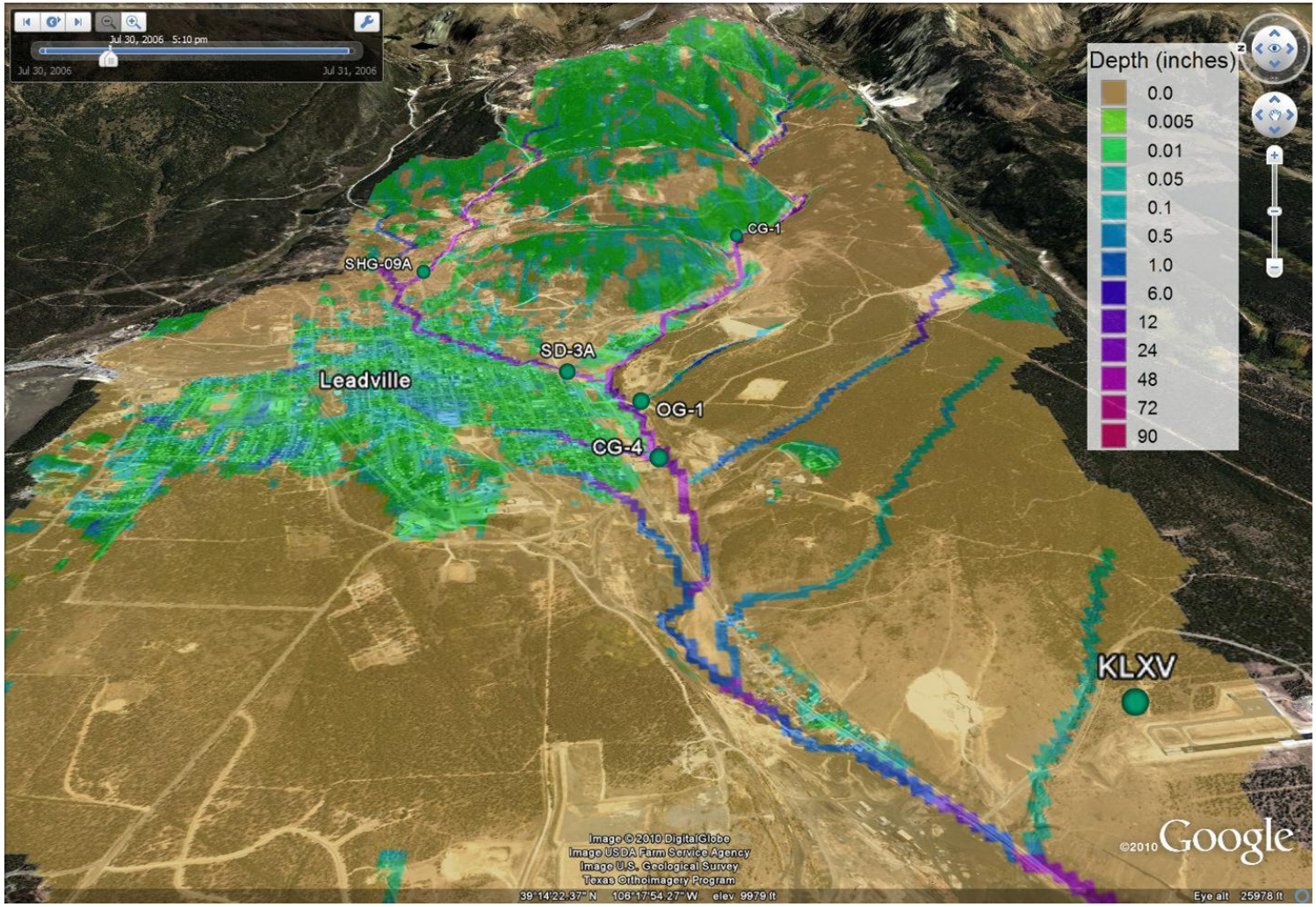


**Figure 6.6: Simulated depth of flow on the land surface and in channels at California Gulch for July 30, 2006, 5:10 p.m., shortly after cessation of rainfall. Upland areas receive intense rain but also have a high infiltration rate which creates the piebald arrangement of wet and dry areas.**

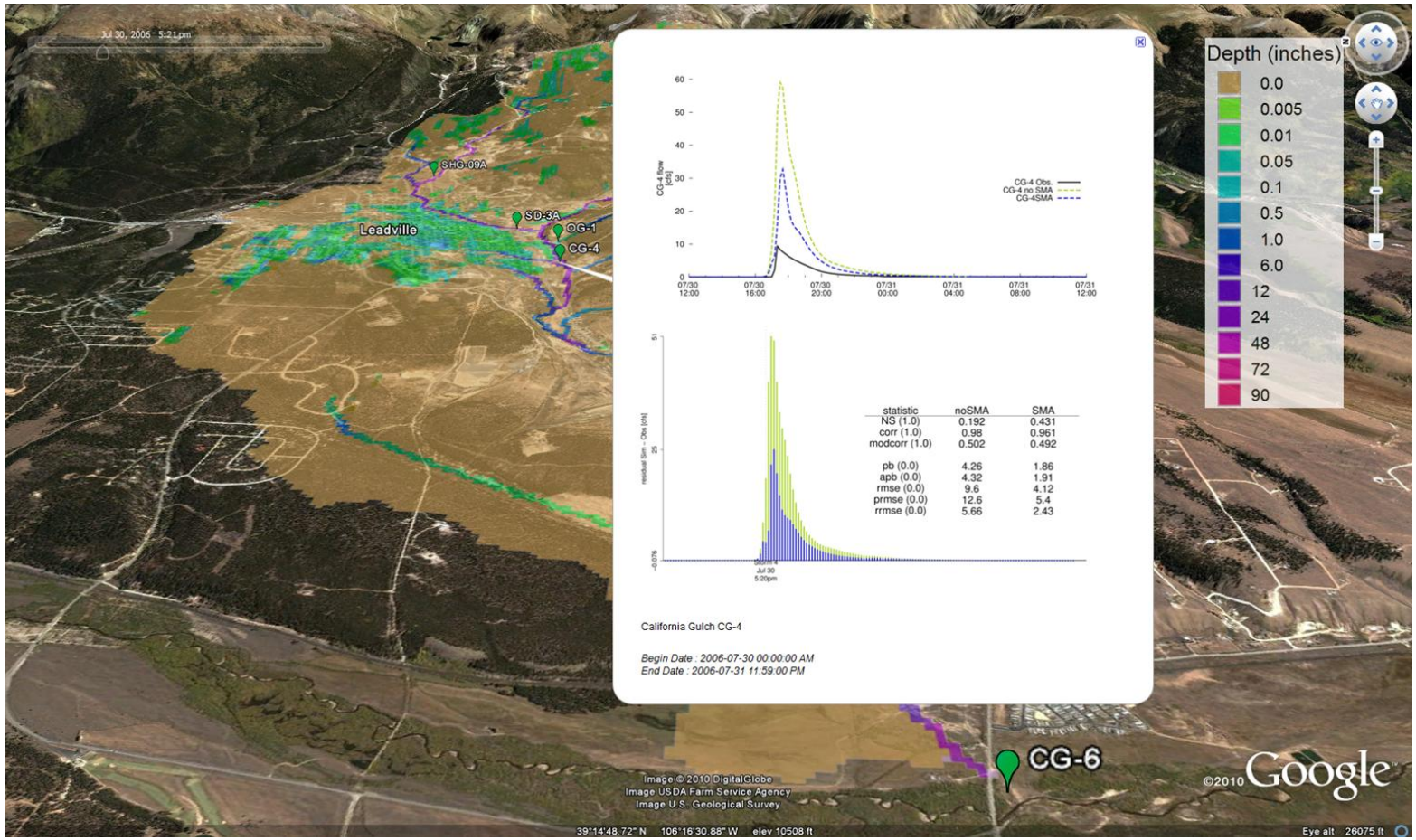


**Figure 6.7: Example of statistical plots dynamically connected to gauge positions using KML scripting and Google Earth. Callout balloon in center shows hydrograph and statistical information for CG-4 during Storm 4. The water depth display is for 5:20 p.m. on July 30, when the observed peak passed CG-4. The simulated peak lagged the observed slightly and can be seen passing through the channel just upstream of the confluence of California Gulch and Stray Hors Gulch, below SD-3A.**

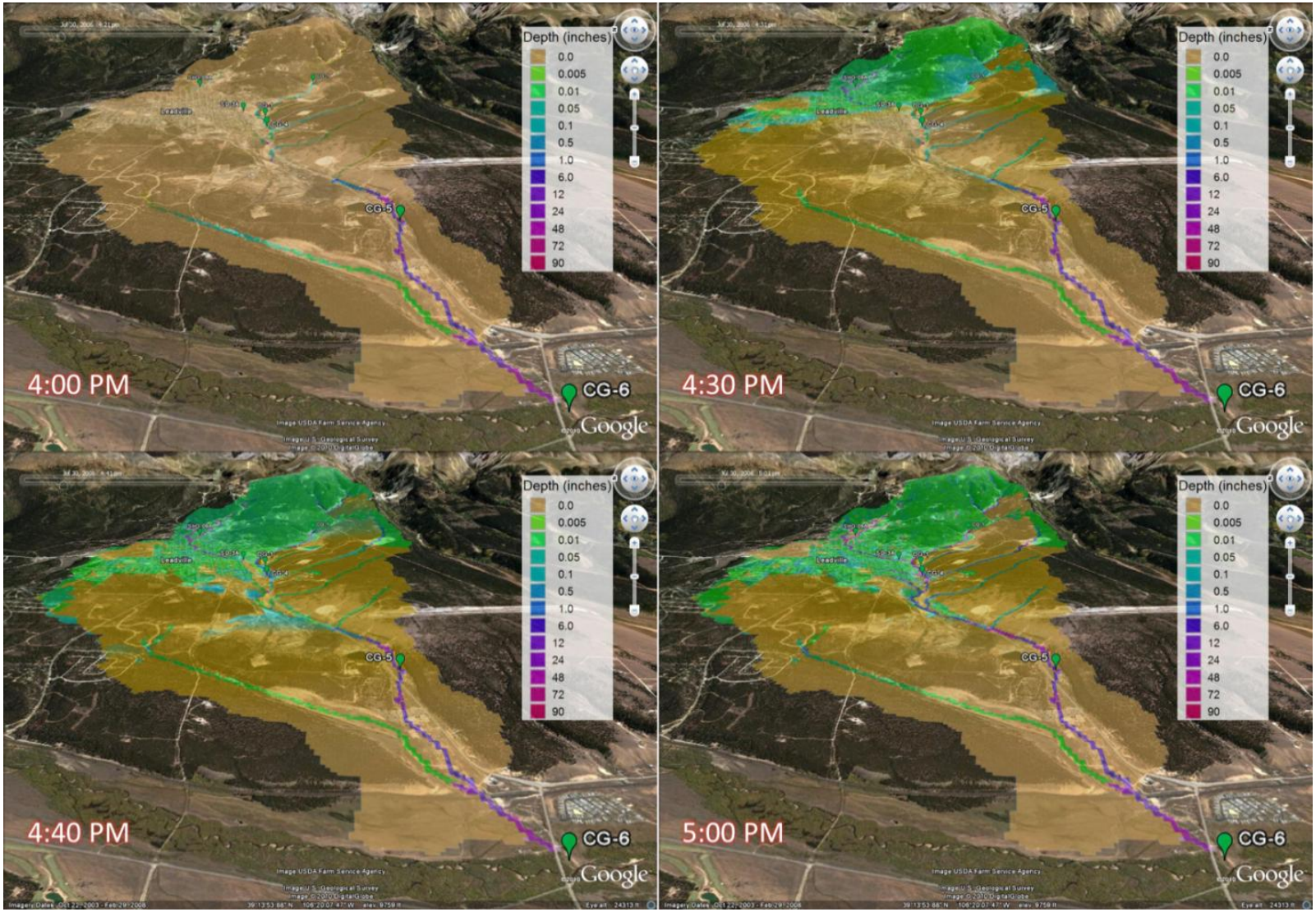


**Figure 6.8: Selected frames from loop sequence showing depth of water on land surface using the Google Earth and KML scripting techniques described in this chapter.**

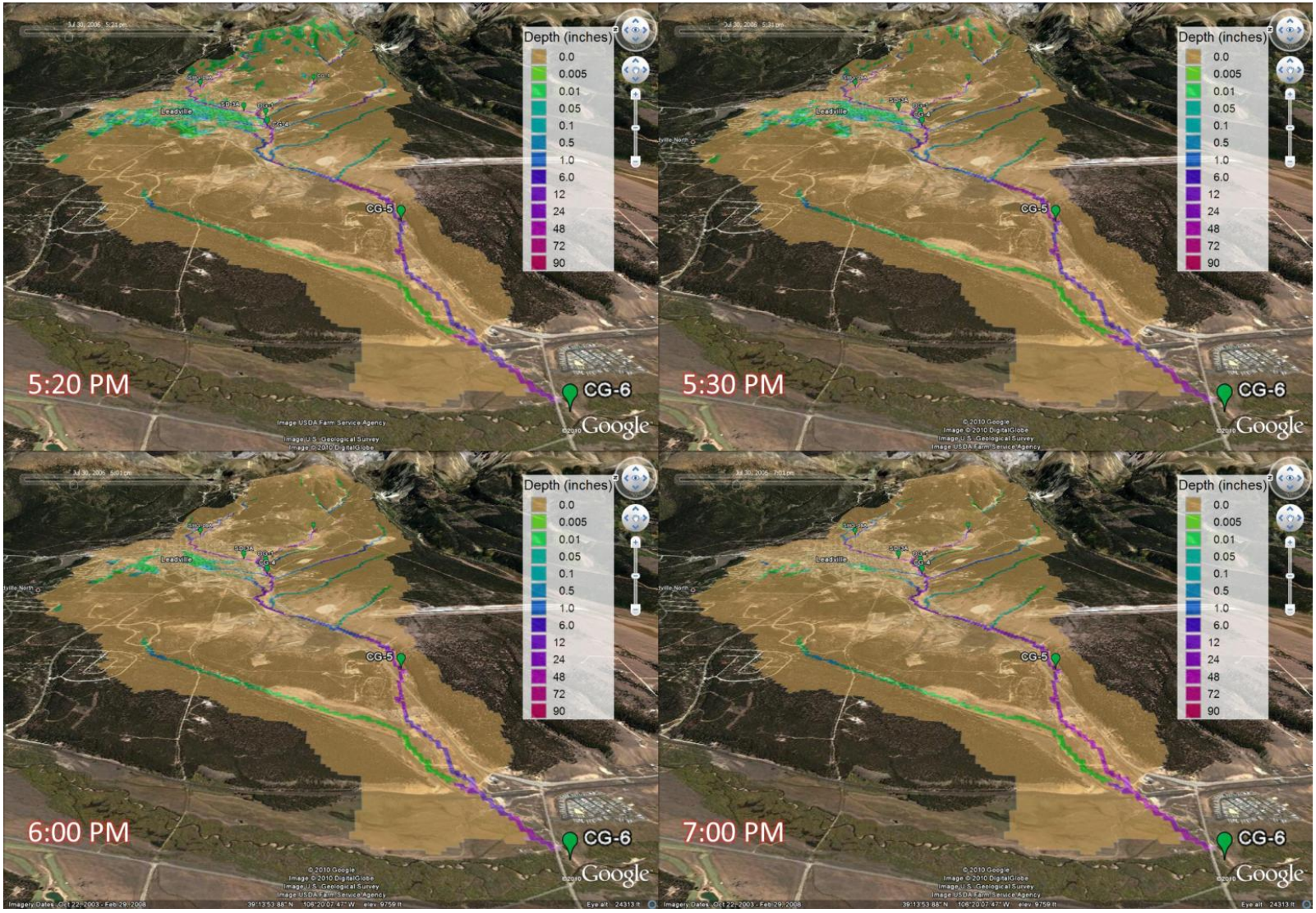


**Figure 6.9: Additional frames from loop sequence showing depth of water on land surface and in the channel.**

### *6.2.4 Overall Statistical Performance*

For this research, little calibration was performed since parameter values were derived from established sources. Therefore, statistical performance is an indication of what may be achieved with a direct hybrid. Joint calibration of the hybrid model was not feasible as part of this research: each 50-day simulation requires two–three days of computing time, and the hundreds of simulation runs necessary to perform manual (or automatic) calibration would require years of computing time. Automatic calibration has not currently been incorporated with the TREX-SMA model though the technical advances described in this research allow more rapid evaluation of model output.

Each of the statistical parameters presented in section 2.3.3 was computed to compare the observed and simulated time series for the with- and without-soil moisture accounting simulations as shown in Table 6.2. The number of gauges which showed improvement for each statistical measure is given in the final column of the table.

**Table 6.2: Statistical analysis of multi-event model showing improvement at nearly all gauges.**

| | cg-1 | | cg-4 | | cg-5 | | cg-6 | | sd-3A | | shg-09A | | Number Improved with SMA |
|---|---|---|---|---|---|---|---|---|---|---|---|---|---|
| Statistic (Optimal Value) | No SMA | SMA | No SMA | SMA | No SMA | SMA | No SMA | SMA | No SMA | SMA | No SMA | SMA | |
| NS (1.0) | 0.12 | 0.16 | 0.17 | 0.19 | 0.27 | 0.04 | 0.44 | 0.46 | 0.29 | 0.25 | 0.28 | 0.31 | 4 |
| corr (1.0) | 0.65 | 0.66 | 0.60 | 0.56 | 0.74 | 0.71 | 0.67 | 0.70 | 0.67 | 0.57 | 0.81 | 0.82 | 3 |
| modcorr (1.0) | 0.45 | 0.46 | 0.48 | 0.46 | 0.54 | 0.52 | 0.49 | 0.52 | 0.60 | 0.51 | 0.74 | 0.75 | 3 |
| pb (0.0) | 6.60 | 4.02 | 0.31 | 0.25 | 0.44 | 0.48 | -0.03 | 0.00 | 0.97 | 0.42 | 1.79 | 1.35 | 6 |
| apb (0.0) | 7.44 | 4.93 | 0.37 | 0.31 | 0.46 | 0.50 | 0.15 | 0.13 | 1.49 | 1.36 | 2.53 | 2.24 | 5 |
| rmse (0.0) | 0.58 | 0.39 | 4.16 | 3.33 | 1.29 | 1.08 | 0.78 | 0.57 | 2.51 | 2.31 | 1.33 | 1.19 | 6 |
| prmse (0.0) | 102.00 | 69.20 | 2.79 | 2.24 | 0.89 | 0.75 | 0.36 | 0.26 | 22.20 | 20.50 | 44.00 | 39.40 | 6 |
| rrmse (0.0) | 9.45 | 6.39 | 4.93 | 3.96 | 1.69 | 1.42 | 1.14 | 0.83 | 3.19 | 2.93 | 4.26 | 3.81 | 6 |

A majority of all gauges showed improved Nash-Sutcliffe efficiency and correlation. All gauges improved in percent bias and root mean squared statistics for the SMA relative to the no-

SMA case. Unfortunately, as shown in Table 6.3, even though the parameters showed improvement, the only parameter with values in the "satisfactory" range was percent bias. It is notable that the gauge with the best performance was CG-6 with a Nash-Sutcliffe index of 0.46 for the SMA simulation. This is likely due to the fact that the overland flow parameters had been originally calibrated primarily for the response at this gauge.

**Table 6.3: Optimal and Satisfactory values of key statistics (cf. Table 2.1).**

| Statistic Name | Abbreviation | Optimal | Satisfactory | Number in range no-SMA | Number in range SMA |
|---|---|---|---|---|---|
| Nash-Sutcliffe Efficiency Index | NS | 1.0 | > 0.50 | 0 | 0 |
| Pearson Correlation Coefficient | corr | 1.0 | | - | - |
| Modified Correlation Coefficient | modcorr | 1.0 | | - | - |
| Percent Bias | pb | 0.0 | < 0.70 | 3 | 4 |
| Absolute Percent Bias | apb | 0.0 | | - | - |
| Root Mean Squared Error | rmse | 0.0 | | - | - |
| Percent Root Mean Squared Error | prmse | 0.0 | | - | - |
| RMSE Ratio | rrmse | 0.0 | < 0.50 | 0 | 0 |

In addition to the gnuplot output showing hydrographs, a similar technique was developed to display real-time statistical information about the model run underway. The technique produces statistical plots and descriptive statistics using the open-source statistical program, called ‘R’ (R Development Core Team 2010). Simple web scripts direct R to read and incorporate observed data with the live model results to generate plots showing correlation, time-corrected peak correlation, and residual. Each plot includes a superimposed table with the Nash-Sutcliffe coefficient, percent bias, absolute percent bias, RMSE ratio, and other descriptive statistics.

The R statistical plots and gnuplot hydrograph plots may be easily combined for display to show model performance across a range of gauges and storm events as already shown in Figure 6.7.

As noted in section 2.3.4, an inverse hyperbolic sine transform can make possible the interpretation of both large and small variations in a residual plot. Figure 6.10 shows an example from gauge CG-6 with the full series from the multi-event simulation.

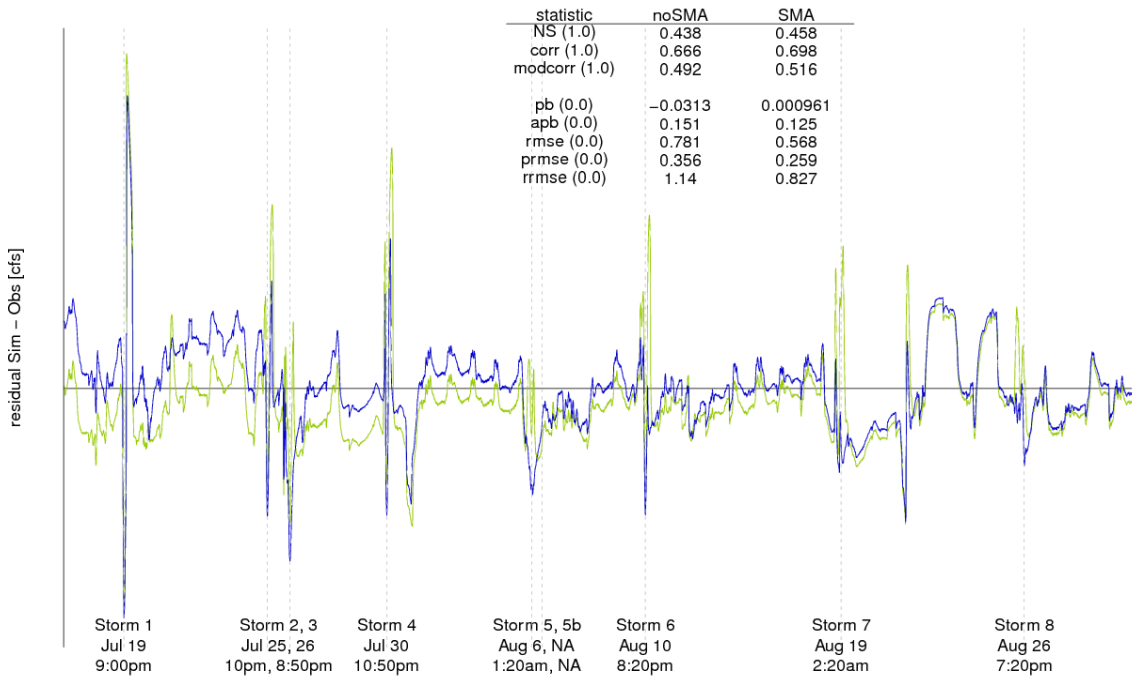


**Figure 6.10: Residual plot with inverse hyperbolic sine (arcsinh) scaling. The arcsinh transform enhances visibility of inner values for a series with both positive and negative values.**

### *6.2.5 Peaks and flow correlations*

Some of the error between the observed and simulated values is a result of timing errors. For each of the storms, the peak simulated flow rate was compared to the peak observed flow rate regardless of timing. These "time-corrected" peaks are plotted in Figure 6.11 and further tabulated in Table 6.5. The plots also show the correlation of all flows in the simulated series with observed and give a 1:1 correlation line for reference. Generally the peak values can be seen to move toward better agreement with observations with the TREX-SMA model.

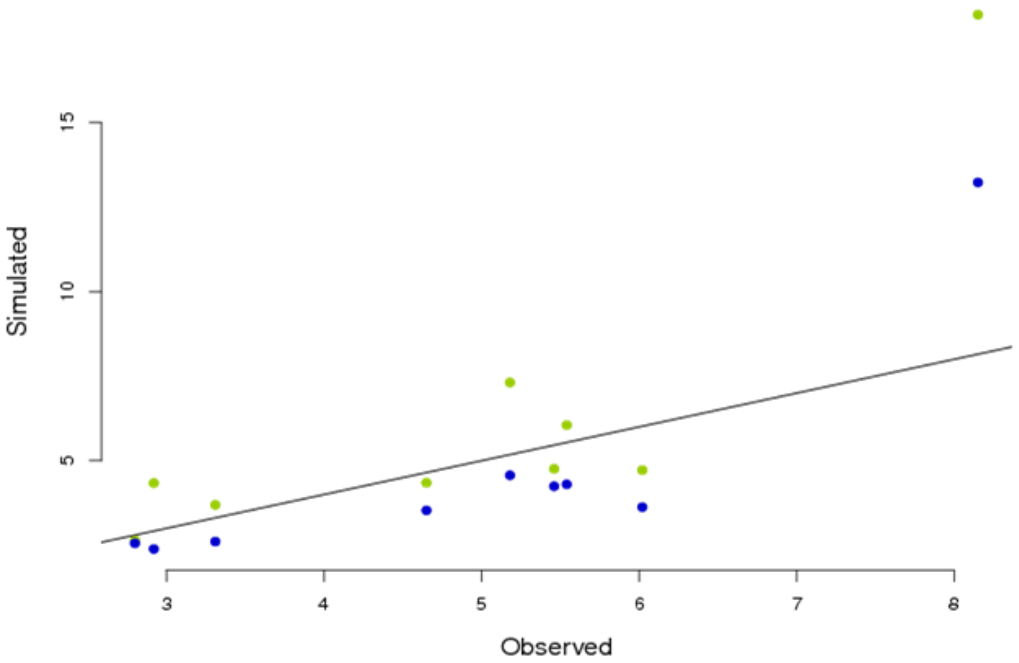


**Figure 6.11: Flow correlation at CG-6. Blue indicates simulations performed with the SMA model active and green without. The simulated peaks are time-corrected to correlate with the individual observed peaks.**

The peak flows in Figure 6.10 have been correlated to take the maximum flow from each simulation for the given storm, regardless of timing. This ensures that the actual scale of the forecast peak flow may be accurately compared. The peaks from the SMA runs are clearly reduced for all gauges; for CG-1, SHG-09A, CG4, and CG-5, this reduction apparently brings the peak value closer to the 1:1 line meaning that the values are closer to observed. Peaks for SD-3A and CG-6 SMA simulations are shifted lower but the correlation is then reduced, because the no-SMA values are relatively close to the 1:1 line. Similar patterns are visible in the plots of Figure 6.10 except that the looping obscures some of the correlation. The looping is caused by timing errors between simulated and observed flows.

**Table 6.4: Improvement in peak flow values at CG-6 for TREX-SMA model compared to TREX only.**

| Storm | Peak Flow | | | Percent Error | | Absolute Error | | |
|---|---|---|---|---|---|---|---|---|
| | Observed | noSMA | SMA | noSMA | SMA | noSMA | SMA | |
| Storm1 | 8.15 | +10.04 | +5.08 | 123% | 62% | 10.04 | 5.08 | + |
| Storm2 | 5.46 | -0.70 | -1.22 | -13% | -22% | 0.70 | 1.22 | - |
| Storm3 | 6.02 | -1.30 | -2.39 | -22% | -40% | 1.30 | 2.39 | - |
| Storm4 | 5.18 | +2.13 | -0.61 | 41% | -12% | 2.13 | 0.61 | + |
| Storm5 | 4.65 | -0.30 | -1.12 | -7% | -24% | 0.30 | 1.12 | - |
| Storm5b | 2.8 | -0.15 | -0.24 | -5% | -9% | 0.15 | 0.24 | - |
| Storm6 | 5.54 | +0.51 | -1.24 | 9% | -22% | 0.51 | 1.24 | - |
| Storm7 | 2.92 | +1.42 | -0.53 | 49% | -18% | 1.42 | 0.53 | + |
| Storm8 | 3.31 | +0.38 | -0.70 | 12% | -21% | 0.38 | 0.70 | - |

Improvement is noted in the final column of the table denoted with a "plus" (+) to indicate an absolute improvement, or if the SMA case has a smaller absolute difference but has overshot so that the error is of the opposite sign. A "minus" (-) indicates that the SMA case has a larger absolute error than the no-SMA case. For the correlation: Out of 54 evaluations, 25 are absolutely improved, four are marginally improved, and 25 did not improve. If we consider the upper watershed storms only (Storms 1, 2, 4, 5b, and 6), we expect that the improvement will be more marked since the surface parameters were calibrated for the lower watershed storm. Table 6.5 shows that all of the upper watershed storms perform well; of 30 SMA evaluations, 20 show improvement, one is marginally improved, and only nine have reduced performance over the no-SMA cases.

### *6.2.6 Individual storm analysis*

One important measure of the performance of the multi-event simulation is the performance during individual storms within the simulation. If a full calibration scheme were to be carried out with this model, the fit for the individual storms could be used as an indicator statistic to guide the parameter selection. Table 6.5 gives Nash-Sutcliffe efficiencies for the 24-hour period surrounding each of the major storms during the multi-event simulation period. As with the peak

matching, the performance indicated by the Nash-Sutcliffe statistic shows an improvement for a majority of upper watershed storms, 1, 2, 4, 5b, and 6. Out of 30 upper watershed evaluations (five gauges, six storms) 17 showed improvement for the SMA case. It is clear that the reduction in the peaks due to the soil moisture re-initialization is an over-correction in some cases. A complete table with numerous statistics for each gauge during each storm is found in Appendix D.

**Table 6.5: Nash-Sutcliffe efficiency values for individual storms from multi-event simulation.**

| | cg-1 | | | sd-3A | | | shg-09A | | | cg-4 | | | cg-5 | | | cg-6 | | |
|---|---|---|---|---|---|---|---|---|---|---|---|---|---|---|---|---|---|---|
| **Storm** | **No SMA** | **SMA** | | **No SMA** | **SMA** | | **No SMA** | **SMA** | | **No SMA** | **SMA** | | **No SMA** | **SMA** | | **No SMA** | **SMA** | |
| Overall | 0.12 | 0.16 | + | 0.29 | 0.25 | - | 0.28 | 0.31 | + | 0.17 | 0.19 | + | 0.27 | 0.04 | - | 0.44 | 0.46 | + |
| Storm1 | 0.02 | 0.07 | + | 0.16 | 0.18 | + | 0.22 | 0.26 | + | 0.01 | 0.03 | + | 0.14 | 0.06 | - | 0 | -0.1 | - |
| Storm2 | 0.05 | 0.08 | + | 0.61 | -0.22 | - | 0.34 | 0.39 | + | 0.18 | 0.3 | + | 0.09 | -0.04 | - | 0.42 | 0.28 | - |
| Storm3 | 0.07 | 0.19 | + | -0.23 | -132 | - | -4.72 | -15.6 | - | 0.5 | -0.36 | - | 0.7 | -6.15 | - | 0.37 | -8.68 | - |
| Storm4 | -0.08 | -0.04 | + | 0.66 | 0.58 | - | 0.27 | 0.38 | + | 0.19 | 0.44 | + | 0.21 | 0.53 | + | 0.36 | 0.73 | + |
| Storm5 | -0.45 | -0.45 | - | 0.72 | -0.94 | - | -43.9 | -43.9 | | 0.45 | 0.77 | + | 0.05 | -1.35 | - | 0.61 | -4.95 | - |
| Storm5b | -384 | -920 | - | NaN | NaN | | -2.41 | -2.41 | | -1.17 | -4.82 | - | -29.3 | -97 | - | -8.72 | -8.33 | + |
| Storm6 | 0.01 | 0.39 | + | 0.69 | 0.78 | + | 0.93 | 0.66 | - | 0.2 | 0.54 | + | 0.33 | 0.57 | + | 0.42 | 0.34 | - |
| Storm7 | -0.94 | -7.19 | - | 0.69 | -6.03 | - | -24.9 | -64.6 | - | 0.47 | 0.62 | + | 0.28 | 0.56 | + | 0.59 | -0.38 | - |
| Storm8 | -0.19 | -1.91 | - | -0.82 | -448 | - | -74.7 | -117 | - | 0.58 | -8.34 | - | -2.14 | -33.3 | - | 0.42 | -12.5 | - |

### *6.2.7 Sources of uncertainty*

A number of sources contribute to the uncertainty in the model. These are not failings in the model—uncertainty is part of engineering modeling (Pappenberger et al. 2005).

Clearly, the assumptions used to create the individual models introduce uncertainty. As discussed in section 3.2.4, the approximate solution of the governing equations of flow creates some uncertainties. Also, the hybrid model concept itself introduces some uncertainty as addressed in the previous question.

Specific assumptions in this implementation of the model produce uncertainty. For the California Gulch model, in an isolated headwater, we assumed that volumes of water not recovered by evaporation from the soil moisture zones or accounted for by return flows, are assumed to discharge through the subsurface to the adjoining downstream watershed. A multi-basin application including the receiving watersheds would be necessary to quantify the uncertainty of this assumption.

Grid scales provide additional uncertainty since the calibrated parameters are really "effective" parameters for the given grid size, averaging the properties of minute variations across the cell.

Measurement error may be present in the data sources used for the precipitation inputs and for comparison of output. For instance, the gauge record for the CG-5 gauge clearly shows the diurnal signature from the waste treatment plant; however, the gauge is located several hundred yards upstream of the effluent discharge point into California Gulch. The current location of CG-5 may not correspond to the location during the 2006 measurement period. The four rain gauges are generally well-correlated (see Figure 4.11 showing cumulative rainfall), lending confidence to the measurements.

Only four rainfall gauges characterize the precipitation distribution in the basin and the most elevated of these, SHG-09A and CG-1 (10450 ft. and 10331 ft., respectively) are still more than 1500 ft. below the summit of the watershed. Significant additional orographic precipitation may be found at the greater elevation. The distribution of these gauges is not biased—simple visual inspection shows that the gauges are well spaced throughout the watershed. However, the significant variation in elevation makes it difficult to capture the significant spatial and temporal variability of rainfall precipitation common in this area.

This is especially critical because about 95% of the water infiltrates in these simulations; so, infiltration location will play a large role in the timing of flood peak arrival. This sensitivity is demonstrated as discussed in section 6.2.1 where the model performance favors simulations with precipitation patters similar to the calibration data.

# 7.0 IMPROVED MODEL TECHNOLOGY

A hydrologic model consists of a hydrologic core and a separate technological shell which is "the programming, user interface, pre- and post-processing facilities, etc." (Refsgaard and Abbott 1996). As part of this research, improvements were made to both the core and to the shell of TREX. These improvements are significant with regard to the applicability and utility of the model. Improvements to the graphical display of results, in particular, have impacted how well results of the model are understood and communicated. Other improvements were made with respect to the manner of handling the input data and the modification of source code. All these changes have increased the usability of the TREX model and create opportunities for improved collaborative research in the future.

The multi-event model becomes a test case for these tools as demonstrated in this section.

## 7.1 CODE ENHANCEMENTS

Database and internet technology were also applied to improve the reliability of the coding process and to increase opportunities for collaboration. One of the historical trademarks of the CASC2D-based models has been free availability of the source code. Working with the engineering school network administrators, a first-of-its-kind at CSU web-available subversion source code control database (Pilato et al. 2008) was implemented in conjunction with this research. This source control database now allows many researchers to simultaneously collaborate on development. Different branches of the code may be maintained without creating conflicts, and simple tools allow for merging the branches as needed. Researchers using the same branch of the code can "commit" their changes and make them instantly available to other users of the repository. For more information about the code repository, see Appendix B.

This research benefited from the code repository in the form of the differencing features which allowed for straightforward assessment of the changes made from the original TREX code. The availability of the repository from anywhere in the world allowed researchers based in various locations to continue work on the code.

Also in conjunction with this research, impediments to parallelization were removed from the code and a parallel version was tested with the multi-event simulation. Performance gains were initially modest, but the codebase is now available for further optimization.

## 7.2 Data Analysis Tools

Relational databases are used to increase the accessibility and reliability of data. "Further development of modelling tools…will place information management at a central position in the modelling process" (Nachtnebel et al. 1993). As models become more sophisticated, "databases will become the central component in the architecture of these systems" (Deckers and Stroet 1996).

California Gulch data provided by Tetra-tech included nearly a million observed flows and precipitation values collected at six different real-time sites on ten-minute intervals, along with thousands of point samples in other locations across three years of collection. In tabular form, these data were intractable. Database integration was used with internet technology to improve the process of preparing these data as a source for precipitation inputs for TREX-SMA input files. The data were ingested into a MySQL database and made available via web-based query. Several scripts were designed to convert the rainfall data output from the web tool for a given simulation period into a series of time-value pairs suitable for direct inclusion as model input. For the multi-event model, this allowed for easy changes to accommodate different model start dates and simplified the process of choosing the best interval for modeling.

## 7.3 GRASS+NVIZ AND GOOGLE EARTH KML

GIS in modeling serves to assist where "the hydrologist needs to co-operate intensively with experts in the field of ecology, agriculture, urban planning, and economics" (Engelen and Kloosterman 1996). This is because "the pure numerical results of a simulation are no longer the final products delivered by the hydrologist. The results have to be translated systematically into hydrological effects and subsequently into socially relevant quantities… the hydrologist can no longer depend on tabular representations of his data…graphical tools [are] a necessity" (Deckers and Stroet 1996).

Modeling studies with TREX and CASC2D started with austere tabular representation in early years but have moved across the continuum toward coupling with various forms of GIS and graphical outputs to demonstrate, analyze, and communicate results in "socially relevant" ways, especially with respect to demonstrating inundated area. The objectives of CASC2D developers in incorporating GIS and graphic display with the model input and output provide comprehensive analysis that is difficult to obtain with text outputs from a model (i.e. a picture is worth a thousand words.) Johnson et al. (2000) says that the spatial capabilities of the model, combined with GIS data for input parameters are the *raison d'être* for CASC2D-SED: "The strength of the model CASC2D-SED lies in its tremendous potential and visual output…"

The present research has further improved graphical interpretation of results, making model output more accessible to a wider range of technical and non-technical users. The improved graphics communicate multiple layers of contextual meaning, moving the TREX model toward becoming part of a decision support tool.

A demonstration of these graphical methods was performed using the 2004 application of CASC2D by Velleux at California Gulch near Leadville, Colorado. The 100-year storm was

simulated as 1.73 inches of uniformly distributed rain falling in two hours over the entire watershed. The 100-year analysis was used to demonstrate the effect of applying the improved graphical techniques. In Figures 7.1 through 7.5 below, the various methods to visualize output are compared, beginning with a snapshot (Figure 7.1) of pure text from the model output.

**Figure 7.1: Pure ASCII gridded output from the model showing depth of water on the land surface. The apparent contours are an artifact of the greatly reduced size of the text display.**

Figure 7.2 is an extract from the previously-available method to animate a sequence of grids using ESRI ArcInfo. The animations immensely improve the accessibility of the modeling results as the flood waves are visible passing through various portions of the model domain and different rates of infiltration can be observed as certain areas lose depth more rapidly, and so forth.

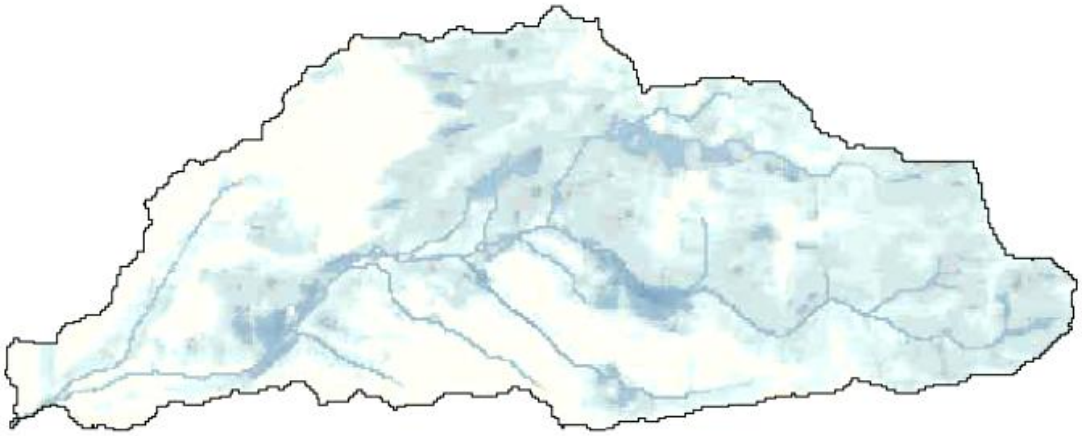

**Figure 7.2: Example—frame from time series animation created using ArcInfo.**

Figure 7.3 shows a series of 3-D perspective frames from a time lapse movie created using GRASS GIS. To produce the animation, the same process described in section 6.2.3 was used to create flat frames showing the depth of water on the land surface at various times through the simulation. The maps were colorized according to the data values for each cell and then draped on a digital elevation model, also contained in the GIS. The 3-D visualization module of the GRASS systems, NVIZ, was used to produce perspective views of each of the time series; these views were assembled into an animation depicting the accumulation of runoff into distinct channels, and flood interaction between channel and floodplain. Any of the distributed model states can be incorporated into this type graphical representation. Figure 7.3 shows six frames from the 100-year storm animation created using this method.

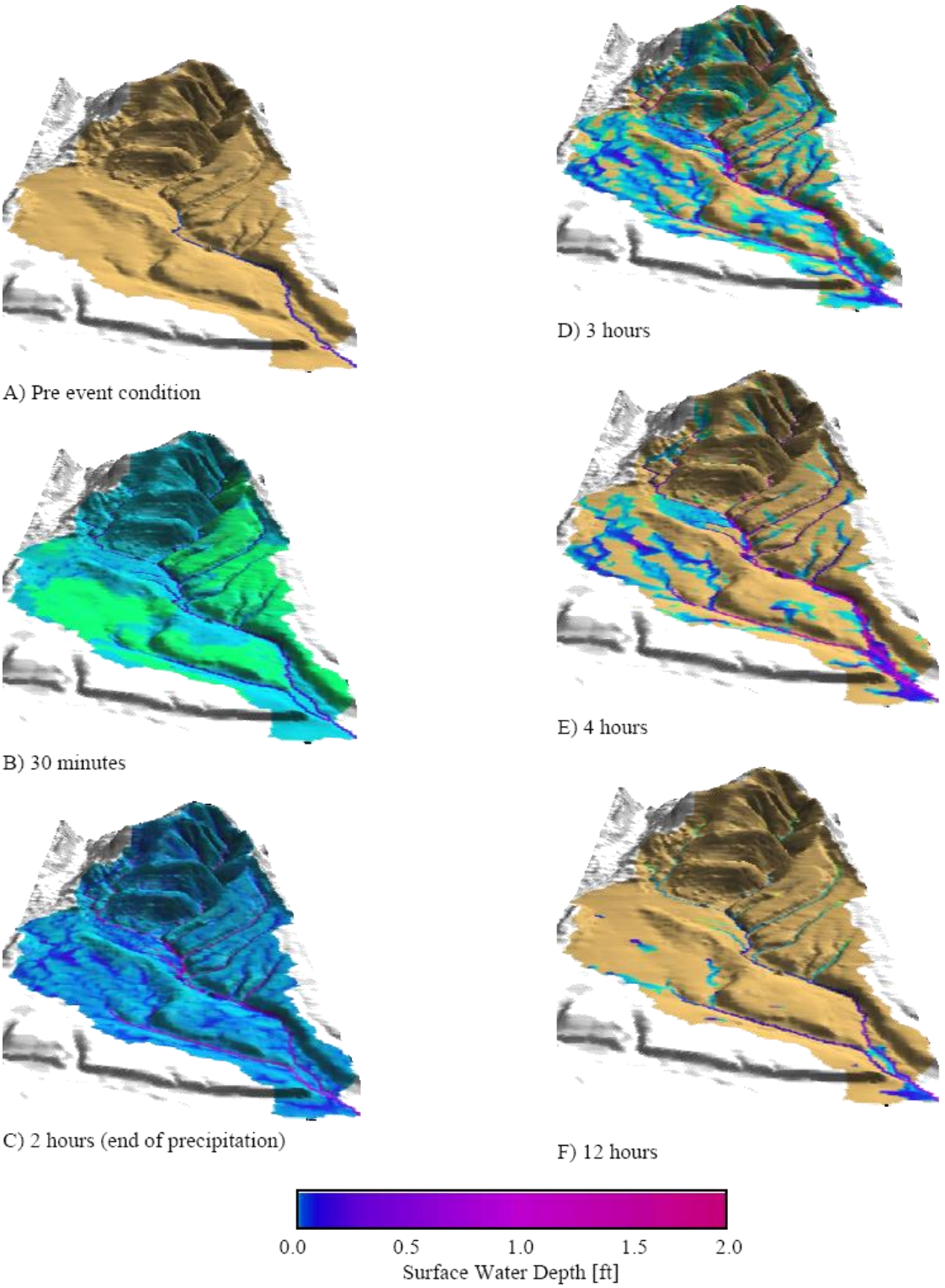


**Figure 7.3: Overland and channel flow depth for the 100-year event (1.73 inches in two hours) at California Gulch near Leadville, CO (Velleux et al. 2008a, b).**

Figure 7.4 and Figure 7.5 show the 100-year inundation extent on a background of an aerial image of Leadville and California Gulch, providing valuable information in an integrated view to better visualize surface processes including: (1) extent of inundation and flow interaction between main channel and the floodplain; (2) runoff from urban and forested hill slopes; and (3) flow convergence and divergence from surface runoff and detention storage. In the sequence of frames from the figure, the progression of flooding mechanism is visible between the Malta Gulch Channel and the main California Gulch channel. In the initial frames, immediately after cessation of rainfall, flooding infiltration creates a thin layer of ponded water between the channels. After the rain stops, the water infiltrates and the depth of water is observed to be minimal. In the last frame, the flood pulse from the channel upstream has arrived and the water begins to inundate the area between the channels again, this time due to hydraulic factors.

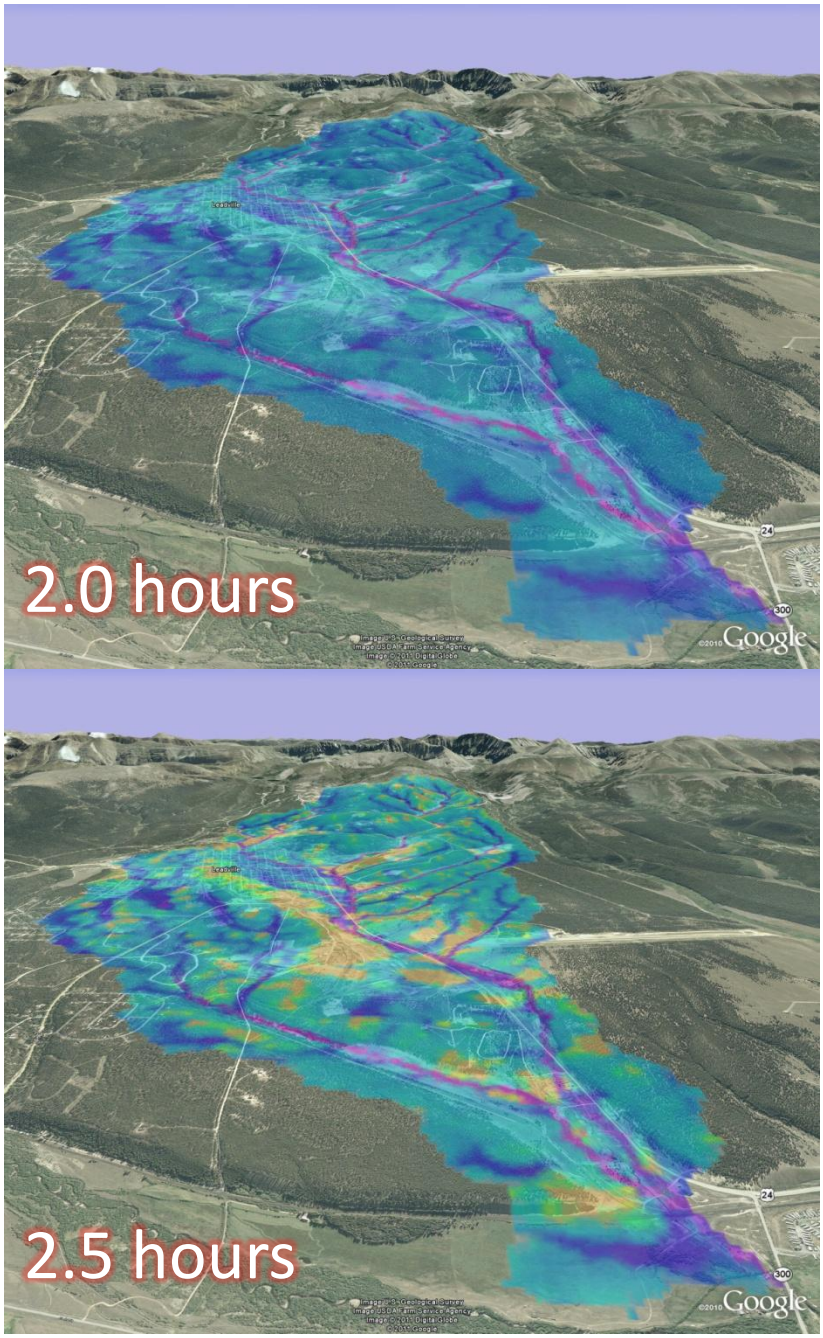


**Figure 7.4: Selected frames from a loop showing the depth of water on a land surface using Google Earth 3-D terrain and imagery for a hypothetical two-hour duration, 100-year return period event. Red text indicates number of hours after beginning of rainfall. Rainfall ends at 2.0 hours.**

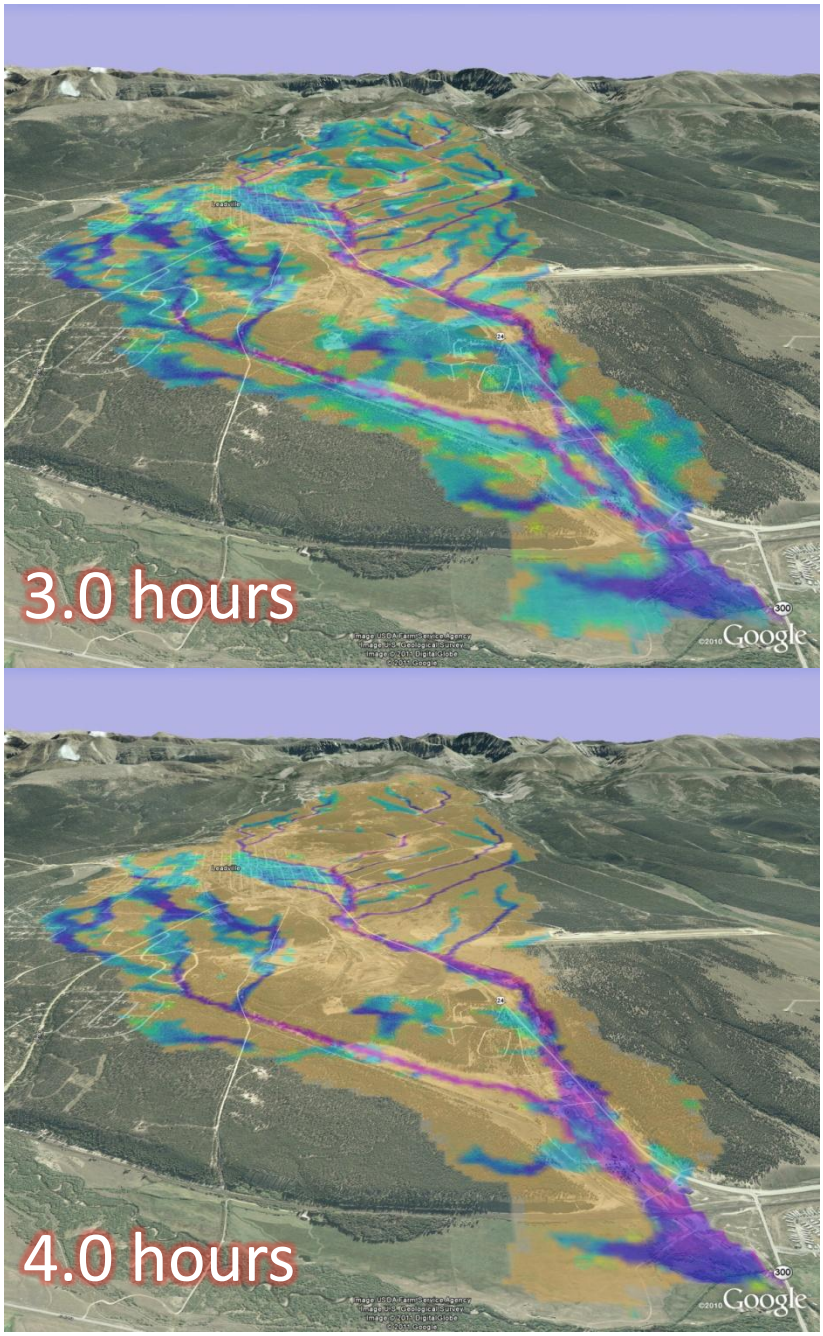


**Figure 7.5: Additional selected frames from a loop showing the depth of water on a land surface using Google Earth 3-D terrain and imagery for a hypothetical 2-hour duration, 100-year return period event. Red text indicates number of hours after beginning of rainfall. Rainfall ends at 2.0 hours.**

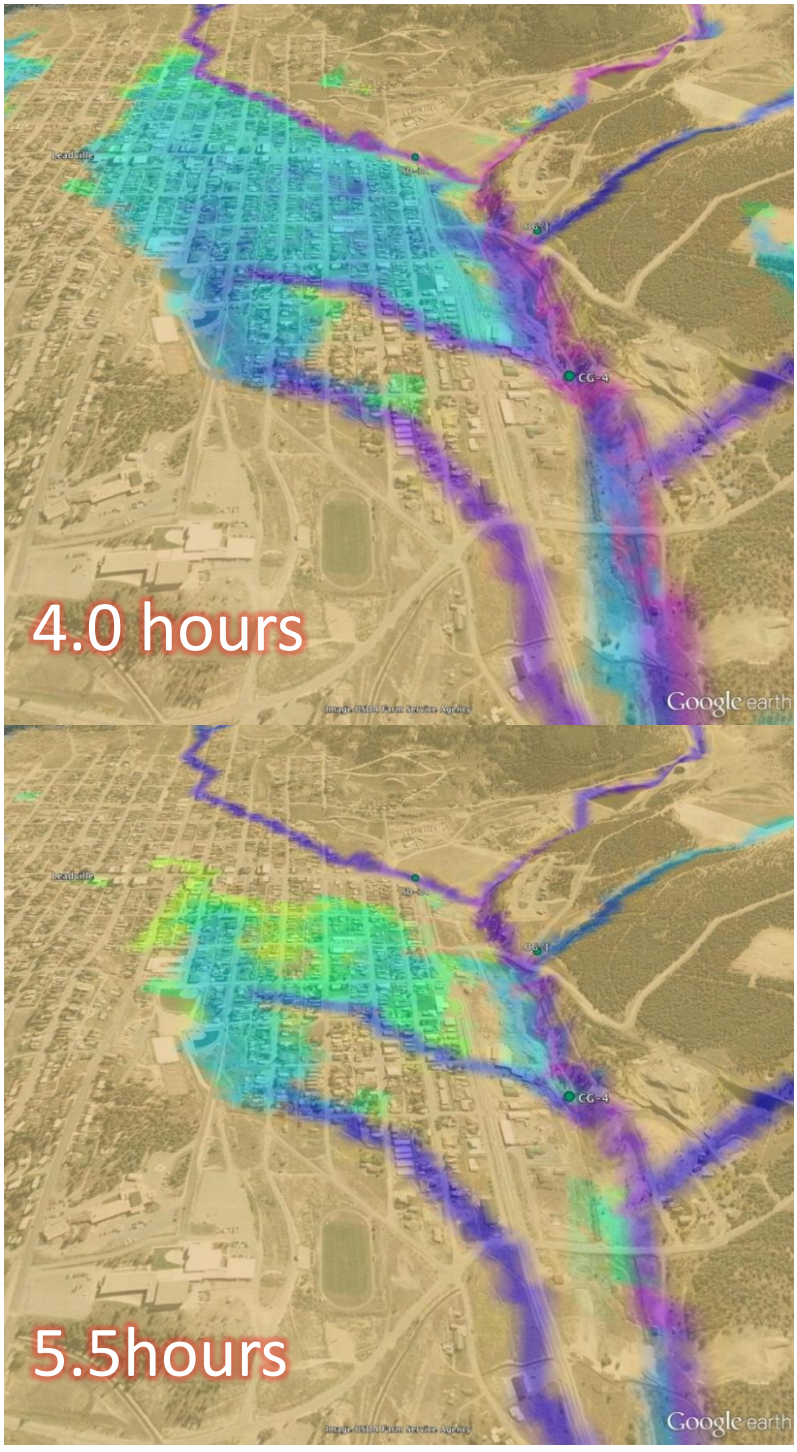


**Figure 7.6: Close-up showing potential for interactive evaluation of flash-flood inundation using KML to interpret output from 100-year storm TREX model on Google Earth 3-D oblique imagery. Red text indicates number of hours after beginning of rainfall.**

A final figure, Figure 7.6, demonstrates the capability for detailed evaluation of flood effects using the KML and Google Earth overlays. The two images in the figure show dissipation of the surface flood wave out of the City of Leadville. Emergency responders can use the Google Earth application interactively to "zoom-in" and highlight areas where flooding is most severe and determine appropriate action to minimize hazards. In the case of California Gulch, there are few structures or hazards in the floodplain; however, the possibility of catastrophic flooding exists. In 2008, the trailer park at the outlet of California Gulch into the Arkansas river was threatened by the possibility of a bursting mine drainage tunnel (Frosch 2008; Lipsher 2008).

For researchers, the Google Earth views can help highlight areas where the model may be behaving in an unexpected way or highlight areas for further parameter refinement. For instance, at the edge of the simulation shown in Figures 7.4 and 7.5, water is spilling out of the channel and forming a lake upstream into the Arkansas flood plain. It is possible that this ponding is actually an artifact of the boundary condition in the stream channel passing inadequate quantities of flow. Further experiments with the DEM in that area could be prompted by these views. Also in the Figure 7.6, a significant flow accumulation is visible through a portion of the city of Leadville, where flow would likely be obstructed by the buildings and infrastructure. The simulation results viewed in this context show the possible inconsistency and allow for the modeler to make a compensating correction.

# 8.0 CONCLUSIONS

The hybrid modeling concept has been implemented with TREX-SMA by combining the physics-based distributed surface hydrology model, TREX, and the conceptual lumped parameter model, SAC-SMA. The California Gulch watershed has provided a field site for developing and demonstrating multi-event modeling with TREX-SMA

This research has provided significant improvements with data and code management, integrated statistical analysis, and graphical display of results for TREX as demonstrated in Chapter 7.

A database of observed measurements from the automated gauging stations was created with a web-based interface to extract data. A script converts precipitation measurements into a format for inclusion in the model. Another database was created which contains all the model code used for this research. A simple web interface to the code database allowed for changes checked-in incrementally so that improvements were immediately available to all users of the code.

Approximately 7500 lines of R and gnuplot scripts allow for real-time viewing of statistical summaries and hydrograph plots from the multi-event simulation. Simple modification to these scripts allowed for display of 54 different storm hydrographs from the six gauges in California Gulch during the nine storms identified for analysis.

Two new processes have been investigated for creating 3-D animations of the distributed model results. The techniques include a KML-based method of projecting distributed parameters on the terrain and satellite imagery delivered in Google Earth and another technique using GRASS GIS and the 3-D submodel Nviz. Both of these techniques were employed to generate animated sequences of water depth on the land surface. Within Google Earth, a “fly-through”

tour was created, showing the evolution of the water depth on the land surface during one of the events in the multi-event simulation.

Another KML-based time series was prepared which displays the hydrographs and statistical plots and tables associated with the individual gauges and storms linked to markers, showing their location and associated with the correct time within the multi-event simulation. These techniques require only about 1000 lines of KML script to implement and provide a powerful and simple method of sharing spatial model results.

The following may be concluded from this research:

1) TREX-SMA has been successfully implemented.

The requirements stated in Chapter 2 (i.e. spatially variable surface processes, lumped soil moisture accounting) are satisfied by the TREX-SMA model as described in Chapter 3. Approximately 1700 lines of code were added to TREX to implement the SAC-SMA procedure and to address the concerns of their different time and spatial scales. Connecting the lumped, conceptual SAC-SMA to the explicit, physical TREX model bridges the gaps between hydrologic events to allow multi-event simulation. Hybridizing these two models represents an innovative approach to multi-event modeling of distributed surface hydrology.

2) Green and Ampt parameters can be reinitialized using lumped soil moisture states. The process-based, internally responsive baseflow and soil-moisture effects on the hydrograph are shown in the example solutions in Chapter 5, in Figure 5.5 and Figure 5.9.

3) Continuous, multi-event modeling is possible using TREX-SMA.

Multi-event model results are detailed in Table 6.3 and Table 6.5 as well as in Figures 6.1, 6.5, and 6.6. The implementation of the TREX-SMA soil moisture accounting algorithm to re-initialize the infiltration parameters reduces the total absolute peak error from 180% to 135% of

the observed peak flow rates. The Nash-Sutcliffe coefficient improved by 43%, 11%, 5%, and 10% at CG-1, CG-4, CG-6, and SHG-09A, respectively.

4) Improved representation of results is achieved by applying GIS and web technology.

Techniques were presented in Chapter 7 which are a clear improvement and make model results instantly accessible and understandable in a relevant geographic context.

The NWS recently supported a conference paper (Reed and Halgren 2011) about operational dam break flood forecasting. A key point of the paper is that for an operational forecaster, there needs to be very quick feedback from a model in order for the output to be useful. The tools developed for this research begin to allow TREX to have the type of short turn-around time needed for utility in operational forecasting. Any model results can now be shared instantly, even while the model is running. TREX-SMA model run-times are not currently fast enough for use as an operational forecasting platform, but computing advances and optimized coding could make that a possibility. And, when TREX is operational, there is already an initial framework for distributing the model results in real-time as products for forecasters.

## 9.0 WORKS CITED


Abbott, M. B., and Refsgaard, J. C. (1996). *Distributed hydrological modelling*. Springer.

Abdulrazzak, M. J., and Morel-Seytoux, H. J. (1983). "Recharge From an Ephemeral Stream Following Wetting Front Arrival to Water Table." *Water Resources Research*, 19(1), 194–200.

Alexiades, V., Amiez, G., and Gremaud, P.-A. (1996). "Super-time-stepping acceleration of explicit schemes for parabolic problems." *Communications in Numerical Methods in Engineering*, 12(1), 31–42.

Anderson, R. M., Koren, V. I., and Reed, S. M. (2006). "Using SSURGO data to improve Sacramento Model a priori parameter estimates." *Journal of Hydrology*, 320(1–2), 103–116.

Aral, M. M., and Gunduz, O. (2003). "Scale effects in large scale watershed modeling." *Advances in Hydrology*, V. P. Singh and R. N. Yadava, eds., Allied Publishers, 37–51.

Aral, M. M., and Gunduz, O. (2006). "Large-Scale Hybrid Watershed Modeling." *Watershed models*, V. P. Singh and D. K. Frevert, eds., CRC/Taylor & Francis, Boca Raton, FL, 75–95.

Beven, K. J. (1986). "Runoff production and flood frequency in catchments of order n: an alternative approach." *Scale Problems in Hydrology: Runoff Generation and Basin Response*, V. K. Gupta, I. Rodriguez-Iturbe, and E. F. Wood, eds., D. Reidel, Dordrecht, 107–131.

Beven, K. J. (2000). *Rainfall-Runoff Modelling: The Primer*. J. Wiley, Chichester, UK.

Beven, K. J. (2004). "Robert E. Horton's perceptual model of infiltration processes." *Hydrological Processes*, 18(17), 3447–3460.

Beven, K. J., and Kirkby, M. J. (1979). "A physically-based, variable contributing area model of basin hydrology / Un modèle à base physique de zone d'appel variable de l'hydrologie du bassin versant." *Hydrological Sciences Bulletin*, 24(1), 43.

Bureau of Reclamation. (2006). "Reclamation: Fryingpan-Arkansas Project—Annual Operating Plan—Water Year 2006 Operations."

Burnash, R., and Ferral, L. (2002). "Conceptualization of the Sacramento Soil Moisture Accounting Model." *NWSRFS User Manual Documentation*, National Weather Service, NOAA, Silver Spring, MD.

Byrd, A., Nelson, E. J., and Downer, C. W. (2005). "Primer: Using Watershed Modeling System (WMS) for Gridded Surface Subsurface Hydrologic Analysis (GSSHA) Data Development—WMS 7.1 and GSSHA 2.0," <http://chl.erdc.usace.army.mil/softwarex/gssha/Primer_20/wf_njs.htm> (May 28, 2010).

Caruso, B. S., Cox, T. J., Runkel, R. L., Velleux, M. L., Bencala, K. E., Nordstrom, D. K., Julien, P. Y., Butler, B. A., Alpers, C. N., Marion, A., and Smith, K. S. (2008). "Metals fate and transport modelling in streams and watersheds: state of the science and USEPA workshop review." *Hydrological Processes*, 22(19), 4011–4021.

Cheney, W., and Kincaid, D. (1999). *Numerical Mathematics and Computing*. Brooks/Cole Pub Co, Pacific Grove, California.

Courant, R., Friedrichs, K., and Lewy, H. (1928). "Über die partiellen Differenzengleichungen der mathematischen Physik." *Mathematische Annalen*, 100(1), 32–74.

Deckers, and Stroet. (1996). "Use of GIS and Database with Distributed Modelling." *Distributed hydrological modelling*, M. B. Abbott and J. C. Refsgaard, eds., Springer.

Downer, C. W., and Ogden, F. L. (2004). "GSSHA: Model to simulate diverse stream flow producing processes." *Journal of Hydrologic Engineering*, 9(3), 161–174.

Downer, C. W., Ogden, F. L., Martin, W. D., and Harmon, R. S. (2002). "Theory, development, and applicability of the surface water hydrologic model CASC2D." *Hydrological Processes*, 16(2), 255–275.

Dunne, T., and Black, R. D. (1970a). "Partial Area Contributions to Storm Runoff in a Small New England Watershed." *Water Resources Research*, 6(5), 1296–1311.

Dunne, T., and Black, R. D. (1970b). "An Experimental Investigation of Runoff Production in Permeable Soils." *Water Resources Research*, 6(2), 478–490.

Eagleson, P. S. (1970). *Dynamic hydrology*. McGraw-Hill, New York.

Ebel, B. A., and Loague, K. (2006). "Physics-based hydrologic-response simulation: Seeing through the fog of equifinality." *Hydrological Processes*, 20(13), 2887–2900.

Ebel, B. A., Loague, K., Montgomery, D. R., and Dietrich, W. E. (2008). "Physics-based continuous simulation of long-term near-surface hydrologic response for the Coos Bay experimental catchment." *Water Resources Research*, 44, W07417.

Engelen, G. B., and Kloosterman, F. H. (1996). *Hydrological Systems Analysis: Methods and Applications*. Water science and technology library, Kluwer, Dordrecht.

England, J. F., Velleux, M. L., and Julien, P. Y. (2007). "Two-dimensional simulations of extreme floods on a large watershed." *Journal of Hydrology*, 347(1–2), 229–241.

Freeze, R. A., and Harlan, R. L. (1969). "Blueprint for a physically-based, digitally-simulated hydrologic response model." *Journal of Hydrology*, 9(3), 237–258.

Freyberg, D. L. (1983). "Modeling the Effects of a Time-Dependent Wetted Perimeter on Infiltration From Ephemeral Channels." *Water Resources Research*, 19(2), 559–566.

Frosch, D. (2008). “Mine Water Poses Danger of a Toxic Gusher.” *The New York Times*.

Gelman, A. (2004). “Exploratory Data Analysis for Complex Models.” *Journal of Computational and Graphical Statistics*, 13(4), 755–779.

Green, W. H., and Ampt, G. A. (1911). “Studies on soil physics Part I - The flow of air and water through soils.” *Journal of Agricultural Science*, 4, 1–24.

Gunduz, O. (2004). “Coupled flow and contaminant transport modeling in large watersheds.”

Gupta, H. V., Sorooshian, S., and Yapo, P. O. (1998). “Toward improved calibration of hydrologic models: Multiple and noncommensurable measures of information.” *Water Resources Research*, 34(4), 751–763.

HDR Engineering. (2002). “Final Focused Feasibility Study: Operable Unit 6.”

Henning, I., and Henning, D. (1981). “Potential Evapotranspiration in Mountain Geoecosystems of Different Altitudes and Latitudes.” *Mountain Research and Development*, 1(3/4), 267–274.

Horton, R. E. (1933). “The role of infiltration in the hydrologic cycle.” *Transactions of the American Geophysical Union*, 14, 446–460.

Jain, S. K., and Sudheer, K. P. (2008). “Fitting of Hydrologic Models: A Close Look at the Nash-Sutcliffe Index.” *Journal of Hydrologic Engineering*, 13(10), 981–986.

Janert, P. K. (2010). *Gnuplot in Action: Understanding data with graphs*. Manning Publications Co.

Johnson, B. E. (1997). “Development of a storm event based two-dimensional upland erosion model.” PhD Dissertation, Colorado State University. Dept. of Civil Engineering.

Johnson, B. E., and Gerald, T. K. (2006). “Development of nutrient submodules for use in the gridded surface subsurface hydrologic analysis (GSSHA) distributed watershed model.” *Journal of the American Water Resources Association*, 42(6), 1503–1525.

Johnson, B. E., Julien, P. Y., Molnár, D. K., and Watson, C. C. (2000). “The two-dimensional Upland erosion model CASC2D-SED.” *Journal of the American Water Resources Association*, 36(1), 31–42.

Julien, P. Y., Saghafian, B., and Ogden, F. L. (1995). “Raster-Based Hydrologic Modeling of Spatially-Varied Surface Runoff.” *Water Resources Bulletin*, 31(3), 523–536.

Kampf, S. K., and Burges, S. J. (2007). “A framework for classifying and comparing distributed hillslope and catchment hydrologic models.” *Water Resources Research*, 43(5).

Kavvas, M. L., Chen, Z. Q., Dogrul, C., Yoon, J. Y., Ohara, N., Liang, L., Aksoy, H., Anderson, M. L., Yoshitani, J., Fukami, K., and Matsuura, T. (2004). "Watershed Environmental Hydrology (WEHY) model based on upscaled conservation equations: Hydrologic module." *Journal of Hydrologic Engineering*, 9(6), 450–464.

Kirchner, J. W. (2003). "A double paradox in catchment hydrology and geochemistry." *Hydrological Processes*, 17(4), 871–874.

Kirchner, J. W. (2006). "Getting the right answers for the right reasons: Linking measurements, analyses, and models to advance the science of hydrology." *Water Resources Research*, 42(3), W03S04.

Koren, V. I., Reed, S. M., Smith, M. B., Zhang, Z., and Seo, D.-J. (2004). "Hydrology laboratory research modeling system (HL-RMS) of the US national weather service." *Journal of Hydrology*, 291(3–4), 297–318.

Koren, V. I., Smith, M. B., and Duan, Q. (2003). "Use of a priori parameter estimates in the derivation of spatially consistent parameter sets of rainfall-runoff models." *Calibration of Watershed Models*, Water Science and Application, Q. Duan, H. V. Gupta, S. Sorooshian, A. N. Rousseau, and R. Turcotte, eds., American Geophysical Union, Washington, D.C, 239–254.

Koren, V. I., Smith, M. B., Wang, D., and Zhang, Z. (2000). "Use of Soil Property Data in the Derivation of Conceptual Rainfall-Runoff Model Parameters." *15th Conference on Hydrology*, American Meteorological Society, Long Beach, California, 403.

Lettenmaier, D. P., and Wood, E. F. (1993). "Hydrologic Forecasting." *Handbook of Hydrology*, D. R. Maidment, ed., McGraw-Hill, New York, 26.1–26.30.

Linsley, R. K., Kohler, M. A., and Paulhus, J. L. H. (1982). *Hydrology for engineers*. McGraw-Hill series in water resources and environmental engineering., McGraw-Hill, New York.

Lipsher, S. (2008). "Feds to pump mine water to avert Leadville flooding." *The Denver Post*.

Lupton, R. H., Gunn, J. E., and Szalay, A. S. (1999). "A Modified Magnitude System that Produces Well-Behaved Magnitudes, Colors, and Errors Even for Low Signal-to-Noise Ratio Measurements." *The Astronomical Journal*, 118(3), 1406–1410.

McCuen, R. H., Knight, Z., and Cutter, A. G. (2006). "Evaluation of the Nash-Sutcliffe Efficiency Index." *Journal of Hydrologic Engineering*, 11(6), 597–602.

McCuen, R. H., and Snyder, W. M. (1975). "A Proposed Index for Comparing Hydrographs." *Water Resources Research*, 11(6), 1021–1024.

Millares, A., Polo, M. J., and Losada, M. A. (2009). "The hydrological response of baseflow in fractured mountain areas." *Hydrology and Earth System Sciences Discussions*, 6, 3359–3384.

Molnár, D. K., and Julien, P. Y. (2000). "Grid-Size Effects on Surface Runoff Modeling." *Journal of Hydrologic Engineering*, 5(1), 8–16.

Moriasi, D. N., Arnold, J., Van Liew, M., Bingner, R., Harmel, D., and Veith, T. (2007). "Model evaluation guidelines for systematic quantification of accuracy in watershed simulations." *Transactions of the ASABE*, 50(3), 885–900.

Nachtnebel, H. P., Furst, J., and Holzmann, H. (1993). "Application of geographical information systems to support groundwater modelling." *Application of Geographic Information Systems in Hydrology and Water Resources Management*, K. Kovar and H. P. Nachtnebel, eds., IAHS Press.

Nash, J. E., and Sutcliffe, J. V. (1970). "River flow forecasting through conceptual models part I —A discussion of principles." *Journal of Hydrology*, 10(3), 282–290.

National Climatic Data Center. (2010). "NCDC: Weather Station." <http://www4.ncdc.noaa.gov/cgi-win/wwcgi.dll?wwDI%7EStnSrch%7EStnID%7E20003674> (Jun. 4, 2010).

National Oceanographic and Atmospheric Administration. (2004). "Statistical Analysis of Two Time Series."

Neteler, M., and Mitasova, H. (2008). *Open Source GIS: A GRASS GIS Approach*. Springer, New York.

Ogden, F. L. (1992). "Two-Dimensional Runoff Modeling with Weather Radar Data." PhD Dissertation, Colorado State University, Fort Collins, CO.

Ogden, F. L., and Julien, P. Y. (1993). "Runoff sensitivity to temporal and spatial rainfall variability at runoff plane and small basin scales." *Water Resources Research*, 29(8), PP. 2589–2597.

Ogden, F. L., and Saghafian, B. (1997). "Green and Ampt Infiltration with Redistribution." *Journal of Irrigation and Drainage Engineering*, 123(5), 386–393.

Panday, S., and Huyakorn, P. S. (2004). "A fully coupled physically-based spatially-distributed model for evaluating surface/subsurface flow." *Advances in Water Resources*, 27(4), 361–382.

Pappenberger, F., Beven, K. J., Hunter, N. M., Bates, P. D., Gouweleeuw, B. T., Thielen, J., and De Roo, A. P. J. (2005). "Cascading model uncertainty from medium range weather forecasts(10 days) through a rainfall-runoff model to flood inundation predictions within the European Flood Forecasting System(EFFS)." *Hydrology and Earth System Sciences*, 9(4), 381–393.

Parks, D. R., Roederer, M., and Moore, W. A. (2006). "A new 'Logicle' display method avoids deceptive effects of logarithmic scaling for low signals and compensated data." *Cytometry. Part A: The Journal of the International Society for Analytical Cytology*, 69(6), 541–551.

Perry, M. A., and Niemann, J. D. (2007). "Analysis and estimation of soil moisture at the catchment scale using EOFs." *Journal of Hydrology*, 334(3–4), 388–404.

Pilato, C. M., Collins-Sussman, B., and Fitzpatrick, B. W. (2008). *Version Control with Subversion*. O'Reilly Media.

R Development Core Team. (2010). "R: A Language and Environment for Statistical Computing." R Foundation for Statistical Computing.

Ramírez, J. A. (2000). "Prediction and modeling of flood hydrology and hydraulics." *Inland Flood Hazards: Human, Riparian, and Aquatic Communities*, E. E. Wohl, ed., Cambridge University Press, Cambridge.

Rawls, W. J., Brakensiek, D. L., and Miller, N. (1983). "Green and Ampt Infiltration Parameters from Soils Data." *Journal of Hydraulic Engineering*, 109(1), 62–70.

Rawls, W. J., Brakensiek, D. L., and Saxton, K. E. (1982). "Estimation of Soil Water Properties." *Transactions of the ASAE*, 25(5).

Reed, S. M., and Halgren, J. S. (2011). "Validation of a New GIS Tool to Rapidly Develop Simplified Dam Break Models." *Dam Safety 2011*, Association of State Dam Safety Officials, Washington, D.C.

Reed, S. M., Schaake, J. C., and Zhang, Z. (2007). "A distributed hydrologic model and threshold frequency-based method for flash flood forecasting at ungauged locations." *Journal of Hydrology*, 337(3–4), 402–420.

Refsgaard, J. C. (1996). "Terminology, Modelling Protocol and Classification of Hydrological Model Codes." *Distributed hydrological modelling*, M. B. Abbott and J. C. Refsgaard, eds., Kluwer Academic Publishers.

Refsgaard, J. C., and Abbott, M. B. (1996). "The Role of Distributed Hydroloical Modelling in Water Resources Management." *Distributed hydrological modelling*, M. B. Abbott and J. C. Refsgaard, eds., Kluwer Academic Publishers.

Refsgaard, J. C., and Storm, B. (1996). "Construction, Calibration and Validation of Hydrological Models." *Distributed hydrological modelling*, M. B. Abbott and J. C. Refsgaard, eds., Kluwer Academic Publishers.

Reggiani, P., and Schellekens, J. (2003). "Modelling of hydrological responses: the representative elementary watershed approach as an alternative blueprint for watershed modelling." *Hydrological Processes*, 17(18), 3785–3789.

Richards, L. A. (1931). “Capillary Conduction of Liquids Through Porous Mediums.” *Physics*, 1(5), 318–333.

Richardson, J. R., and Julien, P. Y. (1994). “Suitability of simplified overland flow equations.” *Water resources research*, 30(3), 665–672.

Rojas Sánchez, R. (2002). “GIS-based upland erosion modeling, geovisualization and grid size effects on erosion simulations with CASC2D-SED.” PhD Dissertation, Colorado State University, Department of Civil Engineering.

Rojas Sánchez, R., Julien, P. Y., and Johnson, B. E. (2003). *CASC2D-SED v 1.0 Reference Manual: A 2-Dimensional Rainfall-Runoff and Sediment Model*. Colorado State University, 2003.

Rojas Sánchez, R., Velleux, M. L., Julien, P. Y., and Johnson, B. E. (2008). “Grid Scale Effects on Watershed Soil Erosion Models.” *Journal of Hydrologic Engineering*, 13(9), 793–802.

Saghafian, B. (1992). “Hydrologic analysis of watershed response to spatially varied infiltration.” PhD Dissertation, Colorado State University. Dept. of Civil Engineering.

Saghafian, B., and Julien, P. Y. (1991). *CASC2D user’s manual : a two-dimensional watershed rainfall-runoff model*. Colorado State University, Center for Geosciences, Hydrologic Modeling Group, Fort Collins, Colo.

Senarath, S. U. S., Ogden, F. L., Downer, C. W., and Sharif, H. O. (2000). “On the Calibration and Verification of Two-Dimensional, Distributed, Hortonian, Continuous Watershed Models.” *Water Resources Research*, 36(6), 1495–1510.

Simons and Associates, Inc. (1997). “Hydrologic Analysis of the California Gulch Watershed.” Simons and Associates, Inc.

Singh, V. P., and Frevert, D. K. (2006). *Watershed models*. CRC/Taylor & Francis, Boca Raton, FL.

Singh, V. P., and Woolhiser, D. A. (2002). “Mathematical Modeling of Watershed Hydrology.” *Journal of Hydrologic Engineering*, 7(4), 270–292.

Smith, M. B., Koren, V. I., Reed, S. M., and Zhang, Z. (2003). “Hydrologic Model Calibration in the National Weather Service.” *Calibration of watershed models*, Watershed Science and Application, American Geophysical Union.

Smith, M. B., Seo, D.-J., Koren, V. I., Reed, S. M., Zhang, Z., Duan, Q., Moreda, F., and Cong, S. (2004). “The distributed model intercomparison project (DMIP): motivation and experiment design.” *Journal of Hydrology*, 298(1–4), 4–26.

Smith, R. E., and Hebbert, R. H. B. (1983). “Mathematical Simulation of Interdependent Surface and Subsurface Hydrologic Processes.” *Water Resources Research*, 19(4), 987–1001.

Storm, and Refsgaard, J. C. (1996). “Modelling the Entire Land Phase of the Hydrological Cycle.” *Distributed hydrological modelling*, M. B. Abbott and J. C. Refsgaard, eds., Kluwer Academic Publishers.

US EPA. (2010). “US EPA Superfund Website.” *CERCLA Overview*, <http://www.epa.gov/superfund/policy/cercla.htm> (Sep. 21, 2010).

US EPA Region 8. (2010). “US EPA Region 8 Superfund Colorado Cleanup Sites.” *California Gulch*, <http://www.epa.gov/region8/superfund/co/calgulch/#2> (Sep. 21, 2010).

Velleux, M. L. (2005). “Spatially distributed model to assess watershed contaminant transport and fate.” Ph.D. Dissertation, Colorado State University, United States—Colorado.

Velleux, M. L., England, J. F., and Julien, P. Y. (2008a). “TREX: Spatially Distributed Model to Assess Watershed Contaminant Transport and Fate.” *Science of the Total Environment*, 404(1), 113–128.

Velleux, M. L., Julien, P. Y., and England, J. F. (2008b). *TREX Watershed Modeling Framework User’s Manual: Model Theory and Description*. Department of Civil Engineering, Colorado State University, Fort Collins, CO.

Velleux, M. L., Julien, P. Y., Rojas Sánchez, R., Clements, W. H., and England, J. F. (2006). “Simulation of Metals Transport and Toxicity at a Mine-Impacted Watershed: California Gulch, Colorado.” *Environ. Sci. Technol.*, 40(22), 6996–7004.

Wagener, T. (2004). *Rainfall-Runoff Modelling in Gauged and Ungauged Catchments*. Imperial College Press, London.

Wagener, T., Sivapalan, M., Troch, P., and Woods, R. (2007). “Catchment Classification and Hydrologic Similarity.” *Geography Compass*, 1(4), 901–931.

Watershed Management Committee, Irrigation and Drainage Division. (1993). “Criteria for Evaluation of Watershed Models.” *Journal of Irrigation and Drainage Engineering*, 119(3), 429–442.

Whitmeyer, S., Nicoletti, J., and De Paor, D. (2010). “The digital revolution in geologic mapping.” *GSA Today*, 4–10.

# APPENDIX A: RECOMMENDATIONS

Within this work, there are several complete, significant contributions to the field of engineering hydrology. The strength of the contributions, in some ways, may be measured by the number of new questions raised and doors opened to further investigation and research. Following are a number of suggested areas for continued work with the TREX-SMA model and the modeling tools developed with this research. These recommendations are subdivided into topics directly related to the current research at California Gulch with TREX-SMA and other topics peripheral to the current research.

## A.1 Ideas for Directly Related Research

A number of ideas for further research pertain directly to the TREX-SMA application at California Gulch as presented in this dissertation.

### *A.1.1 Evaluation of a priori parameter applicability*

The a priori parameters used for the soil moisture accounting algorithm were designed for use in a different model: National Weather Service Hydrology Laboratory Research Distributed Hydrology Model (NWS HL-RDHM). Some validation of the approach used in this research would be achieved by obtaining the results from that model and observing the effect of parallel changes to that model and the TREX-SMA implementation.

### *A.1.2 SAC-SMA calibration for California Gulch*

The HL-RDHM model, operated on a 4km grid, has somewhat different parameter dependencies from the traditional SAC-SMA, which is purely lumped. Unfortunately, no SAC-SMA model has been created for California Gulch alone. By creating NWSRFS run for California Gulch alone, or by expanding the TREX-SMA run to include the Arkansas river to a point where SAC-SMA has been calibrated, a helpful comparison would result. Prior research with TREX by John England on the Arkansas would potentially provide as starting point.

### *A.1.3 Refine the No SMA case*

The No-SMA case in this research was simply the TREX model run with no re-initialization of infiltration parameters. The simulation could be redesigned to re-initialize the infiltration parameters to the given initial conditions for each of the storms during which the SMA case re-initialized based on the SMA states.

### *A.1.4 Extension of California Gulch simulation through entire year*

During the site visit to Leadville in June 2010, Colorado Mountain College professors Kato Dee and Dirk Monroe expressed interest in a model to help them predict peak runoff for snowmelt sampling.

### *A.1.5 Another Basin*

The TREX-SMA model might be applied at another location with more significant baseflow signature. Several watersheds with research-quality datasets to support modeling include Little Washita, Oklahoma; Loch Vale, Colorado; Goodwin Creek, Mississippi; or any of the basins in the National Critical Zone Observatory program: Boulder Creek CZO, Christina River Basin CZO, Jemez River Basin CZO, Luquillo CZO, Southern Sierra CZO, and the Susquehanna Shale Hills CZO.

## A.2 PERIPHERAL TOPICS

Additional research or development topics naturally follow from the current research, though they may not be directly related. Many of these are in cross-discipline research areas would require expertise in both hydrology and computer science to be successfully investigated.

### *A.2.1 SNODAS and snow*

During this research, a three-year, hourly SNODAS dataset extending from September 1, 2004 to March 1, 2007 was acquired, but never used. This dataset contains estimated snow water equivalent, frozen precipitation, and liquid precipitation for each hour over the contiguous United States on a

1km x 1km grid. Additionally, the dataset provides estimated snowpack sublimation, snowmelt, blowing snow sublimation, snow average temperature, and snow depth on a 24-hour basis. TREX-SMA could be modified to explore the possibilities of continuous modeling with SNODAS data as a driving parameter.

Another possibility for modeling snow and snow-based flows has become a reality with work executed by Dr. Mark Velleux at Hydroqual, Inc. Since the initiation of the current research, Dr. Velleux has developed a version of TREX that models snow melt using an energy balance model. This model could be incorporated into TREX-SMA for year-round continuous modeling.

### *A.2.2 Automatic parameter optimization*

The TREX and TREX-SMA models both contain parameters that require "tuning." By coupling the model with an automatic parameter optimization algorithm, modelers could avoid the very arduous process of manually calibrating these values. To implement such an automatic optimization scheme would presuppose some of the other efforts such as input generation interface (to spawn the calibration runs), integrated statistics (to guide the optimization), and model speedup (so that it doesn't take so long and can potentially be interactive). The existing "hot-start" capabilities in the TREX main code could be used to create calibration points, i.e. "things look good to here, lets run from here and tune a few times, then go back to the beginning."

### *A.2.3 Web interface for input generation*

Why web? A web interface is portable to all platforms and would reach a wider audience in its use, consistent with the policy of distributing the source code for free. A web interface to the program would also be consistent with various web sources of data such as USGS and NOAA. In fact, a tool could be developed that, with some reasonable estimates, would automatically provide the TREX-SMA input file for a given location clicked on a map (examples of this kind of model include the USDA model WEPP/FuMe and work by Dr. Mazdak Arabi called eRAMS). ArcGIS online or

Google Earth could be used in a mash-up to provide a base imagery or map layer data with scientific landuse, soils, topography, and other data provided by connections to appropriate databases or represented with surrogates.

The result of using such a tool might be a compressed electronic package of the necessary files which could be run on the computer of choice. Alternatively, the web interface could initiate a model simulation directly on a processing workstation linked to the web server.

### *A.2.4 Web interface for output*

The techniques for viewing output developed in this research might be coalesced into a single web-based interface. A model simulation initiated with the web-based input generation and model initiation tool discussed in 138, could be monitored simultaneously by any number of by collaborators, and their collective input could drive corrections and improvements. This would provide a significant benefit to military advisors who may have difficulty obtaining expert opinion in the field, especially in hydrology and meteorology.

### *A.2.5 Integrated Statistics*

In order to automatically evaluate moel output, the statistical analysis of the ouput time series must be integrated with the model operation. This has been largely accomplished in this research. Additional statistical measures may be incorporated and output tailored to different needs. For instance, precipitation and flow frequency plots could be generated from observed or simulated data.

### *A.2.6 Collaborative coding environment*

A open source collaborative coding environment has been implemented as part of this research. This allows for edits to the TREX code to be made simultaneously by any number of users; these edits can then be combined into a single main code branch with minimal complication. Further improvements to this environment would include a clear open source copyright statement in the code files, improved interface to the repository with bug tracking,  wiki-type documentation, etc.

### *A.2.7 Parallelization /Optimization*

Forecasting, operational use, and scenario testing all demand short simulation times. Several possibilities exist for improving simulation time:

- Modify array declarations to create longer contiguous memory segments
- Parallelize code by re-writing water, sediment, and chemical flux code to "pull" information from adjacent cells
- Implement library lookups for complex calculations

All three of these modifications have already been either tested or partially examined. The first of these modifications has been fully impelemented in a hydrology-only test case under the direction of Dr. Sanjay Rajopadhye with up to 20% improvement in speed reported. Parallelization has been implemented with TREX-SMA test cases but requires further re-coding of major algorithms in order to benefit from potential improvements. Library lookups are under investigation by one of Dr. Michelle Strout's students.

## APPENDIX B: PROGRAM CODE

Approximately 1700 lines of C were added as significant revisions to the main TREX code body as part of this research. These changes include:

- Addition of the main function which performs soil moisture accounting
- A new data structure to contain a soil moisture zone state and flux variables
- Inclusion of functions for converting simulation time to human readable dates
- Modifications to include return flows from SMA computations

Pertinent files or sections of files have been included for reference in section 140. Vertical ellipses such as this:

⋮

indicate sections of code which have been omitted for brevity. The most recent version of the complete source code may be obtained by visiting http://www.engr.colostate.edu/trex.

An additional 7500 lines of script code were generated to create the plots and statistical analyses shown in Chapters 5 and 6. These scripts were duplicated for the various gauges and individual storms. Typical examples of the different scripts are found in Section 161.

The GRASS GIS and Google earth based KML scripts account for approximately 1000 additional lines of code. Examples of the scripts used to produce the overlays, distribute the time series, and display georeferenced plots are included in section 182.

The subversion repository with all code may be accessed on-line at:

https://www.engr.colostate.edu/trex/repos/TREX

## B.1 TREX-SMA CODE

### *B.1.1 Soil Moisture Accounting*

```
/*-----------------------------------------------------------------------
C-  Function:    percolationSMA.c
C-
C-  Purpose/    percolationSMA.c performs soil moisture accounting
C-         using a method similar to the Sacramento Soil Moisture
C-        Accounting procedure.
C-  Methods:
C-
C-  Inputs:
C-
C-  Outputs:
C-
C-  Controls:
C-
C-  Calls:      None
C-
C-  Called by:  Infiltration
C-
C-  Created:    James Halgren (CSU)
C-         Fred Ogden made significant contributions by providing "Sac-mini.c", created by the
C-         NWS as a non-Fortran (ANSI C) version of the SAC-SMA routine.
C-
C-  Date:       Wed Mar  7 11:56:19 MST 2007
C-  Date:       Thu Nov 21 16:55:36 MDT 2008
C-
C-  Revised:
C-
C-  Date:
C-
C-----------------------------------------------------------------------*/

//trex global variable declarations
#include "trex_general_declarations.h"

//trex global variable declarations for water transport
#include "trex_water_declarations.h"

//variable declarations and definitions specific to the
//soil moisture accounting procedure.
#include "trex_SMA_declarations.h"

void percolationSMA (void)
{
    //JSH ADD This file has been slightly modified in the
    //JSH ADD sma2optimize branch of this code.

    //Local variable declaration
    //For volume balance checking
    //JSH DEL DO WE NEED THESE???
    double lf1c0, lf1c1, lf1m, lf2c0, lf2c1, lf2m, ltc0, ltc1, ltm;
    double uf1c0, uf1c1, uf1m, uf2c0, uf2c1, uf2m, utc0, utc1, utm;
    //JSH DEL DO WE NEED THESE???

    //Note that the state variables and outputs are passed by reference - JSH
    //All other values are not being modified. - JSH
    //These are the passed variables in the function call to sac_mini - JSH
    double *uztwc               //Upper zone tension water current volume
     , *uzfwctotal              //Total volume of free water in all upper zones
     , uzfwmtotal               //Total volume of free water capacity in all upper zones
     , *lztwc                   //Lower zone tension water current volume
     , *lzfwctotal              //Total volume of free water in all lower zones
     , lzfwmtotal               //Total volume of free water in all lower zones
     , *uzfwc                   //Upper zone free water current volume
     , *lzfwc                   //Lower zone free water current volume
     , uztwm                    //Upper zone tension water capacity
     , uzfwm                    //Upper zone free water capacity
     , lztwm                    //Lower zone tension water capacity
     , lzfwm                    //Lower zone free water capacity
     , saved                    //Lower zone free water not available to resupply tension water
     , zperc                    //Percolocation multiplier applied to pbase
     , rexp                     //Exponent defining percolation change between wet adn dry soils
     , pfree                    //Minimum fraction of percolated water resupplying deep free
water
```

```
 , *pcp                     //
 , pbase                    //
 , *flowsf                  //
 , *flowin                  //
 , *flowbf                  //
 , *edmnd                   //
 , *e1                      //
 , *e2                      //
 , *e3;                     //

//These are the locally declared variables in sac_mini - JSH
// I have modified some to be pointers
double *perc                //
 , *percdemand              //
 , *pav                     //
 , rperc                    //
 , red                      //
 , a                        //
 , b                        //
 , del                      //
 , duz                      //
 , duzr                     //
 , dlz                      //
 , dlzr                     //
 , check;                   //

double *F, ratlcmtot        //
 , ratucmtot                //
 , ratumm                   //
 , ratucm                   //
 , ratlmm                   //
 , ratlcm                   //
 , pcpreserve               //
 , percreserve;             //

double kpart                //
 , kperc;                   //
double kbfeff               //
 , kifeff;                  //

/*Variables for Reinitialization code */
long isoil;                 //Index of soil type.
/*Variables for Reinitialization code */

//JSH DEL These are unused declarations from Fred Ogden Sac-mini.c - JSH
//JSH DEL double ratlp,dcuz,
//JSH DEL dclz,  hpl, percs;
//JSH DEL double dinc, pinc, evap;
//JSH DEL int skip, ninc, nskip, inc;

//JSH ADD Fill the upper zone buckets by looping through each cell
//JSH ADD this loop could occur under a conditional (infopt == 2)
//JSH ADD in the infiltration.c super-loop

/* 01_EVAPORATION BEGIN */
// Loop over upper zones
for (k = 1; k <= nuz; k++)
{
    uzSMA[k]->etdemand = 0;
    /*
       for (i = 1; i <= nrows; i++)
       {
       for (j = 1; j <= ncols; j++)
       {
       if (imask[i][j] != nodatavalue)
       {
       //Extract ET before accounting for additional infiltration
       //Each upperzone has an evaporation demand computed from the
       //accumulation of individual cell demands across the domain.
       //The cell ET demand is applied to the cumulative value for
       //each upperzone according to the partition coefficient which,
       //though it could be different, shall be defined as equal to
       //the kuzSMA partition coefficient.
       uzSMA[k]->etdemand += kuzSMA[k][i][j] * etdemand[i][j];
       }
       }
       }
     */
}
/* The evaporation demand for the entire domain is calcuated
   for all upper zones and then, theoretically, there should
```

```
   be some comparison to the upper zone storages in order to
   determine if the demand will be met and if not, which zone's
   demand will be reduced -- otherwise, we give preference to
   the first zone in any cell with hybrid upper zones.

   Of course, this complication is an argument for having only
   one zone per cell, similar to how there probably should only
   be one lowerzone per upper zone. Inverted pyramid style,
   from top to bottom, we always decrease in complexity. */

for (k = 1; k <= nuz; k++)
{
    /* JSH DEL Fixed ET to function for CG Case
     * JSH DEL This is a temporary workaround and needs to be replaced
     edmnd = &(uzSMA[k]->etdemand);
     //Scale the input by the number (and portion) of contributing cells
     (*edmnd) /= uzSMA[k]->areafactor;
     //Convert to millimeters, the internal units for the SMA procedure
     (*edmnd) *= 1000;
     END JSH DEL */

    uzSMA[k]->etdemand = 0.18;      //depth of evaporation in inches per day
    uzSMA[k]->etdemand *= (.3048 / 12);     //convert to meters per day
    uzSMA[k]->etdemand *= (1.0 / 86400);    //convert to meters per second
    uzSMA[k]->etdemand *= (1000 / 1);       //convert to millimeters per second
    edmnd = &(uzSMA[k]->etdemand);
    (*edmnd) *= dt[idt];    //multiply by the time step for meters

    // Calculate actual upper zone ET
    e1 = &(uzSMA[k]->et);
    uztwc = &(uzSMA[k]->twc);
    uztwm = uzSMA[k]->twm;

    //upper zone evaporation is scaled by the available upperzone tension water
    *e1 = (*edmnd) * ((*uztwc) / uztwm);
    (*uztwc) -= (*e1);

    //If upperzone tension water does not satisfy the ET demand ...
    if (*uztwc < 0.0)
    {
        *e1 = (*edmnd) + (*uztwc);
        *uztwc = 0.0;
    }
    //remaining evaporation demand is initialized for use during the rest of the loop.
    red = (*edmnd) - (*e1);
    if (red > 0)
    {
        e2 = &(uzSMA[k]->et_deep);
        (*e2) = 0;
        for (m = 1; m <= nlz; m++)
        {
            // Calculate actual lower zone ET
            e3 = &(lzSMA[m]->et);
            lztwc = &(lzSMA[m]->twc);
            lztwm = lzSMA[m]->twm;
            kperc = uzSMA[k]->kperc[m];

            //lower zone evaporation is scaled by the kperc partition coefficient
            (*e3) = red * kperc * ((*lztwc) / lztwm);
            (*lztwc) -= (*e3);

            //If lower zone tension water does not satisfy the ET demand ...
            if (*lztwc < 0.0)
            {
                *e3 += (*lztwc);
                *lztwc = 0.0;
            }
            (*e2) += (*e3);
        }
        //remaining evaporation demand is initialized for use during the rest of the loop.
        red -= (*e2);
        if (red > 0)
        {
            // Go to upper zone free water first for evaporation
            uzfwctotal = &(uzSMA[k]->fwctotal);
            *uzfwctotal = 0;
            for (h = 1; h <= uzSMA[k]->nparts; h++)
            {
                e3 = &(uzSMA[k]->part[h]->et);
                uzfwc = &(uzSMA[k]->part[h]->fwc);
                uzfwm = uzSMA[k]->part[h]->fwm;
```

```
                kpart = uzSMA[k]->kpart[h];

                //If evap demand is greater than the free water volume,
                //Add all the free water to evap and set free water to zero
                if ((*uzfwc - (red * kpart)) < 0.0)
                {
                    (*e3) += (*uzfwc);
                    *uzfwc = 0.0;
                    printf ("evap not satisfied\n");
                }
                //Otherwise, just reduce the free water by the evap amount.
                else
                {
                    (*e3) += (red * kpart);
                    (*uzfwc) -= (red * kpart);
                }
                (*uzfwctotal) += (*uzfwc);
            }
            red -= (*e3);
        }
    }
}                           /* 01_EVAPORATION END */


/* 02_REDISTRIBUTION BEGIN */
// Loop over upper zones
for (k = 1; k <= nuz; k++)
{
    uztwc = &(uzSMA[k]->twc);
    uztwm = uzSMA[k]->twm;
    uzfwctotal = &(uzSMA[k]->fwctotal);
    uzfwmtotal = uzSMA[k]->fwmtotal;

    //Initialize free water total to make sure it adds up
    *uzfwctotal = 0;
    //Loop over free water storages in each lower zone
    for (h = 1; h <= uzSMA[k]->nparts; h++)
    {
        uzfwc = &(uzSMA[k]->part[h]->fwc);
        (*uzfwctotal) += (*uzfwc);
    }

    // if uztwc/uztwm < uzfwc/uzfwm, make them equal */
    // JSH ADD This should actually balance the
    // JSH ADD storage volumes according to kpart
    a = (*uztwc) / uztwm;
    b = (*uzfwctotal) / uzfwmtotal;
    if (a < b)
    {
        a = ((*uztwc) + (*uzfwctotal)) / (uztwm + uzfwmtotal);
        // JSH The following is the algebraic proof that the redistribution
        // JSH is not modifying the mass balance in this loop.
        // a = (tc0 + fc0) / (tm + fm);
        // tc1 = tm * (tc0 + fc0) / (tm + fm);
        // fc1 = fm * (tc0 + fc0) / (tm + fm);
        // tc1 + fc1 = tc0 + fc0;
        // try it -- it works!
        *uztwc = uztwm * a;
        *uzfwctotal = 0;
        for (h = 1; h <= uzSMA[k]->nparts; h++)
        {
            uzfwc = &(uzSMA[k]->part[h]->fwc);
            uzfwm = uzSMA[k]->part[h]->fwm;
            *uzfwc = uzfwm * a;
            (*uzfwctotal) += (*uzfwc);
        }
    }
    //JSH During debugging, it was noted that if the upper zone
    //JSH free water exceeds the maximum, then the rebalancing
    //JSH procedure can put more than the maximum possible into
    //JSH the upper zone tension water which in turn has the effect of
    //JSH making the available precip increase out of control
    //JSH (because it is computed as the difference between incoming precipitation
    //JSH and the tension water deficit -- which means subtracting a negative number
    //JSH if twc > twm).
    if ((*uztwc) > uztwm)
    {
        printf ("Upper zone tension water has exceeded the maximum\n\
              A serious error has occured in the mass balance.\n");
    }
}
```

```
// Loop over lower zones
for (k = 1; k <= nlz; k++)
{
    lztwc = &(lzSMA[k]->twc);
    lztwm = lzSMA[k]->twm;
    saved = lzSMA[k]->saved;
    lzfwctotal = &(lzSMA[k]->fwctotal);
    lzfwmtotal = lzSMA[k]->fwmtotal;

    //Initialize free water total to make sure it adds up
    *lzfwctotal = 0;
    //Loop over free water storages in each lower zone
    for (h = 1; h <= lzSMA[k]->nparts; h++)
    {
        lzfwc = &(lzSMA[k]->part[h]->fwc);
        (*lzfwctotal) += (*lzfwc);
    }

    // if lower zone tension water becomes small, pull some water up from s & p
    a = (*lztwc) / lztwm;
    b = ((*lzfwctotal) + (*lztwc) - saved) / (lzfwmtotal + lztwm - saved);
    if (a < b)
    {
        del = (b - a) * lztwm;
        (*lztwc) += del;
        *lzfwctotal = 0;
        //Loop backward through the zones
        //Filling tension water with last free water first.
        for (h = lzSMA[k]->nparts; h >= 1; h--)
        {
            // This has been checked for mass balance errors
            lzfwc = &(lzSMA[k]->part[h]->fwc);
            (*lzfwc) -= del;
            //JSH ADD put a debugging stop here if del gets below 0, which it shouldn't
            //JSH ADD Erroneous array access could occur ...
            if ((*lzfwc) < 0.0)
            {
                del = -1.0 * (*lzfwc);
                (*lzfwc) = 0.0;
            }
            else
            {
                del = 0.0;
            }
            (*lzfwctotal) += (*lzfwc);
        }
    }
}                           /* 02_REDISTRIBUTION END */


/* 03_PRECIP BEGIN PART I */
for (k = 1; k <= nuz; k++)
{
    uzSMA[k]->wnew = 0;
    uzSMA[k]->precip = 0;
    for (i = 1; i <= nrows; i++)
    {
        for (j = 1; j <= ncols; j++)
        {
            if (imask[i][j] != nodatavalue)
            {
                //Apply portion of cumulative infiltration to each upper zone
                uzSMA[k]->wnew +=
                    kuzSMA[k][i][j] * SMAinfiltrationvol[i][j];
                uzSMA[k]->precip += kuzSMA[k][i][j] * SMAprecipvol[i][j];
            }
        }
    }
}

for (k = 1; k <= nuz; k++)
{
    pcp = &(uzSMA[k]->pcp);
    pav = &(uzSMA[k]->pav);
    *pcp = 0;
    *pcp = uzSMA[k]->wnew;
    //Scale the input by the number (and portion) of contributing cells
    (*pcp) /= uzSMA[k]->areafactor;
    //Convert to millimeters, the internal units for the SMA procedure
    (*pcp) *= 1000;
```

```
        uztwc = &(uzSMA[k]->twc);
        uztwm = uzSMA[k]->twm;

        //Does all the precip fit in the available upper zone tension?
        *pav = 0.0;
        (*pav) = (*pcp) - (uztwm - (*uztwc));
        //If it does, fill up the upper zone tension and clear the precip var.
        if ((*pav) < 0.0)
        {
            (*uztwc) += (*pcp);
            *pav = 0.0;
        }
        //If there is some leftover, set tension to max ...
        else
        {
            *uztwc = uztwm;
        }
        //... and
        //Store remaining precip in wnew (via *pcp pointer)
        *pcp = *pav;
    }                           /* 03_PRECIP END PART I */

    //JSH ADD This scaling (below) would be important
    //JSH ADD if we used longer time steps.
    //JSH ADD This is just a code excerpt from sac_mini.c
    //JSH ADD So please refer to the original for further work
///*############################################################################*/
///* determine the number of time increments required so that no one increment  */
///* will exceed 5.0 mm of (*uzfwc+pav).  pinc is the precip available in each  */
///* time increment.                                                            */
///*############################################################################*/
//                ninc = (int) (1.00001 + ((*uzfwc) + pav) / 5.0);        /* uzfwc, pav in  mm,
5.0 is max rate */
//                dinc = 1.0 / (float) ninc;
//                pinc = pav * dinc;
//                *flowbf = 0.0;
//                *flowsf = 0.0;
//                *flowin = 0.0;
//                duz = uzSMA[k]->part[h]->k;
//                nskip = 1;
//                if (pav > 5.08)
//                {
//                    nskip = 0;
//                }
//
///* if there are sub-increments, modify the rate constants accordingly  */
//                if (ninc > 1)
//                {
//                    duz = 1.0 - pow ((1.0 - dcuz), (double) dinc);
//                }


    /* 04.00_Initialize SMA outlets BEGIN */
    for (m = 1; m <= nio; m++)
    {
        ioSMA[m]->wnew = 0;
    }                           /* 04.00_Initialize SMA outlets END */


    /* 04_BASEFLOW BEGIN */
    for (k = 1; k <= nlz; k++)
    {
        lzSMA[k]->basftotal = 0.0;
        lzfwctotal = &(lzSMA[k]->fwctotal);
        *lzfwctotal = 0;
        //Loop over free water storages in each lower zone
        for (h = 1; h <= lzSMA[k]->nparts; h++)
        {
            lzfwc = &(lzSMA[k]->part[h]->fwc);
            dlz = lzSMA[k]->part[h]->k;

            //Compute baseflow from the previous time step's lower zone free water.
            kbfeff = dlz;
            // Convert depletion coefficient from mm / mm / day
            // To mm / mm / s and multiply by the time step to determine straight volume
            kbfeff /= (24       // hours / day
                       * 60     // minutes / hour
                       * 60);   // seconds / minute
            kbfeff *= dt[idt];  //seconds
```

```
            //Total infiltration [mm] from this lower zone part is accumulated in the variable
'basf'.
            lzSMA[k]->part[h]->basf = ((*lzfwc) * kbfeff);
            //Amount of interflow is subtracted from fwc
            (*lzfwc) -= lzSMA[k]->part[h]->basf;
            //Amount of baseflow is added to total for the zone
            lzSMA[k]->basftotal += lzSMA[k]->part[h]->basf;
            //Free water total is updated
            (*lzfwctotal) += (*lzfwc);
            //Distribute baseflow to nio interflow outlets
            for (m = 1; m <= nio; m++)
            {
                flowbf = &(ioSMA[m]->wnew);
                (*flowbf) += lzSMA[k]->part[h]->basf
                    * lzSMA[k]->part[h]->kbasf[m]
                    * lzSMA[k]->areafactor * w * w / 1000;
            }
        }
    }                           /* 04_BASEFLOW END */


    /* 05_PERCOLATION_DEMAND BEGIN */
    for (k = 1; k <= nlz; k++)
    {
        lztwc = &(lzSMA[k]->twc);
        lztwm = lzSMA[k]->twm;
        lzfwctotal = &(lzSMA[k]->fwctotal);
        lzfwmtotal = lzSMA[k]->fwmtotal;
        percdemand = &(lzSMA[k]->percdemand);
        pbase = lzSMA[k]->pbase;
        zperc = lzSMA[k]->zperc;
        rexp = lzSMA[k]->rexp;

        //Initialize free water total to make sure it adds up
        *lzfwctotal = 0;
        //Loop over free water storages in each lower zone
        for (h = 1; h <= lzSMA[k]->nparts; h++)
        {
            lzfwc = &(lzSMA[k]->part[h]->fwc);
            (*lzfwctotal) += (*lzfwc);
        }

        //Compute percolation demand for this time step in this lower zone
        //Limit demand to the minimum of pbase
        a = lzfwmtotal - (*lzfwctotal) + lztwm - (*lztwc);      /* sum of lwr zone deficits */
        b = lzfwmtotal + lztwm;
        *percdemand = pbase * (1 + zperc * pow ((a / b), rexp));
    }
    /* 05_PERCOLATION_DEMAND END */


    /* 06_PERCOLATION BEGIN */
    for (k = 1; k <= nlz; k++)
    {
        //initialize lower zone new water
        lzSMA[k]->wnew = 0;
    }

    for (k = 1; k <= nuz; k++)
    {
        //Initialize upper zone to lower zone percolation
        uzSMA[k]->perctotal = 0;
        uzfwctotal = &(uzSMA[k]->fwctotal);
        *uzfwctotal = 0;
        for (h = 1; h <= uzSMA[k]->nparts; h++)
        {
            uzfwc = &(uzSMA[k]->part[h]->fwc);
            uzfwm = uzSMA[k]->part[h]->fwm;
            perc = &(uzSMA[k]->part[h]->percolation);
            *perc = 0;

            //Compute percolation to lower zone from previous
            //time step percdemand and current time step uzfwc/uzfwm ratio.
            for (m = 1; m <= nlz; m++)
            {
                /* JSH Comment: 2009 12:34:21 GMT-0700 */
                //I am going to make the strategic decision that from upper to
                //lower, the zones can only aggregate (1 to many relation for lower to upper).
                //This should mean that this loop shouldn't be necessary since
                //for a given upper zone, there will be one lower zone.
                //(Other upper zones may have the same index
```

```
            //but each upper zone will have only one index.)
            //Someone later could make an array of indexes and liven things up a bit.
            //
            // The problem is that if there is more than
            // one upper zone contributing to a particular lower zone,
            // the first upper zone may max out the lower storage volume
            // (i.e. the check parameter is triggered at > 0 above)
            // but the the storages are not updated until the next
            // step and this could lead to overfilling of the wnew
            // and THEN what do we do?
            //
            // This might be a reason to wrap the mass transfer
            // steps (05 -- 08) into a larger loop (though not necessarily
            // for the reasons that FLO did it--to compute the incremental
            // volumes for long time steps). In the larger loop, we could
            // check for such errors
            /* JSH Comment: 2009 12:34:43 GMT-0700 */

            lztwc = &(lzSMA[k]->twc);
            lztwm = lzSMA[k]->twm;
            lzfwctotal = &(lzSMA[k]->fwctotal);
            lzfwmtotal = lzSMA[k]->fwmtotal;
            percdemand = &(lzSMA[m]->percdemand);
            kperc = uzSMA[k]->kperc[m];

            //Set aside volume for percolation
            rperc = (*percdemand);
            // Convert demand mm / mm / day
            // To mm / mm / s and multiply by the time step to determine straight volume
            rperc /= (24    // hours / day
                      * 60  // minutes / hour
                      * 60);        // seconds / minute
            rperc *= dt[idt];       //seconds
            //percolation is scaled by available upper zone free water
            rperc *= (*uzfwc) / uzfwm;

            //percolation is scaled by the free water portion contributing to each outlet
            //similar to the scaling of evaporation demand.
            rperc *= kperc;
            //If demand is greater than free water supply, take as much as possible
            if (rperc > (kperc * (*uzfwc)))
            {
                rperc = (kperc * (*uzfwc));
            }
            else
            {
                //This check reserves as upper zone free water any amount which
                //does not fit in the lower zone storages.
                check = (*lzfwctotal) + (*lztwc) - lzfwmtotal - lztwm;
                check *= kperc;
                check += rperc;

                if (check > 0.0)
                {
                    (rperc) -= check;
                }
            }

            // Mass Balance Check
            lzSMA[m]->wnew += rperc;
            (*perc) += rperc;
        }                   //end loop over lower zones within upper zone loop
        // Mass Balance Check
        (*uzfwc) -= (*perc);
        (*uzfwctotal) += (*uzfwc);
        uzSMA[k]->perctotal += (*perc);
    }
}                           //end Loop over upper zones
/* 06_PERCOLATION END */


/* 07_INTERFLOW BEGIN */
for (k = 1; k <= nuz; k++)
{
    uzSMA[k]->intftotal = 0.0;
    uzfwctotal = &(uzSMA[k]->fwctotal);
    *uzfwctotal = 0;
    //Loop over free water storages in each upper zone
    for (h = 1; h <= uzSMA[k]->nparts; h++)
    {
        uzfwc = &(uzSMA[k]->part[h]->fwc);
```

```
        duz = uzSMA[k]->part[h]->k;

        // After satisfying percolation demand, interflow
        // is computed from the remaining upper zone free water.
        kifeff = duz;
        // Convert depletion coefficient from mm / mm / day
        // To mm / mm / s and multiply by the time step to determine straight volume
        kifeff /= (24       // hours / day
                   * 60     // minutes / hour
                   * 60);   // seconds / minute
        kifeff *= dt[idt];  //seconds
        //Total infiltration from this lower zone is accumulated in the variable 'intf'.
        uzSMA[k]->part[h]->intf = ((*uzfwc) * kifeff);
        //Amount of interflow is subtracted from fwc
        (*uzfwc) -= uzSMA[k]->part[h]->intf;
        //Amount of interflow is added to total for the zone
        uzSMA[k]->intftotal += uzSMA[k]->part[h]->intf;
        //Free water total is updated
        (*uzfwctotal) += (*uzfwc);
        for (m = 1; m <= nio; m++)
        {
            flowin = &(ioSMA[m]->wnew);
            (*flowin) += uzSMA[k]->part[h]->intf
                * uzSMA[k]->part[h]->kintf[m]
                * uzSMA[k]->areafactor * w * w / 1000;
        }
    }
}                           /* 07_INTERFLOW END */


/* 08_NEW WATER BEGIN */
for (k = 1; k <= nlz; k++)
{
    perc = &(lzSMA[k]->wnew);
    lztwc = &(lzSMA[k]->twc);
    lztwm = lzSMA[k]->twm;
    lzfwctotal = &(lzSMA[k]->fwctotal);
    lzfwmtotal = lzSMA[k]->fwmtotal;
    pfree = lzSMA[k]->pfree;
    F = &(lzSMA[k]->fwdeficitratio);

    //rperc is used in this loop in a slightly difference sense than in the top loop.
    rperc = (*perc) * (1.0 - pfree);

    //check if percolation is less than the lowerzone deficit.
    //If it is, dump the percolated water into the tension bucket,
    //clear perc, and move on.
    if (rperc <= (lztwm - (*lztwc)))        /* chgd order of m and c - flo */
    {
        *lztwc += rperc;
        rperc = 0.0;
    }
    //If there is more incoming water than the twc can hold ...
    else
    {
        rperc -= (lztwm - (*lztwc));        /* chgd from + to - flo */
        *lztwc = lztwm;
    }
    //Add the pfree portion back in and distribute
    //this water to the lower zone free water storages
    rperc += (*perc) * pfree;
    if (rperc > 0.0)
    {
        // Distribute Percolated Water according to demand
        for (h = 1; h <= lzSMA[k]->nparts; h++)
        {
            lzfwc = &(lzSMA[k]->part[h]->fwc);
            lzfwm = lzSMA[k]->part[h]->fwm;
            (*F) = (lzfwm - (*lzfwc)) / (lzfwmtotal - (*lzfwctotal));
            (*lzfwc) += (rperc * (*F));
        }

    }                       // end if tension water leaves water for percolation
}                           // end loop over lower zones

for (k = 1; k <= nlz; k++)
{
    //Initialize free water total to make sure it adds up
    *lzfwctotal = 0;
    //Loop over free water storages in each lower zone
    for (h = 1; h <= lzSMA[k]->nparts; h++)
```

```
    {
        lzfwc = &(lzSMA[k]->part[h]->fwc);
        (*lzfwctotal) += (*lzfwc);
    }
}

//Loop over upper zones to determine new water distribution
for (k = 1; k <= nuz; k++)
{
    pcp = &(uzSMA[k]->pcp);
    if (*pcp > 0)
    {
        // Distribute remaining precipitation according to demand
        for (h = 1; h <= uzSMA[k]->nparts; h++)
        {
            uzfwc = &(uzSMA[k]->part[h]->fwc);
            uzfwm = uzSMA[k]->part[h]->fwm;
            (*F) = (uzfwm - (*uzfwc)) / (uzfwmtotal - (*uzfwctotal));
            (*uzfwc) += ((*pcp) * (*F));
        }

    }
}

for (k = 1; k <= nuz; k++)
{
    //Initialize free water total to make sure it adds up
    *uzfwctotal = 0;
    //Loop over free water storages in each lower zone
    for (h = 1; h <= uzSMA[k]->nparts; h++)
    {
        uzfwc = &(uzSMA[k]->part[h]->fwc);
        (*uzfwctotal) += (*uzfwc);
    }
}                           /* 08_NEW WATER END */


/* 09_SATURATION_EXCESS BEGIN */
// JSH ADD This (09) and (10) are the real research problems
// JSH ADD (09): How to spit water back i.e.
// JSH ADD if, after the percolation and interflow has been satisfied,
// JSH ADD there is excess free water (fwc > fwm), then
// JSH ADD what do we do with the extra water?
// JSH ADD Note, since the lower zones have a check in the percolation routines,
// JSH ADD only the upper zones need to be checked for super-charging.
// JSH ADD and
// JSH ADD (10): How to correlate the SAC parameters to the GA parameters.

// Loop over upper zones
for (k = 1; k <= nuz; k++)
{

    uztwc = &(uzSMA[k]->twc);
    uztwm = uzSMA[k]->twm;

    //Initialize free water total to make sure it adds up
    *uzfwctotal = 0;
    for (h = 1; h <= uzSMA[k]->nparts; h++)
    {
        uzfwc = &(uzSMA[k]->part[h]->fwc);
        uzfwm = uzSMA[k]->part[h]->fwm;
        flowsf = &(uzSMA[k]->wreject);
        (*flowsf) = 0.0;
        //The remaining precipitated water is added to the
        //upper zone free water in the distribution step (08)
        if ((*uzfwc) > uzfwm)
        {
            // Surface flow (from saturation excess) is computed
            // from the excess upper zone free water
            (*flowsf) = (*uzfwc) - uzfwm;
            switch (SMArejectionMethod)
            {
            case 0:         //Allow upperzone to simply overfill (with a warning).
                //(*uzfwc) = uzfwm;
                printf ("The SMA routine indicates %g millimeters \
                            saturation excess runoff is ocurring due to over \
                            filling of the upper zone %5.0d, \
                            free water part %5.0d. \n\
                            Please check fwm values and consider \
                            a modification to your model.\n", (*flowsf), k, h);
                break;
```

```
            case 1:        //Redistribute excess just according to kuzSMA
                // Upper zone free water is set to the maximum
                (*uzfwc) = uzfwm;
                printf
                    ("You are now using the saturation excess rejection algorithm.\n");
                for (i = 1; i <= nrows; i++)
                {
                    for (j = 1; j <= ncols; j++)
                    {
                        if (imask[i][j] != nodatavalue)
                        {
                            //Apply portion of excess to each overland cell in the upper zone
                            smaRejectvolume =
                                (*flowsf) / uzSMA[k]->areafactor *
                                kuzSMA[k][i][j];
                        }
                    }
                }
                break;
            case 2:        //Redistribution excess based on infiltrated volume
                // Upper zone free water is set to the maximum
                (*uzfwc) = uzfwm;
                for (i = 1; i <= nrows; i++)
                {
                    for (j = 1; j <= ncols; j++)
                    {
                        if (imask[i][j] != nodatavalue)
                        {
                            //Redistribute based on infiltration
                            smaRejectvolume =
                                (*flowsf) * (SMAinfiltrationvol[i][j] /
                                             uzSMA[k]->wnew);
                        }
                    }
                }
                break;
            case 3:        //Deliver excess to channel outlets
                // Upper zone free water is set to the maximum
                (*uzfwc) = uzfwm;
                break;
            case 4:        //Resdistribute based on topographic index
                // Upper zone free water is set to the maximum
                (*uzfwc) = uzfwm;
                break;
            case 5:        //Set infiltration Rate to zero --- MLV suggestion (a good one)
                //"When there's none --- there's 'Dunne'".
                break;
            }
        }
        (*uzfwctotal) += (*uzfwc);
    }
          //ADD Would there be any advantage to allowing
          //The super-charging of fwm becomes something of a feature that maybe
          //ADD could be selectively turned on and off--assuming I can figure out
          //ADD how to turn it off in the first place. With the feature on, it allows
          //ADD the Green and Ampt piston to completely determine the Hortonian rate
          //ADD and just figuratively stacks up water to drive more percolation and
          //ADD interflow through the SMA procedure.
          //ADD Alternatively, this could be added to the interflow value.
          //ADD this would require a synthetic hydrograph (except for these extremely
          //ADD short time steps, the variation would be negligible).
          //ADD The initialization of these collector variables should occur in one
          //ADD place and should be the same place that allows them to be printed if
          //ADD that is desired. These collector variables are, for the most part,
          //ADD the sacramento model states and fluxes so we would likely want to see
          //ADD them in action.
}                           /* 09_SATURATION_EXCESS END */


/* 10_REINITIALIZE_INFILTRATION_PARAMS BEGIN */
//Loop over upper zone again to pass the information back about losses.

switch (SMAinfReinitMethod)
{
case 0:                     //For this case, do not reinitialize parameters
    printf ("SMA-based infiltration \n\
             parameter re-initialization is inactive.\n");
    break;
case 1:                     //Reinitialize parameters based on the precip
    //threshold definining the break between storms.
    //Infiltrated depth will revert to 0, and the
```

```
//moisture deficit for each soil group will be
//set to the SMASummaryState value.
SMASummaryState = 0;
SMASummaryDivisor = 0;
for (k = 1; k <= nuz; k++)
{
    for (m = 1; m <= nlz; m++)
    {
        lzSMA[m]->includeSummaryState = 1;
        if (lzSMA[m]->includeSummaryState)
        {
            lztwc = &(lzSMA[m]->twc);
            lztwm = lzSMA[m]->twm;
            SMASummaryState += (*lztwc);
            SMASummaryDivisor += lztwm;
        }
        for (h = 1; h <= lzSMA[m]->nparts; h++)
        {
            lzSMA[m]->part[h]->includeSummaryState = 0;
            if (lzSMA[m]->part[h]->includeSummaryState)
            {
                lzfwc = &(lzSMA[m]->part[h]->fwc);
                lzfwm = lzSMA[m]->part[h]->fwm;
                SMASummaryState += (*lzfwc);
                SMASummaryDivisor += lzfwm;
            }
        }

    }

    uzSMA[k]->includeSummaryState = 1;
    if (uzSMA[k]->includeSummaryState)
    {
        uztwc = &(uzSMA[k]->twc);
        uztwm = uzSMA[k]->twm;
        SMASummaryState += (*uztwc);
        SMASummaryDivisor += uztwm;
    }
    for (h = 1; h <= uzSMA[k]->nparts; h++)
    {
        uzSMA[k]->part[h]->includeSummaryState = 1;
        if (uzSMA[k]->part[h]->includeSummaryState)
        {
            uzfwc = &(uzSMA[k]->part[h]->fwc);
            uzfwm = uzSMA[k]->part[h]->fwm;
            SMASummaryState += (*uzfwc);
            SMASummaryDivisor += uzfwm;
        }
    }
}

SMASummaryState /= SMASummaryDivisor;

//if the amount of precipitation is less than the threshold
if (uzSMA[1]->precip < smaReinitializationStormEpsilon)
{
    switch (smaReinitializationStormToggle)
    {
    case -1:           //Do nothing if no storm has occurred yet
        if (smaReinitializationPrintMessageToggle != 1)
        {
            printf ("There has not yet been a storm\n");
            smaReinitializationPrintMessageToggle = 1;
        }
        break;
    case 0:            // If there has been no storm and the infiltration
        // remains below epsilon, do nothing.
        if (smaReinitializationPrintMessageToggle != 2)
        {
            printf ("There has been a storm\n");
            printf ("but it is over and another \n");
            printf ("has not yet started\n");
            smaReinitializationPrintMessageToggle = 2;
        }
        break;
    case 1:            // If there was a storm and it is now over, flip the toggle
        smaReinitializationStormToggle = 0;
        if (smaReinitializationPrintMessageToggle != 3)
        {
            printf ("The storm is over.\n");
            printf
```

```
                ("The volume of incoming water averaged per cell\n");
            printf ("on this upper zone is now less than the \n");
            printf ("specified minimum of ");
            printf ("%g\n", smaReinitializationStormEpsilon);
            printf ("The SMA parameters will continue adjusting.\n");
            printf ("When a new storm begins, the SMA parameters\n");
            printf
                ("will be used to re-initialize the infiltration parameters.\n");
            smaReinitializationPrintMessageToggle = 3;
        }
        break;
    }
}
//else if the amount of precipitation is greater than the threshold
else
{
    switch (smaReinitializationStormToggle)
    {
    case -1:           // If no storm has occurred yet,
        // set the toggle to reflect the onset of the first storm
        if (smaReinitializationPrintMessageToggle != 4)
        {
            printf ("The first storm is beginning.\n");
            smaReinitializationPrintMessageToggle = 4;
        }
        smaReinitializationStormToggle = 1;
        break;
    case 0:            // If there has been no storm and the infiltration
        // rises above epsilon, flip the toggle
        // and proceed with infiltration parameter reinitialization.
        if (smaReinitializationPrintMessageToggle != 5)
        {
            printf ("Another storm is beginning.\n");
            printf
                ("Infiltration parameters will be re-initialized\n");
            printf ("based on SMA parameter states.\n");

            printf ("Current Soil Settings are: \n");
            printf ("soil\tkhsoil\tcapshsoil\tsoilmd\n");
            smaReinitializationPrintMessageToggle = 5;
        }
        for (isoil = 1; isoil <= nsoils; isoil++)
        {
            //modify the terms for infiltration rate equation
            //The infiltration equation in infiltration-rN.c
            /*
               p1 = (float) (khsoil[isoil] * dt[idt] -
               2.0 * infiltrationdepth[i][j]);
               p2 = khsoil[isoil] * (infiltrationdepth[i][j] +
               capshsoil[isoil] * soilmd[isoil]);
             */
            printf ("%d\t", isoil);
            printf ("%g\t", khsoil[isoil]);
            //JSH ADD the infiltration depth varies by cell
            //JSH ADD the soil parameters vary by soil type
            //JSH ADD and the reset values are determined by the SMA
            //JSH ADD parameter states which come from SMA zones.
            //JSH ADD The multiple geometries are starting to get problematic.
            printf ("%g\t", capshsoil[isoil]);
            printf ("%g\n", soilmd[isoil]);
            soilmd[isoil] = SMASummaryState;
        }
        //loop through rows and columns to reset infiltration depth to 0
        //printf("%g \t", infiltrationdepth[i][j]);
        for (i = 1; i <= nrows; i++)
        {
            for (j = 1; j <= ncols; j++)
            {
                if (imask[i][j] != nodatavalue)
                {
                    /*
                     * JSH ADD --
                     * Code to account for the continuously
                     * increasing infiltration needs to be added
                     *
                     infiltrationdepth[i][j]
                     [smaReinitializationStormCount];
                     infiltrationdepth[i][j]
                     [smaReinitializationStormCount + 1] -=
                     kuzSMA[k][i][j];
                     */
```

```
                            infiltrationdepth[i][j] = 0;
                        }
                    }
                }
                smaReinitializationStormCount++;
                smaReinitializationStormToggle = 1;
                break;
            case 1:             // If there has been a storm and the infiltration
                // remains above epsilon, do nothing.
                if (smaReinitializationPrintMessageToggle != 6)
                {
                    printf ("The storm is continuing\n");
                    smaReinitializationPrintMessageToggle = 6;
                }
            }
        }
        break;
    }                           /* 10_REINITIALIZE_INFILTRATION_PARAMS END */

            //ADD How does the Sacramento model decide how much to send to primary
            //ADD and secondary lower zones? Is there a balancing process so they
            //ADD are the same percent full after each filling step?
            //ADD I know they are filled based on demand so perhaps that is the balancing
            //ADD factor.
            //ADD I am inclined to use 1-c/m (current/max) and compare that between
            //ADD the various lower zone parts but that lends itself to a problem
            //ADD with floating point error if the zones are very empty or if
            //ADD the difference in c/m ratio is very small.
}                               /* End of function percolationSMA(void): Return to WaterTransport
*/
```

### *B.1.2 Human Readable Date Display*

```
/*-----------------------------------------------------------------------
C-  File:        UtilityFunctions.c
C-
C-    Purpose/
C-    Methods:    Concatenated group of general utility functions for
C-               statistics
C-
C-  Function
C-   Listing:   Min, Max, dateshift
C-
C-      Created:    John F. England, Jr.
C-                  Bureau of Reclamation
C-                  Flood Hydrology Group, D-8530
C-                  Bldg. 67, Denver Federal Center, Denver, CO  80225
C-
C-                  Mark Velleux
C-                Department of Civil Engineering
C-                Colorado State University
C-                  Fort Collins, CO 80523
C-
C-    Date:         31-OCT-2003
C-
C-    Revised:  James Halgren
C-
C-    Date:         07-Jul-2010
C-
C-    Revisions:  added dateshift function
C-
C-----------------------------------------------------------------------*/

//trex general variable declarations
#include "trex_general_declarations.h"
#include <time.h>
#define  ONEDAY         60*60*24
#define  ONEHOUR        60*60

.
.
.

                        /*************************************/
                        /*               FUNCTION: Dateshift */
                        /*************************************/


/* JSH Comment: 2009-12-18 12:10:36 GMT-0700
 * Portions of this code based on work by Dave Taylor
 * found at http://www.askdavetaylor.com/date_math_in_linux_shell_script.html
 * (C) Copyright 2005 by Dave Taylor. Free to redistribute
 * if this copyright is left intact. Thanks.
 * JSH Comment: 2009-12-18 12:13:00 GMT-0700 */

void dateshift (char *out_ptr,       //ouput of dateshift is a variable containing
           // the offset time in the format YYYY-MM-DD HH:MM:SS
                double offset,                  //number of hours forward or backward from start
date
                long startyear,                 //year of time 0 in simulation
                long startmonth,                //month of time 0 in simulation
                long startday,                  //day of time 0 in simulation
                long starthour,                 //hour of time 0 in simulation
                long startminute,               //minute of time 0 in simulation
                long startsecond,               //second of time 0 in simulation
                long gmt_offset,                //difference in hours of start time zone from
Greenwich mean time (WITHOUT DAYLIGHT SAVINGS)
                long daylightsavings)           //=1 if given start time is in daylight savings
(USUALLY the summer time), =0 otherwise
{
    struct tm time_struct;
    time_t theTime;


    time_struct.tm_year = startyear;
    time_struct.tm_year -= 1900;
    time_struct.tm_mon = startmonth - 1; //Months are indexed from 0=January
                                  //But the input file expects human readable 1=January
    time_struct.tm_mday = startday;
    time_struct.tm_hour = starthour;
```

```
    time_struct.tm_min = startminute;
    time_struct.tm_sec = startsecond;
    time_struct.tm_isdst = daylightsavings;

    theTime = mktime (&time_struct);
    if (mktime (&time_struct) == -1)
    {
        printf ("Error getting time.\n");
    }

    theTime += (double) (offset * ONEHOUR);
    theTime -= (double) (gmt_offset * ONEHOUR);
    strftime (out_ptr, 20, "%Y-%m-%d %H:%M:%S", gmtime (&theTime));

}
```

### *B.1.3 Return of SMA flows to Channel*

```
/*----------------------------------------------------------------------
C-  Function:    ChannelWaterRoute.c
C-
C-    Purpose/    Explicit, one-dimensional channel water routing using
C-    Methods:    diffusive wave approximation.
C-
C-
C-    Inputs:        hov[][], landuse[][], nmanningch[][], storagedepth[][],
C-              interceptionrate[][], dt[], ichnrow[][], ichncol[][],
C-              chanlength[][]  (Globals)
C-
C-    Outputs:    dqch[][] (Global)
C-              dqchin[][][] (Global)
C-              dqchout[][][] (Global)
C-
C-    Called by:    WaterTransport.c
C-

.
.
.

C-
C-    Revised:    Mark Velleux
C-                HydroQual, Inc.
C-                1200 MacArthur Boulevard
C-                Mahwah, NJ 07430
C-
C-    Date:        20-May-2008
C-
C-    Revisions:    Reorganized code to assign point source flows.
C-              Imbedded if/then in main link/node loops was
C-              replaced with code to loop over loads to make
C-              direct assignment of values.
C-
C-    Revised:      James Halgren
C-
C-    Date:         01-DEC-2008
C-
C-    Revisions:    Added interflow outlet addition to channel if
C-                  infopt = 2
C----------------------------------------------------------------------*/

//trex global variable declarations
#include "trex_general_declarations.h"

//trex global variable declarations for water transport
#include "trex_water_declarations.h"

//variable declarations and definitions specific to the
//soil moisture accounting procedure.
#include "trex_SMA_declarations.h"

void ChannelWaterRoute (void)
{

.
.
.

    //Add external flows...
    //
    //Note: Only flow sources (qwch > 0) are safely considered.
    //      Sources bring flow to the node and are added as
    //      dqchin[][][0]. Sinks (qwch < 0) take flow from the
    //      node and should be added as dqchout[][][0] but
    //      should also have a check comparing the sink volume
    //      (qwchinterp[] * dt[]) to the available volume.  The
    //      check should also consider total outflow potential
    //      due to channel flow as well as the sink.  As the
    //      code stands, a sink can be specified but it would
    //      be tracked as a negative source and does not have a
    //      check to make sure the sink is smaller than volume
    //      available for flow.
    //
    //Loop over number of external flow sources
    for (k = 1; k <= nqwch; k++)
```

```
    {
        //set link and node references for the flow point source
        i = qwchlink[k];
        j = qwchnode[k];

        //Add (temporally interpolated) external flow to channel flow
        dqch[i][j] = dqch[i][j] + qwchinterp[k];

        //In case there is more than one external flow source
        //to this node, flows must be summed.  This summation
        //is ok because we do not need to sperately track each
        //possible external flow source...
        //
        //Gross inflow to present node from external source
        dqchin[i][j][0] = dqchin[i][j][0] + qwchinterp[k];

        //Developer's Note:  Since dqchinvol[][][0] is the same as qwchvol[][],
        //                   the qwchvol array could be eliminated.  For now both
        //                   arrays are retained because they provide a separate
        //                   check on point source flows.
        //
        //increment cumulative node flow volume
        dqchinvol[i][j][0] = dqchinvol[i][j][0] + qwchinterp[k] * dt[idt];

        //Compute sum of external flow volumes (m3)
        qwchvol[i][j] = qwchvol[i][j] + qwchinterp[k] * dt[idt];
        if (infopt == 2)
        {
            // loop over SMA interflow outlets
            for (m = 1; m <= nio; m++)
            {
                //SMA Flows may also be added to the overland domain.
                //SMA But that is not yet implemented.
                if ((ioSMA[m]->intfout_i == i) && (ioSMA[m]->intfout_j == j))
                {
                    // Add interflow
                    dqch[i][j] += ioSMA[m]->wnew / dt[idt];
                    dqchin[i][j][0] += ioSMA[m]->wnew / dt[idt];
                    dqchinvol[i][j][0] += ioSMA[m]->wnew;
                    //DEBUG printf ("\nThe first loop delivered to interflow outlet\n");
                    //DEBUG printf ("%g m^3\n", ioSMA[m]->wnew);
                    //DEBUG printf ("in %g seconds\n", dt[idt]);
                    qwchvol[i][j] += ioSMA[m]->wnew;
                }
            }                   // end loop over SMA interflow outlets
        }                       // end if (infopt ==2) SMA
    }                           //end loop over number of external flow sources

.
.
.

//End of Function: Return to WaterTransport
}
```

### *B.1.4 Computation of SMA Influx*

```
/*---------------------------------------------------------------------
C-  Function:   Infiltration.c
C-
C-  Purpose/    Infiltration.c computes the infiltration rate
C-  Methods:    and cumulative depth of infiltration for each
C-              cell in the overland plane.  Uses the Green-Ampt
C-              equation neglecting a term for head for the ponded
C-              water depth.
C-
C-              After performing infiltration computations
C-              Infiltration.c computes the new infiltration depth
C-              which is used for soil moisture accounting in the
C-              upper soil zone and initializes lower zone values
C-              using a method similar to the Sacramento Soil Moisture
C-              Accounting procedure.
C-
C-  Inputs:     hov[][] (at time t),
C-              infiltrationdepth[][] (at time t),
C-              soiltype[][][]
C-
C-  Outputs:    infiltrationrate[][] (at time t),
C-              infiltrationdepth[][] (at time t+dt)
C-              infiltrationvol[][] (at time t+dt)
```

```
C-
C-  Controls:   hov[][] (at time t)
C-
C-  Calls:      None
C-
C-  Called by:  WaterTransport
C-
C-  Created:    P. Y. Julien, B. Saghafian, B. Johnson,
C-              and R. Rojas (CSU)
C-
C-  Date:       1991
C-
C-  Revised:    Mark Velleux (CSU)
C-              John England (USBR)
C-              James Halgren (CSU)
C-
C-  Date:       03-MAR-2007
C-
C-------------------------------------------------------------------------*/
.
.
.
void Infiltration (void)
{
.
.
.
    //Loop over rows
    for (i = 1; i <= nrows; i++)
    {
        //Loop over columns
        for (j = 1; j <= ncols; j++)
        {
            //if the cell is in the domain
            if (imask[i][j] != nodatavalue)
            {
.
.
.
                //compute cumulative infiltration volume for this cell (m3)
                infiltrationvol[i][j] = infiltrationvol[i][j] +
                    infiltrationrate[i][j] * dt[idt] * (w * w - achsurf);
                if (infopt == 2)
                {
                    smainfiltrationvol[i][j] =
                        infiltrationrate[i][j] * dt[idt];
                    smaprecipvol[i][j] = netrainrate[i][j] * dt[idt];
                }               //end if infopt == 2
            }                   //end if cell is in domain
        }                       //end loop over columns
    }                           //end loop over rows
//End of function: Return to WaterTransport
}
```

## B.2 PLOTTING SCRIPTS

### *B.2.1 Php front-end script to arrange plots*

This is a typical front end which produces a grid of both hydrograph and statistical analysis plots for the entire multi-event simulation series.

```
<?php
  //The plotcall is in the parent directory
  //so all subsequent paths are relative to that location.
  //The paths inside of each gnuplot script are also relative
  //to the parent directory.
    $plotcall="../gnuplot_call.png.php";
    $Rplotcall="../R_call.png.php";
    $cellwidth=1200;

  //Identify the plot scripts to be placed on the page
    $pltprecip_max="precip/precipitation-max-multi.gnup";
    $pltprecip="precip/precipitation.multi.gnup";
    $pltSMA="multi/SMA/zone1.gnup";
    $plt1="multi/CG-1.gnup";
    $plt2="multi/SHG-09A.gnup";
    $plt3="multi/SD-3A.gnup";
    $plt4="multi/CG-4.gnup";
    $plt5="multi/CG-5.gnup";
    $plt6="multi/CG-6.gnup";
    $Rplt1="multi/cg-1.R";
    $Rplt2="multi/shg-09A.R";
    $Rplt3="multi/sd-3A.R";
    $Rplt4="multi/cg-4.R";
    $Rplt5="multi/cg-5.R";
    $Rplt6="multi/cg-6.R";

  //Set the refresh in seconds for the plot
    $refresh=0;

  //passvar.php is a debugging script
  //which simply prints the variable 'gnuplot_script'
  //$plotcall="test/passvar.php";
  print "<html>";
  print "<head>";
  print "</head>";
  print "<body>";

    print "<table width=\"2400\" border=\"0\" cellspacing=\"0\" cellpadding=\"0\">";
      print "<tr>";
        print "<td>";
          echo "<object type='image/png' width='$cellwidth'
data='$plotcall?gnuplot_script=$pltprecip&refresh_period=$refresh'></object>";
        print "</td>";

        print "<td>";
          echo "<object type='image/png' width='$cellwidth'
data='$plotcall?gnuplot_script=$pltprecip&refresh_period=$refresh'></object>";
        print "</td>";

        print "<td>";
          echo "<object type='image/png' width='$cellwidth'
data='$plotcall?gnuplot_script=$pltprecip&refresh_period=$refresh'></object>";
        print "</td>";
      print "</tr>";

      print "<tr>";
        print "<td>";
          echo "<object type='image/png' width='$cellwidth'
data='$plotcall?gnuplot_script=$pltSMA&refresh_period=$refresh'></object>";
        print "</td>";

        print "<td>";
          echo "<object type='image/png' width='$cellwidth'
data='$plotcall?gnuplot_script=$pltSMA&refresh_period=$refresh'></object>";
        print "</td>";
```

```
        print "<td>";
          echo "<object type='image/png' width='$cellwidth'
data='$plotcall?gnuplot_script=$pltSMA&refresh_period=$refresh'></object>";
        print "</td>";
      print "</tr>";

      print "<tr>";
        print "<td>";
          print "<table width=\"1200\" border=\"0\" cellspacing=\"0\" cellpadding=\"0\">";
               print "<tr><td>";
                 echo "<object type='image/png' width='$cellwidth'
data='$plotcall?gnuplot_script=$plt1&refresh_period=$refresh'></object>";
               print "</td></tr>";

               print "<tr><td>";
                 echo "<object type='image/png' width='$cellwidth'
data='$Rplotcall?R_script=$Rplt1&refresh_period=$refresh'></object>";
               print "</td></tr>";
          print "</table>";
        print "</td>";

        print "<td>";
          print "<table width=\"1200\" border=\"0\" cellspacing=\"0\" cellpadding=\"0\">";
               print "<tr><td>";
                 echo "<object type='image/png' width='$cellwidth'
data='$plotcall?gnuplot_script=$plt2&refresh_period=$refresh'></object>";
               print "</td></tr>";

               print "<tr><td>";
                 echo "<object type='image/png' width='$cellwidth'
data='$Rplotcall?R_script=$Rplt2&refresh_period=$refresh'></object>";
               print "</td></tr>";
          print "</table>";
        print "</td>";

        print "<td>";
          print "<table width=\"1200\" border=\"0\" cellspacing=\"0\" cellpadding=\"0\">";

               print "<tr><td>";
                 echo "<object type='image/png' width='$cellwidth'
data='$plotcall?gnuplot_script=$plt3&refresh_period=$refresh'></object>";
               print "</td></tr>";

               print "<tr><td>";
                 echo "<object type='image/png' width='$cellwidth'
data='$Rplotcall?R_script=$Rplt3&refresh_period=$refresh'></object>";
               print "</td></tr>";
          print "</table>";
        print "</td>";
      print "</tr>";

      print "<tr>";
        print "<td>";
          print "<table width=\"1200\" border=\"0\" cellspacing=\"0\" cellpadding=\"0\">";
               print "<tr><td>";
                 echo "<object type='image/png' width='$cellwidth'
data='$plotcall?gnuplot_script=$plt4&refresh_period=$refresh'></object>";
               print "</td></tr>";

               print "<tr><td>";
                 echo "<object type='image/png' width='$cellwidth'
data='$Rplotcall?R_script=$Rplt4&refresh_period=$refresh'></object>";
               print "</td></tr>";
          print "</table>";
        print "</td>";

        print "<td>";
          print "<table width=\"1200\" border=\"0\" cellspacing=\"0\" cellpadding=\"0\">";
               print "<tr><td>";
                 echo "<object type='image/png' width='$cellwidth'
data='$plotcall?gnuplot_script=$plt5&refresh_period=$refresh'></object>";
               print "</td></tr>";

               print "<tr><td>";
                 echo "<object type='image/png' width='$cellwidth'
data='$Rplotcall?R_script=$Rplt5&refresh_period=$refresh'></object>";
               print "</td></tr>";
          print "</table>";
        print "</td>";

        print "<td>";
```

```
          print "<table width=\"1200\" border=\"0\" cellspacing=\"0\" cellpadding=\"0\">";
              print "<tr><td>";
                echo "<object type='image/png' width='$cellwidth'
data='$plotcall?gnuplot_script=$plt6&refresh_period=$refresh'></object>";
              print "</td></tr>";

              print "<tr><td>";
                echo "<object type='image/png' width='$cellwidth'
data='$Rplotcall?R_script=$Rplt6&refresh_period=$refresh'></object>";
              print "</td></tr>";
          print "</table>";
        print "</td>";
      print "</tr>";
    print "</table>";
  print "</body>";
  print "</html>";

?>
```

### *B.2.2 Php back-end script for creating gnuplot and R plots*

The gnuplot backend is called with this php code which references the gnuplot script, and defines the refresh period. The .png graphic is produced with an in-line call to the convert command.

```
<?php
//If png output is desired, change the header comment type
//and the $other array created for the proc_open call
//The gnuplot script will need to be modified accordingly.
  header('Content-Type: image/png');
  //header('Content-Type: image/svg+xml');
  $gnuplot_script=$_GET['gnuplot_script'];
  $refresh_period=$_GET['refresh_period'];
  if ($refresh_period > 0) {
    header("Refresh: $refresh_period");
  }
  $png_res=$_GET['png_res'];
  if ($png_res == 0) {
    $png_res= 192;
  }

  $procname ="/usr/bin/gnuplot $gnuplot_script | convert -rotate 90 -density $png_res ps:- png:-";
  //$procname ="/usr/bin/gnuplot $gnuplot_script | convert -rotate 90 -density $png_res -resample
49 ps:- png:-";
  $descriptorspec = array(
    0 => array("pipe", "r"),  // stdin is a pipe that the child will read from
    1 => array("pipe", "w"),  // stdout is a pipe that the child will write to
    //2 => array("file", "tmp/error-output.txt", "a") // stderr is a file to write to
    2 => array("file", "tmp/error-output.txt", "w") // stderr is a file to write to
    //2 => array("file", "/dev/null", "w") // stderr is a file to write to
  );
  $cwd = getcwd();
  $env = array();
  //$other = array();
  $other = array('binary_pipes'=>true);

  $process = proc_open($procname, $descriptorspec, $pipes, $cwd, $env, $other);

  if (is_resource($process)) {

    // $pipes now looks like this:
    // 0 => writeable handle connected to child stdin
    // 1 => readable handle connected to child stdout
    // Any error output will be appended to /tmp/error-output.txt

    fclose($pipes[0]);

    // Pass the pipe back to the browser
    // to produce the png graphic.
    fpassthru($pipes[1]);
    fclose($pipes[1]);

    // It is important that you close any pipes before calling
    // proc_close in order to avoid a deadlock
    proc_close($process);
  }

?>
```

The R scripts are referenced with a similar php script.

```
<?php
//For png output, it may be necessary to change the
//$other array created for the proc_open call.
//The R script is spitting out a postscript file
//in so the convert command needs to be modified accordingly.
  header('Content-Type: image/png');
  //header('Content-Type: image/svg+xml');
  $R_script=$_GET['R_script'];
  $refresh_period=$_GET['refresh_period'];
  if ($refresh_period > 0) {
    header("Refresh: $refresh_period");
  }

  $procname ="/usr/bin/Rscript $R_script | convert -rotate 90 ps:- png:-";
  //$procname ="/usr/bin/Rscript $R_script | convert -density 384 -resample 32 -rotate 90 ps:-
png:-";
  //
  //$procname ="/usr/bin/Rscript $R_script | convert -rotate 90 ps:- svg:-";
  //$procname ='/usr/bin/R'; //R does not read and write pipes ...
  // so we get rid of the fwrite command below.
  // (see gnuplot_call.svg.php for comparison.)
  $descriptorspec = array(
    0 => array("pipe", "r"),  // stdin is a pipe that the child will read from
    1 => array("pipe", "w"),  // stdout is a pipe that the child will write to
    //2 => array("file", "tmp/error-output.txt", "a") // stderr is a file to write to
    2 => array("file", "tmp/error-output.txt", "w") // stderr is a file to write to
  );
  $cwd = getcwd();
  $env = array();
  $other = array();
  //$other = array('binary_pipes'=>true);

  $process = proc_open($procname, $descriptorspec, $pipes, $cwd, $env, $other);

  if (is_resource($process)) {

    // $pipes now looks like this:
    // 0 => writeable handle connected to child stdin
    // 1 => readable handle connected to child stdout
    // Any error output will be appended to /tmp/error-output.txt

    // Any text written to stdin ($pipes[0])
    // would manipulate the R interface
    //fwrite($pipes[0], "load \"$gnuplot_script\"\n");
    // but since R doesn't accept input from stdin, we
    // just use the postscript kludge to hack a live
    // web graphic using imagemagick (convert).
    fclose($pipes[0]);

    // Pass the pipe back to the browser
    // to produce the png graphic.
    fpassthru($pipes[1]);
    fclose($pipes[1]);

    // It is important that you close any pipes before calling
    // proc_close in order to avoid a deadlock
    proc_close($process);
  }

?>
```

### *B.2.3 Gnuplot Script for observed data*

```
#!/usr/bin/gnuplot
#set terminal svg enhanced size 2000 1000 fixed lw 0.75 fs 14.0;
#set terminal postscript enhanced color dl 1.8 lw 0.75 clip size 18, 9.0;
set terminal postscript enhanced color dl 1.8 lw 1.67 clip size 18, 7.0;
set macros; #enable string substitution
#set zero 1e-08;
#todo -- perl/php to get this file automatically.

# Set date range for plot parameters
begindate = "'2006-07-01 00:00:00'"
enddate = "'2006-09-01 00:00:00'"

# Create pointer to data file and set comma flag
set datafile separator ",";
grepline = "\"<grep -E '2006-0[6789]'
cg_realtime/AllContinuous.gnup.withcumulativeprecip.commadelim\""

# Set values which do not change for all plots
set xdata time;
set timefmt "%Y-%m-%d %H:%M:%S";
set xrange [ @begindate : @enddate ] noreverse writeback;
unset border;
set border lt 1 lc rgbcolor "#999999";
unset grid;

# Initiate multiplot mode
set multiplot;

# Prepare CG flow plot
set origin 0,0.15;
set size 1.0,0.59;
set key at screen 0.79, screen 0.55;
set rmargin 3; set lmargin 10;
set tmargin 0; set bmargin 0;
set title "";

# Set x-axis parameters
set format x "";
set xlabel "" offset 0.000000,0.000000  font "";
set xtics "2006-06-01 00:00:00", 604800, "2006-09-31" nomirror;
set mxtics;

# Set y-axis parameters
set ylabel "CG flow [cfs]" offset 1.3,0  font "";
set yrange [ 0.0 : 26 ] noreverse nowriteback;
set ytics 0,2,25 nomirror\
      textcolor rgb "#000000";

#Plot measured flow in California Gulch
#Date and time are a single column so the 'using' number is slightly off
#of what might be expected.

labelposition1="graph 1.00"
labelposition2="graph 0.96"
labelposition3="graph 1.9"

#these need to be plotted in the first graph so they don't overlap the labels plotted in the
second graph.
set arrow from "2006-07-19 16:00:00", graph .97 to "2006-07-19 16:00:00", @labelposition2 nohead
lc rgb "grey";
set arrow from "2006-07-25 16:00:00", graph .67 to "2006-07-25 16:00:00", @labelposition2 nohead
lc rgb "grey";
set arrow from "2006-07-26 16:00:00", graph .62 to "2006-07-26 16:00:00", @labelposition2 nohead
lc rgb "grey";
set arrow from "2006-07-30 16:00:00", graph .75 to "2006-07-30 16:00:00", @labelposition2 nohead
lc rgb "grey";
set arrow from "2006-08-05 16:00:00", graph .23 to "2006-08-05 16:00:00", @labelposition2 nohead
lc rgb "grey";
set arrow from "2006-08-06 16:00:00", graph .23 to "2006-08-06 16:00:00", @labelposition2 nohead
lc rgb "grey";
set arrow from "2006-08-10 16:00:00", graph .42 to "2006-08-10 16:00:00", @labelposition2 nohead
lc rgb "grey";
set arrow from "2006-08-18 20:00:00", graph .38 to "2006-08-18 20:00:00", @labelposition2 nohead
lc rgb "grey";
set arrow from "2006-08-26 16:00:00", graph .27 to "2006-08-26 16:00:00", @labelposition2 nohead
lc rgb "grey";
```

```
#label vertical position defined relative to y axis.
set label 1 "1" at "2006-07-19 16:00:00", @labelposition1 center;
set label 2 "2  3" at "2006-07-26 05:00:00", @labelposition1 center;
set label 3 "4" at "2006-07-30 16:00:00", @labelposition1 center;
set label 4 "5 5b" at "2006-08-06 05:00:00", @labelposition1 center;
set label 5 "6" at "2006-08-10 16:00:00", @labelposition1 center;
set label 6 "7" at "2006-08-18 21:00:00", @labelposition1 center;
set label 7 "8" at "2006-08-26 16:00:00", @labelposition1 center;
#set label 8 "July 1" at "2006-07-01 00:00:00", @labelposition1 center;
#set label 9 "August 31" at "2006-08-31 00:00:00", @labelposition1 center;
set label 8 "Storm Number:" at "2006-07-14 00:00:00", @labelposition1 center;

plot @grepline u 1:14 w line t 'CG-1 Obs.' lt 1 lc rgbcolor "#99CC00" lw 1 pt 2 ps 0.35,\
  @grepline u 1:44 w line t 'SD-3 Obs.' lt 1 lc rgbcolor "#000099" lw 1 pt 2 ps 0.35,\
  @grepline u 1:50 w line t 'SD-3A Obs.' lt 1 lc rgbcolor "#000099" lw 1 pt 2 ps 0.35,\
  @grepline u 1:56 w line t 'SHG-09A Obs.' lt 1 lc rgbcolor "#CC0000" lw 1 pt 2 ps 0.35,\
  @grepline u 1:20 w line t 'CG-4 Obs.' lt 1 lc rgbcolor "#FF6600" lw 1 pt 2 ps 0.35,\
  @grepline u 1:26 w line t 'CG-5 Obs.' lt 1 lc rgbcolor "#FFCC00" lw 1 pt 2 ps 0.35,\
  @grepline u 1:32 w line t 'CG-6 Obs.' lt 1 lc rgbcolor "#000000" lw 1 pt 2 ps 0.35;

#@grepline u 1:38 w line t 'OG-1 Obs.' lt 2 lc rgbcolor "#660000" lw 3 pt 2 ps 0.35,\
unset arrow 1;
unset arrow 2;
unset arrow 3;
unset arrow 4;
unset arrow 5;
unset arrow 6;
unset arrow 7;
unset arrow 8;
unset arrow 9;

unset label 1;
unset label 2;
unset label 3;
unset label 4;
unset label 5;
unset label 6;
unset label 7;
unset label 8;
unset label 9;

# Prepare Arkansas River flow plot
set origin 0,0.01;
set size 1.0,0.13;
set key at screen 0.89, screen .12 box lt -2;
set rmargin 3; set lmargin 10;
set tmargin 0; set bmargin 2.0;
set title "";

# Set x-axis parameters
set format x "%d %b";
set xlabel "" offset 0.000000,0.000000  font "";
set xtics "2006-06-01 00:00:00", 604800, "2006-09-31" nomirror textcolor rgb "#000000";
set mxtics;

# Set y-axis parameters
set ylabel "AR flow [cfs]" offset 1.5,0  font "";
set yrange [ 1 : 250 ] noreverse nowriteback;
set ytics 0,100,250 nomirror\
      textcolor rgb "#000000";

#Plot measured flow in Arkansas River
plot @grepline u 1:2 w line axes x1y2 t 'AR-1 Obs.' lt 1 lc rgbcolor "#CC0000" lw 1,\
  @grepline u 1:8 w line axes x1y2 t 'AR-3A Obs.' lt 1 lc rgbcolor "#99CC00" lw 1;

# Prepare precip (i and cum) plot
set origin 0,0.70;
set size 1.0,0.30;
set key at screen 0.79, screen 0.87;
set rmargin 3; set lmargin 10;
set tmargin 2; set bmargin 0;
set title "Observed Flow and Precipitation in California Gulch and Arkansas River" offset 0.00,
0.00  font "";

# Set x-axis parameters
set format x "";
set xlabel "" offset 0.000000,0.000000  font "";
set xtics "2006-06-01 00:00:00", 604800, "2006-09-31" mirror;
set mxtics;

# Set y-axis parameters
```

```
set ylabel "10-min precip. [in]" offset 1.3,0;
set yrange [ 0 : 0.5 ] reverse nowriteback;
set ytics 0,0.1,0.4 nomirror\
      textcolor rgb "#000000";

#Precipitation - Intensity
plot @grepline u 1:($19>0 ? $19 : 1/0) w impulses t 'CG-1 Precip' lt 1 lc rgbcolor "#99CC00" lw 1
pt 1 ps 0.95,\
@grepline u 1:($61>0 ? $61 : 1/0) w impulses t 'SHG-09A Precip' lt 1 lc rgbcolor "#CC0000" lw 1
pt 6 ps 0.95,\
@grepline u 1:($25>0 ? $25 : 1/0) w impulses t 'CG-4 Precip' lt 1 lc rgbcolor "#FF6600" lw 1 pt 2
ps 0.95,\
@grepline u 1:($37>0 ? $37 : 1/0) w impulses t 'CG-6 Precip' lt 1 lc rgbcolor "#000000" lw 1 pt 4
ps 0.95;

# Terminate multiplot mode
unset multiplot;

# EOF!
```

### *B.2.4 Gnuplot Script for precipitation data*

```
#!/usr/bin/gnuplot -persist
#set terminal svg size 2048 1024 fixed lw 0.75 fsize 20;
set terminal postscript enhanced color dl 1.8 lw 0.75 clip size 12,6.0;
set macros;
#set output "2006storm1.svg";

#set zero 1e-08;
#todo -- perl/php to get this file automatically.

# Set date range for plot parameters
set xdata time;
set timefmt "%Y-%m-%d %H:%M:%S";
begindate = "'2006-07-01 00:00:00'"
enddate = "'2006-09-01 00:00:00'"
set xrange [ @begindate : @enddate ] noreverse writeback;
set datafile separator ",";
set title "";
set format x "";

grepline =
"\"/home/halgrenj/gnuplot/AllContinuous.gnup.withcumulativeprecip.commadelim.Rtext.trunc\"";
KLXVdata = "\"cg_realtime/KLXV.Summer2006.csv\"";

# set the zero value for the cumulative precipitation plots
h = `grep '2006-07-01 00:00:00'
cg_realtime/AllContinuous.gnup.withcumulativeprecip.commadelim.Rtext.trunc | awk -F, '{print
$62}'`;
i = `grep '2006-07-01 00:00:00'
cg_realtime/AllContinuous.gnup.withcumulativeprecip.commadelim.Rtext.trunc | awk -F, '{print
$63}'`;
j = `grep '2006-07-01 00:00:00'
cg_realtime/AllContinuous.gnup.withcumulativeprecip.commadelim.Rtext.trunc | awk -F, '{print
$64}'`;
k = `grep '2006-07-01 00:00:00'
cg_realtime/AllContinuous.gnup.withcumulativeprecip.commadelim.Rtext.trunc | awk -F, '{print
$65}'`;
#l = `grep '2006-07-01 00:00:00' cg_realtime/KLXV.Summer2006.csv | awk -F, '{print $26}'`;
l = 0.3;

set multiplot;

# Prepare precip (i and cum) plot
set origin 0,0.1;
set size 1.0,0.9;
set rmargin 5; set lmargin 8;
set tmargin 1; set bmargin 1;
unset grid;
unset ytics;
unset y2tics;
set yrange [ 0 : 0.6 ] reverse nowriteback;
set y2range [ 0 : 10. ] noreverse nowriteback;
unset ylabel;
unset y2label;
unset border;

#Precipitation - Intensity
unset key;

#these need to be plotted in the first graph so they don't overlap the labels plotted in the
second graph.
set arrow from "2006-07-19 16:00:00", graph .31 to "2006-07-19 16:00:00", graph .05 nohead lc rgb
"grey";
set arrow from "2006-07-25 16:00:00", graph .54 to "2006-07-25 16:00:00", graph .05 nohead lc rgb
"grey";
set arrow from "2006-07-26 16:00:00", graph .67 to "2006-07-26 16:00:00", graph .05 nohead lc rgb
"grey";
set arrow from "2006-07-30 16:00:00", graph .62 to "2006-07-30 16:00:00", graph .05 nohead lc rgb
"grey";
set arrow from "2006-08-05 16:00:00", graph .86 to "2006-08-05 16:00:00", graph .05 nohead lc rgb
"grey";
set arrow from "2006-08-06 16:00:00", graph .83 to "2006-08-06 16:00:00", graph .05 nohead lc rgb
"grey";
set arrow from "2006-08-10 16:00:00", graph .72 to "2006-08-10 16:00:00", graph .05 nohead lc rgb
"grey";
set arrow from "2006-08-18 20:00:00", graph .78 to "2006-08-18 20:00:00", graph .05 nohead lc rgb
"grey";
```

```
set arrow from "2006-08-26 16:00:00", graph .83 to "2006-08-26 16:00:00", graph .05 nohead lc rgb
"grey";

plot @grepline u 1:($19>0 ? $19 : 1/0) w impulses notitle 'CG-1 Precip' lt 1 lc rgbcolor
"#99CC00" lw 1.0 pt 1 ps 0.95,\
@grepline u 1:($61>0 ? $61 : 1/0) w impulses notitle 'SHG-09A Precip' lt 1 lc rgbcolor "#CC0000"
lw 1.0 pt 6 ps 0.95,\
@KLXVdata u 1:($15>0 ? $15/6 : 1/0) w impulses notitle 'KLXV (airport) Precip' lt 1 lc rgbcolor
"#6666FF" lw 1.0 pt 4 ps 0.95,\
@grepline u 1:($25>0 ? $25 : 1/0) w impulses notitle 'CG-4 Precip' lt 1 lc rgbcolor "#FF6600" lw
1.0 pt 2 ps 0.95,\
@grepline u 1:($37>0 ? $37 : 1/0) w impulses notitle 'CG-6 Precip' lt 1 lc rgbcolor "#000000" lw
1.0 pt 4 ps 0.95;

#Precipitation - Cumulative
set key at screen 0.33, screen 0.60;
# The preciptation at each gauge is accumulated in a second field.
# The followign grep procdure extracts the cumulative precip
# to define a zero point on the graph.
# It may be easier to generate these
# values using Perl, rather than depending on the gnuplot
# environment to exist where the grep and awk programs will
# work properly.
plot @grepline u 1:($62-h) w line axes x1y2 notitle 'CG-1 Cumulative Precip' lt 1 lc rgbcolor
"#99CC00" lw 2 pt 1 ps 0.00,\
@grepline u 1:($65-k) w line axes x1y2 notitle 'SHG-09A Cumulative Precip' lt 1 lc rgbcolor
"#CC0000" lw 2 pt 1 ps 0.00,\
@KLXVdata u 1:($26-l) w line axes x1y2 notitle 'KLXV (airport) Precip' lt 1 lc rgbcolor "#6666ff"
lw 2 pt 1 ps 0.00,\
@grepline u 1:($63-i) w line axes x1y2 notitle 'CG-4 Cumulative Precip' lt 1 lc rgbcolor
"#FF6600" lw 2 pt 1 ps 0.00,\
@grepline u 1:($64-j) w line axes x1y2 notitle 'CG-6 Cumulative Precip' lt 1 lc rgbcolor
"#000000" lw 2 pt 1 ps 0.00;

#Preciptation - Cum. + Int. for legend
set title "Precipitation in California Gulch and Arkansas River" offset 0.000000,0.000000  font
"";
#set xtics '2006-07-01 00:00:00', 604800 lt 2;# lc rgbcolor "#000000" lw 0.25;
#set mxtics
#set grid mxtics mytics lt 2 lc rgbcolor "#000000" lw 0.25;
#set grid xtics lt 2 lc rgbcolor "#000000" lw 0.5;
#set grid mxtics mytics lt 2 lc rgbcolor "#000000" lw 0.25;
#set ylabel "10-minute precipitation intensity [inches / 10 min]" offset 1.3,4.50 font
"Helvetica,20";
set ylabel "10-minute precipitation intensity\n[inches / 10 min]" offset 1.5,4.50;
#set y2label "cumulative preciptation depth [inches]" offset -1.5,-5.3 font "Helvetica,20";
set y2label "cumulative preciptation depth [inches]" offset -1.5,-4.4;
set ytics 0,0.1,0.4 nomirror;
set y2tics 0,1.0,7.0 nomirror;

##label vertical position defined relative to y axis.
#set format x "";
#set label 1 "July 19\nStorm 1" at "2006-07-19 16:00:00", .615 center;
#set label 2 "July 25, 26\nStorm 2, 3" at "2006-07-26 10:00:00", .615 center;
#set label 3 "July 30\nStorm 4" at "2006-07-30 16:00:00", .615 center;
#set label 4 "August 5, 6\nStorm 5, 5b" at "2006-08-05 16:00:00", .615 center;
#set label 5 "August 10\nStorm 6" at "2006-08-10 16:00:00", .615 center;
#set label 6 "August 18\nStorm 7" at "2006-08-18 16:00:00", .615 center;
#set label 7 "August 26\nStorm 8" at "2006-08-26 16:00:00", .615 center;
#set label 8 "July 1" at "2006-07-01 00:00:00", .615 center;
#set label 9 "August 31" at "2006-08-31 00:00:00", .615 center;

#set arrow from "2006-07-19 16:00:00", .41 to "2006-07-19 16:00:00", .608 nohead lc rgb "grey";
#set arrow from "2006-07-25 16:00:00", .26 to "2006-07-25 16:00:00", .608 nohead lc rgb "grey";
#set arrow from "2006-07-26 16:00:00", .21 to "2006-07-26 16:00:00", .608 nohead lc rgb "grey";
#set arrow from "2006-07-30 16:00:00", .24 to "2006-07-30 16:00:00", .608 nohead lc rgb "grey";
#set arrow from "2006-08-05 16:00:00", .09 to "2006-08-05 16:00:00", .608 nohead lc rgb "grey";
#set arrow from "2006-08-06 16:00:00", .11 to "2006-08-06 16:00:00", .608 nohead lc rgb "grey";
#set arrow from "2006-08-10 16:00:00", .17 to "2006-08-10 16:00:00", .608 nohead lc rgb "grey";
#set arrow from "2006-08-18 20:00:00", .12 to "2006-08-18 20:00:00", .608 nohead lc rgb "grey";
#set arrow from "2006-08-26 16:00:00", .08 to "2006-08-26 16:00:00", .608 nohead lc rgb "grey";

unset arrow 1;
unset arrow 2;
unset arrow 3;
unset arrow 4;
unset arrow 5;
unset arrow 6;
unset arrow 7;
unset arrow 8;
unset arrow 9;
```

```
#label vertical position defined relative to y axis.
set format x "%b %d";
set label 1 "1" at "2006-07-19 16:00:00", .575 center;
set label 2 "2  3" at "2006-07-26 05:00:00", .575 center;
set label 3 "4" at "2006-07-30 16:00:00", .575 center;
set label 4 "5 5b" at "2006-08-06 05:00:00", .575 center;
set label 5 "6" at "2006-08-10 16:00:00", .575 center;
set label 6 "7" at "2006-08-18 21:00:00", .575 center;
set label 7 "8" at "2006-08-26 16:00:00", .575 center;
#set label 8 "July 1" at "2006-07-01 00:00:00", .615 center;
#set label 9 "August 31" at "2006-08-31 00:00:00", .615 center;
set label 8 "Storm Number:" at "2006-07-14 00:00:00", .575 center;

plot @grepline u 1:($19>0 ? $20-40 : 1/0) w lines t 'CG-1 Precip' lt 1 lc rgbcolor "#99CC00" lw 2
pt 1 ps 1.35,\
  @grepline u 1:($61>0 ? $62-40 : 1/0) w lines t 'SHG-09A Precip' lt 1 lc rgbcolor "#CC0000" lw 2
pt 6 ps 0.95,\
  @grepline u 1:($25>0 ? $26-40 : 1/0) w lines t 'CG-4 Precip' lt 1 lc rgbcolor "#FF6600" lw 2 pt
2 ps 1.35,\
  @grepline u 1:($37>0 ? $38-40 : 1/0) w lines t 'CG-6 Precip' lt 1 lc rgbcolor "#000000" lw 2 pt
4 ps 1.35,\
  @KLXVdata u 1:($26>0 ? $26-40 : 1/0) w lines t 'KLXV (airport) Precip' lt 1 lc rgbcolor
"#6666ff" lw 2 pt 4 ps 0.95;
# Terminate multiplot mode

unset multiplot;
unset output;
# EOF!
```

### *B.2.5 Gnuplot script for single gauge*

```
#!/usr/bin/gnuplot
#set terminal svg enhanced size 1024 568 fixed dashed lw 0.75;
#set terminal svg enhanced size 1024 568 dynamic dashed lw 0.75;
#set terminal png size 1024 568 dashed lw 0.75;
#When gnuplot 4.3+ becomes available, I expect the
#dashlength option will be available for the svg terminal.
set terminal postscript enhanced color dl 1.8 lw 0.75 clip size 15,7.5;
set macros; #enable string substitution

# Set date range for plot parameters
set xdata time;
set timefmt "%Y-%m-%d %H:%M:%S";
#set format x "%m/%d \n%H:00";
set format x "%m/%d";

begindate = "'2006-07-19 00:00:00'"
enddate = "'2006-08-30 12:00:00'"

obsfield = "$32";
simfield = "$31";

gaugename="'CG-6'";

grepline = "\"<grep -E '2006-0[78]-'
cg_realtime/AllContinuous.gnup.withcumulativeprecip.commadelim\""
modelfile_SMA = "\"multi/out/export/r26SMA.exp\""
modelfile_noSMA = "\"multi/out/export/r26noSMA.exp\""

set xrange [ @begindate : @enddate ] noreverse writeback;
set datafile separator ",";

ft2m (ft) =  (ft  * 0.3048) #Function for converting feet to meters
m2ft (m) =  (m  * 0.3048) #Function for converting meters to feet
cfs2cms (cfs) =  (cfs  * (0.3048**3)) #Function for converting cubic feet to cubic meters
cms2cfs (cms) =  (cms  / (0.3048**3)) #Function for converting cubic meters to cubic feet
Obs = "1"
noSMA = "2"
SMA = "3"
set style line @Obs lt 1 lc rgb "#000000" lw 5 pt 2 ps 0.35;
set style line @noSMA lt 2 lc rgb "#99CC00" lw 5 pt 2 ps 0.35;
set style line @SMA lt 2 lc rgb "#0000CC" lw 5 pt 2 ps 0.35;

#Set parameters to be used for all/whole plot(s)
set origin 0,0;
set size 1.0,1.0;
set rmargin 10; set lmargin 10;
set tmargin 3; set bmargin 3;
set yrange [ 0.0 : * ] noreverse nowriteback;
set ylabel @gaugename . " flow\n[cfs]" offset 1.5,0  font "";
set xtics nomirror;
set ytics nomirror;

#Measured Flow
#Date and time are a single column
#so the 'using' number is slightly off
#of what might be expected.
set key at screen .9, screen 0.50;

unset border;
plot @grepline u 1:(@obsfield) w line t @gaugename . ' Obs.' ls @Obs,\
     @modelfile_noSMA u 1:(cms2cfs(@simfield)) w line t @gaugename . ' no SMA' ls @noSMA,\
     @modelfile_SMA u 1:(cms2cfs(@simfield)) w line t @gaugename . 'SMA' ls @SMA;
# EOF
```

### *B.2.6 R script for residual analysis*

```
#Rscript cg-6.R | convert -rotate 90 ps:- png:cg-6.png

{
  #load required libraries/packages
  library (topmodel, lib.loc="/home/halgrenj/R/x86_64-pc-linux-gnu-library/2.10/");
  library (boot, lib.loc="/home/halgrenj/R/x86_64-pc-linux-gnu-library/2.10/");
  library (plotrix, lib.loc="/home/halgrenj/R/x86_64-pc-linux-gnu-library/2.10/");
  #library (RSvgDevice);
}

{
```

```
#arcsinh <- function (x) { log(x + (x^2 + 1)^(0.5)) };
  arcsinh <- function (x) { x };
}

{
  #read data --- linux
  obstrunc = read.table
("cg_realtime/AllContinuous.gnup.withcumulativeprecip.commadelim.Rtext.trunc", header = FALSE,
sep = ",");
  r22 = read.table ("multi/out/export/r26SMA.exp", header = TRUE, sep = ",");
  r16n = read.table ("multi/out/export/r26noSMA.exp", header = TRUE, sep = ",");
  ##read data --- windows
#  obstrunc = read.table
("z_R_temp/AllContinuous.gnup.withcumulativeprecip.commadelim.Rtext.trunc", header = FALSE, sep =
",");
#  r22 = read.table ("z_R_temp/cg20060719Storm-r22SMA.exp", header = TRUE, sep = ",");
#  r16n = read.table ("z_R_temp/cg20060719Storm-r16noSMA.exp", header = TRUE, sep = ",");
}

{
  #Offset parameters
  obs0 = 5761;   #the point where the simulated and observed dates are matched
                 #5761 -- the ordinal number of the July 11th 2006 00:00:00 observation

  obso = 0;          #This SHOULD be the optimum shift ... no data tinkering.
  obs0 = obs0 + obso #shift observations (positive number shifts observations to the left)
  obso_noSMA = 13;   #at r22, this shift provides the best correlation and NSeff
  obso_SMA = -20;    #for the noSMA and SMA cases, respectively

  sim0 = 1;      #for the moment, there is no reason to count from anywhere but the start of
                 #simulation. But if someday there were a longer simulated series,
                 #then this would be useful.

  analysisstart = 1152;     #start analysis series relative from sim0 or obs0
  analysislength = 24 * 6 * 52;     #end analysis series relative from sim0 or obs0

  plotstart = 1152;     #start plotting series relative from sim0 or obs0
  plotlength = 6000;  #end plotting series relative from sim0 or obs0

  obs1 = obs0 + analysisstart;
  obsn = obs0 + analysisstart + analysislength;

  sim1 = sim0 + analysisstart;     #first element of time series relative from simulation start
  simn = sim0 + analysisstart + analysislength; #last element of time series

  plotend = plotstart+plotlength;
}

{ #Plot Parameters
  simdate = r16n[sim0:simn, 1];
  simtime = r16n[sim0:simn, 2];
}

#Observed
#14 CG-1
#44 SD-3
#50 SD-3A
#56 SHG-09A
#20 CG-4
#26 CG-5
#32 CG-6
#38 OG-1

#Simulated
#4 CG-1
#7 CG-1
#10 SHG-09A
#13 SD-3A
#16 CG-4
#19 OG-1
#22 OG-1
#25 CG-5
#28 CG-5 + WWTP
#31 CG-6

{ #time series
  obs_cg6_all <- data.frame (obstrunc[obs0:obsn,1], obstrunc[obs0:obsn,32]);
  r16n_cg6_all <- data.frame (r16n[sim0:simn, 1],r16n[sim0:simn, 31]  * (1 / 0.3048) ** 3);
  r22_cg6_all <- data.frame (r22[sim0:simn, 1],r22[sim0:simn, 31]  * (1 / 0.3048) ** 3);
}
```

```
{
  obs_cg6_analysis = obs_cg6_all[sim1:simn, 2];
  r16n_cg6_analysis = r16n_cg6_all[sim1:simn, 2];
  r22_cg6_analysis = r22_cg6_all[sim1:simn, 2];
#  obs_cg6_analysis = obs_cg6_all[analysisstart:analysisstart+analysislength, 2];
#  r16n_cg6_analysis = r16n_cg6_all[analysisstart:analysisstart+analysislength, 2];
#  r22_cg6_analysis = r22_cg6_all[analysisstart:analysisstart+analysislength, 2];
}

{
  obsmean = mean (na.omit(obs_cg6_analysis));
  obsstdv = sd (na.omit(obs_cg6_analysis));
  NS_n = NSeff (r16n_cg6_analysis, obs_cg6_analysis);  #Nash-SutCliffe
  NS_s = NSeff (r22_cg6_analysis, obs_cg6_analysis);  #Nash-SutCliffe
  corr_n = corr (na.omit (cbind (r16n_cg6_analysis, obs_cg6_analysis))); #Correlation Coefficient
  corr_s = corr (na.omit (cbind (r22_cg6_analysis, obs_cg6_analysis))); #Correlation Coefficient
  modcorr_n = corr (na.omit (cbind (r16n_cg6_analysis, obs_cg6_analysis))) * min (sd (na.omit
(r16n_cg6_analysis)), sd (na.omit (r22_cg6_analysis))) / max (sd (na.omit (r16n_cg6_analysis)),
sd (na.omit (r22_cg6_analysis)));     #Modified Correlation Coefficient
  modcorr_s = corr (na.omit (cbind (r22_cg6_analysis, obs_cg6_analysis))) * min (sd (na.omit
(r16n_cg6_analysis)), sd (na.omit (r22_cg6_analysis))) / max (sd (na.omit (r16n_cg6_analysis)),
sd (na.omit (r22_cg6_analysis)));     #Modified Correlation Coefficient
  pb_n = sum (na.omit (r16n_cg6_analysis - obs_cg6_analysis)) / sum (na.omit (obs_cg6_analysis));
#Percent Bias
  pb_s = sum (na.omit (r22_cg6_analysis - obs_cg6_analysis)) / sum (na.omit (obs_cg6_analysis));
#Percent Bias
  apb_n = sum (abs (na.omit (r16n_cg6_analysis - obs_cg6_analysis))) / sum (na.omit
(obs_cg6_analysis));        #Absolute Percent Bias
  apb_s = sum (abs (na.omit (r22_cg6_analysis - obs_cg6_analysis))) / sum (na.omit
(obs_cg6_analysis));        #Absolute Percent Bias
  rmse_n = sqrt (1 / NROW (na.omit (obs_cg6_analysis)) * sum ((na.omit (r16n_cg6_analysis -
obs_cg6_analysis) ** 2)));   #Root Mean Squared Error (RMSE)
  prmse_n = rmse_n / obsmean;  #percent RMSE
  rrmse_n = rmse_n / obsstdv;  #RMSE ratio
  rmse_s = sqrt (1 / NROW (na.omit (obs_cg6_analysis)) * sum ((na.omit (r22_cg6_analysis-
obs_cg6_analysis) ** 2)));  #Root Mean Squared Error (RMSE)
  prmse_s = rmse_s / obsmean;  #percent RMSE
  rrmse_s = rmse_s / obsstdv;  #RMSE ratio
}

{ #Build all storm plot
  r22_cg6max = max(na.omit(r22_cg6_analysis - obs_cg6_analysis));
  r22_cg6min = min(na.omit(r22_cg6_analysis - obs_cg6_analysis));
  r16n_cg6max = max(na.omit(r16n_cg6_analysis - obs_cg6_analysis));
  r16n_cg6min = min(na.omit(r16n_cg6_analysis - obs_cg6_analysis));
  plotmax = max(na.omit(r22_cg6_analysis - obs_cg6_analysis),na.omit(r16n_cg6_analysis -
obs_cg6_analysis)) + 0.3;
  plotmin = min(na.omit(r22_cg6_analysis - obs_cg6_analysis),na.omit(r16n_cg6_analysis -
obs_cg6_analysis)) - 0.3;
  # Residual Plot
  postscript(file="", command="cat", title="Residuals Plot", width=17, height=11,
paper='special');
  #plot (0, ylim = c (plotmin, plotmax), xlim = c (plotstart, plotend), yaxt ='n', xaxt = 'n',
bty = "n", xlab = "", ylab = "residual Sim - Obs [cfs]" , cex.lab=1.5);
  plot (0, ylim = c (arcsinh(plotmin), arcsinh(plotmax)), xlim = c (plotstart, plotend), yaxt
='n', xaxt = 'n', bty = "n", xlab = "", ylab = "residual Sim - Obs [cfs]" , cex.lab=1.5);
  points (c (-1000, 10000), c (0, 0), col = '#000000', type = 'l');
  points (simdate, arcsinh(r16n_cg6_all[,2] - obs_cg6_all[,2]), type = 'l', col = '#99CC00');
  points (simdate, arcsinh(r22_cg6_all[,2] - obs_cg6_all[,2]), col = '#0000CC', type = 'l');
}

{
  sd3A_peaks = c(1248, 2111, 2249, 2837, 3714, 4000, 4406, 5593, 6704);
  shg09A_peaks = c(1247, 2116, 2250, 2837, 3715, 3816, 4403, 5594, 6706);
  cg1_peaks = c(1247, 2115, 2251, 2837, 3563, 3850, 4410, 5594, 6705);
  og1_peaks = c(1249, 2117, 2251, 2839, 3718, 3816, 4407, 5594, 6707);
  cg4_peaks = c(1249, 2114, 2253, 2840, 3719, 4006, 4409, 5598, 6710);
  cg5_peaks = c(1267, 2139, 2275, 2864, 3744, 3879, 4432, 5620, 6731);
  cg6_peaks = c(1278, 2148, 2285, 2873, 3752, 3816, 4442, 5630, 6740);
  ar1_peaks = c(1398, 2176, 2258, 2849, 3786, 3816, 4488, 5657, 6811);
  ar3A_peaks = c(1402, 2175, 2263, 2873, 3789, 3816, 4495, 5669, 6821);

  sd3A_label_x <- c(0,1248,2180,2837,3857,4406,5593,6704);
  shg09A_label_x <- c(0,1247,2183,2837,3765.5,4403,5594,6706);
  cg1_label_x <- c(0,1247,2183,2837,3706.5,4410,5594,6705);
  og1_label_x <- c(0,1249,2184,2839,3767,4407,5594,6707);
  cg4_label_x <- c(0,1249,2183.5,2840,3862.5,4409,5598,6710);
  cg5_label_x <- c(0,1267,2207,2864,3811.5,4432,5620,6731);
  cg6_label_x <- c(0,1278,2216.5,2873,3784,4442,5630,6740);
  ar1_label_x <- c(0,1398,2217,2849,3801,4488,5657,6811);
  ar3A_label_x <- c(0,1402,2219,2873,3802.5,4495,5669,6821);
```

```
  sd3A_label <- c("Jul 11", "Storm 1\nJul 19\n4:00pm" , "Storm 2\nJul 25\n3:50pm" , "Storm 3\nJul
26\n2:50pm" , "Storm 4\nJul 30\n4:50pm" , "Storm 5\nAug 5\n7:00pm" , "Storm 5b\nAug 7\n6:40pm" ,
"Storm 6\nAug 10\n2:20pm" , "Storm 7\nAug 18\n8:10pm" , "Storm 8\nAug 26\n1:20pm");
  shg09A_label <- c("Jul 11", "Storm 1\nJul 19\n3:50pm" , "Storm 2\nJul 25\n4:40pm" , "Storm
3\nJul 26\n3:00pm" , "Storm 4\nJul 30\n4:50pm" , "Storm 5\nAug 5\n7:10pm" , "Storm 5b\nAug
6\n12:00pm" , "Storm 6\nAug 10\n1:50pm" , "Storm 7\nAug 18\n8:20pm" , "Storm 8\nAug 26\n1:40pm");
  cg1_label <- c("Jul 11", "Storm 1\nJul 19\n3:50pm" , "Storm 2\nJul 25\n4:30pm" , "Storm 3\nJul
26\n3:10pm" , "Storm 4\nJul 30\n4:50pm" , "Storm 5\nAug 4\n5:50pm" , "Storm 5b\nAug 6\n5:40pm" ,
"Storm 6\nAug 10\n3:00pm" , "Storm 7\nAug 18\n8:20pm" , "Storm 8\nAug 26\n1:30pm");
  og1_label <- c("Jul 11", "Storm 1\nJul 19\n4:10pm" , "Storm 2\nJul 25\n4:50pm" , "Storm 3\nJul
26\n3:10pm" , "Storm 4\nJul 30\n5:10pm" , "Storm 5\nAug 5\n7:40pm" , "Storm 5b\nAug 6\n12:00pm" ,
"Storm 6\nAug 10\n2:30pm" , "Storm 7\nAug 18\n8:20pm" , "Storm 8\nAug 26\n1:50pm");
  cg4_label <- c("Jul 11", "Storm 1\nJul 19\n4:10pm" , "Storm 2\nJul 25\n4:20pm" , "Storm 3\nJul
26\n3:30pm" , "Storm 4\nJul 30\n5:20pm" , "Storm 5\nAug 5\n7:50pm" , "Storm 5b\nAug 7\n7:40pm" ,
"Storm 6\nAug 10\n2:50pm" , "Storm 7\nAug 18\n9:00pm" , "Storm 8\nAug 26\n2:20pm");
  cg5_label <- c("Jul 11", "Storm 1\nJul 19\n7:10pm" , "Storm 2\nJul 25\n8:30pm" , "Storm 3\nJul
26\n7:10pm" , "Storm 4\nJul 30\n9:20pm" , "Storm 5\nAug 6\n12:00am" , "Storm 5b\nAug 6\n10:30pm" ,
"Storm 6\nAug 10\n6:40pm" , "Storm 7\nAug 19\n12:40am" , "Storm 8\nAug 26\n5:50pm");
  cg6_label = c("Jul 11", "Storm 1\nJul 19\n9:00pm" , "Storm 2\nJul 25\n10:00pm" , "Storm 3\nJul
26\n8:50pm" , "Storm 4\nJul 30\n10:50pm" , "Storm 5\nAug 6\n1:20am" , "Storm 5b\nAug 6\n12:00pm" ,
"Storm 6\nAug 10\n8:20pm" , "Storm 7\nAug 19\n2:20am" , "Storm 8\nAug 26\n7:20pm");
  ar1_label <- c("Jul 11", "Storm 1\nJul 20\n5:00pm" , "Storm 2\nJul 26\n2:40am" , "Storm 3\nJul
26\n4:20pm" , "Storm 4\nJul 30\n6:50pm" , "Storm 5\nAug 6\n7:00am" , "Storm 5b\nAug 6\n12:00pm" ,
"Storm 6\nAug 11\n4:00am" , "Storm 7\nAug 19\n6:50am" , "Storm 8\nAug 27\n7:10am");
  ar3A_label <- c("Jul 11", "Storm 1\nJul 20\n5:40pm" , "Storm 2\nJul 26\n2:30am" , "Storm 3\nJul
26\n5:10pm" , "Storm 4\nJul 30\n10:50pm" , "Storm 5\nAug 6\n7:30am" , "Storm 5b\nAug 6\n12:00pm" ,
"Storm 6\nAug 11\n5:10am" , "Storm 7\nAug 19\n8:50am" , "Storm 8\nAug 27\n8:50am");

  sd3A_label_adj <- c("Jul 11", "Storm 1\nJul 19\n4:00pm" , "Storm 2, 3\nJul 25, 26\n3:50pm,
2:50pm" , "Storm 4\nJul 30\n4:50pm" , "Storm 5, 5b\nAug 5, 7\n7:00pm, 6:40pm" , "Storm 6\nAug
10\n2:20pm" , "Storm 7\nAug 18\n8:10pm" , "Storm 8\nAug 26\n1:20pm");
  shg09A_label_adj <- c("Jul 11", "Storm 1\nJul 19\n3:50pm" , "Storm 2, 3\nJul 25, 26\n4:40pm,
3:00pm" , "Storm 4\nJul 30\n4:50pm" , "Storm 5, 5b\nAug 5, 6\n7:10pm, 12:00pm" , "Storm 6\nAug
10\n1:50pm" , "Storm 7\nAug 18\n8:20pm" , "Storm 8\nAug 26\n1:40pm");
  cg1_label_adj <- c("Jul 11", "Storm 1\nJul 19\n3:50pm" , "Storm 2, 3\nJul 25, 26\n4:30pm,
3:10pm" , "Storm 4\nJul 30\n4:50pm" , "Storm 5, 5b\nAug 4, 6\n5:50pm, 5:40pm" , "Storm 6\nAug
10\n3:00pm" , "Storm 7\nAug 18\n8:20pm" , "Storm 8\nAug 26\n1:30pm");
  og1_label_adj <- c("Jul 11", "Storm 1\nJul 19\n4:10pm" , "Storm 2, 3\nJul 25, 26\n4:50pm,
3:10pm" , "Storm 4\nJul 30\n5:10pm" , "Storm 5, 5b\nAug 5, 6\n7:40pm, 12:00pm" , "Storm 6\nAug
10\n2:30pm" , "Storm 7\nAug 18\n8:20pm" , "Storm 8\nAug 26\n1:50pm");
  cg4_label_adj <- c("Jul 11", "Storm 1\nJul 19\n4:10pm" , "Storm 2, 3\nJul 25, 26\n4:20pm,
3:30pm" , "Storm 4\nJul 30\n5:20pm" , "Storm 5, 5b\nAug 5, NA\n7:50pm,NA" , "Storm 6\nAug
10\n2:50pm" , "Storm 7\nAug 18\n9:00pm" , "Storm 8\nAug 26\n2:20pm");
  cg5_label_adj <- c("Jul 11", "Storm 1\nJul 19\n7:10pm" , "Storm 2, 3\nJul 25, 26\n8:30pm,
7:10pm" , "Storm 4\nJul 30\n9:20pm" , "Storm 5, 5b\nAug 6, 6\n12:00am, 10:30pm" , "Storm 6\nAug
10\n6:40pm" , "Storm 7\nAug 19\n12:40am" , "Storm 8\nAug 26\n5:50pm");
  cg6_label_adj = c("Jul 11", "Storm 1\nJul 19\n9:00pm" , "Storm 2, 3\nJul 25, 26\n10pm, 8:50pm" ,
"Storm 4\nJul 30\n10:50pm" , "Storm 5, 5b\nAug 6, NA\n1:20am, NA" , "Storm 6\nAug 10\n8:20pm" ,
"Storm 7\nAug 19\n2:20am" , "Storm 8\nAug 26\n7:20pm");
  ar1_label_adj <- c("Jul 11", "Storm 1\nJul 20\n5:00pm" , "Storm 2, 3\nJul 26, 26\n2:40am,
4:20pm" , "Storm 4\nJul 30\n6:50pm" , "Storm 5, 5b\nAug 6, 6\n7:00am, 12:00pm" , "Storm 6\nAug
11\n4:00am" , "Storm 7\nAug 19\n6:50am" , "Storm 8\nAug 27\n7:10am");
  ar3A_label_adj <- c("Jul 11", "Storm 1\nJul 20\n5:40pm" , "Storm 2, 3\nJul 26, 26\n2:30am,
5:10pm" , "Storm 4\nJul 30\n10:50pm" , "Storm 5, 5b\nAug 6, 6\n7:30am, 12:00pm" , "Storm 6\nAug
11\n5:10am" , "Storm 7\nAug 19\n8:50am" , "Storm 8\nAug 27\n8:50am");
}

{ #Build axes, etc for all storm plot
#  axis (2, at = c (r22_cg6max, r22_cg6min, r16n_cg6max, r16n_cg6min), labels = c ("SMA2 Max
positive deviation", "SMA2 Max negative deviation", "TREX Max positive deviation", "TREX Max
negative deviation"));
  axis (2,
      at = c (r22_cg6max, r22_cg6min, r16n_cg6max, r16n_cg6min)
      , labels = c (signif(r22_cg6max,digits=2)
        , signif(r22_cg6min,digits=2)
        , signif(r16n_cg6max,digits=2)
        , signif(r16n_cg6min,digits=2))
      , cex.axis=1.5);

  axis (1, at = cg6_label_x, labels = cg6_label_adj, lty=0, cex.axis=1.5);
  abline (v = cg6_peaks, lty=2, col="grey");
  statistic = c("NS (1.0)","corr (1.0)","modcorr (1.0)", "", "pb (0.0)","apb (0.0)","rmse
(0.0)","prmse (0.0)","rrmse (0.0)");
  noSMA =
c(signif(NS_n,digits=3),signif(corr_n,digits=3),signif(modcorr_n,digits=3),"",signif(pb_n,digits=
3),signif(apb_n,digits=3),signif(rmse_n,digits=3),signif(prmse_n,digits=3),signif(rrmse_n,digits=
3));
  SMA =
c(signif(NS_s,digits=3),signif(corr_s,digits=3),signif(modcorr_s,digits=3),"",signif(pb_s,digits=
```

```
3),signif(apb_s,digits=3),signif(rmse_s,digits=3),signif(prmse_s,digits=3),signif(rrmse_s,digits=
3));
  resultstable = cbind(statistic,noSMA,SMA);
  addtable2plot(x=3600,y=arcsinh(3.5),table=resultstable,bty="n", cex=1.5);
  write.csv(resultstable, file="cg6.csv");
}
```

### *B.2.7 R script for peak plotting*

```
#Rscript cg-6.peak.R | convert -rotate 90 ps:- png:cg-6.peak.R.png

{
  #load required libraries/packages
  library (topmodel, lib.loc="/home/halgrenj/R/x86_64-pc-linux-gnu-library/2.10/");
  library (boot, lib.loc="/home/halgrenj/R/x86_64-pc-linux-gnu-library/2.10/");
  library (plotrix, lib.loc="/home/halgrenj/R/x86_64-pc-linux-gnu-library/2.10/");
  #library (RSvgDevice);
}

{
  #read data --- linux
  obstrunc = read.table
("cg_realtime/AllContinuous.gnup.withcumulativeprecip.commadelim.Rtext.trunc", header = FALSE,
sep = ",");
  A = read.table ("multi/out/export/r26SMA.exp", header = TRUE, sep = ",");
  B = read.table ("multi/out/export/r26noSMA.exp", header = TRUE, sep = ",");
  ##read data --- windows
#  obstrunc = read.table
("z_R_temp/AllContinuous.gnup.withcumulativeprecip.commadelim.Rtext.trunc", header = FALSE, sep =
",");
#  A = read.table ("z_R_temp/cg20060719Storm-ASMA.exp", header = TRUE, sep = ",");
#  B = read.table ("z_R_temp/cg20060719Storm-BoSMA.exp", header = TRUE, sep = ",");
}

{
  #Offset parameters
  obs0 = 5761;   #the point where the simulated and observed dates are matched
                 #5761 -- the ordinal number of the July 11th 2006 00:00:00 observation

  obso = 0;          #This SHOULD be the optimum shift ... no data tinkering.
  obs0 = obs0 + obso #shift observations (positive number shifts observations to the left)
  obso_noSMA = 13;   #at A, this shift provides the best correlation and NSeff
  obso_SMA = -20;    #for the noSMA and SMA cases, respectively

  sim0 = 1;      #for the moment, there is no reason to count from anywhere but the start of
                 #simulation. But if someday there were a longer simulated series,
                 #then this would be useful.

  analysisstart = 1152;     #start analysis series relative from sim0 or obs0
  analysislength = 24 * 6 * 52;     #end analysis series relative from sim0 or obs0

  plotstart = 1152;     #start plotting series relative from sim0 or obs0
  plotlength = 6000;  #end plotting series relative from sim0 or obs0

  obs1 = obs0 + analysisstart;
  obsn = obs0 + analysisstart + analysislength;

  sim1 = sim0 + analysisstart;     #first element of time series relative from simulation start
  simn = sim0 + analysisstart + analysislength; #last element of time series

  plotend = plotstart+plotlength;
}

{ #Plot Parameters
  simdate = B[sim0:simn, 1];
  simtime = B[sim0:simn, 2];
}

{ #Identify storm intervals
  #First number is from Excel Spreadsheet precip.ods
  #and is the number of timesteps from July 1st.
  #The second number adjusts the interval to begin July 11th.
  Storm1_begin=2602-1440;
  Storm1_end=2800-1440;
  Storm2_begin=3466-1440;
  Storm2_end=3600-1440;
  Storm3_begin=3665-1440;
  Storm3_end=3750-1440;
  Storm4_begin=4187-1440;
  Storm4_end=4400-1440;
```

```
  Storm5_begin=5050-1440;
  Storm5_end=5250-1440;
  Storm5b_begin=5303-1440;
  Storm5b_end=5450-1440;
  Storm6_begin=5734-1440;
  Storm6_end=5950-1440;
  Storm7_begin=6922-1440;
  Storm7_end=7150-1440;
  Storm8_begin=8074-1440;
  Storm8_end=8300-1440;
}

#{ #Identify storm intervals
#  #First number is from Excel Spreadsheet precip.ods
#  #and is the number of timesteps from July 1st.
#  #The second number adjusts the interval to begin July 11th.
#  Storm1_begin=2602-1440;
#  Storm1_end=2889-1440;
#  Storm2_begin=3466-1440;
#  Storm2_end=3663-1440;
#  Storm3_begin=3665-1440;
#  Storm3_end=3838-1440;
#  Storm4_begin=4187-1440;
#  Storm4_end=4473-1440;
#  Storm5_begin=5050-1440;
#  Storm5_end=5301-1440;
#  Storm5b_begin=5303-1440;
#  Storm5b_end=5499-1440;
#  Storm6_begin=5734-1440;
#  Storm6_end=6016-1440;
#  Storm7_begin=6922-1440;
#  Storm7_end=7209-1440;
#  Storm8_begin=8074-1440;
#  Storm8_end=8361-1440;
#}

#Observed
#14 CG-1
#44 SD-3
#50 SD-3A
#56 SHG-09A
#20 CG-4
#26 CG-5
#32 CG-6
#38 OG-1

#Simulated
#4 CG-1
#7 CG-1
#10 SHG-09A
#13 SD-3A
#16 CG-4
#19 OG-1
#22 OG-1
#25 CG-5
#28 CG-5 + WWTP
#31 CG-6

{ #time series
  obs_all <- data.frame (obstrunc[obs0:obsn,1], obstrunc[obs0:obsn,32]);
#  obs_all = obstrunc[obs0:obsn, c(1,14)];
  A_all <- data.frame (A[sim0:simn, 1],A[sim0:simn, 31]  * (1 / 0.3048) ** 3);
  B_all <- data.frame (B[sim0:simn, 1],B[sim0:simn, 31]  * (1 / 0.3048) ** 3);
}

{
  obs_analysis = obs_all[sim1:simn, 2];
  B_analysis = B_all[sim1:simn, 2];
  A_analysis = A_all[sim1:simn, 2];
#  obs_analysis = obs_all[analysisstart:analysisstart+analysislength, 2];
#  B_analysis = B_all[analysisstart:analysisstart+analysislength, 2];
#  A_analysis = A_all[analysisstart:analysisstart+analysislength, 2];
  obs_storm1 = obs_all[Storm1_begin:Storm1_end, ];
  A_storm1 = A_all[Storm1_begin:Storm1_end, ];
  B_storm1 = B_all[Storm1_begin:Storm1_end, ];
  obs_storm2 = obs_all[Storm2_begin:Storm2_end, ];
  A_storm2 = A_all[Storm2_begin:Storm2_end, ];
  B_storm2 = B_all[Storm2_begin:Storm2_end, ];
  obs_storm3 = obs_all[Storm3_begin:Storm3_end, ];
  A_storm3 = A_all[Storm3_begin:Storm3_end, ];
  B_storm3 = B_all[Storm3_begin:Storm3_end, ];
```

```
  obs_storm4 = obs_all[Storm4_begin:Storm4_end, ];
  A_storm4 = A_all[Storm4_begin:Storm4_end, ];
  B_storm4 = B_all[Storm4_begin:Storm4_end, ];
  obs_storm5 = obs_all[Storm5_begin:Storm5_end, ];
  A_storm5 = A_all[Storm5_begin:Storm5_end, ];
  B_storm5 = B_all[Storm5_begin:Storm5_end, ];
  obs_storm5b = obs_all[Storm5b_begin:Storm5b_end, ];
  A_storm5b = A_all[Storm5b_begin:Storm5b_end, ];
  B_storm5b = B_all[Storm5b_begin:Storm5b_end, ];
  obs_storm6 = obs_all[Storm6_begin:Storm6_end, ];
  A_storm6 = A_all[Storm6_begin:Storm6_end, ];
  B_storm6 = B_all[Storm6_begin:Storm6_end, ];
  obs_storm7 = obs_all[Storm7_begin:Storm7_end, ];
  A_storm7 = A_all[Storm7_begin:Storm7_end, ];
  B_storm7 = B_all[Storm7_begin:Storm7_end, ];
  obs_storm8 = obs_all[Storm8_begin:Storm8_end, ];
  A_storm8 = A_all[Storm8_begin:Storm8_end, ];
  B_storm8 = B_all[Storm8_begin:Storm8_end, ];
}

{ #peak value statistics
  S1obs=obs_storm1[obs_storm1[, 2]==max(obs_storm1[, 2]),];
  S1A=A_storm1[A_storm1[, 2]==max(A_storm1[, 2]),];
  S1B=B_storm1[B_storm1[, 2]==max(B_storm1[, 2]),];
  S2obs=obs_storm2[obs_storm2[, 2]==max(obs_storm2[, 2]),];
  S2A=A_storm2[A_storm2[, 2]==max(A_storm2[, 2]),];
  S2B=B_storm2[B_storm2[, 2]==max(B_storm2[, 2]),];
  S3obs=obs_storm3[obs_storm3[, 2]==max(obs_storm3[, 2]),];
  S3A=A_storm3[A_storm3[, 2]==max(A_storm3[, 2]),];
  S3B=B_storm3[B_storm3[, 2]==max(B_storm3[, 2]),];
  S4obs=obs_storm4[obs_storm4[, 2]==max(obs_storm4[, 2]),];
  S4A=A_storm4[A_storm4[, 2]==max(A_storm4[, 2]),];
  S4B=B_storm4[B_storm4[, 2]==max(B_storm4[, 2]),];
  S5obs=obs_storm5[obs_storm5[, 2]==max(obs_storm5[, 2]),];
  S5A=A_storm5[A_storm5[, 2]==max(A_storm5[, 2]),];
  S5B=B_storm5[B_storm5[, 2]==max(B_storm5[, 2]),];
  S5bobs=obs_storm5b[obs_storm5b[, 2]==max(obs_storm5b[, 2]),];
  S5bA=A_storm5b[A_storm5b[, 2]==max(A_storm5b[, 2]),];
  S5bB=B_storm5b[B_storm5b[, 2]==max(B_storm5b[, 2]),];
  S6obs=obs_storm6[obs_storm6[, 2]==max(obs_storm6[, 2]),];
  S6A=A_storm6[A_storm6[, 2]==max(A_storm6[, 2]),];
  S6B=B_storm6[B_storm6[, 2]==max(B_storm6[, 2]),];
  S7obs=obs_storm7[obs_storm7[, 2]==max(obs_storm7[, 2]),];
  S7A=A_storm7[A_storm7[, 2]==max(A_storm7[, 2]),];
  S7B=B_storm7[B_storm7[, 2]==max(B_storm7[, 2]),];
  S8obs=obs_storm8[obs_storm8[, 2]==max(obs_storm8[, 2]),];
  S8A=A_storm8[A_storm8[, 2]==max(A_storm8[, 2]),];
  S8B=B_storm8[B_storm8[, 2]==max(B_storm8[, 2]),];
}

{ #format for display
  names(S1obs) <- c("date", "flow");
  names(S1A) <- c("date", "flow");
  names(S1B) <- c("date", "flow");
  names(S2obs) <- c("date", "flow");
  names(S2A) <- c("date", "flow");
  names(S2B) <- c("date", "flow");
  names(S3obs) <- c("date", "flow");
  names(S3A) <- c("date", "flow");
  names(S3B) <- c("date", "flow");
  names(S4obs) <- c("date", "flow");
  names(S4A) <- c("date", "flow");
  names(S4B) <- c("date", "flow");
  names(S5obs) <- c("date", "flow");
  names(S5A) <- c("date", "flow");
  names(S5B) <- c("date", "flow");
  names(S5bobs) <- c("date", "flow");
  names(S5bA) <- c("date", "flow");
  names(S5bB) <- c("date", "flow");
  names(S6obs) <- c("date", "flow");
  names(S6A) <- c("date", "flow");
  names(S6B) <- c("date", "flow");
  names(S7obs) <- c("date", "flow");
  names(S7A) <- c("date", "flow");
  names(S7B) <- c("date", "flow");
  names(S8obs) <- c("date", "flow");
  names(S8A) <- c("date", "flow");
  names(S8B) <- c("date", "flow");
}

{ #format for display
```

```
  S1obs_f = S1obs;
  S1A_f = S1A;
  S1B_f = S1B;
  S2obs_f = S2obs;
  S2A_f = S2A;
  S2B_f = S2B;
  S3obs_f = S3obs;
  S3A_f = S3A;
  S3B_f = S3B;
  S4obs_f = S4obs;
  S4A_f = S4A;
  S4B_f = S4B;
  S5obs_f = S5obs;
  S5A_f = S5A;
  S5B_f = S5B;
  S5bobs_f = S5bobs;
  S5bA_f = S5bA;
  S5bB_f = S5bB;
  S6obs_f = S6obs;
  S6A_f = S6A;
  S6B_f = S6B;
  S7obs_f = S7obs;
  S7A_f = S7A;
  S7B_f = S7B;
  S8obs_f = S8obs;
  S8A_f = S8A;
  S8B_f = S8B;
}

{ #format for display v3
  S1obs_f$date = substr(S1obs_f$date,7,16); S1obs_f$flow=signif(S1obs_f$flow,digits=3);
  S1A_f$date = substr(S1A_f$date,7,16); S1A_f$flow=signif(S1A_f$flow,digits=3);
  S1B_f$date = substr(S1B_f$date,7,16); S1B_f$flow=signif(S1B_f$flow,digits=3);
  S2obs_f$date = substr(S2obs_f$date,7,16); S2obs_f$flow=signif(S2obs_f$flow,digits=3);
  S2A_f$date = substr(S2A_f$date,7,16); S2A_f$flow=signif(S2A_f$flow,digits=3);
  S2B_f$date = substr(S2B_f$date,7,16); S2B_f$flow=signif(S2B_f$flow,digits=3);
  S3obs_f$date = substr(S3obs_f$date,7,16); S3obs_f$flow=signif(S3obs_f$flow,digits=3);
  S3A_f$date = substr(S3A_f$date,7,16); S3A_f$flow=signif(S3A_f$flow,digits=3);
  S3B_f$date = substr(S3B_f$date,7,16); S3B_f$flow=signif(S3B_f$flow,digits=3);
  S4obs_f$date = substr(S4obs_f$date,7,16); S4obs_f$flow=signif(S4obs_f$flow,digits=3);
  S4A_f$date = substr(S4A_f$date,7,16); S4A_f$flow=signif(S4A_f$flow,digits=3);
  S4B_f$date = substr(S4B_f$date,7,16); S4B_f$flow=signif(S4B_f$flow,digits=3);
  S5obs_f$date = substr(S5obs_f$date,7,16); S5obs_f$flow=signif(S5obs_f$flow,digits=3);
  S5A_f$date = substr(S5A_f$date,7,16); S5A_f$flow=signif(S5A_f$flow,digits=3);
  S5B_f$date = substr(S5B_f$date,7,16); S5B_f$flow=signif(S5B_f$flow,digits=3);
  S5bobs_f$date = substr(S5bobs_f$date,7,16); S5bobs_f$flow=signif(S5bobs_f$flow,digits=3);
  S5bA_f$date = substr(S5bA_f$date,7,16); S5bA_f$flow=signif(S5bA_f$flow,digits=3);
  S5bB_f$date = substr(S5bB_f$date,7,16); S5bB_f$flow=signif(S5bB_f$flow,digits=3);
  S6obs_f$date = substr(S6obs_f$date,7,16); S6obs_f$flow=signif(S6obs_f$flow,digits=3);
  S6A_f$date = substr(S6A_f$date,7,16); S6A_f$flow=signif(S6A_f$flow,digits=3);
  S6B_f$date = substr(S6B_f$date,7,16); S6B_f$flow=signif(S6B_f$flow,digits=3);
  S7obs_f$date = substr(S7obs_f$date,7,16); S7obs_f$flow=signif(S7obs_f$flow,digits=3);
  S7A_f$date = substr(S7A_f$date,7,16); S7A_f$flow=signif(S7A_f$flow,digits=3);
  S7B_f$date = substr(S7B_f$date,7,16); S7B_f$flow=signif(S7B_f$flow,digits=3);
  S8obs_f$date = substr(S8obs_f$date,7,16); S8obs_f$flow=signif(S8obs_f$flow,digits=3);
  S8A_f$date = substr(S8A_f$date,7,16); S8A_f$flow=signif(S8A_f$flow,digits=3);
  S8B_f$date = substr(S8B_f$date,7,16); S8B_f$flow=signif(S8B_f$flow,digits=3);
}

{ #format for analysis
  S1 <- cbind(S1obs[1,],S1A[1,],S1B[1,]);
  S2 <- cbind(S2obs[1,],S2A[1,],S2B[1,]);
  S3 <- cbind(S3obs[1,],S3A[1,],S3B[1,]);
  S4 <- cbind(S4obs[1,],S4A[1,],S4B[1,]);
  S5 <- cbind(S5obs[1,],S5A[1,],S5B[1,]);
  S5b <- cbind(S5bobs[1,],S5bA[1,],S5bB[1,]);
  S6 <- cbind(S6obs[1,],S6A[1,],S6B[1,]);
  S7 <- cbind(S7obs[1,],S7A[1,],S7B[1,]);
  S8 <- cbind(S8obs[1,],S8A[1,],S8B[1,]);
  peaktable <- rbind(S1, S2, S3, S4, S5, S5b, S6, S7, S8);
}

{
  obsmean = mean (na.omit(obs_analysis));
  obsstdv = sd (na.omit(obs_analysis));
  NS_n = NSeff (B_analysis, obs_analysis);  #Nash-SutCliffe
  NS_s = NSeff (A_analysis, obs_analysis);  #Nash-SutCliffe
  corr_n = corr (na.omit (cbind (B_analysis, obs_analysis))); #Correlation Coefficient
  corr_s = corr (na.omit (cbind (A_analysis, obs_analysis))); #Correlation Coefficient
```

```
  modcorr_n = corr (na.omit (cbind (B_analysis, obs_analysis))) * min (sd (na.omit (B_analysis)),
sd (na.omit (A_analysis))) / max (sd (na.omit (B_analysis)), sd (na.omit (A_analysis)));
#Modified Correlation Coefficient
  modcorr_s = corr (na.omit (cbind (A_analysis, obs_analysis))) * min (sd (na.omit (B_analysis)),
sd (na.omit (A_analysis))) / max (sd (na.omit (B_analysis)), sd (na.omit (A_analysis)));
#Modified Correlation Coefficient
  pb_n = sum (na.omit (B_analysis - obs_analysis)) / sum (na.omit (obs_analysis));      #Percent
Bias
  pb_s = sum (na.omit (A_analysis - obs_analysis)) / sum (na.omit (obs_analysis));      #Percent
Bias
  apb_n = sum (abs (na.omit (B_analysis - obs_analysis))) / sum (na.omit (obs_analysis));
#Absolute Percent Bias
  apb_s = sum (abs (na.omit (A_analysis - obs_analysis))) / sum (na.omit (obs_analysis));
#Absolute Percent Bias
  rmse_n = sqrt (1 / NROW (na.omit (obs_analysis)) * sum ((na.omit (B_analysis - obs_analysis) **
2)));   #Root Mean Squared Error (RMSE)
  prmse_n = rmse_n / obsmean;  #percent RMSE
  rrmse_n = rmse_n / obsstdv;  #RMSE ratio
  rmse_s = sqrt (1 / NROW (na.omit (obs_analysis)) * sum ((na.omit (A_analysis- obs_analysis) **
2)));  #Root Mean Squared Error (RMSE)
  prmse_s = rmse_s / obsmean;  #percent RMSE
  rrmse_s = rmse_s / obsstdv;  #RMSE ratio
}

{ #Set plot limits
  A_max = max(na.omit(A_analysis - obs_analysis));
  A_min = min(na.omit(A_analysis - obs_analysis));
  B_max = max(na.omit(B_analysis - obs_analysis));
  B_min = min(na.omit(B_analysis - obs_analysis));
  plotmax = max(na.omit(A_analysis - obs_analysis),na.omit(B_analysis - obs_analysis)) + 0.3;
  plotmin = min(na.omit(A_analysis - obs_analysis),na.omit(B_analysis - obs_analysis)) - 0.3;
  allmax = max(na.omit(obs_analysis), na.omit(B_analysis), na.omit(A_analysis));
  allmin = min(na.omit(obs_analysis), na.omit(B_analysis), na.omit(A_analysis));
  maxsim = max(na.omit(B_analysis), na.omit(A_analysis));
  minsim = min(na.omit(B_analysis), na.omit(A_analysis));
  maxobs = max(na.omit(obs_analysis));
  minobs = min(na.omit(obs_analysis));
  peakminobs = min(na.omit(peaktable[c(2)]));
  peakminsim = min(na.omit(peaktable[c(4,6)]));
}

{
  statistic = c("NS (1.0)","corr (1.0)","modcorr (1.0)", "", "pb (0.0)","apb (0.0)","rmse
(0.0)","prmse (0.0)","rrmse (0.0)");
  noSMA =
c(signif(NS_n,digits=3),signif(corr_n,digits=3),signif(modcorr_n,digits=3),"",signif(pb_n,digits=
3),signif(apb_n,digits=3),signif(rmse_n,digits=3),signif(prmse_n,digits=3),signif(rrmse_n,digits=
3));
  SMA =
c(signif(NS_s,digits=3),signif(corr_s,digits=3),signif(modcorr_s,digits=3),"",signif(pb_s,digits=
3),signif(apb_s,digits=3),signif(rmse_s,digits=3),signif(prmse_s,digits=3),signif(rrmse_s,digits=
3));
  resultstable = cbind(statistic,noSMA,SMA);
}

{
  postscript(file="", command="cat", title="CG-6 Flow Comparison Plot", width=9, height=14,
paper='special');
  par(mfrow=c(2,1))
}

{ #plot the observed peaks versus simulated for the selected storms
#  plot (0, ylim = c (0 , peakmax), xlim = c (0, peakmax), yaxt ='n', xaxt = 'n', bty = "n", xlab
= "", ylab = "" );
  plot (-500, ylim = c (peakminsim , maxsim)
      , xlim = c (peakminobs , maxobs)
      , bty = "n"
      , xlab = "Observed"
      , ylab = "Simulated"
      , cex.lab=1.3 );
  title(main = "CG-6 flow correlation: time corrected peaks"
      , sub = NULL
      , xlab = NULL
      , ylab = NULL
      , line = NA
      , outer = FALSE
      , cex.main=1.5);
  points(peaktable[c(2,6)], col="#99cc00", type="p", pch=19);
  points(peaktable[c(2,4)], col="#0000cc", type="p", pch=19);
  lines (x=c(allmin,allmax), y=c(allmin,allmax), lty=1);
}
```

```
{ #Plot observed flow versus simulated flow for the entire series on logscale
#  plot (0, ylim = c (0.01 , peakmax), xlim = c (0.01, peakmax), log="yx", yaxt ='n', xaxt = 'n',
bty = "n", xlab = "", ylab = "" );
#  plot (0.000001, ylim = c (0.01 , peakmax), xlim = c (0.01, peakmax), log="yx", bty = "n", xlab
= "", ylab = "" );
  plot (0.000001, ylim = c (minsim , maxsim)
      , xlim = c (minobs, maxobs), log="yx"
      , bty = "n"
      , xlab = "Observed"
      , ylab = "Simulated"
      , cex.lab=1.3 );
  title(main = "CG-6 flow correlation: all flows"
      , sub = NULL
      , xlab = NULL
      , ylab = NULL
      , line = NA
      , outer = FALSE
      , cex.main=1.5);

  points(obs_analysis, B_analysis, col="#99cc00", type="p", pch=19);
  points(obs_analysis, A_analysis, col="#0000cc", type="p", pch=19);
  lines (x=c(allmin,allmax), y=c(allmin,allmax), lty=1);
}

{
  write.csv(peaktable, file="multi/cg-6.peak.csv");
}
```

## B.3 GRASS AND KML SCRIPTS

The GRASS scripts are executed from a bash prompt inside the GRASS program. KML scripts may be read directly by Google earth.

### *B.3.1 Import model output into GRASS*

```
#!/bin/bash
SUFFIX=.grassgrid
prefixdir=$1 # If directory name given as a script argument ...
echo "This script creates a list of all files"
echo "$prefixdir*"
echo "and adds them to the current grass database"
echo "with the same name and '.SUFFIX'."
echo "(.i.e. this script must be run within a "
echo "grass shell.)"
a=0
for file in $prefixdir* # Filename globbing
do
  fullfilename=$file$SUFFIX
  filename=$fullfilename
  a=1
  while [ $a -ne 0 ]
  do
    a=`expr index "$filename" '/'`
    filename=${filename:$a}
  done
  if [ ! -d $file ]
  then
    echo "r.in.gdal input='$file' \
        output='$filename'"
    r.in.gdal input=$file \
      output=$filename
  fi
done

exit 0
```

### *B.3.2 Export 2-D graphics*

Prior to exporting, the color must be set using a script such as the following:

```
#!/bin/bash
prefixdir=$1 # If directory name given as a script argument ...
colorfile=$2    # file name of color "rule" file
echo "This script creates a list of all files"
echo "$prefixdir*"
echo "and sets the colortable to $colorfile."
a=0
for file in $prefixdir* # Filename globbing
do
  fullfilename=$file
  filename=$fullfilename
  a=1
  while [ $a -ne 0 ]
  do # strip the leading directory name and use only the grass grid name
    a=`expr index "$filename" '/'`
    filename=${filename:$a}
  done
  if [ ! -d $file ]
  then
    cat $colorfile | r.colors map=$filename color=rules
    echo "cat $colorfile | r.colors map=$filename color=rules"
  fi
done

#exit 0
```

The colorfile refers to a text file with the data value breaks listed each follwed by an RGB color triple.

```
0 208 167 90
0.000003 190 150 0
0.0003 0 198 208
0.001 0 208 0
0.003 0 195 85
0.01 0 149 208
0.03 0 66 208
0.1 184 0 208
0.3 101 0 208
1.0 184 0 208
3.0 208 0 31
end
```

Finally, the export is accomplished via the following:

```
#!/bin/bash
graphicssuffix=".ppm"
prefixdir=$1 # If directory name given as a script argument ...
newpath=$2 # second command line argument is path for new ppms
echo "This script creates a list of all files"
echo "$prefixdir*"
echo "and displays them on a grass monitor, one by one."
echo "The displays are exported to a graphic file using"
echo "the extension $graphicssuffix"
a=0
for file in $prefixdir* # Filename globbing
do
  fullfilename=$file
  filename=$fullfilename
  a=1
  while [ $a -ne 0 ]
  do # strip the leading directory name and use only the grass grid name
    a=`expr index "$filename" '/'`
    filename=${filename:$a}
  done
  if [ ! -d $file ]
  then
    #echo "d.rast output=$filename"
    r.out.ppm input=$filename output=$newpath$filename$graphicssuffix
    convert -trim -transparent white $newpath$filename$graphicssuffix $newpath$filename".png"
    rm $newpath$filename$graphicssuffix
    echo "r.out.ppm input=$filename output=$newpath$filename$graphicssuffix"


    echo "file created in $newpath$filename$graphicssuffix"
  fi
done

#exit 0
```

### *B.3.3 Display time series KML*

```
<?xml version="1.0" encoding="UTF-8"?>
<kml xmlns="http://www.opengis.net/kml/2.2" xmlns:gx="http://www.google.com/kml/ext/2.2"
xmlns:kml="http://www.opengis.net/kml/2.2" xmlns:atom="http://www.w3.org/2005/Atom">
<Document>
  <name>Summer 2006 storm frames</name>
  <open>1</open>
    <Folder>
      <name>July 30 2006 storm simulation</name>
      <open>1</open>
      <NetworkLink id="Legend">
        <name>Legend</name>
        <visibility>1</visibility>
        <open>1</open>
        <description>Legend for flow depth from depth.label.4 script</description>
        <refreshVisibility>0</refreshVisibility>
        <flyToView>0</flyToView>
        <Link><href>legend.kml</href></Link>
      </NetworkLink>
      <Folder>
        <name>simulation frames</name>
        <open>0</open>
        <GroundOverlay><name>Jul301200CG20060719Storm-r23SMA_AROutlet-waterdepth.005616
        </name><TimeSpan><begin>2006-07-30T12:00:00-06:00  </begin><end>2006-07-30T12:05:00-06:00
        </end></TimeSpan><color>87ffffff  </color><Icon><href>files//CG20060719Storm-
        r23SMA_AROutlet-waterdepth.005616.t.png  </href><viewBoundScale>0.75
        </viewBoundScale></Icon><LatLonBox><north>39.26216056263301</north>
        <south>39.22252677946483</south> <east>-106.2267295233106</east> <west>-
        106.3558339684977</west>
        <rotation>0.8404321523684434</rotation></LatLonBox></GroundOverlay>
        <GroundOverlay><name>Jul301205CG20060719Storm-r23SMA_AROutlet-waterdepth.005617
        </name><TimeSpan><begin>2006-07-30T12:05:00-06:00  </begin><end>2006-07-30T12:10:00-06:00
        </end></TimeSpan><color>87ffffff  </color><Icon><href>files//CG20060719Storm-
        r23SMA_AROutlet-waterdepth.005617.t.png  </href><viewBoundScale>0.75
        </viewBoundScale></Icon><LatLonBox><north>39.26216056263301</north>
        <south>39.22252677946483</south> <east>-106.2267295233106</east> <west>-
        106.3558339684977</west>
        <rotation>0.8404321523684434</rotation></LatLonBox></GroundOverlay>

        .
        .
        .

        <GroundOverlay><name>Jul311155CG20060719Storm-r23SMA_AROutlet-waterdepth.005903
        </name><TimeSpan><begin>2006-07-31T11:55:00-06:00  </begin><end>2006-07-31T12:00:00-06:00
        </end></TimeSpan><color>87ffffff  </color><Icon><href>files//CG20060719Storm-
        r23SMA_AROutlet-waterdepth.005903.t.png  </href><viewBoundScale>0.75
        </viewBoundScale></Icon><LatLonBox><north>39.26216056263301</north>
        <south>39.22252677946483</south> <east>-106.2267295233106</east> <west>-
        106.3558339684977</west>
        <rotation>0.8404321523684434</rotation></LatLonBox></GroundOverlay>
        <GroundOverlay><name>Jul311200CG20060719Storm-r23SMA_AROutlet-waterdepth.005904
        </name><TimeSpan><begin>2006-07-31T12:00:00-06:00  </begin><end>2006-07-31T12:05:00-06:00
        </end></TimeSpan><color>87ffffff  </color><Icon><href>files//CG20060719Storm-
        r23SMA_AROutlet-waterdepth.005904.t.png  </href><viewBoundScale>0.75
        </viewBoundScale></Icon><LatLonBox><north>39.26216056263301</north>
        <south>39.22252677946483</south> <east>-106.2267295233106</east> <west>-
        106.3558339684977</west>
        <rotation>0.8404321523684434</rotation></LatLonBox></GroundOverlay>
    </Folder>
</Folder>
</Document>
</kml>
```

### *B.3.4 Display legend on page*

```
<?xml version="1.0" encoding="UTF-8"?>
<kml xmlns="http://www.opengis.net/kml/2.2" xmlns:gx="http://www.google.com/kml/ext/2.2"
xmlns:kml="http://www.opengis.net/kml/2.2" xmlns:atom="http://www.w3.org/2005/Atom">
<Folder id="Legend">
    <name>Legends for GoogleEarth Simulation Displays</name>
    <open>1</open>
    <Folder>
    <name>Hydrology</name>
    <open>0</open>
      <Folder>
      <name>Flow Depth</name>
      <open>0</open>
      <ScreenOverlay id="Legend">
      <name>Flow Depth July 30 2006 storm simulation</name>
      <color>bbffffff</color>
            <description>Legend for flow depth from depth.label.4 script</description>
            <Icon>static/100yr_Legend.png</Icon>
            <overlayXY x="1.5" y="1.1" xunits="fraction" yunits="fraction"/>
            <screenXY x="1.0" y="1.0" xunits="fraction" yunits="fraction"/>
                <size x="165" y="0" xunits="pixels" yunits="pixels"/>
                <rotation>0</rotation>
                <visibility>1</visibility>
                <open>0</open>
      </ScreenOverlay>
    </Folder>
    <Folder>
      <open>0</open>
      <name>Flow Rate</name>
    </Folder>
    <Folder>
      <open>0</open>
      <name>Rain Rate</name>
    </Folder>
  </Folder>
  <Folder>
    <name>Sediment</name>
    <open>0</open>
  </Folder>
  <Folder>
    <name>Chemicals</name>
    <open>0</open>
  </Folder>
</Folder>
</kml>
```

### *B.3.5 Display gauge plots with KML*

Note that this example file refers to static local images for instance,

```
<img src="png/s4/CG-1.gnup.png" width="300">.
```

The image source may be pointed to the live web version of each graphic as well with code such as:

```
<object type='image/png'
data='http://albuquerque.engr.colostate.edu/~halgrenj/plot/gnuplot_call.png.php?gnuplot_script=mu
lti/s4/CG-4.gnup&refresh_period=0'>
```

When pointed to the live image, the graphic will update each time it is viewed in Google Earth, depending on simulation progress.

```
<?xml version="1.0" encoding="UTF-8"?>
<kml xmlns="http://www.opengis.net/kml/2.2" xmlns:gx="http://www.google.com/kml/ext/2.2"
xmlns:kml="http://www.opengis.net/kml/2.2" xmlns:atom="http://www.w3.org/2005/Atom">
<Document>
  <name>Storm 4</name>
  <open>1</open>
    <Schema parent="Placemark" name="TREX-SMA_gauges">
    </Schema>
  <Style id="greengauge"> <IconStyle>
      <color>ff77aa00</color>
      <scale>1.1</scale>
      <Icon> <href>static/shaded_dot.png</href> </Icon>
    </IconStyle>
    <LabelStyle> <scale>1.3</scale> </LabelStyle>
    <LineStyle> <color>00000000</color> </LineStyle>
    <PolyStyle> <color>ff77aa00</color> </PolyStyle>
        <BalloonStyle>
            <bgColor>44ffffff</bgColor> <!-- kml:color -->
            <text>$[description]</text>
        </BalloonStyle>
  </Style>
     <Style id="green_pintag">
    <IconStyle> <color>ff7faa00</color> <colorMode>normal</colorMode>
            <Icon> <href>http://maps.google.com/mapfiles/kml/paddle/grn-blank.png</href> </Icon>
            <hotSpot x="32" y="1" units="pixels" yunits="pixels"/>
    </IconStyle>
    <LabelStyle> <scale>1.3</scale> </LabelStyle>
    <LineStyle> <color>ff7faa00</color> <colorMode>normal</colorMode> </LineStyle>
    <PolyStyle> <color>ff7faa00</color> <colorMode>normal</colorMode> </PolyStyle>
        <BalloonStyle>
            <bgColor>44ffffff</bgColor> <!-- kml:color -->
            <text>$[description]</text>
        </BalloonStyle>
  </Style>
  <StyleMap id="msn_airports">
    <Pair>
      <key>normal</key>
      <styleUrl>#sn_airports</styleUrl>
    </Pair>
    <Pair>
      <key>highlight</key>
      <styleUrl>#sh_airports</styleUrl>
    </Pair>
  </StyleMap>
  <Style id="sh_airports">
    <IconStyle>
      <scale>1.1</scale>
      <Icon>
        <href>http://maps.google.com/mapfiles/kml/shapes/airports.png</href>
      </Icon>
    </IconStyle>
    <LabelStyle>
      <scale>1.1</scale>
    </LabelStyle>
  </Style>
```

```
  <Style id="default+icon=http://maps.google.com/mapfiles/kml/pal4/icon49.png">
    <IconStyle>
      <scale>1.1</scale>
      <Icon>
        <href>http://maps.google.com/mapfiles/kml/pal4/icon49.png</href>
      </Icon>
    </IconStyle>
    <LabelStyle>
      <scale>1.1</scale>
    </LabelStyle>
  </Style>
  <Style id="sn_airports">
    <IconStyle>
      <Icon>
        <href>http://maps.google.com/mapfiles/kml/shapes/airports.png</href>
      </Icon>
    </IconStyle>
  </Style>
  <Folder id="0_All">
    <name>Storm 4</name>
        <open>0</open>
    <TREX-SMA_gauges> <name>CG-1</name> <visibility>1</visibility>
            <TimeSpan>
                <begin>2006-07-30T12:00:00-06:00</begin>
                <end>2006-07-31T12:00:00-06:00</end>
            </TimeSpan>
            <description> <![CDATA[
              <table width="300"> <tbody> <tr> <td> <img src="png/s4/CG-1.gnup.png" width="300">
<br/> </td> </tr> <tr> <td> <img src="png/s4/cg-1.R.png" width="300"> <br/> </td> </tr> <tr>
<td> </td> </tr> <tr> <td>California Gulch CG-1</td> </tr> <tr> <td> </td> </tr> <tr>
<td> <em>Begin Date : 2006-07-30 12:00:00 PM</em> <br/> <em>End Date : 2006-07-31 12:00:00 PM</em>
</td> </tr> </tbody> </table>
               ]]>
           </description>
            <styleUrl>#green_pintag</styleUrl>
            <Point> <coordinates>-106.2703749138755,39.23574655786021,0</coordinates> </Point>
</TREX-SMA_gauges>
    <TREX-SMA_gauges> <name>CG-4</name> <visibility>1</visibility>
            <TimeSpan>
                <begin>2006-07-30T12:00:00-06:00</begin>
                <end>2006-07-31T12:00:00-06:00</end>
            </TimeSpan>
            <TimeSpan>
                <begin>2006-07-30T12:00:00-06:00</begin>
                <end>2006-07-31T12:00:00-06:00</end>
            </TimeSpan>
            <description> <![CDATA[
                <table> <tbody> <tr> <td> <object type='image/png'
data='http://albuquerque.engr.colostate.edu/~halgrenj/plot/gnuplot_call.png.php?gnuplot_script=mu
lti/s4/CG-4.gnup&refresh_period=0'> </object> <!--<img src="png/s4/CG-4.gnup.png" width="500">-->
<br/> </td> </tr> <tr> <td> <object type='image/png'
data='http://albuquerque.engr.colostate.edu/~halgrenj/plot/R_call.png.php?R_script=multi/s4/cg-
4.R&refresh_period=0'> </object> <!--<img src="png/s4/cg-4.R.png" width="500">--> <br/> </td>
</tr> <tr> <td> </td> </tr> <tr> <td>California Gulch CG-4</td> </tr> <tr> <td> </td>
</tr> <tr> <td> <em>Begin Date : 2006-07-30 00:00:00 AM</em> <br/> <em>End Date : 2006-07-31
11:59:00 PM</em> </td> </tr> </tbody> </table>
               ]]>
           </description>
            <styleUrl>#green_pintag</styleUrl>
            <Point> <coordinates>-106.2987192962472,39.23954720283152,0</coordinates> </Point>
</TREX-SMA_gauges>
    <TREX-SMA_gauges> <name>CG-5</name> <visibility>1</visibility>
            <TimeSpan>
                <begin>2006-07-30T12:00:00-06:00</begin>
                <end>2006-07-31T12:00:00-06:00</end>
            </TimeSpan>
            <description> <![CDATA[
              <table width="300"> <tbody> <tr> <td> <img src="png/s4/CG-5.gnup.png" width="300">
<br/> </td> </tr> <tr> <td> <img src="png/s4/cg-5.R.png" width="300"> <br/> </td> </tr> <tr>
<td> </td> </tr> <tr> <td>California Gulch CG-1</td> </tr> <tr> <td> </td> </tr> <tr>
<td> <em>Begin Date : 2006-07-30 00:00:00 AM</em> <br/> <em>End Date : 2006-07-31 11:59:00 PM</em>
</td> </tr> </tbody> </table>
               ]]>
           </description>
            <styleUrl>#green_pintag</styleUrl>
            <Point> <coordinates>-106.3317586064558,39.22698910338171,0</coordinates> </Point>
</TREX-SMA_gauges>
    <TREX-SMA_gauges> <name>CG-6</name> <visibility>1</visibility>
            <TimeSpan>
                <begin>2006-07-30T12:00:00-06:00</begin>
                <end>2006-07-31T12:00:00-06:00</end>
```

```
            </TimeSpan>
            <description> <![CDATA[
              <table width="300"> <tbody> <tr> <td> <img src="png/s4/CG-6.gnup.png" width="300">
<br/> </td> </tr> <tr> <td> <img src="png/s4/cg-6.R.png" width="300"> <br/> </td> </tr> <tr>
<td> </td> </tr> <tr> <td>California Gulch CG-1</td> </tr> <tr> <td> </td> </tr> <tr>
<td> <em>Begin Date : 2006-07-30 00:00:00 AM</em> <br/> <em>End Date : 2006-07-31 11:59:00 PM</em>
</td> </tr> </tbody> </table>
              ]]>
           </description>
            <styleUrl>#green_pintag</styleUrl>
            <Point> <coordinates>-106.3554952979911,39.22200904506989,0</coordinates> </Point>
</TREX-SMA_gauges>
    <TREX-SMA_gauges> <name>OG-1</name> <visibility>1</visibility>
            <TimeSpan>
                <begin>2006-07-30T12:00:00-06:00</begin>
                <end>2006-07-31T12:00:00-06:00</end>
            </TimeSpan>
            <description> <![CDATA[
              <table width="300"> <tbody> <tr> <td> <!--<img src="png/s4/OG-1.gnup.png"
width="300">--> <br/> </td> </tr> <tr> <td> <!--<img src="png/s4/og-1.R.png" width="300">--> <br/>
</td> </tr> <tr> <td> </td> </tr> <tr> <td>California Gulch CG-1</td> </tr> <tr>
<td> </td> </tr> <tr> <td> <em>Begin Date : 2006-07-30 00:00:00 AM</em> <br/> <em>End Date :
2006-07-31 11:59:00 PM</em> </td> </tr> </tbody> </table>
               ]]>
           </description>
            <styleUrl>#green_pintag</styleUrl>
            <Point> <coordinates>-106.2934464846659,39.24025906479917,0</coordinates> </Point>
</TREX-SMA_gauges>
    <TREX-SMA_gauges> <name>SD-3A</name> <visibility>1</visibility>
            <TimeSpan>
                <begin>2006-07-30T12:00:00-06:00</begin>
                <end>2006-07-31T12:00:00-06:00</end>
            </TimeSpan>
            <description> <![CDATA[
              <table width="300"> <tbody> <tr> <td> <img src="png/s4/SD-3A.gnup.png" width="300">
<br/> </td> </tr> <tr> <td> <img src="png/s4/sd-3A.R.png" width="300"> <br/> </td> </tr> <tr>
<td> </td> </tr> <tr> <td>California Gulch CG-1</td> </tr> <tr> <td> </td> </tr> <tr>
<td> <em>Begin Date : 2006-07-30 00:00:00 AM</em> <br/> <em>End Date : 2006-07-31 11:59:00 PM</em>
</td> </tr> </tbody> </table>
              ]]>
           </description>
            <styleUrl>#green_pintag</styleUrl>
            <Point> <coordinates>-106.2901000939475,39.24324993155267,0</coordinates> </Point>
</TREX-SMA_gauges>
    <TREX-SMA_gauges> <name>SHG-09A</name> <visibility>1</visibility>
            <TimeSpan>
                <begin>2006-07-30T12:00:00-06:00</begin>
                <end>2006-07-31T12:00:00-06:00</end>
            </TimeSpan>
            <description> <![CDATA[
              <table width="300"> <tbody> <tr> <td> <img src="png/s4/SHG-09A.gnup.png"
width="300"> <br/> </td> </tr> <tr> <td> <img src="png/s4/shg-09A.R.png" width="300"> <br/> </td>
</tr> <tr> <td> </td> </tr> <tr> <td>California Gulch CG-1</td> </tr> <tr> <td> </td>
</tr> <tr> <td> <em>Begin Date : 2006-07-30 00:00:00 AM</em> <br/> <em>End Date : 2006-07-31
11:59:00 PM</em> </td> </tr> </tbody> </table>
               ]]>
           </description>
            <styleUrl>#green_pintag</styleUrl>
            <Point> <coordinates>-106.2780683695445,39.25069196304045,0</coordinates> </Point>
</TREX-SMA_gauges>
  </Folder>
</Document>
</kml>
```

### *B.3.6 Time series tour KML*

```
<?xml version="1.0" encoding="UTF-8"?>
<kml xmlns="http://www.opengis.net/kml/2.2" xmlns:gx="http://www.google.com/kml/ext/2.2"
xmlns:kml="http://www.opengis.net/kml/2.2" xmlns:atom="http://www.w3.org/2005/Atom">
<Document>
  <name>Storm4Tour.kml</name>
  <open>1</open>
  <Folder>
    <name>California Gulch Tours</name>
    <open>1</open>
    <gx:Tour>
      <name>High, then down to Leadville city</name>
      <gx:Playlist>
          <gx:FlyTo><gx:duration>1</gx:duration> <LookAt> <gx:TimeStamp>  <when>  2006-07-
          30T16:00:01-06:00  </when> </gx:TimeStamp> <longitude>-106.3104803218946</longitude>
          <latitude>39.23132454015865</latitude> <altitude>0</altitude>
          <range>9932.750754596775</range> <tilt>62.10874334115960</tilt>
          <heading>84.72574103179315</heading> <altitudeMode>relativeToGround</altitudeMode>
          <gx:altitudeMode>relativeToSeaFloor</gx:altitudeMode> </LookAt> </gx:FlyTo>
          <gx:FlyTo><gx:flyToMode>smooth</gx:flyToMode> <gx:duration>15</gx:duration> <LookAt>
          <gx:TimeStamp>  <when>  2006-07-30T17:30:01-06:00  </when> </gx:TimeStamp>
          <longitude>-106.3104803218946</longitude> <latitude>39.23132454015865</latitude>
          <altitude>0</altitude> <range>9932.750754596775</range> <tilt>62.10874334115960</tilt>
          <heading>84.72574103179315</heading> <altitudeMode>relativeToGround</altitudeMode>
          <gx:altitudeMode>relativeToSeaFloor</gx:altitudeMode> </LookAt> </gx:FlyTo>
          <gx:FlyTo><gx:flyToMode>smooth</gx:flyToMode> <gx:duration>15</gx:duration> <LookAt>
          <gx:TimeStamp>  <when>  2006-07-30T17:30:01-06:00  </when> </gx:TimeStamp>
          <longitude>-106.3132801473476</longitude> <latitude>39.23309099633818</latitude>
          <altitude>0</altitude> <range>11820.76536643215</range> <tilt>60.63919983268732</tilt>
          <heading>77.61758647869176</heading> <altitudeMode>relativeToGround</altitudeMode>
          <gx:altitudeMode>relativeToSeaFloor</gx:altitudeMode> </LookAt> </gx:FlyTo>
          <gx:FlyTo><gx:flyToMode>smooth</gx:flyToMode> <gx:duration>10</gx:duration> <LookAt>
          <gx:TimeStamp>  <when>  2006-07-30T18:30:01-06:00  </when> </gx:TimeStamp>
          <longitude>-106.3025831821842</longitude> <latitude>39.24080892817672</latitude>
          <altitude>0</altitude> <range>4934.6807046798913</range> <tilt>73.54036809276O6</tilt>
          <heading>78.21591541809711</heading> <altitudeMode>relativeToGround</altitudeMode>
          <gx:altitudeMode>relativeToSeaFloor</gx:altitudeMode> </LookAt> </gx:FlyTo>
          <gx:FlyTo><gx:flyToMode>smooth</gx:flyToMode> <gx:duration>15</gx:duration> <LookAt>
          <gx:TimeStamp>  <when>  2006-07-30T22:00:01-06:00  </when> </gx:TimeStamp>
          <longitude>-106.330171327667</longitude> <latitude>39.23120737497095</latitude>
          <altitude>0</altitude> <range>3000.938259194934</range> <tilt>66.37891775060704</tilt>
          <heading>79.44553869458431</heading> <altitudeMode>relativeToGround</altitudeMode>
          <gx:altitudeMode>relativeToSeaFloor</gx:altitudeMode> </LookAt> </gx:FlyTo>
          <gx:FlyTo><gx:flyToMode>smooth</gx:flyToMode> <gx:duration>10</gx:duration> <LookAt>
          <gx:TimeStamp>  <when>  2006-07-31T00:00:01-06:00  </when> </gx:TimeStamp>
          <longitude>-106.334171327667</longitude> <latitude>39.23120737497095</latitude>
          <altitude>0</altitude> <range>4500.938259194934</range> <tilt>66.37891775060704</tilt>
          <heading>79.44553869458431</heading> <altitudeMode>relativeToGround</altitudeMode>
          <gx:altitudeMode>relativeToSeaFloor</gx:altitudeMode> </LookAt> </gx:FlyTo>
                        <gx:Wait> <gx:duration>5</gx:duration> </gx:Wait>
      </gx:Playlist>
    </gx:Tour>
    </Folder>
</Document>
</kml>
```

# APPENDIX C: LEADVILLE SITE VISIT

On June 15, 2010, a site visit was undertaken to Leadville, Colorado for the purposes of retrieving discharge data from the Leadville and Yak tunnel waste water treatment plants, meeting with Colorado Mountain College professor Kato Dee, and making general observations of the California Gulch watershed.

Photographs taken as part of the visit are shown in Section C.1. Data collected from the Leadville municipal waste treatment plant and the Yak tunnel mine drainage tunnel treatment plant are shown in Section C.2.

## C.1 Site Photographs


Figure C-1: Welcome to Leadville!

Figure C-2: Panorama of upper California Gulch looking east from Mineral Belt trail crossing.

Figure C-3: Culvert outlet below Mineral Belt trail crossing over California Gulch. The series of rock weirs above the lined channel are visible downstream. No flow observed upstream of this point indicating that groundwater may be a source of flow here and downstream.

Figure C-4: Beginning of lined channel above CG-1. A series of five rock weirs is visible upstream of the lined channel.

Figure C-5: View upstream from CG-1. California Gulch is a concrete-lined trapezoidal channel floor approximately 1.5 miles above the CG-1 gauge.

Figure C-6: CG-1 gauge in California Gulch. Flow from left to right. Tan colored container is auto-sampling unit.

Figure C-7: View looking downstream at double channel in California Gulch near Yak Tunnel Portal below CG-1 gauge. Flow from the Yak Tunnel is collected from the left channel and delivered to the treatment plant approximately one-half mile downstream. Any flow from upper California Gulch (there is none in this photo) bypasses the treatment plant via the channel at right. Defunct flume is obscured but the foot bridge shows that its location is just upstream of the Yak ditch.

Figure C-8: Defunct flume adjacent to CG-1 and above Yak ditch. Bridge in foreground crosses the outflow channel below the CG-1 pool.

Figure C-9: View down California Gulch below Yak Tunnel Portal. Channel transmits flow to Yak Water Treatment Plant. Right channel is the California Gulch drainage.

Figure C-10: View looking downstream at double channel in California Gulch near Yak Tunnel Portal below CG-1 gauge. Flow from the Yak Tunnel is collected from the left channel and delivered to the treatment plant approximately one-half mile downstream. Flow from the upper California Gulch (there is none in this photo) bypasses the treatment plant via the channel at right.

Figure C-11: Yak Tunnel Water Treatment Facility. California Gulch is in the foreground. Flow is carried from the tunnel portal via the pipeline on the far embankment.

Figure C-12: Yak Tunnel Water Treatment Plant reservoir. Flow in foreground is California Gulch with Yak Tunnel Treatment Plant discharge included.

Figure C-13: Photomosaic view of Yak Tunnel Treatment Pond (left) and Apache tailings impoundment (right). Flow from California Gulch is passed in a lined channel to bypass each of these features.

Figure C-14: View looking upstream (east) from County Road 6 bridge over California Gulch. Apache Tailings visible in middle background.

Figure C-15: View looking downstream (west) from County Road 6 bridge over California Gulch.

Figure C-16: View looking downstream (west) from County Road 6 bridge over California Gulch.

Figure C-17: Oregon Gulch looking upstream to the southeast at OG-1 gauge. The stream channel is dry.

Figure C-18: Oregon Gulch looking downstream to the northwest from OG-1 gauge. The stream channel is dry.

Figure C-19: View toward California Gulch in Oregon Gulch at OG-1 gauge looking downstream to the northwest. The stream channel is dry.

Figure C-20: View from tailings pile on left bank of California Gulch above CG-4 looking upstream. A sediment fence, apparently placed to protect the stream from tailings erosion, has been breached as the high flows have shifted the primary course of flow.

Figure C-21: View upstream from CG-4 gauge. White material is refuse.

Figure C-22: View from left bank of California Gulch looking upstream at CG-4 gauge.

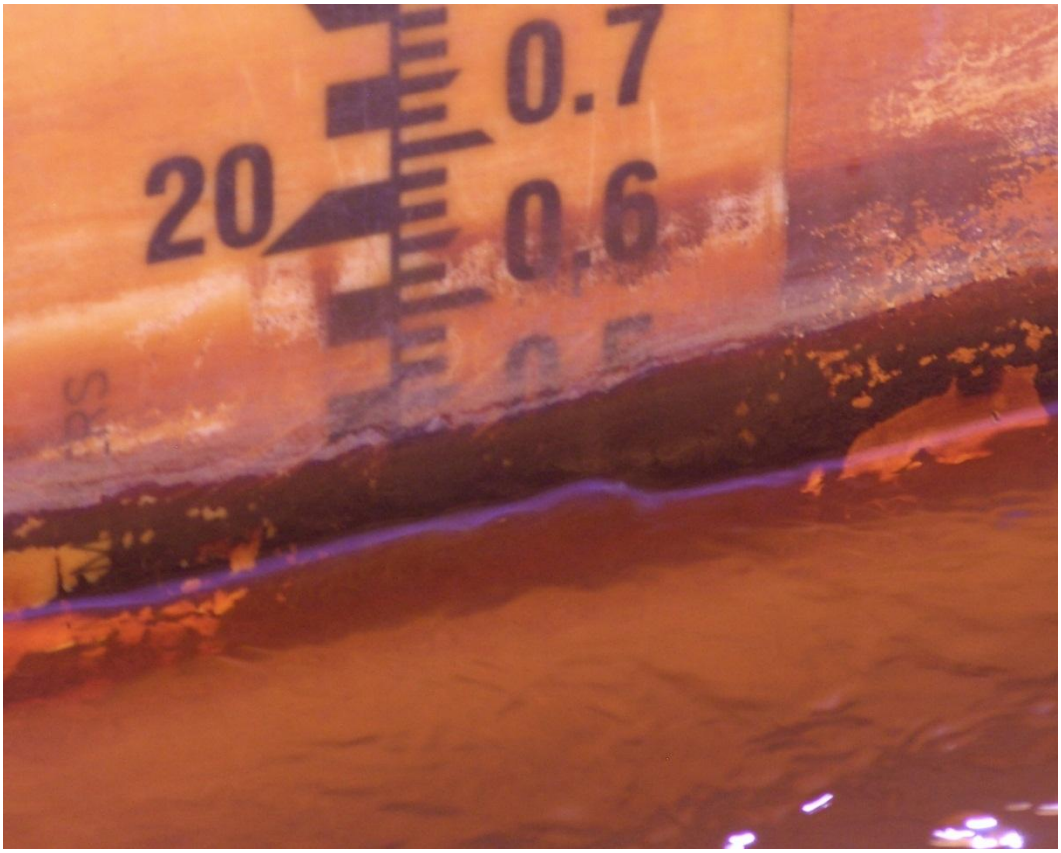


Figure C-23: Stage level indicator inside CG-4 gauge.

Figure C-24: View from left bank of California Gulch looking downstream beyond CG-4 gauge. Note high-flow notch in gauge weir.

Figure C-25: View from left bank of California Gulch looking downstream toward CG-4 gauge.

Figure C-26: Panoramic view looking across and upstream through California Gulch above CG-4 gauge.

Figure C-27: Panoramic view looking downstream (west) through California Gulch from above CG-4 gauge with Colorado Mountain College campus buildings at left; Mt. Elbert and Mt. Massive left and center, respectively, in background; the Arkansas River valley (flowing to the left); and, California Gulch.

Figure C-28: Flow in Channel above CG-5. Note secondary channel at the right of photograph with a lower base level, but no flow.

Figure C-29: California gulch and unnamed dry channel.

Figure C-30: California Gulch looking downstream to the west.

Figure C-31: California Gulch looking downstream to the west.

Figure C-32: View upstream from right bank at CG-5 flume.

Figure C-33: View of CG-5 flume outlet and data recording equipment.

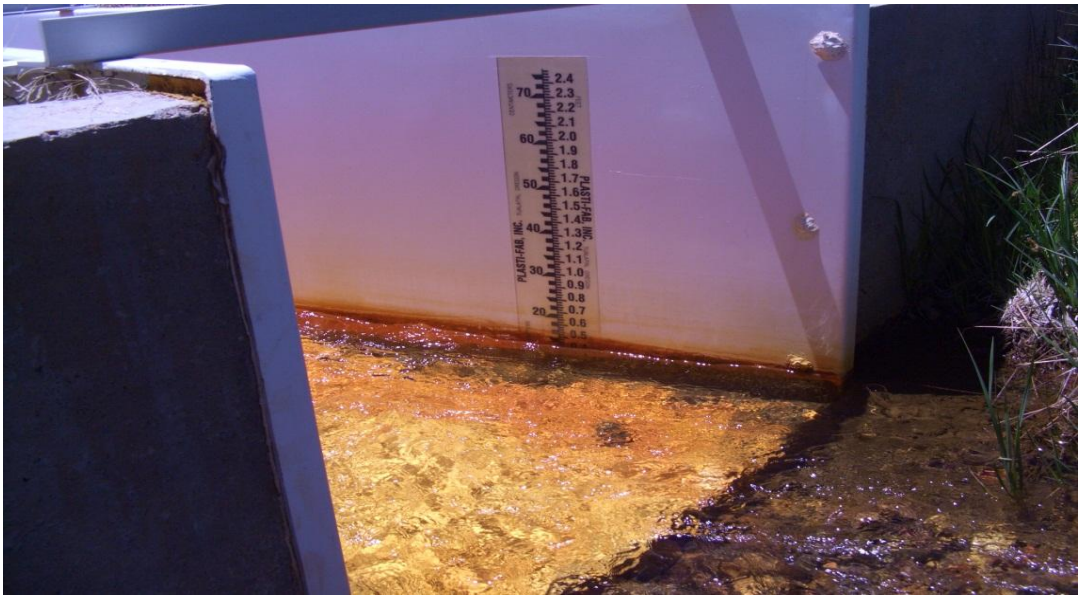


Figure C-34: Stage indicator at CG-5 flume.

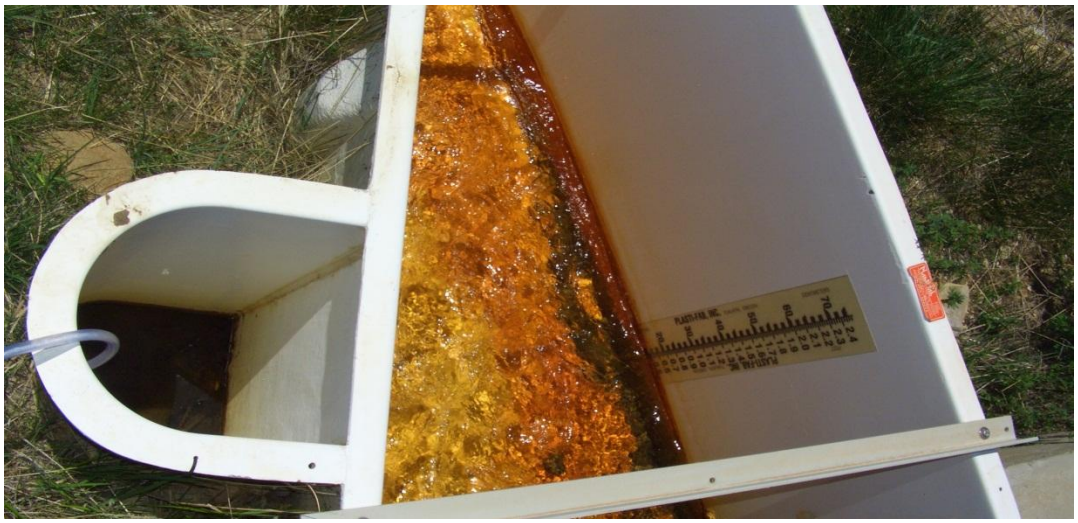

Figure C-35: Stage indicator and bubbler at CG-5 flume.

Figure C-36: CG-5 flume inlet and view downstream.

Figure C-37: Monitoring equipment on installed rip-rap on left bank with CG-5 flume.

Figure C-38: CG-5 flume and surroundings.

Figure C-39: View looking upstream (east) toward CG-5 through floodway channel.

Figure C-40: Photo mosaic view of floodway below CG-5 looking downstream (west).

Figure C-41: Looking upstream from US-24 bridge over California Gulch below CG-5.

Figure C-42: US-24 bridge over California Gulch.


Figure C-43: Entrance to Leadville Waste Water Treatment Plant (WWTP).

Figure C-44: Leadville WWTP final oxidation pond looking west toward Mt. Elbert (left) and Mt. Massive (right).

Figure C-45: Chlorination Building at outlet of oxidation pond. Chlorination is the last treatment step before water is discharged to California Gulch below CG-5.

Figure C-46: WWTP discharge culvert downstream of US-24 bridge. Pink flags are CDOT wetland delineation.

Figure C-47: WWTP discharge confluence (left) with California Gulch (right). Note algae in WWTP channel contrasting with abiotic CG channel.

Figure C-48: California Gulch channel below WWTP confluence.

Figure C-49: California Gulch channel below WWTP confluence.

Figure C-50: California Gulch channel below WWTP confluence. Floodway is visible to left and right. Pink flags are CDOT wetland delineation.

Figure C-51: Photomosaic view looking north into Malta Gulch.

Figure C-52: County Road 5 crossing of California Gulch looking upstream (northeast).

Figure C-53: County Road 5 crossing of California Gulch looking downstream (southwest).

Figure C-54: CG-6 flume.

Figure C-55: CG-6 looking downstream toward confluence with Arkansas River.

Figure C-56: View of California Gulch Channel with CG-6 gauge shack in center. Flow is from left to right to confluence with Arkansas River on right.

Figure C-57: AR-3A looking upstream.

Figure C-58: AR-3A gauge station looking downstream past gauge.

Figure C-59: Panorama of Arkansas River at AR-3A gauge. Flow is from right to left.

Figure C-60: Arkansas River at County Road 4. View of culvert inlets from right looking southwest.

Figure C-61: County Road 4 bridge over Arkansas River, looking upstream (north).

Figure C-62: County Road 4 bridge over Arkansas River, looking downstream (south).

Figure C-63: Arkansas River at County Road 4. View of culvert outlets from left bank looking northwest.

Figure C-64: Arkansas River at County Road 4. Close-up view of east culvert outlet.

Figure C-65: Starr Ditch crossing at 3rd Street. There is no flow in the channel—drainage flows away from the observation position toward California Gulch to the south.

Figure C-66: Stray Horse Gulch looking downstream. Flow from Stray Horse Gulch is intercepted by the Starr Ditch and conveyed south (left) along the eastern edge of Leadville to California Gulch.


Figure C-67: Stray Horse Gulch looking upstream. Note landmark at left—The Matchless Mine.

Figure C-68: Bureau of Reclamation meteorological station at Sugarloaf Dam.


Figure C-69: View from Colorado Mountain College looking north. California Gulch runs right to left at the base of the hill.

Figure C-70: View from Colorado Mountain College looking north over California Gulch into Leadville and beyond into Evans Gulch and Arkansas Valley River.

## C.2 LEADVILLE WASTEWATER TREATMENT PLANT DISCHARGE

### *C.2.1 2006 Daily Total Volumes*

The following tables are reproductions of the Leadville waste water treatment plant record of daily total output for 2006. The flows reported for July–August 2006 were used to create the time series inputs for external point sources for the simulation.

**Leadville Sanitation District**

**Effluent Flow Report**

Report Date : 01/31/2006

| Date | Flow |
|---|---|
| 01/01/2006 | 328580 |
| 01/02/2006 | 414590 |
| 01/03/2006 | 356760 |
| 01/04/2006 | 344200 |
| 01/05/2006 | 354160 |
| 01/06/2006 | 328530 |
| 01/07/2006 | 326610 |
| 01/08/2006 | 309090 |
| 01/09/2006 | 341470 |
| 01/10/2006 | 336450 |
| 01/11/2006 | 320130 |
| 01/12/2006 | 299730 |
| 01/13/2006 | 361070 |
| 01/14/2006 | 312620 |
| 01/15/2006 | 323800 |
| 01/16/2006 | 324230 |
| 01/17/2006 | 317220 |
| 01/18/2006 | 330640 |
| 01/19/2006 | 348600 |
| 01/20/2006 | 364080 |
| 01/21/2006 | 337060 |
| 01/22/2006 | 333640 |
| 01/23/2006 | 340970 |
| 01/24/2006 | 352230 |
| 01/25/2006 | 348100 |
| 01/26/2006 | 347880 |
| 01/27/2006 | 349700 |
| 01/28/2006 | 310410 |
| 01/29/2006 | 335190 |
| 01/30/2006 | 349790 |
| 01/31/2006 | 350240 |
| Total Flow : | 10497770.00 |
| Average Flow : | 338637.74 |
| Maximum Flow : | 414590.00 |
| Minimum Flow : | 299730.00 |

## Leadville Sanitation District

### Effluent Flow Report

Report Date : 03/01/2006

| Date | Flow |
|---|---|
| 02/01/2006 | 343880 |
| 02/02/2006 | 348200 |
| 02/03/2006 | 340080 |
| 02/04/2006 | 363560 |
| 02/05/2006 | 382380 |
| 02/06/2006 | 353190 |
| 02/07/2006 | 360370 |
| 02/08/2006 | 334330 |
| 02/09/2006 | 290320 |
| 02/10/2006 | 367040 |
| 02/11/2006 | 355380 |
| 02/12/2006 | 346930 |
| 02/13/2006 | 358020 |
| 02/14/2006 | 365800 |
| 02/15/2006 | 371200 |
| 02/16/2006 | 324760 |
| 02/17/2006 | 349540 |
| 02/18/2006 | 353200 |
| 02/19/2006 | 230210 |
| 02/20/2006 | 454880 |
| 02/21/2006 | 375990 |
| 02/22/2006 | 355560 |
| 02/23/2006 | 353580 |
| 02/24/2006 | 355750 |
| 02/25/2006 | 363810 |
| 02/26/2006 | 349480 |
| 02/27/2006 | 381920 |
| 02/28/2006 | 387840 |
| Total Flow : | 9917200.00 |
| Average Flow : | 354185.71 |
| Maximum Flow : | 454880.00 |
| Minimum Flow : | 230210.00 |

## Leadville Sanitation District

### Effluent Flow Report

Report Date : 03/31/2006

| Date | Flow |
|---|---|
| 03/01/2006 | 383810 |
| 03/02/2006 | 385330 |
| 03/03/2006 | 381490 |
| 03/04/2006 | 370430 |
| 03/05/2006 | 353980 |
| 03/06/2006 | 381290 |
| 03/07/2006 | 368280 |
| 03/08/2006 | 341590 |
| 03/09/2006 | 358550 |
| 03/10/2006 | 345020 |
| 03/11/2006 | 349140 |
| 03/12/2006 | 347880 |
| 03/13/2006 | 362910 |
| 03/14/2006 | 377710 |
| 03/15/2006 | 345000 |
| 03/16/2006 | 360460 |
| 03/17/2006 | 344220 |
| 03/18/2006 | 295740 |
| 03/19/2006 | 313260 |
| 03/20/2006 | 368110 |
| 03/21/2006 | 381770 |
| 03/22/2006 | 365560 |
| 03/23/2006 | 341320 |
| 03/24/2006 | 343750 |
| 03/25/2006 | 348340 |
| 03/26/2006 | 347460 |
| 03/27/2006 | 225980 |
| 03/28/2006 | 479720 |
| 03/29/2006 | 402690 |
| 03/30/2006 | 349050 |
| 03/31/2006 | 375310 |
| Total Flow : | 11095150.00 |
| Average Flow : | 357908.06 |
| Maximum Flow : | 479720.00 |
| Minimum Flow : | 225980.00 |

## Leadville Sanitation District

### Effluent Flow Report

Report Date : 05/01/2006

| Date | Flow |
|---|---|
| 04/01/2006 | 380860 |
| 04/02/2006 | 363100 |
| 04/03/2006 | 341350 |
| 04/04/2006 | 131180 |
| 04/05/2006 | 552610 |
| 04/06/2006 | 435180 |
| 04/07/2006 | 433810 |
| 04/08/2006 | 411530 |
| 04/09/2006 | 367390 |
| 04/10/2006 | 379870 |
| 04/11/2006 | 372770 |
| 04/12/2006 | 447030 |
| 04/13/2006 | 231200 |
| 04/14/2006 | 171020 |
| 04/15/2006 | 305900 |
| 04/16/2006 | 430980 |
| 04/17/2006 | 660870 |
| 04/18/2006 | 529750 |
| 04/19/2006 | 537190 |
| 04/20/2006 | 514060 |
| 04/21/2006 | 437940 |
| 04/22/2006 | 351910 |
| 04/23/2006 | 469440 |
| 04/24/2006 | 363150 |
| 04/25/2006 | 404930 |
| 04/26/2006 | 388230 |
| 04/27/2006 | 494140 |
| 04/28/2006 | 345170 |
| 04/29/2006 | 506460 |
| 04/30/2006 | 372410 |
| Total Flow : | 12131430.00 |
| Average Flow : | 404381.00 |
| Maximum Flow : | 660870.00 |
| Minimum Flow : | 131180.00 |

## Leadville Sanitation District

### Effluent Flow Report

Report Date : 05/31/2006

| Date | Flow |
|---|---|
| 05/01/2006 | 554030 |
| 05/02/2006 | 345120 |
| 05/03/2006 | 361670 |
| 05/04/2006 | 447150 |
| 05/05/2006 | 427310 |
| 05/06/2006 | 413100 |
| 05/07/2006 | 278540 |
| 05/08/2006 | 407640 |
| 05/09/2006 | 389130 |
| 05/10/2006 | 513650 |
| 05/11/2006 | 412240 |
| 05/12/2006 | 328060 |
| 05/13/2006 | 395400 |
| 05/14/2006 | 331990 |
| 05/15/2006 | 429600 |
| 05/16/2006 | 457330 |
| 05/17/2006 | 336150 |
| 05/18/2006 | 413830 |
| 05/19/2006 | 359440 |
| 05/20/2006 | 308660 |
| 05/21/2006 | 310600 |
| 05/22/2006 | 449510 |
| 05/23/2006 | 409060 |
| 05/24/2006 | 507690 |
| 05/25/2006 | 395840 |
| 05/26/2006 | 388720 |
| 05/27/2006 | 388440 |
| 05/28/2006 | 216640 |
| 05/29/2006 | 261210 |
| 05/30/2006 | 373900 |
| 05/31/2006 | 382820 |
| Total Flow : | 11994470.00 |
| Average Flow : | 386918.39 |
| Maximum Flow : | 554030.00 |
| Minimum Flow : | 216640.00 |

## Leadville Sanitation District

### Effluent Flow Report

**Report Date : 07/05/2006**

| Date | Flow |
|---|---|
| 06/01/2006 | 396350 |
| 06/02/2006 | 373700 |
| 06/03/2006 | 208430 |
| 06/04/2006 | 483760 |
| 06/05/2006 | 395960 |
| 06/06/2006 | 419200 |
| 06/07/2006 | 345570 |
| 06/08/2006 | 420060 |
| 06/09/2006 | 379010 |
| 06/10/2006 | 390190 |
| 06/11/2006 | 349810 |
| 06/12/2006 | 328810 |
| 06/13/2006 | 273290 |
| 06/14/2006 | 308930 |
| 06/15/2006 | 419010 |
| 06/16/2006 | 315480 |
| 06/17/2006 | 317500 |
| 06/18/2006 | 203720 |
| 06/19/2006 | 374260 |
| 06/20/2006 | 320440 |
| 06/21/2006 | 281500 |
| 06/22/2006 | 156380 |
| 06/23/2006 | 531700 |
| 06/24/2006 | 242390 |
| 06/25/2006 | 311680 |
| 06/26/2006 | 346330 |
| 06/27/2006 | 423890 |
| 06/28/2006 | 360040 |
| 06/29/2006 | 370830 |
| 06/30/2006 | 305270 |
| Total Flow : | 10353490.00 |
| Average Flow : | 345116.33 |
| Maximum Flow : | 531700.00 |
| Minimum Flow : | 156380.00 |

## Leadville Sanitation District

### Effluent Flow Report

Report Date : 08/02/2006

| Date | Flow |
|---|---|
| 07/01/2006 | 330170 |
| 07/02/2006 | 344820 |
| 07/03/2006 | 339670 |
| 07/04/2006 | 243140 |
| 07/05/2006 | 461510 |
| 07/06/2006 | 446700 |
| 07/07/2006 | 396078 |
| 07/08/2006 | 296272 |
| 07/09/2006 | 446730 |
| 07/10/2006 | 421150 |
| 07/11/2006 | 376150 |
| 07/12/2006 | 342430 |
| 07/13/2006 | 335650 |
| 07/14/2006 | 325270 |
| 07/15/2006 | 360570 |
| 07/16/2006 | 345960 |
| 07/17/2006 | 352710 |
| 07/18/2006 | 353000 |
| 07/19/2006 | 395900 |
| 07/20/2006 | 395510 |
| 07/21/2006 | 387640 |
| 07/22/2006 | 394150 |
| 07/23/2006 | 371370 |
| 07/24/2006 | 371430 |
| 07/25/2006 | 312620 |
| 07/26/2006 | 406730 |
| 07/27/2006 | 430000 |
| 07/28/2006 | 346930 |
| 07/29/2006 | 338330 |
| 07/30/2006 | 387260 |
| 07/31/2006 | 387960 |
| Total Flow : | 11443810.00 |
| Average Flow : | 369155.16 |
| Maximum Flow : | 461510.00 |
| Minimum Flow : | 243140.00 |

## Leadville Sanitation District

### Effluent Flow Report

Report Date : 08/31/2006

| Date | Flow |
|---|---|
| 08/01/2006 | 406010 |
| 08/02/2006 | 369450 |
| 08/03/2006 | 367280 |
| 08/04/2006 | 345520 |
| 08/05/2006 | 362410 |
| 08/06/2006 | 433790 |
| 08/07/2006 | 390540 |
| 08/08/2006 | 413970 |
| 08/09/2006 | 400030 |
| 08/10/2006 | 370180 |
| 08/11/2006 | 369820 |
| 08/12/2006 | 335180 |
| 08/13/2006 | 371050 |
| 08/14/2006 | 395440 |
| 08/15/2006 | 420400 |
| 08/16/2006 | 352640 |
| 08/17/2006 | 323360 |
| 08/18/2006 | 325570 |
| 08/19/2006 | 357890 |
| 08/20/2006 | 418980 |
| 08/21/2006 | 356080 |
| 08/22/2006 | 355960 |
| 08/23/2006 | 378590 |
| 08/24/2006 | 363030 |
| 08/25/2006 | 326340 |
| 08/26/2006 | 346330 |
| 08/27/2006 | 392100 |
| 08/28/2006 | 346730 |
| 08/29/2006 | 315490 |
| 08/30/2006 | 230590 |
| 08/31/2006 | 356770 |
| Total Flow : | 11297520.00 |
| Average Flow : | 364436.13 |
| Maximum Flow : | 433790.00 |
| Minimum Flow : | 230590.00 |

## Leadville Sanitation District

### Effluent Flow Report

Report Date : 10/02/2006

| Date | Flow |
|---|---|
| 09/01/2006 | 340090 |
| 09/02/2006 | 332590 |
| 09/03/2006 | 291730 |
| 09/04/2006 | 367560 |
| 09/05/2006 | 332530 |
| 09/06/2006 | 328150 |
| 09/07/2006 | 302960 |
| 09/08/2006 | 352680 |
| 09/09/2006 | 373400 |
| 09/10/2006 | 338060 |
| 09/11/2006 | 343830 |
| 09/12/2006 | 315310 |
| 09/13/2006 | 326740 |
| 09/14/2006 | 280200 |
| 09/15/2006 | 341890 |
| 09/16/2006 | 337750 |
| 09/17/2006 | 304530 |
| 09/18/2006 | 295790 |
| 09/19/2006 | 307330 |
| 09/20/2006 | 308690 |
| 09/21/2006 | 353530 |
| 09/22/2006 | 406090 |
| 09/23/2006 | 411730 |
| 09/24/2006 | 350110 |
| 09/25/2006 | 280590 |
| 09/26/2006 | 298600 |
| 09/27/2006 | 414840 |
| 09/28/2006 | 352100 |
| 09/29/2006 | 378350 |
| 09/30/2006 | 303420 |
| Total Flow : | 10071170.00 |
| Average Flow : | 335705.67 |
| Maximum Flow : | 414840.00 |
| Minimum Flow : | 280200.00 |

## Leadville Sanitation District

### Effluent Flow Report

Report Date : 10/31/2006

| Date | Flow |
|---|---|
| 10/01/2006 | 317150 |
| 10/02/2006 | 279120 |
| 10/03/2006 | 317240 |
| 10/04/2006 | 381090 |
| 10/05/2006 | 374110 |
| 10/06/2006 | 261460 |
| 10/07/2006 | 365950 |
| 10/08/2006 | 298650 |
| 10/09/2006 | 382640 |
| 10/10/2006 | 223900 |
| 10/11/2006 | 409020 |
| 10/12/2006 | 342080 |
| 10/13/2006 | 307330 |
| 10/14/2006 | 326350 |
| 10/15/2006 | 354280 |
| 10/16/2006 | 265680 |
| 10/17/2006 | 397480 |
| 10/18/2006 | 307630 |
| 10/19/2006 | 364560 |
| 10/20/2006 | 272990 |
| 10/21/2006 | 349990 |
| 10/22/2006 | 249880 |
| 10/23/2006 | 346950 |
| 10/24/2006 | 325800 |
| 10/25/2006 | 297730 |
| 10/26/2006 | 374910 |
| 10/27/2006 | 376700 |
| 10/28/2006 | 325600 |
| 10/29/2006 | 329910 |
| 10/30/2006 | 305190 |
| 10/31/2006 | 297960 |

| | |
|---|---|
| Total Flow : | 10129330.00 |
| Average Flow : | 326752.58 |
| Maximum Flow : | 409020.00 |
| Minimum Flow : | 223900.00 |

## Leadville Sanitation District

### Effluent Flow Report

Report Date : 11/30/2006

| Date | Flow |
|---|---|
| 11/01/2006 | 330800 |
| 11/02/2006 | 326290 |
| 11/03/2006 | 335960 |
| 11/04/2006 | 319760 |
| 11/05/2006 | 280700 |
| 11/06/2006 | 283070 |
| 11/07/2006 | 344480 |
| 11/08/2006 | 309180 |
| 11/09/2006 | 290360 |
| 11/10/2006 | 337540 |
| 11/11/2006 | 294810 |
| 11/12/2006 | 420960 |
| 11/13/2006 | 292770 |
| 11/14/2006 | 495870 |
| 11/15/2006 | 420720 |
| 11/16/2006 | 348510 |
| 11/17/2006 | 327470 |
| 11/18/2006 | 317590 |
| 11/19/2006 | 305890 |
| 11/20/2006 | 305360 |
| 11/21/2006 | 328610 |
| 11/22/2006 | 322970 |
| 11/23/2006 | 318790 |
| 11/24/2006 | 314630 |
| 11/25/2006 | 317250 |
| 11/26/2006 | 322770 |
| 11/27/2006 | 321190 |
| 11/28/2006 | 342500 |
| 11/29/2006 | 367600 |
| 11/30/2006 | 327490 |
| **Total Flow :** | 9971890.00 |
| **Average Flow :** | 332396.33 |
| **Maximum Flow :** | 495870.00 |
| **Minimum Flow :** | 280700.00 |

## Leadville Sanitation District

### Effluent Flow Report

Report Date : 01/02/2007

| Date | Flow |
|---|---|
| 12/01/2006 | 321490 |
| 12/02/2006 | 332450 |
| 12/03/2006 | 324840 |
| 12/04/2006 | 337320 |
| 12/05/2006 | 344160 |
| 12/06/2006 | 356200 |
| 12/07/2006 | 355690 |
| 12/08/2006 | 334840 |
| 12/09/2006 | 327560 |
| 12/10/2006 | 317600 |
| 12/11/2006 | 322660 |
| 12/12/2006 | 353000 |
| 12/13/2006 | 349620 |
| 12/14/2006 | 326120 |
| 12/15/2006 | 309070 |
| 12/16/2006 | 327750 |
| 12/17/2006 | 303700 |
| 12/18/2006 | 331640 |
| 12/19/2006 | 346350 |
| 12/20/2006 | 347520 |
| 12/21/2006 | 316480 |
| 12/22/2006 | 337380 |
| 12/23/2006 | 330370 |
| 12/24/2006 | 306370 |
| 12/25/2006 | 324760 |
| 12/26/2006 | 307150 |
| 12/27/2006 | 288530 |
| 12/28/2006 | 326590 |
| 12/29/2006 | 388020 |
| 12/30/2006 | 351320 |
| 12/31/2006 | 318950 |
| Total Flow : | 10265500.00 |
| Average Flow : | 331145.16 |
| Maximum Flow : | 388020.00 |
| Minimum Flow : | 288530.00 |

### *C.2.2 Typical Daily Variation*

The following circle plots are reproductions of the Leadville waste water treatment plant daily record for two weeks of flows from 1–7 July 2009 and 1–7 August 2009. These dates were selected as representative of the typical daily variation for the modeled period (July–August 2006). The actual plots for the 2006 period were not available.

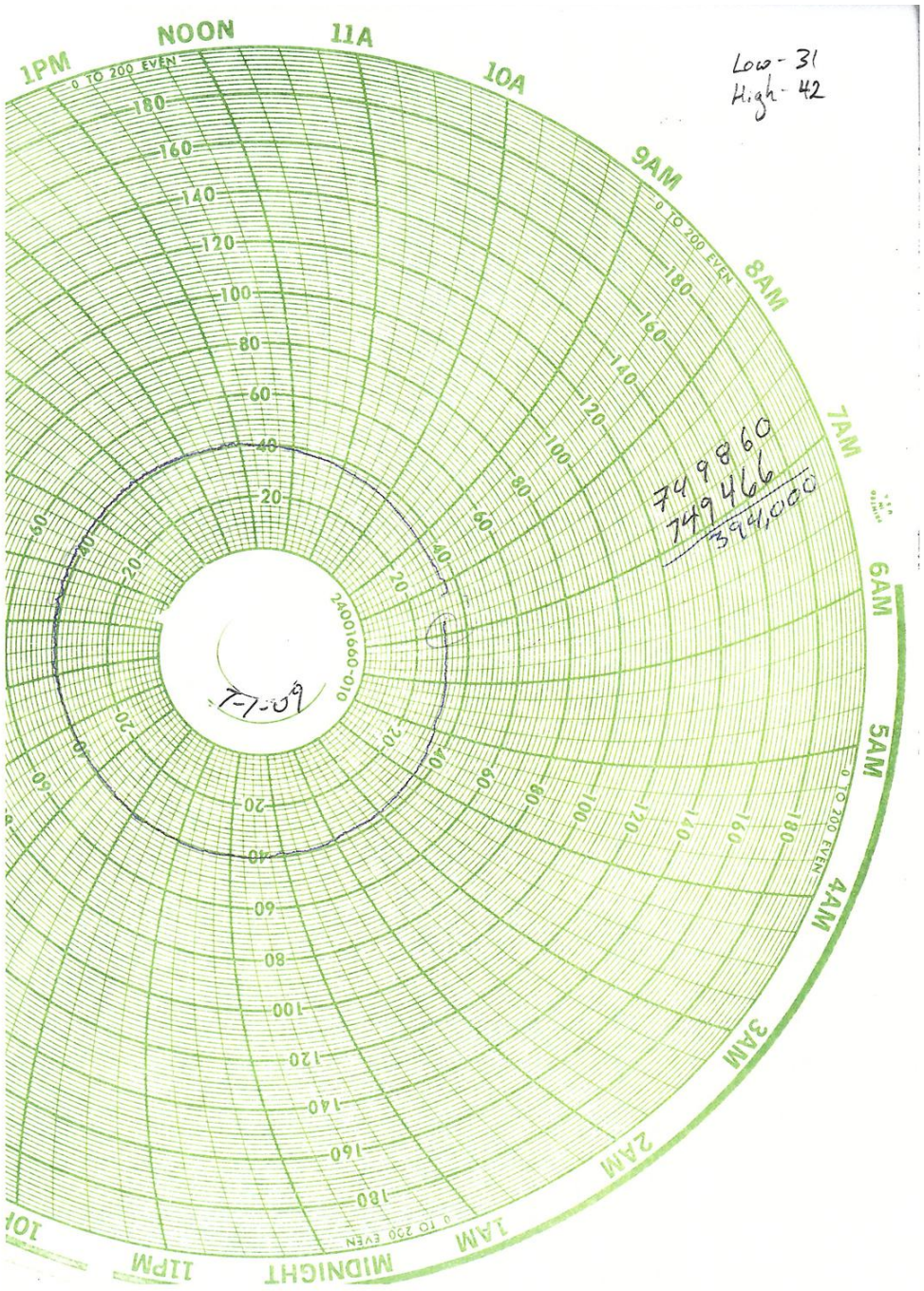

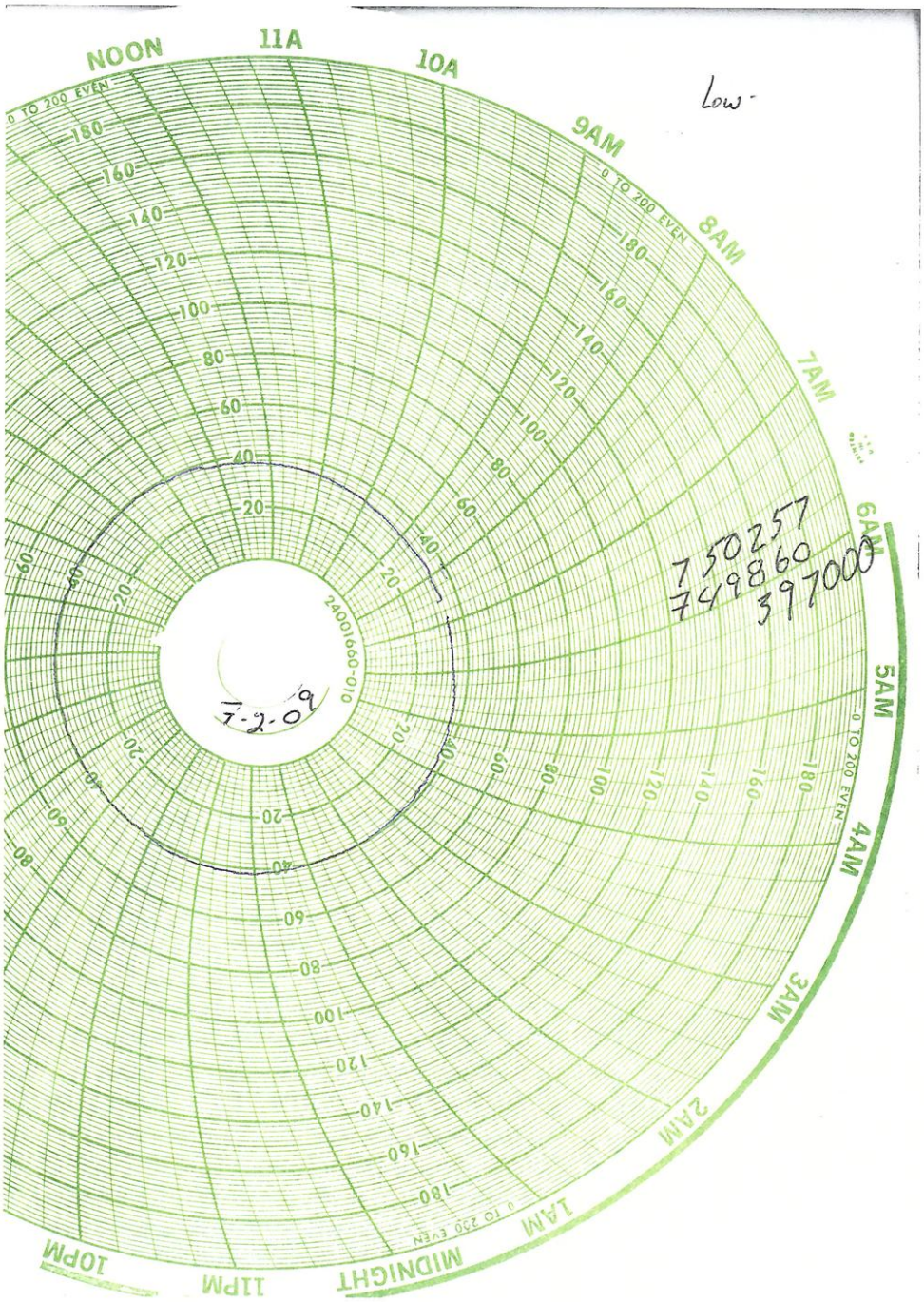
NOON
11A
10A
9AM
8AM
7AM
6AM
5AM
4AM
3AM
2AM
1AM
MIDNIGHT
11PM
10PM
0 TO 200 EVEN
0 TO 230 EVEN
Low-
7502577498603970008
7-2-09

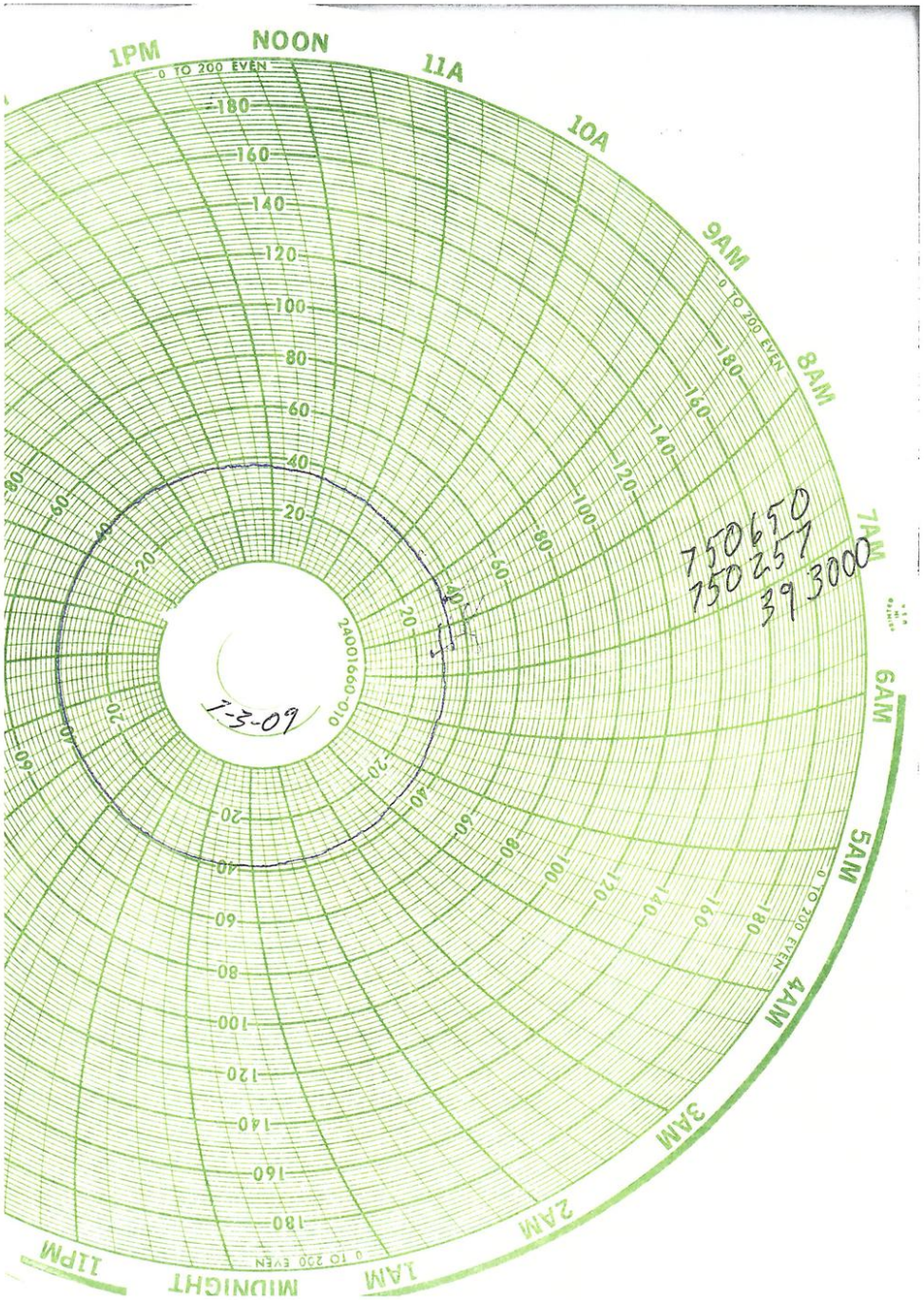
NOON
1PM
11A
10A
9AM
8AM
7AM
6AM
5AM
4AM
3AM
2AM
1AM
MIDNIGHT
11PM
0 TO 200 EVEN
1-3-09
750650
750257
393000

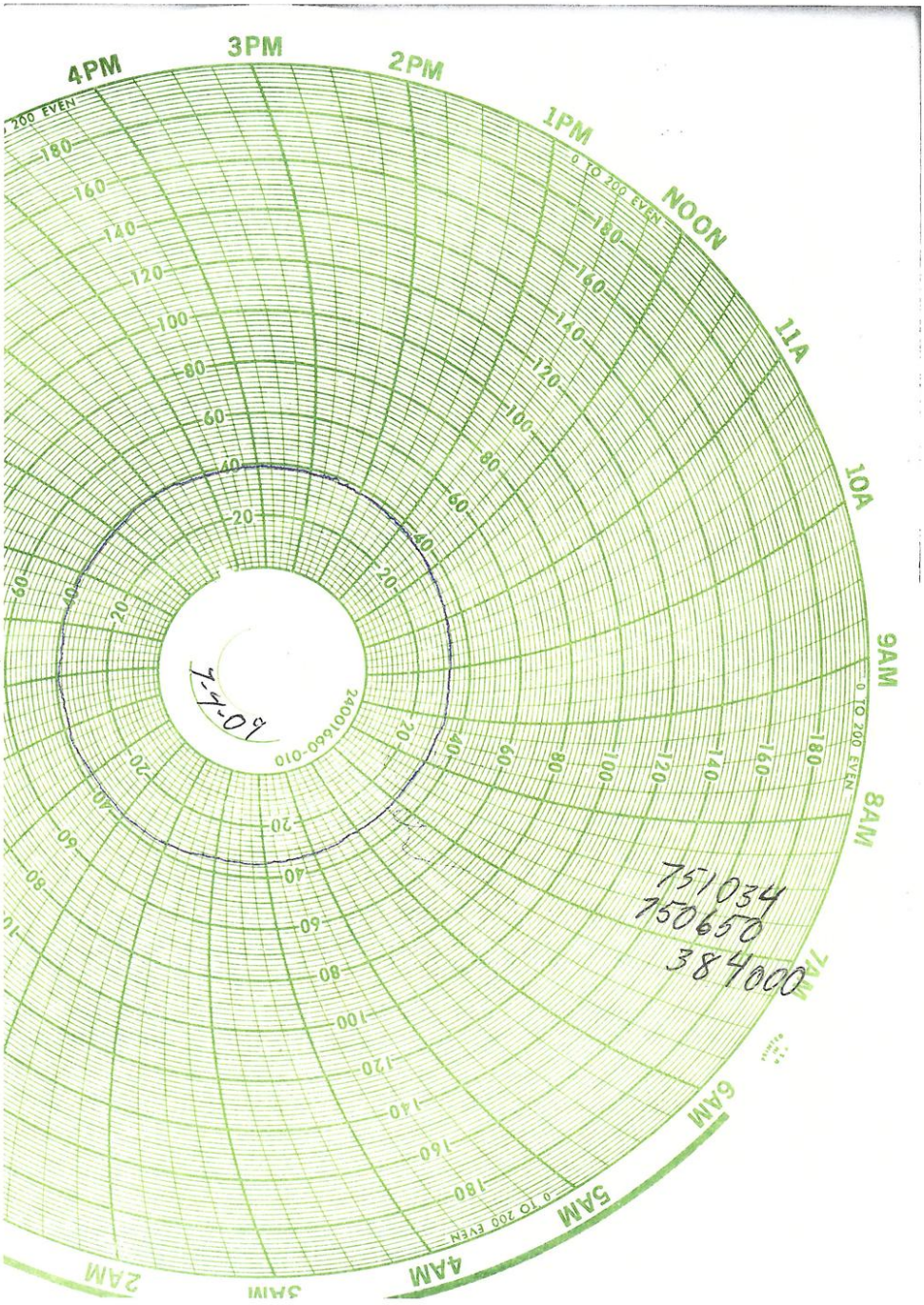
4PM
3PM
2PM
1PM
NOON
11A
10A
9AM
8AM
7AM
6AM
5AM
4AM
3AM
2AM
0 TO 200 EVEN
751034
750650
384000

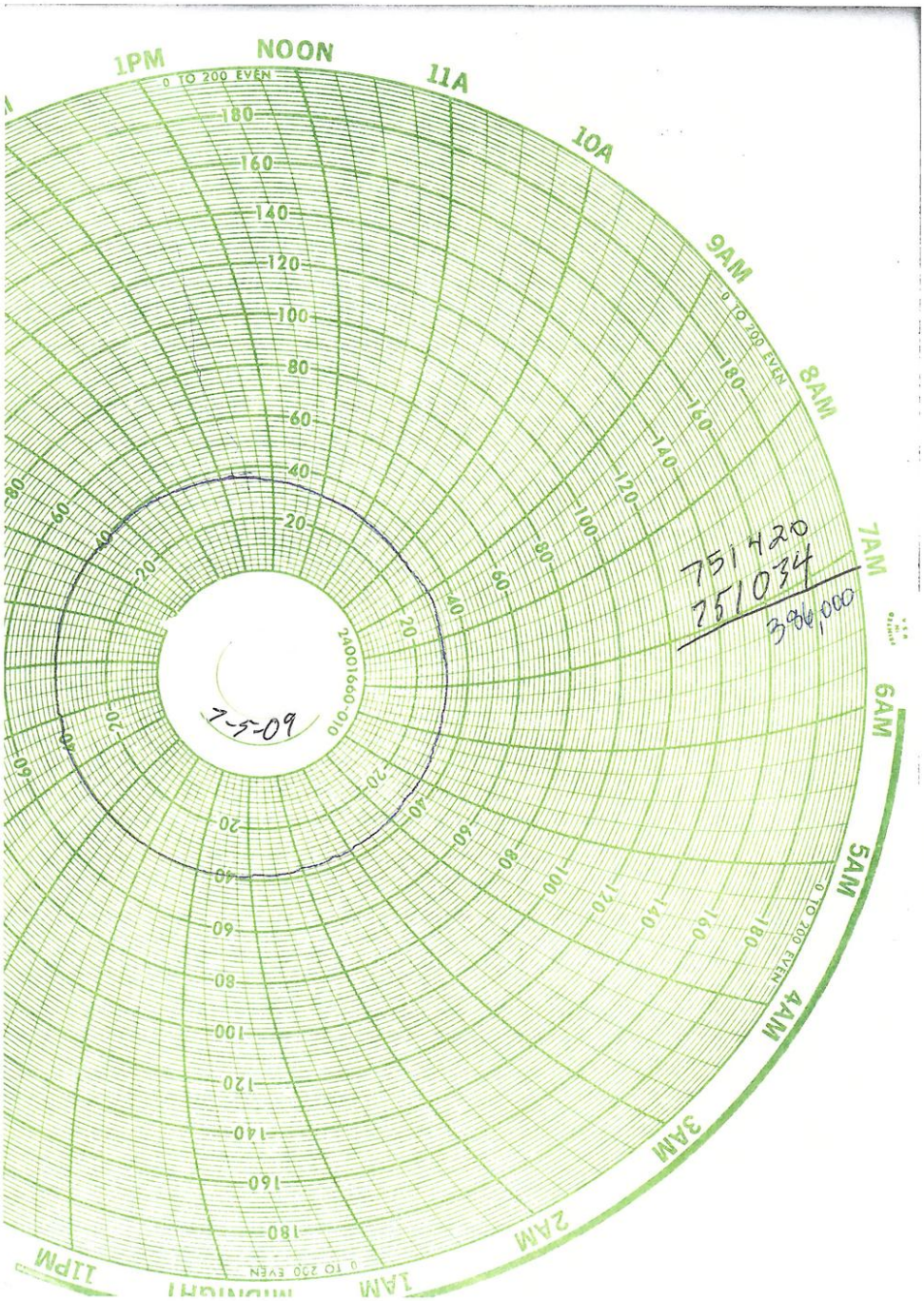
NOON
1PM
11A
10A
9AM
8AM
7AM
6AM
5AM
4AM
3AM
2AM
1AM
MIDNIGHT
11PM
0 TO 200 EVEN
751420
751034
396,000
7-5-09

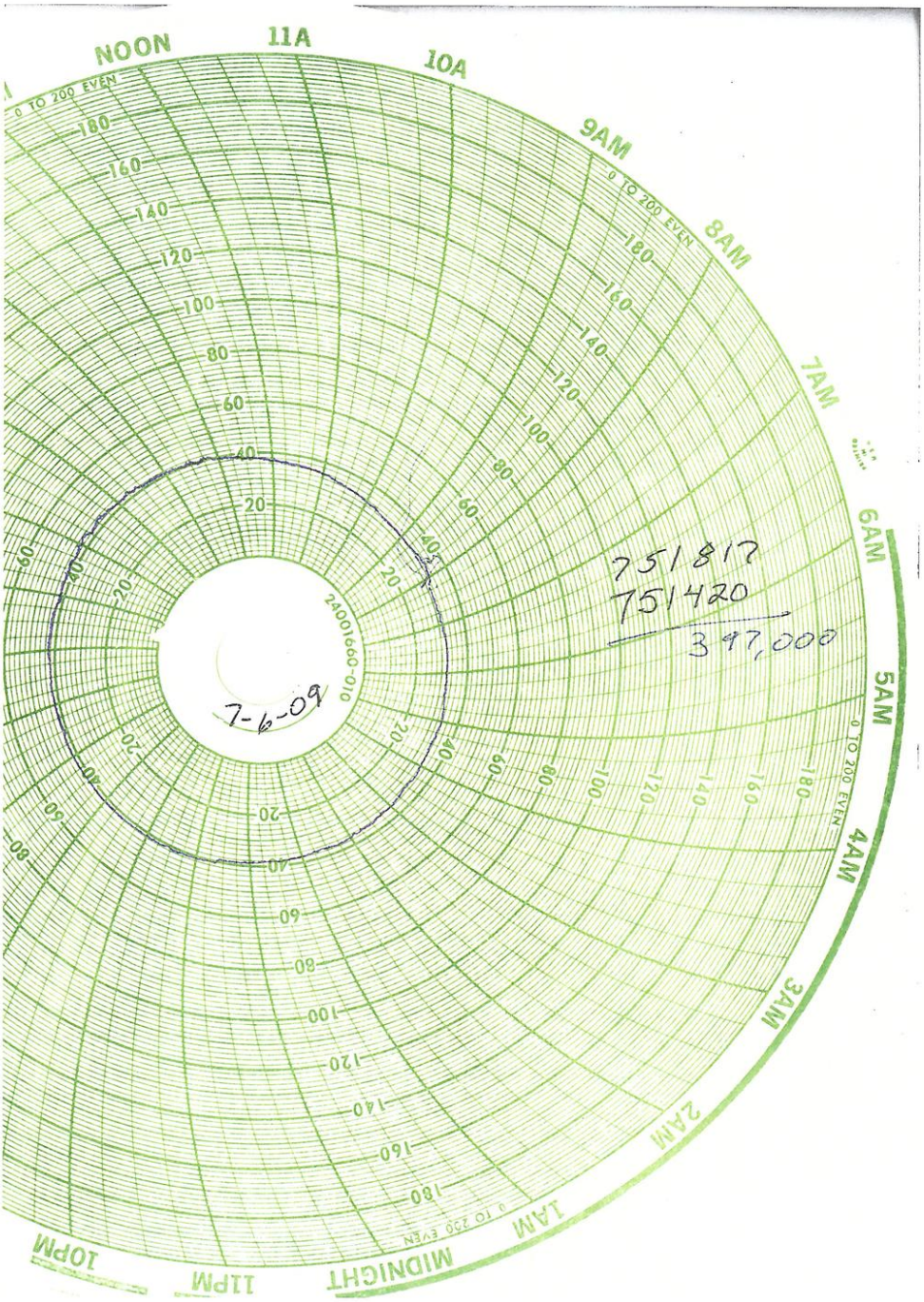
NOON
11A
10A
9AM
8AM
7AM
6AM
5AM
4AM
3AM
2AM
1AM
MIDNIGHT
11PM
10PM
751817
751420
347,000
7-6-09

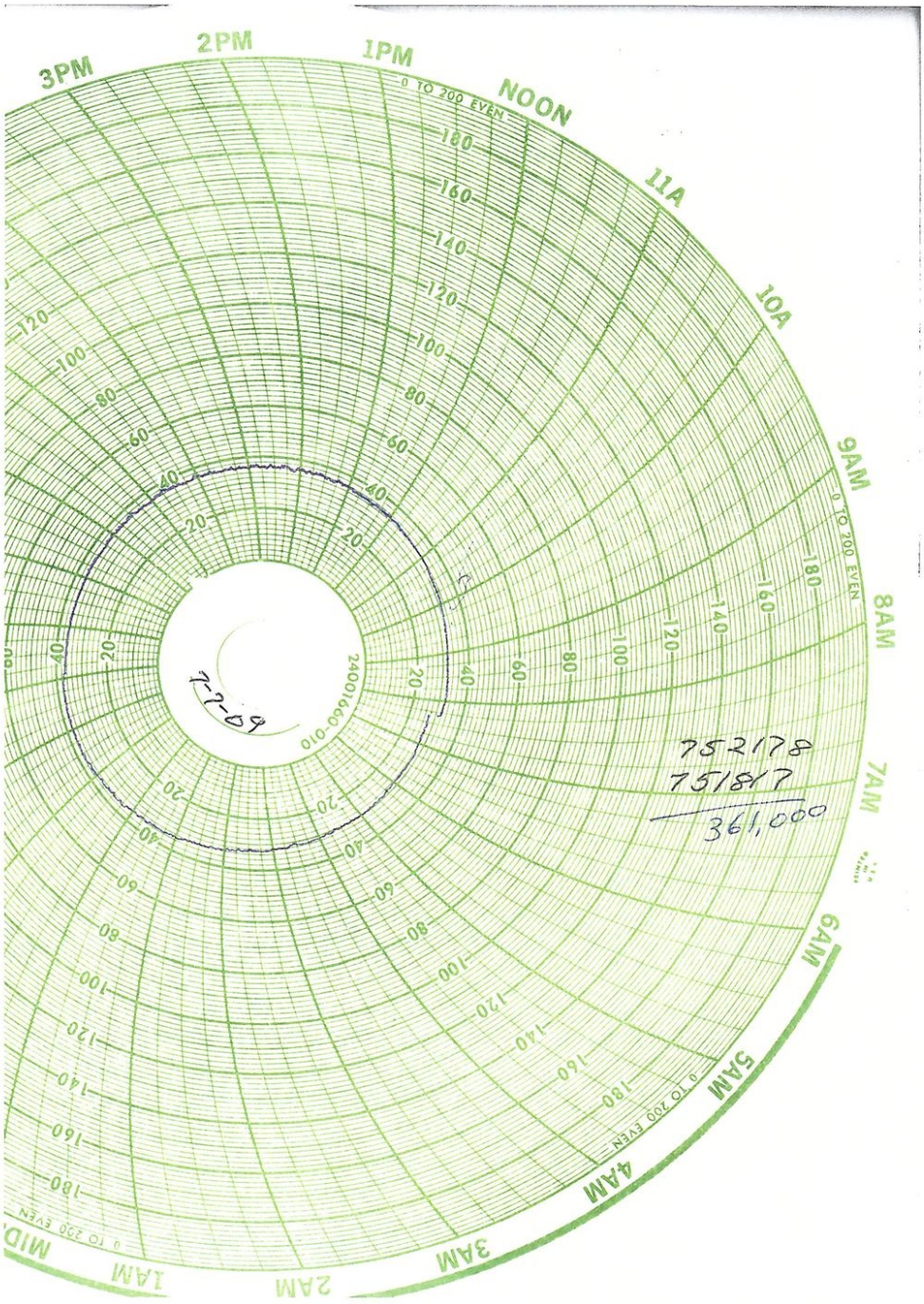
3PM
2PM
1PM
NOON
11A
10A
9AM
8AM
7AM
6AM
5AM
4AM
3AM
2AM
1AM
MID
0 TO 200 EVEN
7-7-09
752178
751817
361,000

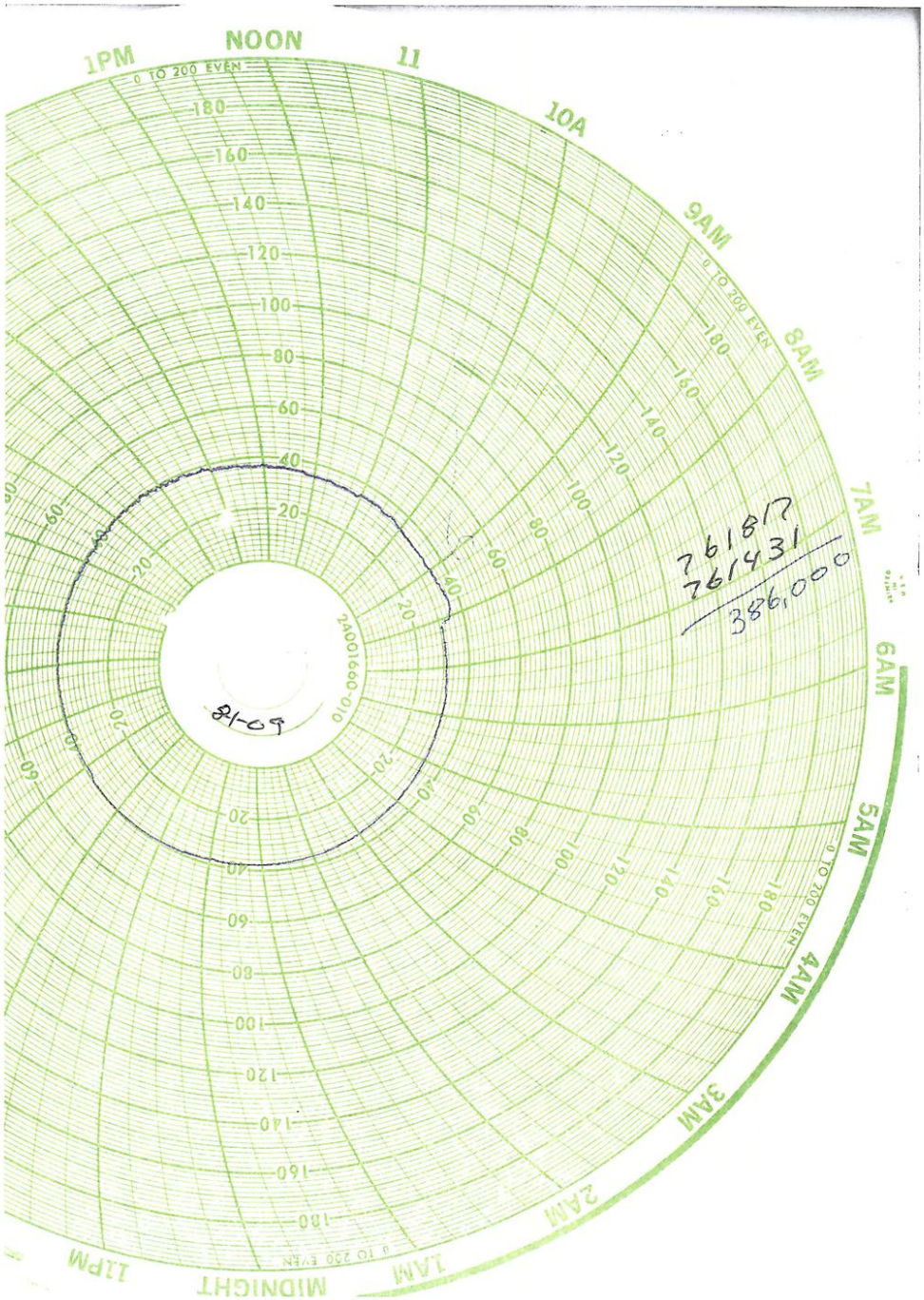
NOON
11
10A
9AM
8AM
7AM
6AM
5AM
4AM
3AM
2AM
1AM
MIDNIGHT
11PM
1PM
0 TO 200 EVEN
761817
761431
386,000

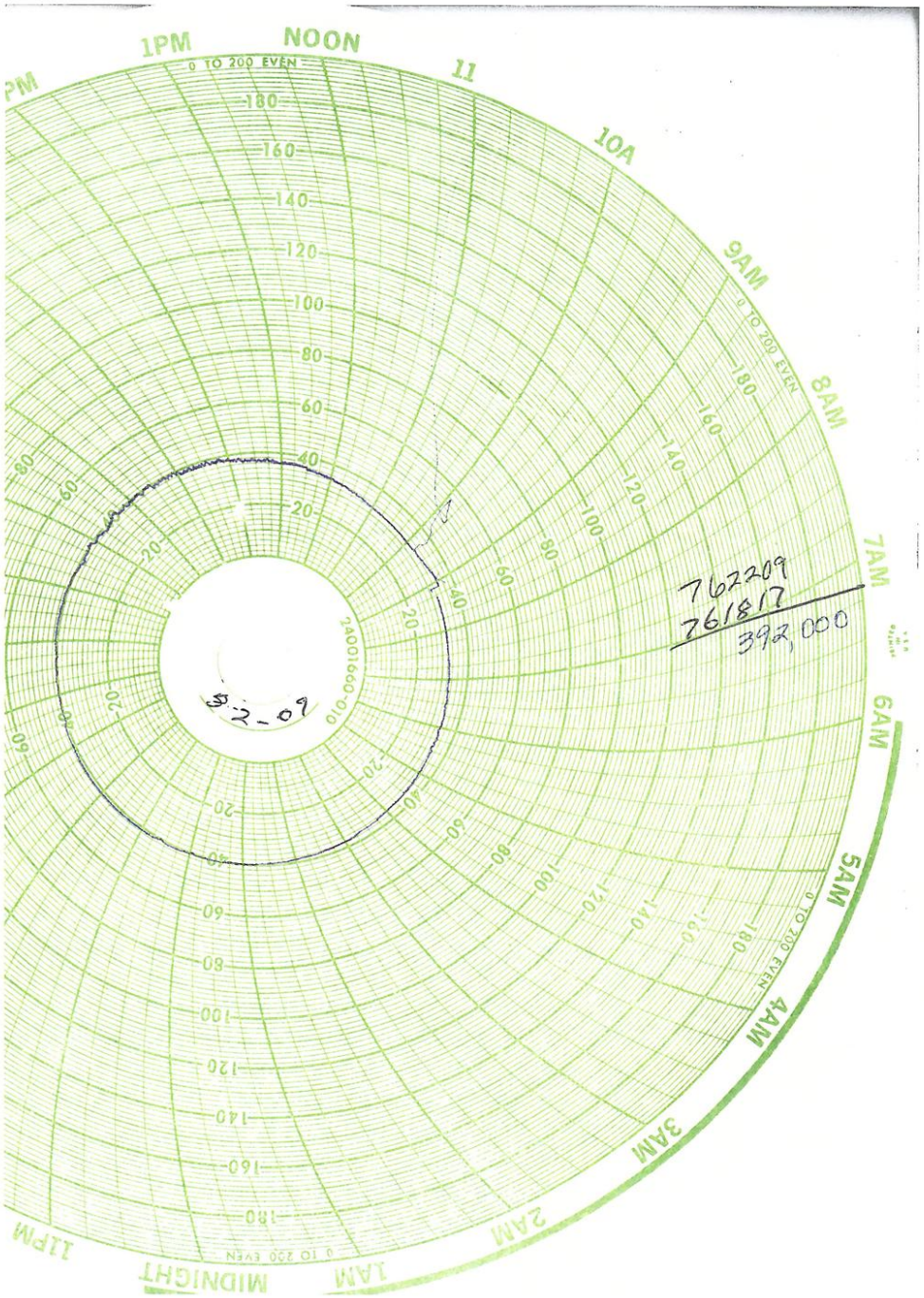
NOON
1PM
11
10A
9AM
8AM
7AM
6AM
5AM
4AM
3AM
2AM
1AM
MIDNIGHT
11PM
0 TO 200 EVEN
7602209
761817
392,000

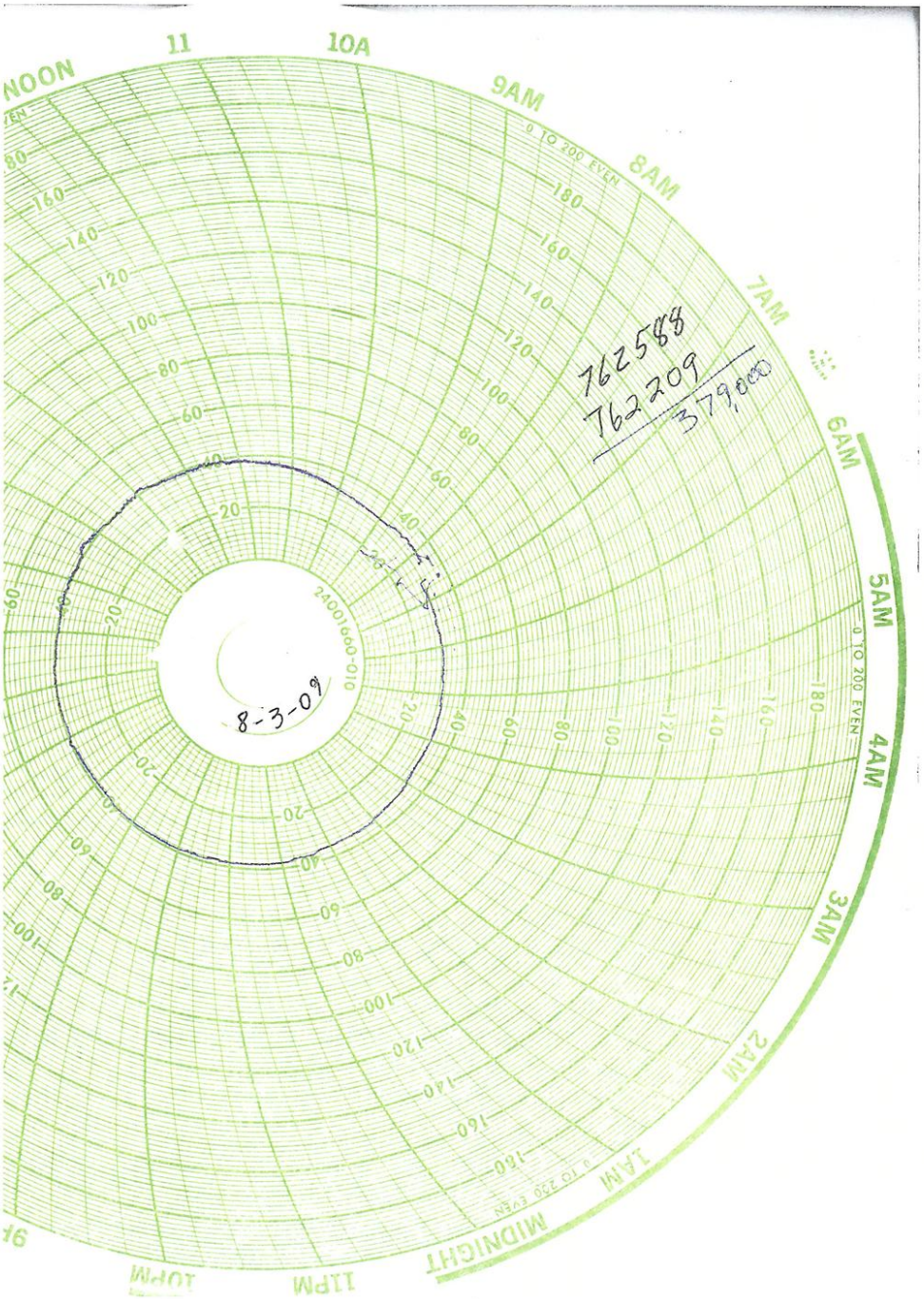
NOON
11
10A
9AM
8AM
7AM
6AM
5AM
4AM
3AM
2AM
1AM
MIDNIGHT
11PM
10PM
0 TO 200 EVEN
762588
762209
379000
8-3-09

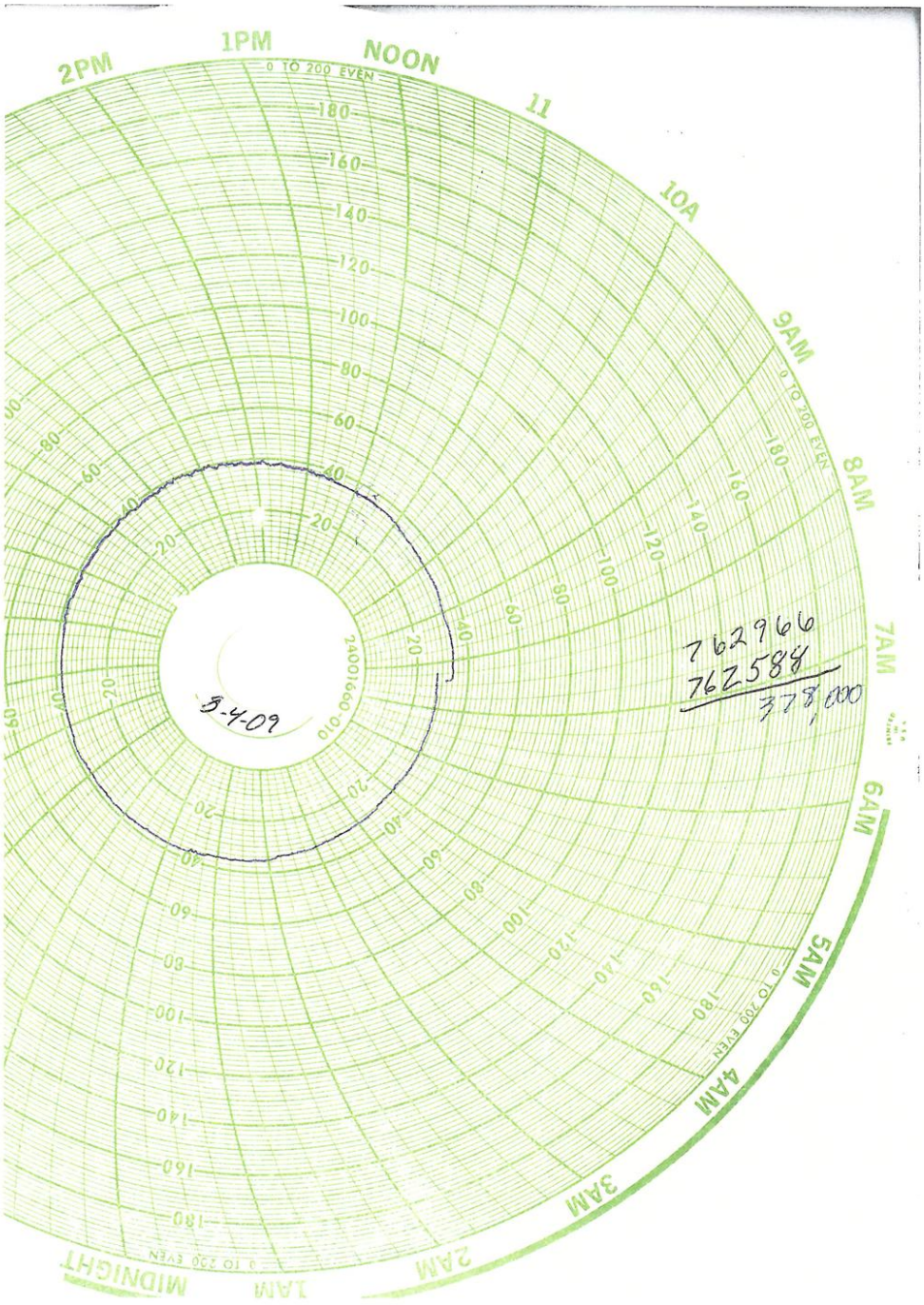
2PM
1PM
NOON
11
10A
9AM
8AM
7AM
6AM
5AM
4AM
3AM
2AM
1AM
MIDNIGHT
0 TO 200 EVEN
0 TO 200 EVEN
0 TO 200 EVEN
0 TO 230 EVEN
3-4-09
762966
762584
378,000

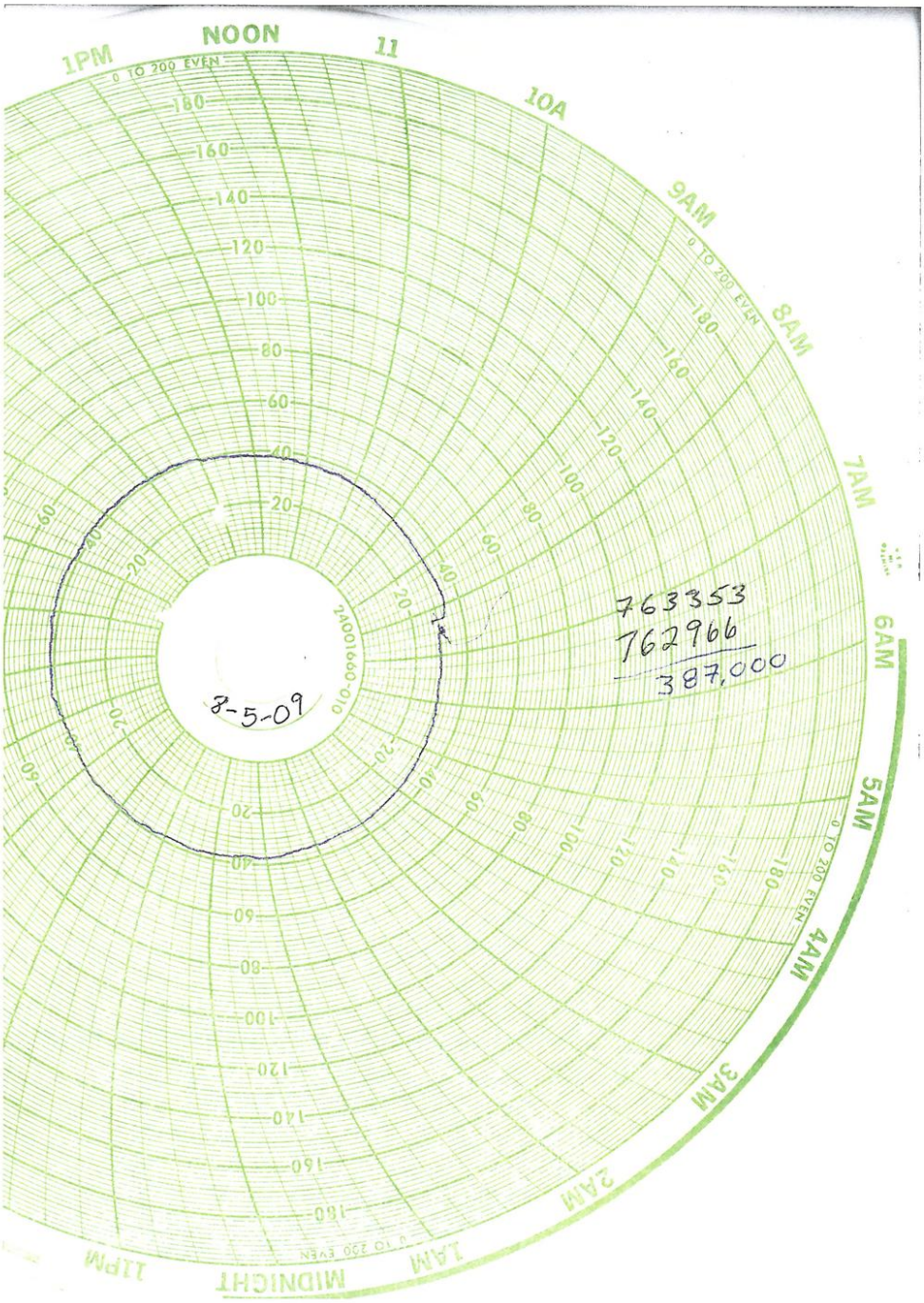
NOON
11
10A
9AM
8AM
7AM
6AM
5AM
4AM
3AM
2AM
1AM
MIDNIGHT
11PM
1PM
763353
762966
387,000
8-5-09

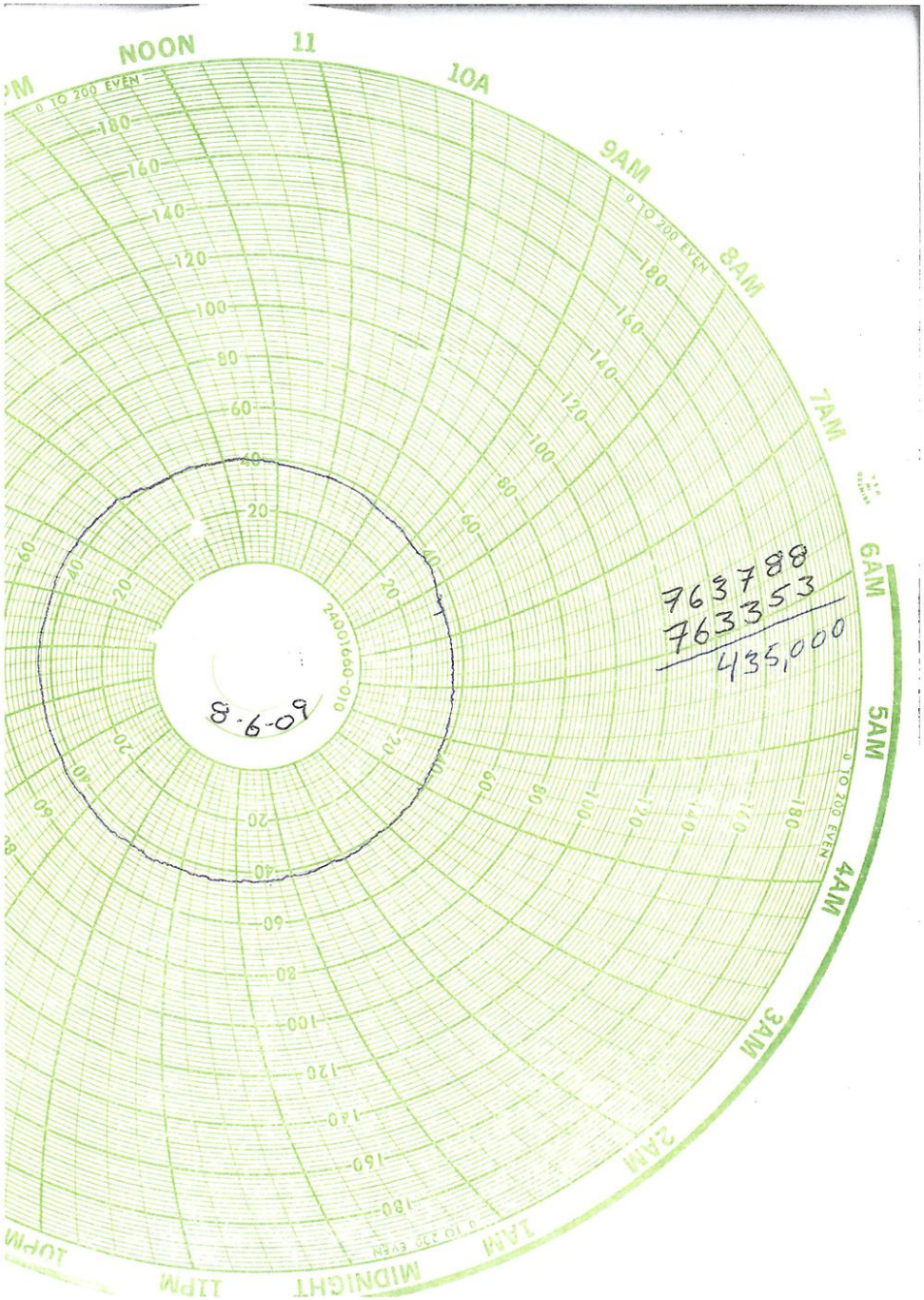
NOON
11
10A
9AM
8AM
7AM
6AM
5AM
4AM
3AM
2AM
1AM
MIDNIGHT
11PM
10PM
763788
763353
435,000
8-6-09

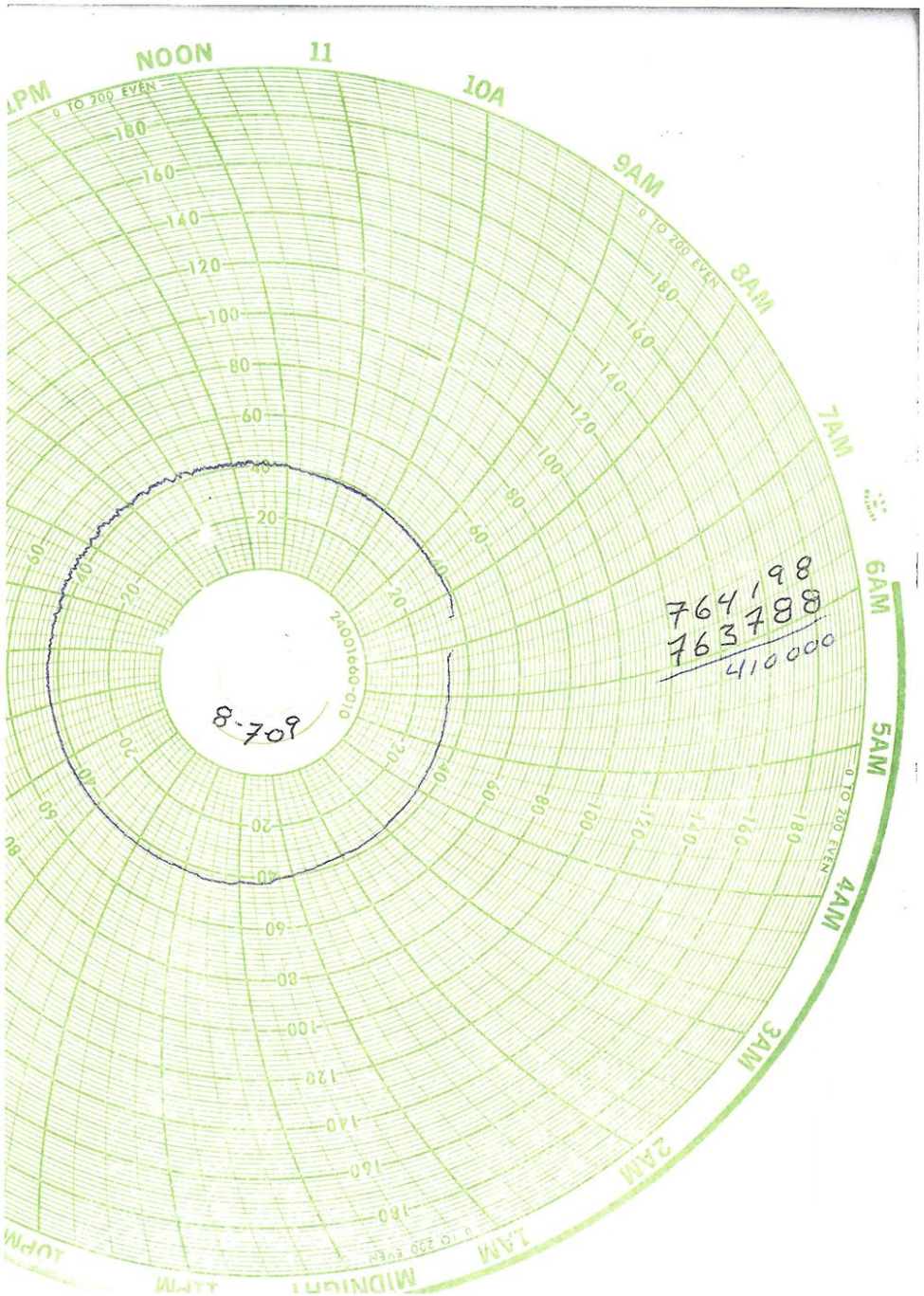
NOON
11
10A
9AM
8AM
7AM
6AM
5AM
4AM
3AM
2AM
1AM
MIDNIGHT
0 TO 200 EVEN
764198
763788
410000
8-709

## C.3 YAK TUNNEL TREATMENT PLANT DISCHARGE

These data were obtained through the gracious cooperation of Bill Lyle of Newmont Mining Corp. and are published here with his permission. Any use of these data for any unauthorized purpose is strictly prohibited.

### Yak Tunnel Water Treatment Plant

**Daily Flow Data** 2006-07-01 to 2006-07-31

| Date | Start Time | End Time | Hours of Operation | Discharge (gallons) | Flow Equivalent (cfs) |
|---|---|---|---|---|---|
| 7/1/2006 | 0:00 | 23:59 | 24.0 | 1,198,048 | 1.85 |
| 7/2/2006 | 0:00 | 23:59 | 24.0 | 1,197,620 | 1.85 |
| 7/3/2006 | 0:00 | 23:59 | 24.0 | 1,197,198 | 1.85 |
| 7/4/2006 | 0:00 | 23:59 | 24.0 | 1,195,442 | 1.85 |
| 7/5/2006 | 0:00 | 23:59 | 24.0 | 1,167,186 | 1.81 |
| 7/6/2006 | 0:00 | 23:59 | 24.0 | 1,166,465 | 1.80 |
| 7/7/2006 | 0:00 | 10:29 | 10.5 | 468,466 | 1.66 |
| 7/8/2006 | | | | 0 | |
| 7/9/2006 | | | | 0 | |
| 7/10/2006 | 5:56 | 23:59 | 18.1 | 904,948 | 1.86 |
| 7/11/2006 | 0:00 | 23:59 | 24.0 | 1,183,483 | 1.83 |
| 7/12/2006 | 0:00 | 23:59 | 24.0 | 1,127,933 | 1.75 |
| 7/13/2006 | 0:00 | 23:59 | 24.0 | 1,125,592 | 1.74 |
| 7/14/2006 | 0:00 | 23:59 | 24.0 | 1,173,946 | 1.82 |
| 7/15/2006 | 0:00 | 23:59 | 24.0 | 1,179,118 | 1.82 |
| 7/16/2006 | 0:00 | 23:59 | 24.0 | 1,179,145 | 1.82 |
| 7/17/2006 | 0:00 | 23:59 | 24.0 | 1,176,478 | 1.82 |
| 7/18/2006 | 0:00 | 23:59 | 24.0 | 1,175,850 | 1.82 |
| 7/19/2006 | 0:00 | 23:59 | 24.0 | 1,177,331 | 1.82 |
| 7/20/2006 | 0:00 | 23:59 | 24.0 | 1,178,298 | 1.82 |
| 7/21/2006 | 0:00 | 23:59 | 24.0 | 1,180,394 | 1.83 |
| 7/22/2006 | 0:00 | 23:59 | 24.0 | 1,183,405 | 1.83 |
| 7/23/2006 | 0:00 | 23:59 | 24.0 | 1,177,592 | 1.82 |
| 7/24/2006 | 0:00 | 23:59 | 24.0 | 1,175,259 | 1.82 |
| 7/25/2006 | 0:00 | 23:59 | 24.0 | 1,178,735 | 1.82 |
| 7/26/2006 | 0:00 | 23:59 | 24.0 | 1,177,273 | 1.82 |
| 7/27/2006 | 0:00 | 23:59 | 24.0 | 1,176,063 | 1.82 |
| 7/28/2006 | 0:00 | 13:59 | 14.0 | 624,523 | 1.66 |
| 7/29/2006 | | | | 0 | |
| 7/30/2006 | | | | 0 | |
| 7/31/2006 | 9:28 | 23:59 | 14.5 | 692,204 | 1.77 |
| | | | | Total | Average |
| | | | | **29,737,995** | **1.81** |

# Yak Tunnel Water Treatment Plant

**Daily Flow Data** 2006-08-01 to 2006-08-31

| Date | Start Time | End Time | Hours of Operation | Discharge (gallons) | Flow Equivalent (cfs) |
|---|---|---|---|---|---|
| 8/1/2006 | 0:00 | 0:00 | 24.0 | 1,187,753 | 1.84 |
| 8/2/2006 | 0:00 | 0:00 | 24.0 | 1,185,207 | 1.83 |
| 8/3/2006 | 0:00 | 0:00 | 24.0 | 1,185,035 | 1.83 |
| 8/4/2006 | 0:00 | 0:00 | 24.0 | 1,186,327 | 1.84 |
| 8/5/2006 | 0:00 | 0:00 | 24.0 | 1,187,791 | 1.84 |
| 8/6/2006 | 0:00 | 0:00 | 24.0 | 1,156,489 | 1.79 |
| 8/7/2006 | 0:00 | 0:00 | 24.0 | 1,055,102 | 1.63 |
| 8/8/2006 | 0:00 | 0:00 | 24.0 | 1,192,093 | 1.84 |
| 8/9/2006 | 0:00 | 0:00 | 24.0 | 1,180,901 | 1.83 |
| 8/10/2006 | 0:00 | 0:00 | 24.0 | 1,172,590 | 1.81 |
| 8/11/2006 | 0:00 | 0:00 | 24.0 | 1,147,988 | 1.78 |
| 8/12/2006 | 0:00 | 0:00 | 24.0 | 1,185,255 | 1.83 |
| 8/13/2006 | 0:00 | 0:00 | 24.0 | 1,183,124 | 1.83 |
| 8/14/2006 | 0:00 | 0:00 | 24.0 | 1,151,669 | 1.78 |
| 8/15/2006 | 0:00 | 0:00 | 24.0 | 1,123,156 | 1.74 |
| 8/16/2006 | 0:00 | 0:00 | 24.0 | 1,145,294 | 1.77 |
| 8/17/2006 | 0:00 | 0:00 | 24.0 | 1,132,544 | 1.75 |
| 8/18/2006 | 0:00 | 0:14 | 0.2 | 7,225 | 1.15 |
| 8/19/2006 | | | | | |
| 8/20/2006 | | | | | |
| 8/21/2006 | 6:02 | 0:00 | 18.0 | 850,719 | 1.76 |
| 8/22/2006 | 0:00 | 8:45 | 8.8 | 420,519 | 1.78 |
| 8/23/2006 | 12:46 | 0:00 | 11.2 | 322,710 | 1.07 |
| 8/24/2006 | 0:00 | 13:12 | 13.2 | 375,712 | 1.06 |
| 8/25/2006 | 7:31 | 0:00 | 16.5 | 828,512 | 1.87 |
| 8/26/2006 | 0:00 | 0:00 | 24.0 | 1,114,006 | 1.72 |
| 8/27/2006 | 0:00 | 0:00 | 24.0 | 1,075,863 | 1.66 |
| 8/28/2006 | 0:00 | 0:00 | 24.0 | 1,218,232 | 1.88 |
| 8/29/2006 | 0:00 | 0:00 | 24.0 | 1,227,656 | 1.90 |
| 8/30/2006 | 0:00 | 0:00 | 24.0 | 1,225,130 | 1.90 |
| 8/31/2006 | 0:00 | 0:00 | 24.0 | 1,074,442 | 1.66 |
| | | | | Total | Average |
| | | | | **29,499,041** | **1.72** |

## APPENDIX D: COMPREHENSIVE MODEL OUTPUT

The six stream gauges in the automated gaging network recorded nine major events through the summer of 2006 that were simulated with TREX-SMA. Each event was designated with a sequential number with one exception. The peak precipitation of Storm 5b occurred less than 24 hours following storm 5 and was particularly concentrated in the upper watershed while Storm 5 was primarily a lower-watershed storm.

Various plots showing the simulation results with and without soil moisture accounting are shown in this appendix. In cases where the plot is concerned with a particular storm event, the date ranges for the plot are as shown in Table D-1.

Table D-1: Date ranges of Storm Specific Plots

| Storm Number | Plot Begin | Plot End |
|---|---|---|
| Storm 1 | 07/19/2006 12:00 PM | 07/20/2006 12:00 PM |
| Storm 2 | 07/25/2006 12:00 PM | 07/26/2006 12:00 PM |
| Storm 3 | 07/26/2006 12:00 PM | 07/27/2006 12:00 PM |
| Storm 4 | 07/30/2006 12:00 PM | 07/31/2006 12:00 PM |
| Storm 5 | 08/05/2006 12:00 PM | 08/06/2006 12:00 PM |
| Storm 5b | 08/06/2006 12:00 PM | 08/07/2006 12:00 PM |
| Storm 6 | 08/10/2006 12:00 PM | 08/11/2006 12:00 PM |
| Storm 7 | 08/18/2006 12:00 PM | 08/19/2006 12:00 PM |
| Storm 8 | 08/26/2006 12:00 PM | 08/27/2006 12:00 PM |

In Table D.3.3 and Table D.3.4, improvement is noted in the final column denoted with a "plus" (+) to indicate an absolute improvement or a degree mark (°) if the SMA case has a smaller absolute difference but has overshot so that the error is of the opposite sign. A minus (-) indicates that the SMA case has a larger absolute error than the no-SMA case.

## D.1 FULL SIMULATION PLOTS

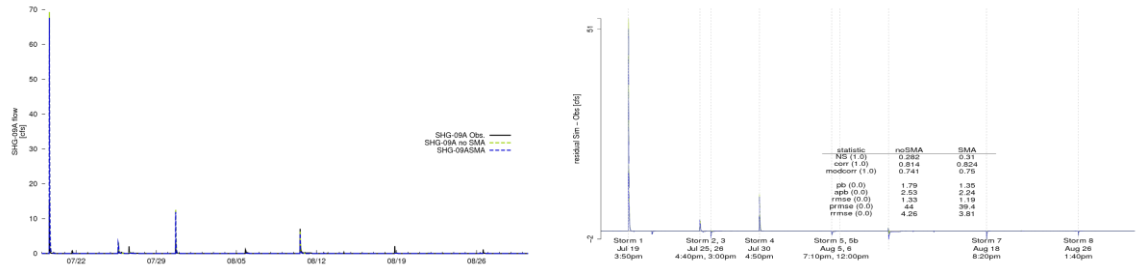


Figure D.1.1: Stray Horse Gulch—SHG-09A gauge from July 19–August 31 2006.

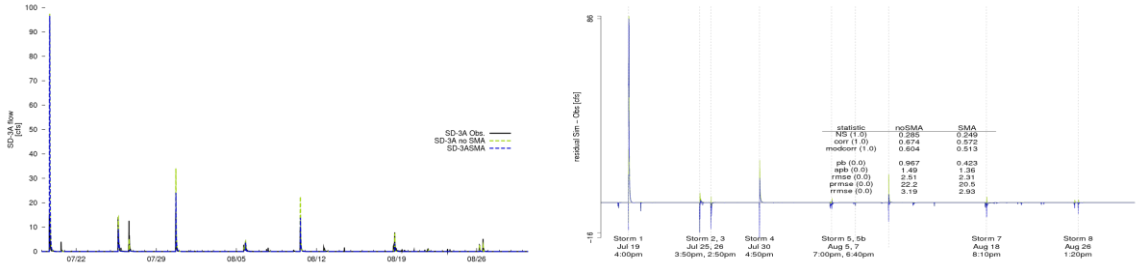


Figure D.1.2: Starr Ditch—SD-3A gauge from July 19–August 31, 2006.

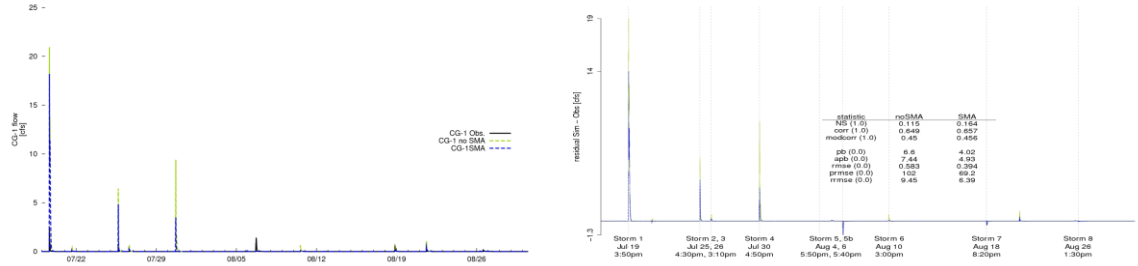


Figure D.1.3: Upper California Gulch—CG-1 gauge from July 19–August 31, 2006.

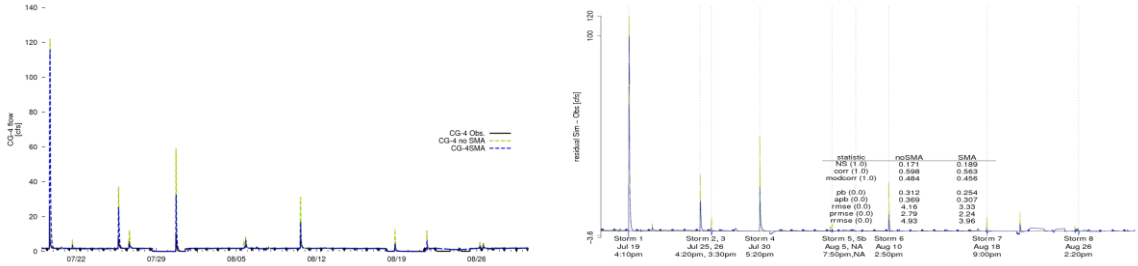


Figure D.1.4: California Gulch below Starr Ditch—CG-4 gauge from July 19–August 31, 2006.

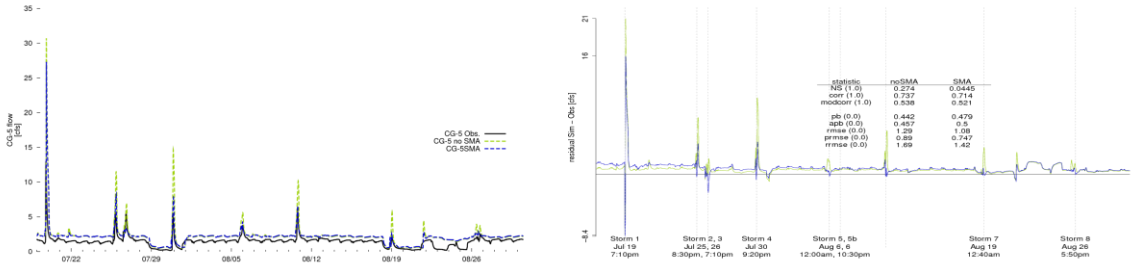


Figure D.1.5: California Gulch above WWTP—CG-5 gauge from July 19–August 31, 2006.

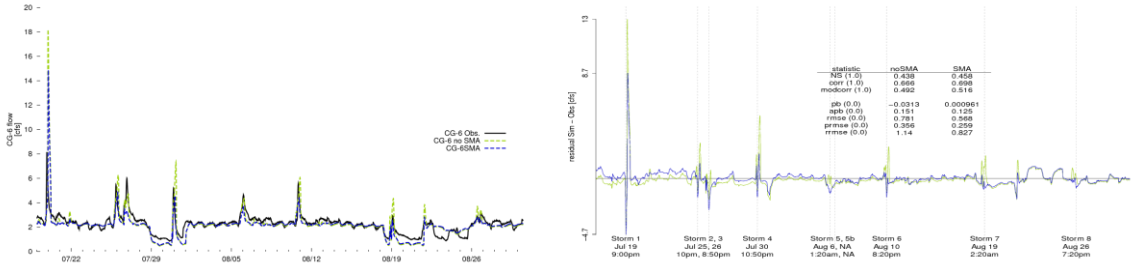


Figure D.1.6: California Gulch at Arkansas—CG-6 gauge from July 19–August 31, 2006.

## D.2 INDIVIDUAL STORM PLOTS

### *D.2.1 Storm 1*

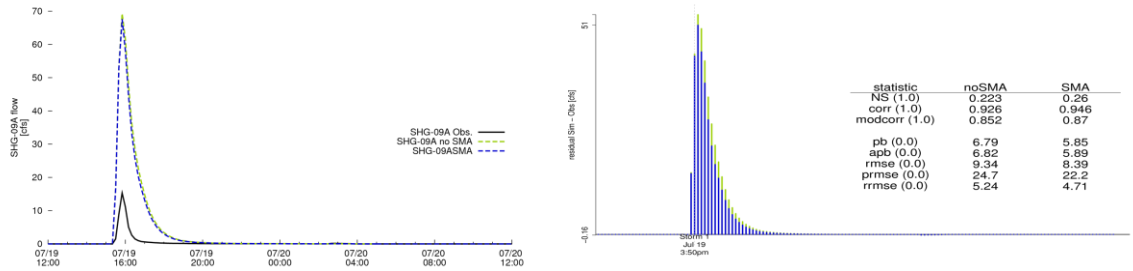


Figure D.2.1: Stray Horse Gulch—SHG-09A gauge from July 19–20, 2006.

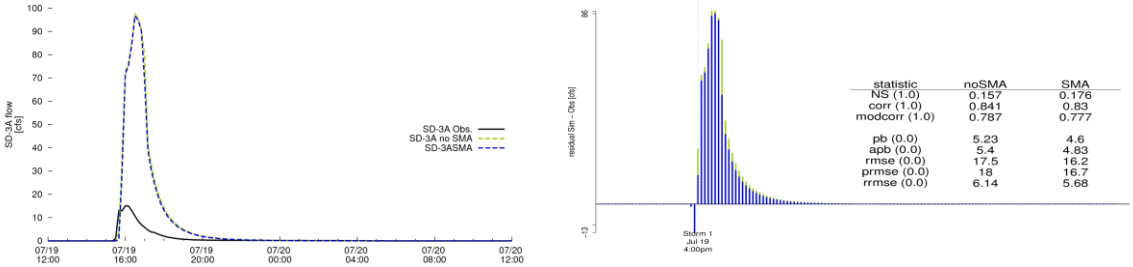


Figure D.2.2: Starr Ditch—SD-3A gauge from July 19–20, 2006.

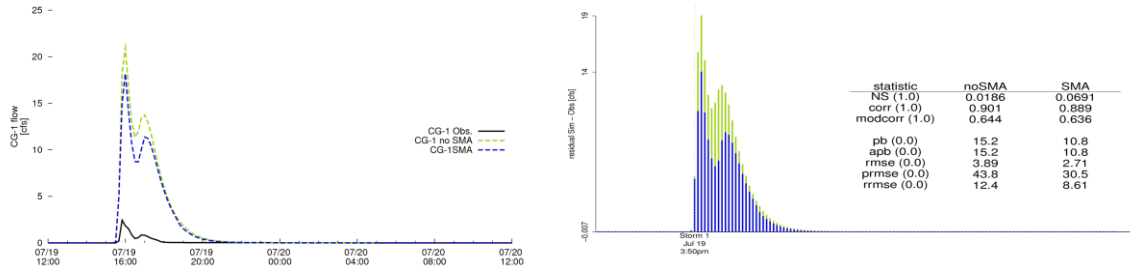


Figure D.2.3: Upper California Gulch—CG-1 gauge from July 19–20, 2006.

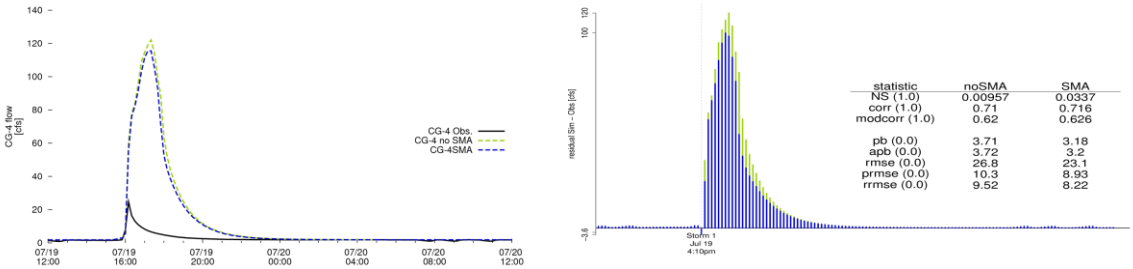


Figure D.2.4: California Gulch below Starr Ditch—CG-4 gauge from July 19–20, 2006.

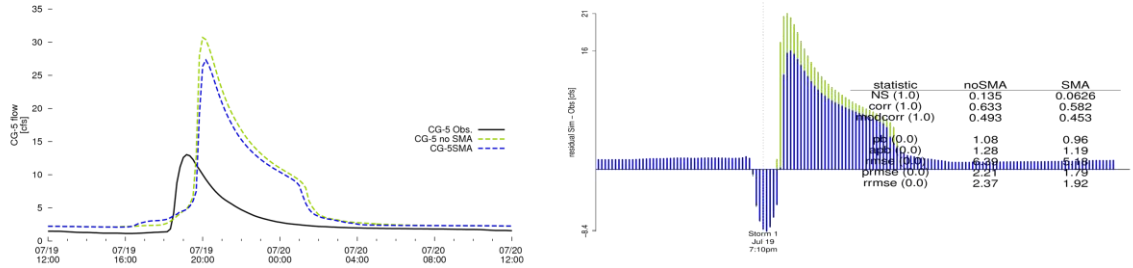


Figure D.2.5: California Gulch above WWTP—CG-5 gauge from July 19–20, 2006.

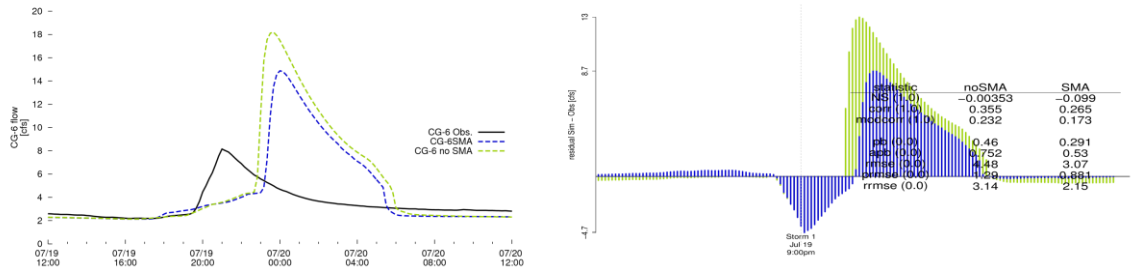


Figure D.2.6: California Gulch at Arkansas—CG-6 gauge from July 19–20, 2006.

### *D.2.2 Storm 2*

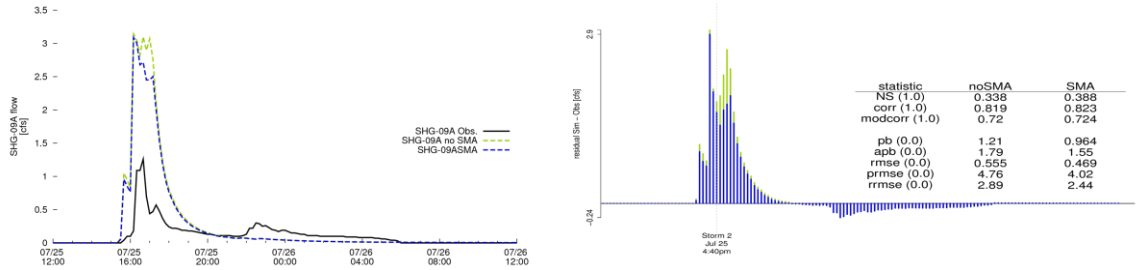


Figure D.2.7: Stray Horse Gulch—SHG-09A gauge from July 25–26, 2006.

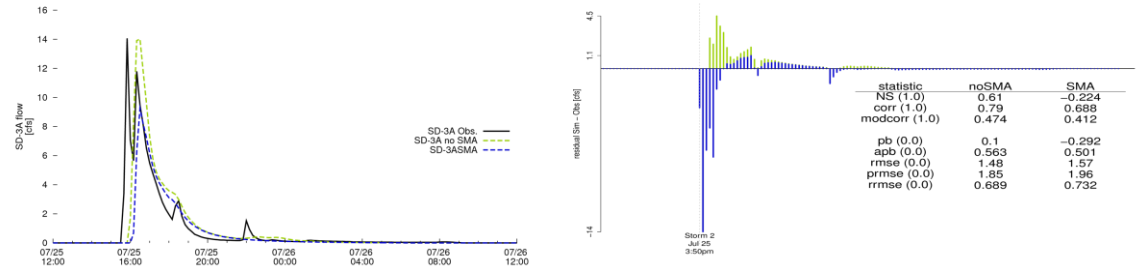


Figure D.2.8: Starr Ditch—SD-3A gauge from July 25–26, 2006.

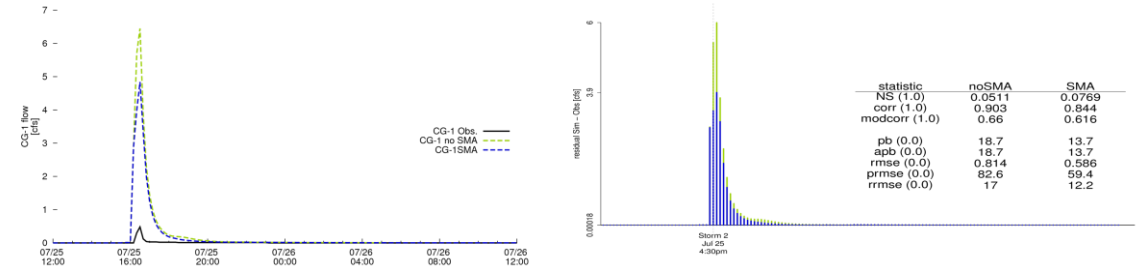


Figure D.2.9: Upper California Gulch—CG-1 gauge from July 25–26, 2006.

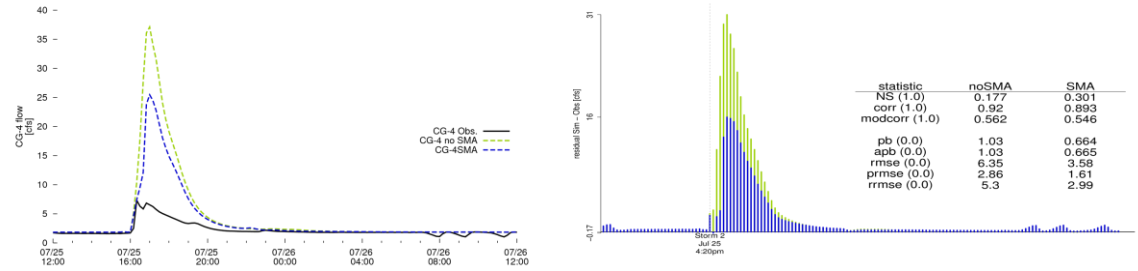


Figure D.2.10: California Gulch below Starr Ditch—CG-4 gauge from July 25–26, 2006.

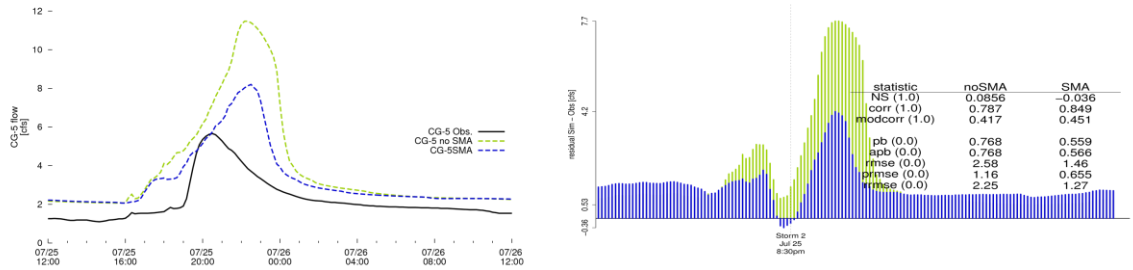


Figure D.2.11: California Gulch above WWTP—CG-5 gauge from July 25–26, 2006.

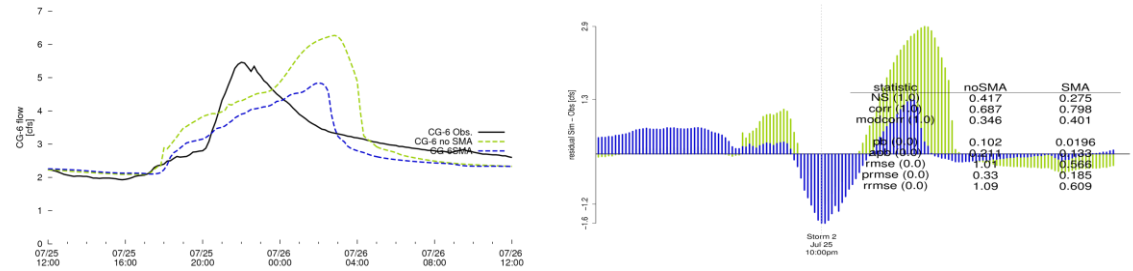


Figure D.2.12: California Gulch at Arkansas—CG-6 gauge from July 25–26, 2006.

### *D.2.3 Storm 3*

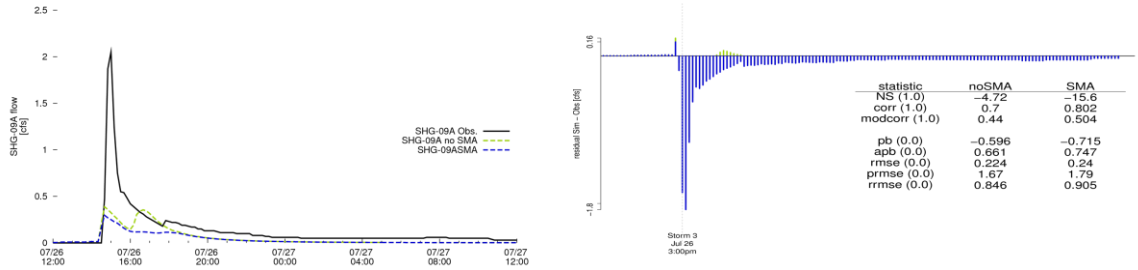


Figure D.2.13: Stray Horse Gulch—SHG-09A gauge from July 26–27, 2006.

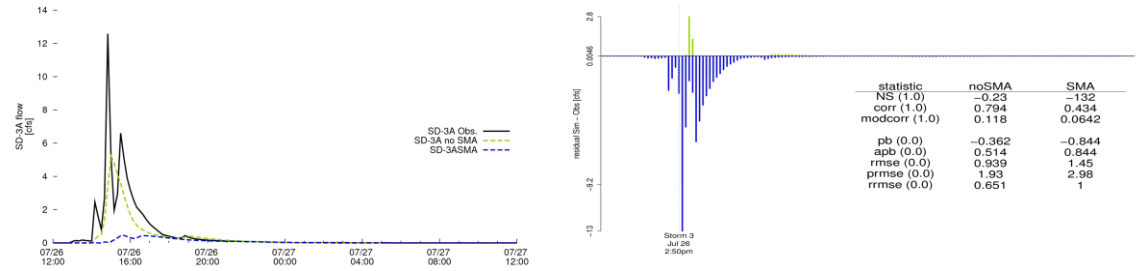


Figure D.2.14: Starr Ditch—SD-3A gauge from July 26–27, 2006.

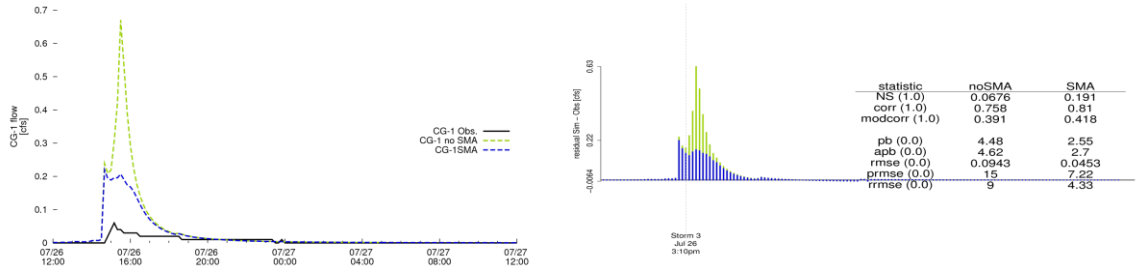


Figure D.2.15: Upper California Gulch—CG-1 gauge from July 26–27, 2006.

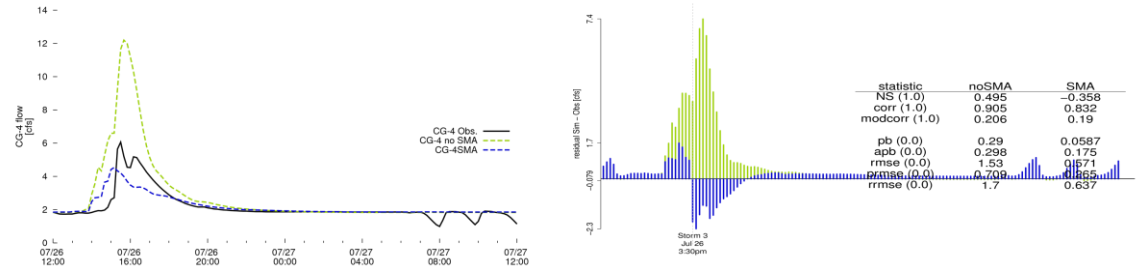


Figure D.2.16: California Gulch below Starr Ditch—CG-4 gauge from July 26–27, 2006.

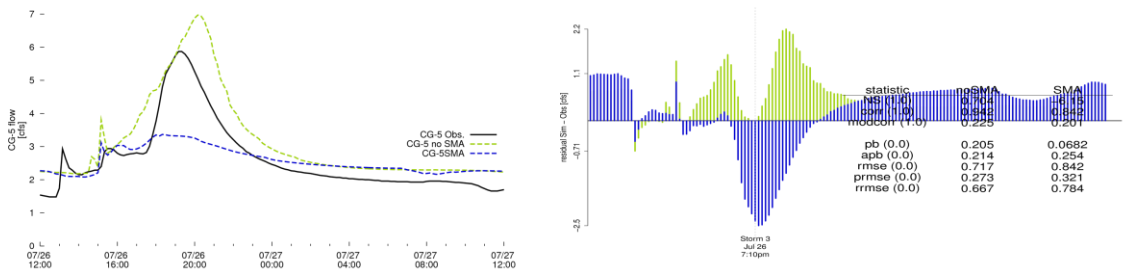


Figure D.2.17: California Gulch above WWTP—CG-5 gauge from July 26–27, 2006.

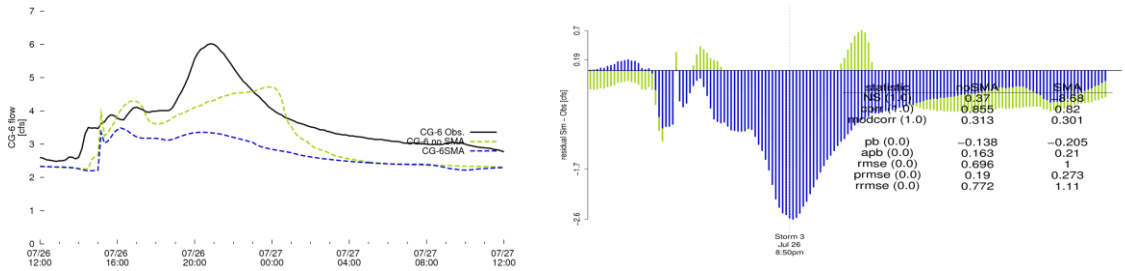


Figure D.2.18: California Gulch at Arkansas—CG-6 gauge from July 26–27, 2006.

### *D.2.4 Storm 4*

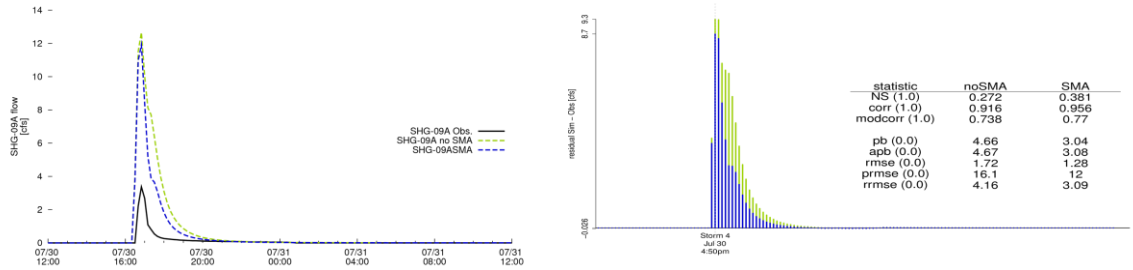


Figure D.2.19: Stray Horse Gulch—SHG-09A gauge from July 30–31, 2006.

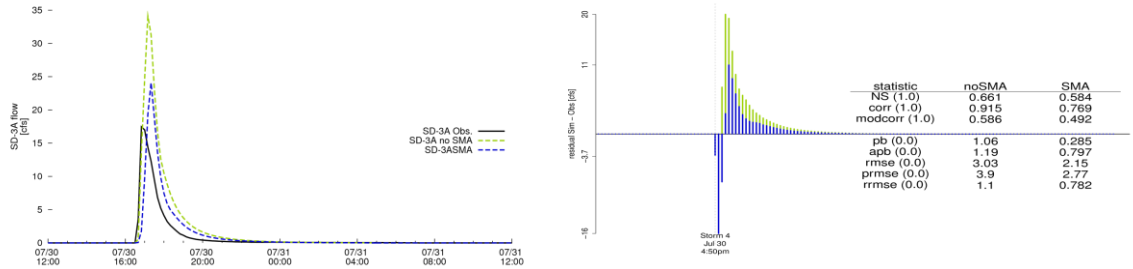


Figure D.2.20: Starr Ditch—SD-3A gauge from July 30–31, 2006.

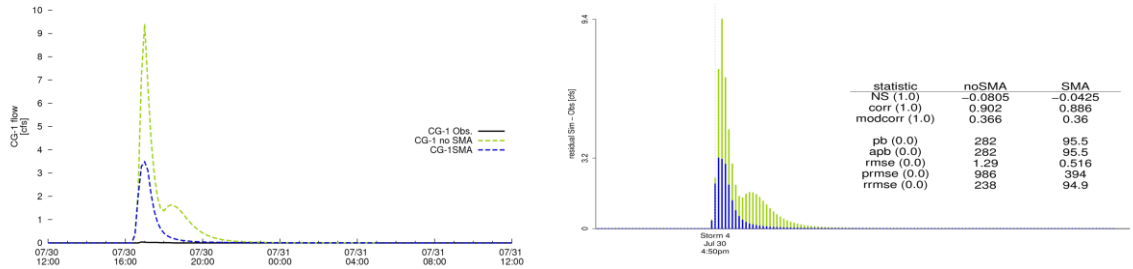


Figure D.2.21: Upper California Gulch—CG-1 gauge from July 30–31, 2006.

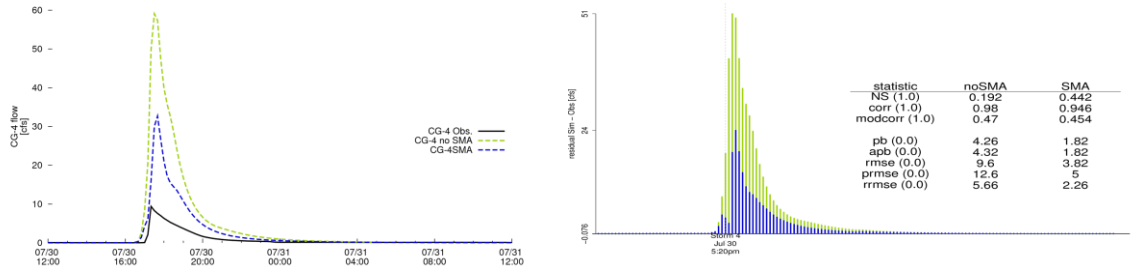


Figure D.2.22: California Gulch below Starr Ditch—CG-4 gauge from July 30–31, 2006.

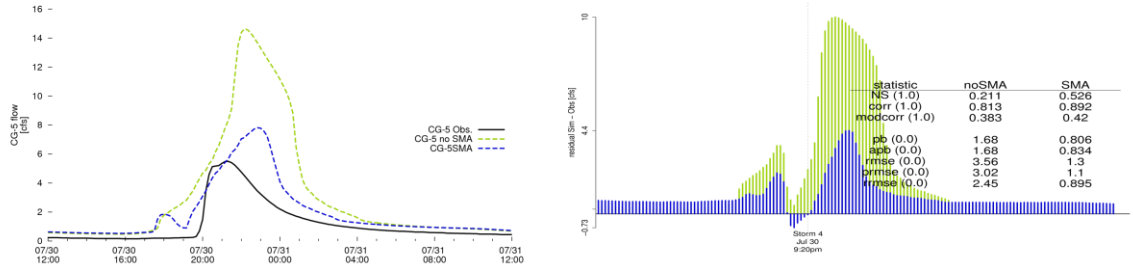


Figure D.2.23: California Gulch above WWTP—CG-5 gauge from July 30–31, 2006.

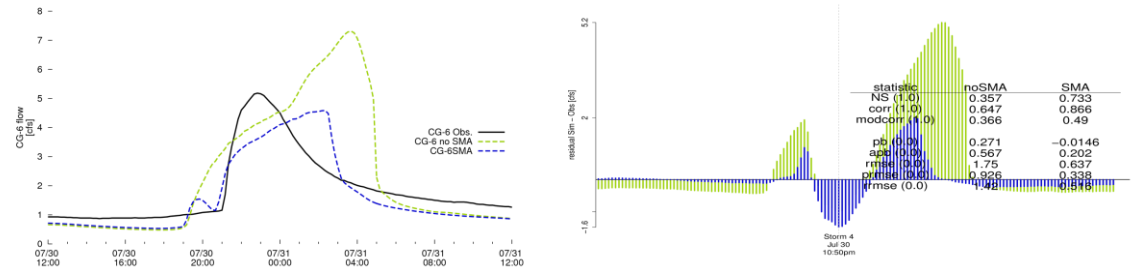


Figure D.2.24: California Gulch at Arkansas—CG-6 gauge from July 30–31, 2006.

### *D.2.5 Storm 5*

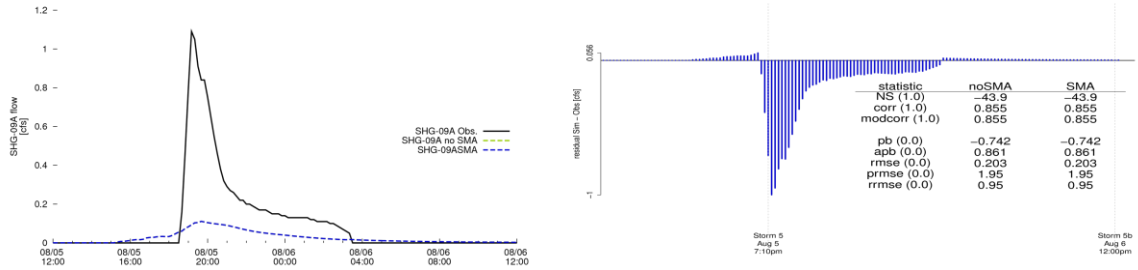


Figure D.2.25: Stray Horse Gulch—SHG-09A gauge from August 5–6, 2006.

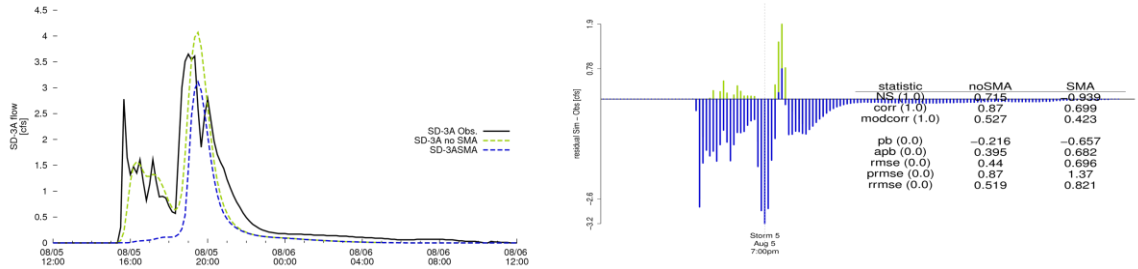


Figure D.2.26: Starr Ditch—SD-3A gauge from August 5–6, 2006.

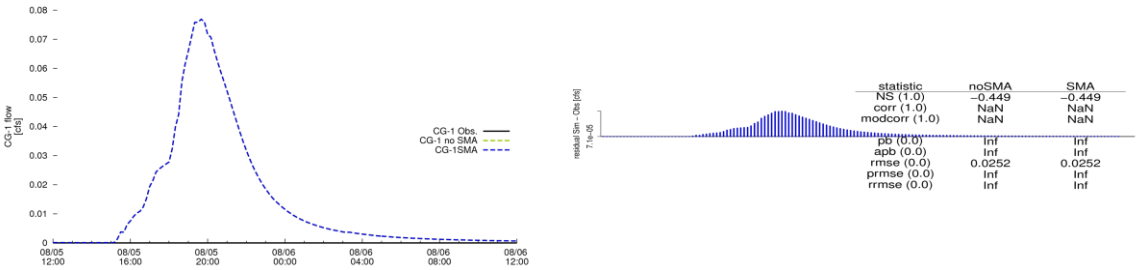


Figure D.2.27: Upper California Gulch—CG-1 gauge from August 5–6, 2006.

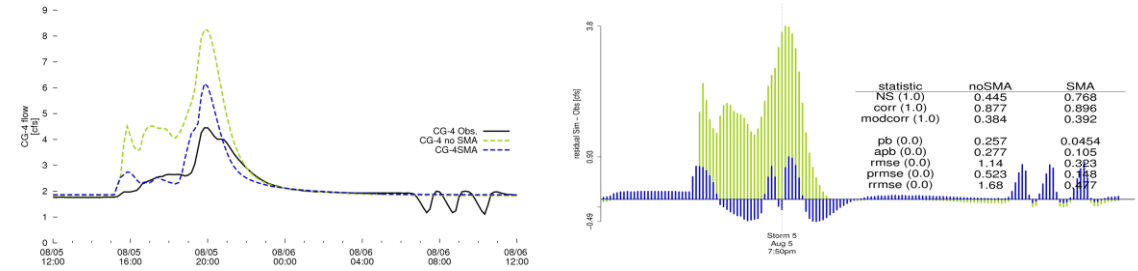


Figure D.2.28: California Gulch below Starr Ditch—CG-4 gauge from August 5–6, 2006.

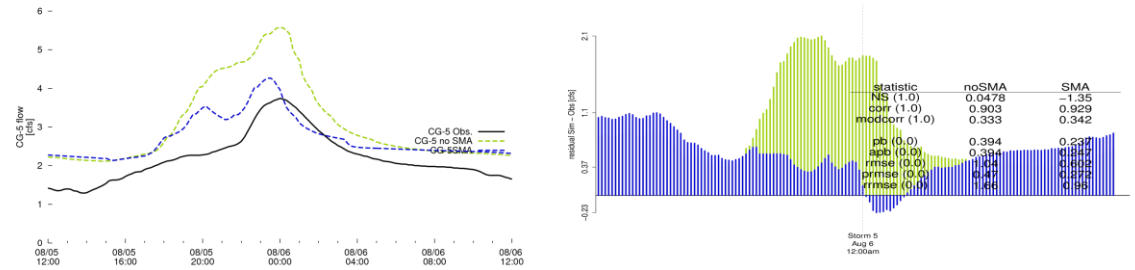


Figure D.2.29: California Gulch above WWTP—CG-5 gauge from August 5–6, 2006.

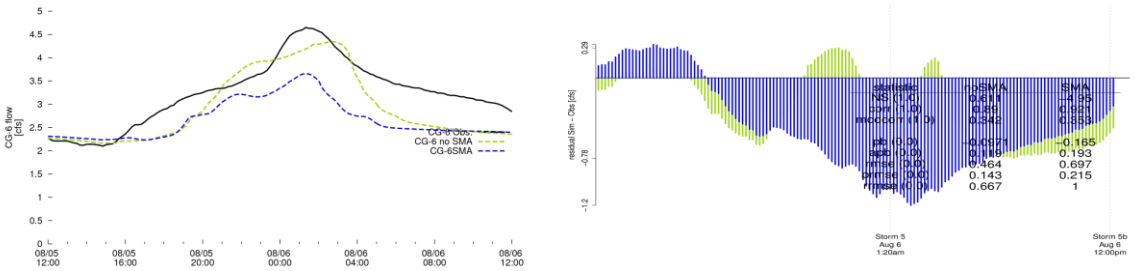


Figure D.2.30: California Gulch at Arkansas—CG-6 gauge from August 5–6, 2006.

### *D.2.6 Storm 5b*

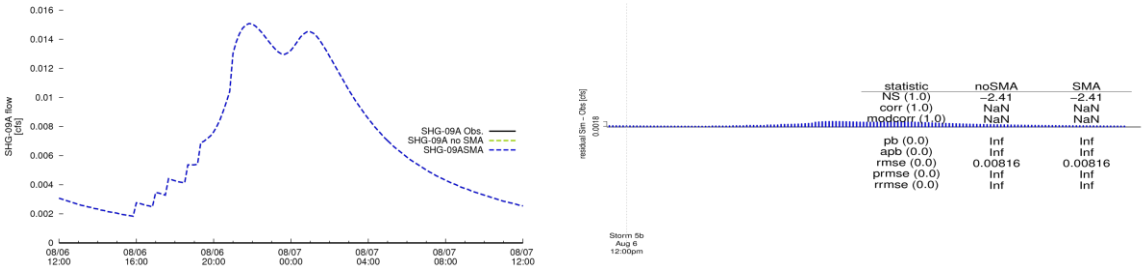


Figure D.2.31: Stray Horse Gulch—SHG-09A gauge from August 6–7, 2006.

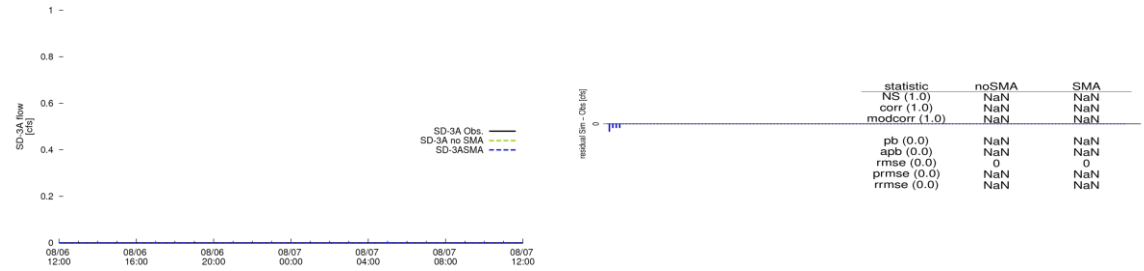


Figure D.2.32: Starr Ditch—SD-3A gauge from August 6–7, 2006.

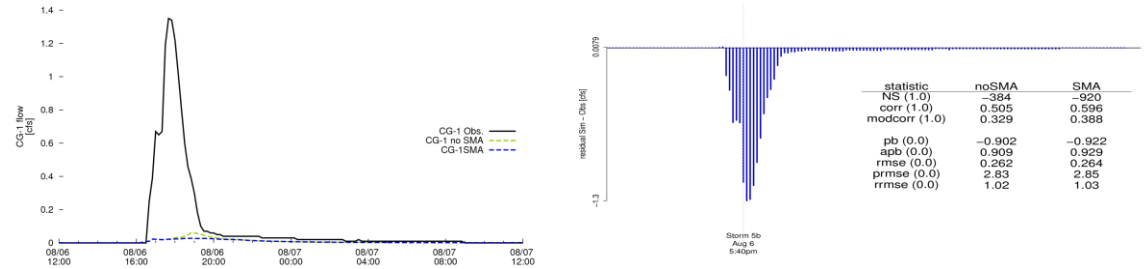


Figure D.2.33: Upper California Gulch—CG-1 gauge from August 6–7, 2006.

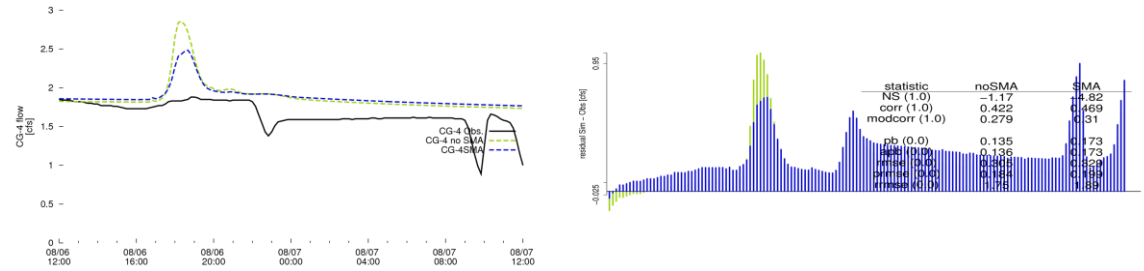


Figure D.2.34: California Gulch below Starr Ditch—CG-4 gauge from August 6–7, 2006.

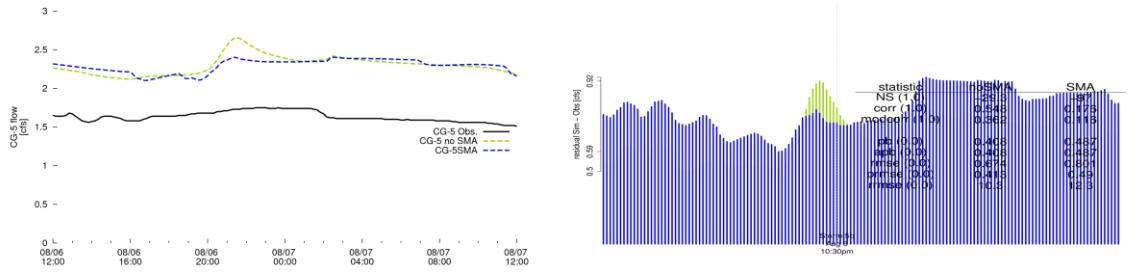


Figure D.2.35: California Gulch above WWTP—CG-5 gauge from August 6–7, 2006.

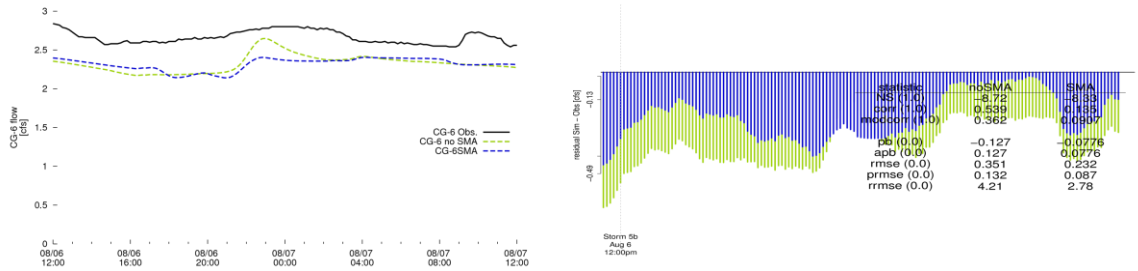


Figure D.2.36: California Gulch at Arkansas—CG-6 gauge from August 6–7, 2006.

### *D.2.7 Storm 6*

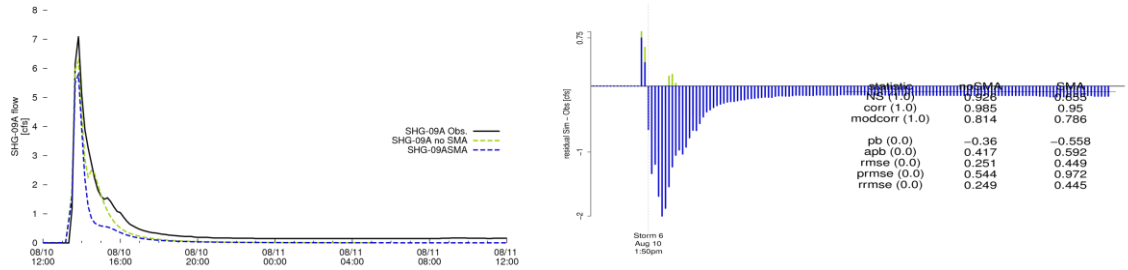


Figure D.2.37: Stray Horse Gulch—SHG-09A gauge from August 10–11, 2006.

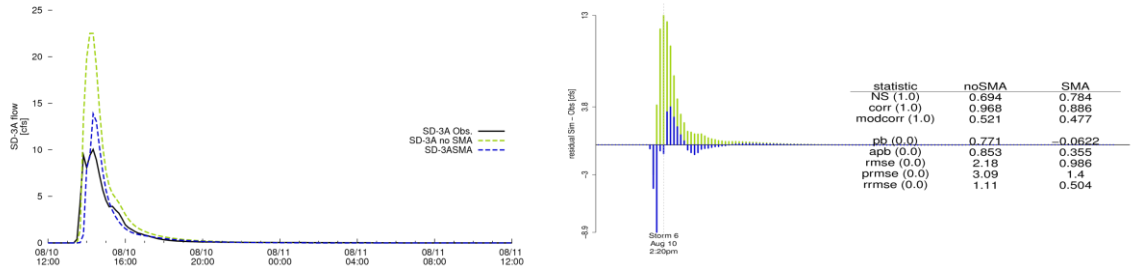


Figure D.2.38: Starr Ditch—SD-3A gauge from August 10–11, 2006.

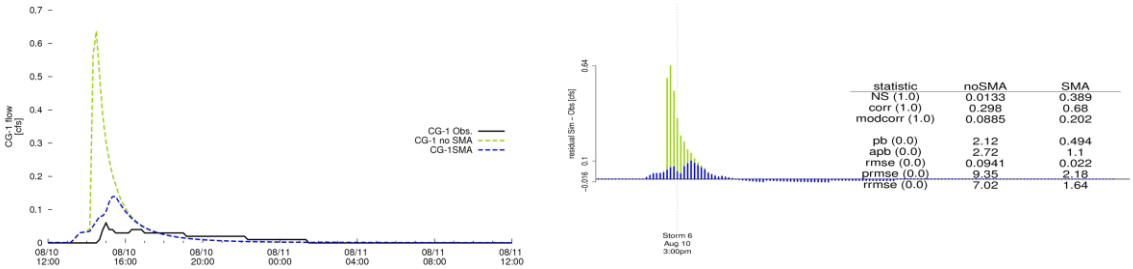


Figure D.2.39: Upper California Gulch—CG-1 gauge from August 10–11, 2006.

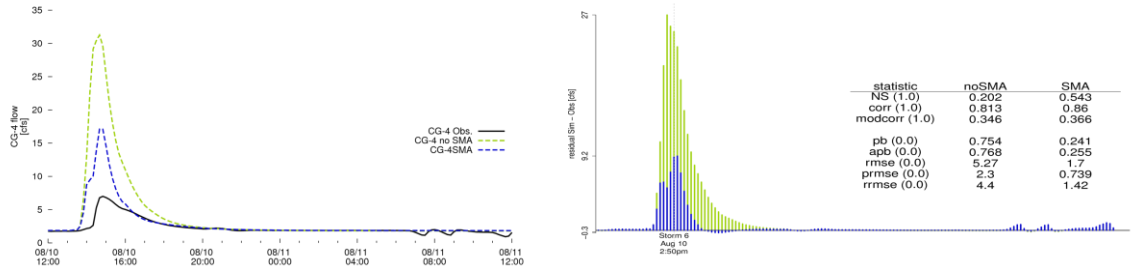


Figure D.2.40: California Gulch below Starr Ditch—CG-4 gauge from August 10–11, 2006.

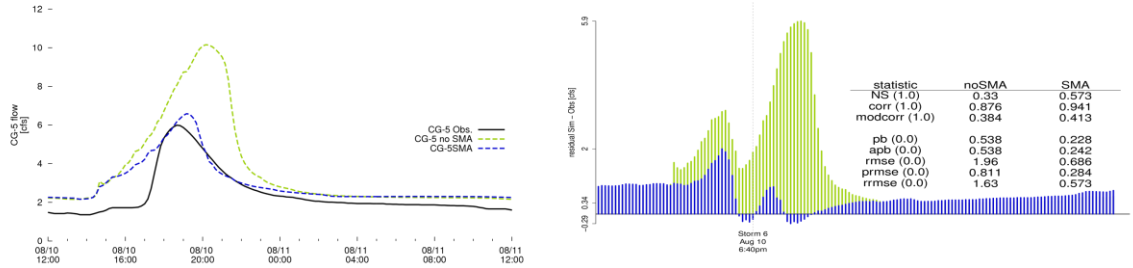


Figure D.2.41: California Gulch above WWTP—CG-5 gauge from August 10–11, 2006.

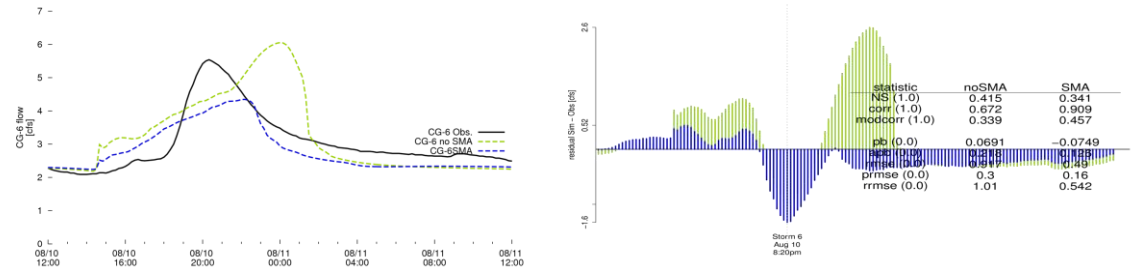


Figure D.2.42: California Gulch at Arkansas—CG-6 gauge from August 10–11, 2006.

### *D.2.8 Storm 7*

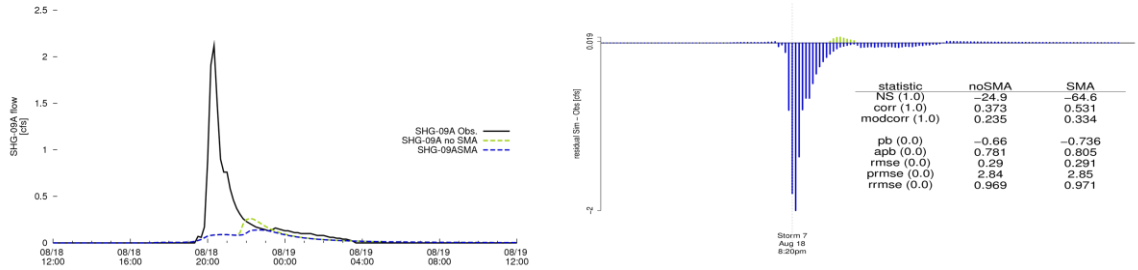


Figure D.2.43: Stray Horse Gulch—SHG-09A gauge from August 18–19, 2006.

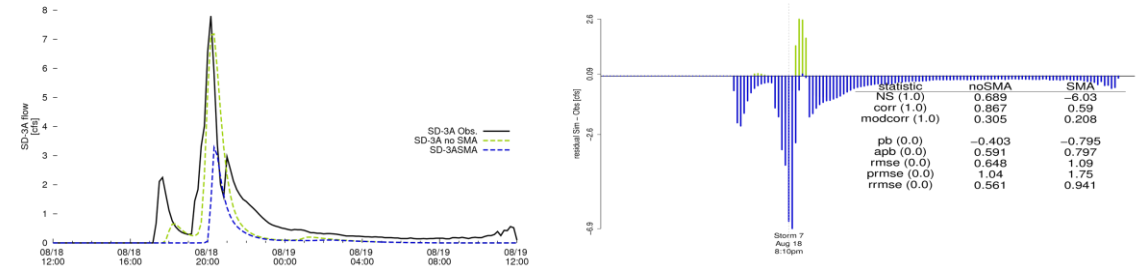


Figure D.2.44: Starr Ditch—SD-3A gauge from August 18–19, 2006.

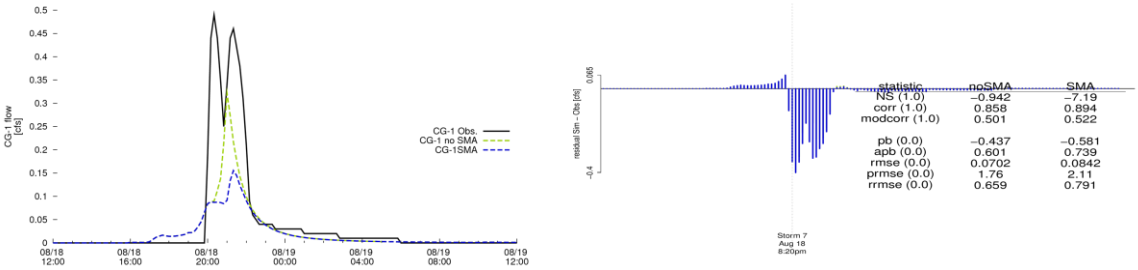


Figure D.2.45: Upper California Gulch—CG-1 gauge from August 18–19, 2006.

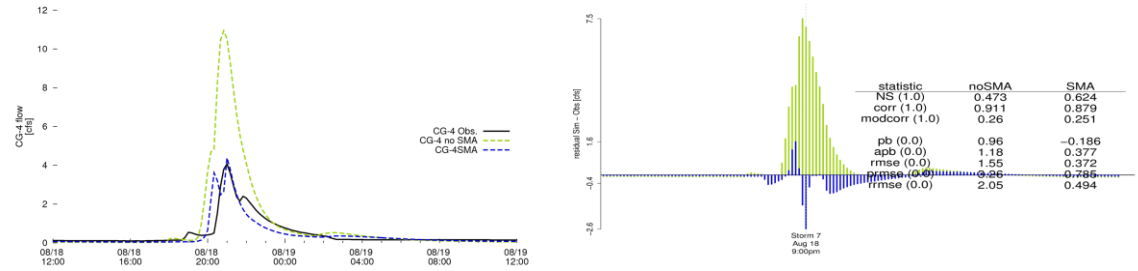


Figure D.2.46: California Gulch below Starr Ditch—CG-4 gauge from August 18–19, 2006.

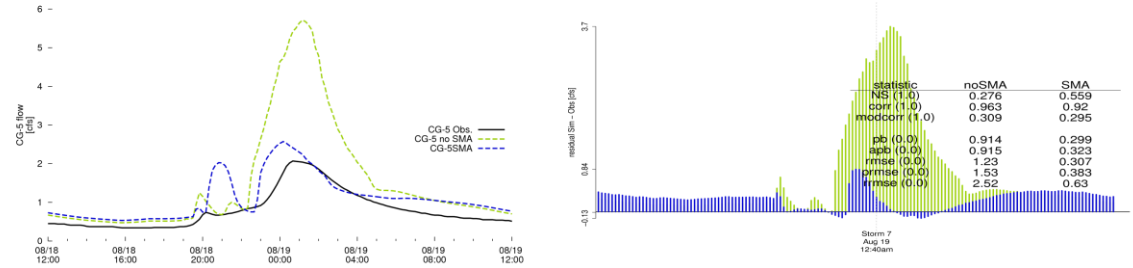


Figure D.2.47: California Gulch above WWTP—CG-5 gauge from August 18–19, 2006.

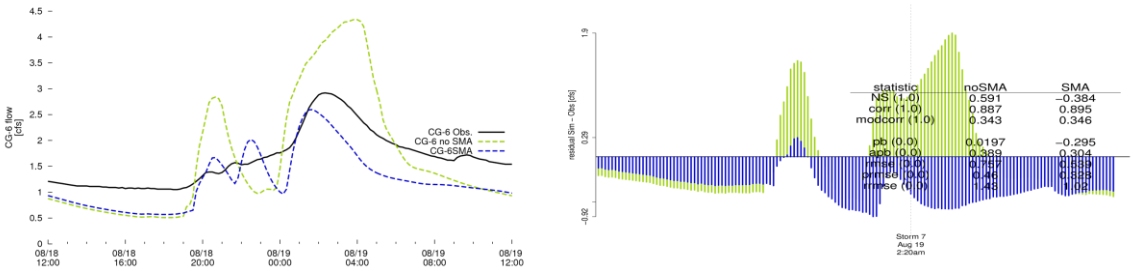


Figure D.2.48: California Gulch at Arkansas—CG-6 gauge from August 18–19, 2006.

### *D.2.9 Storm 8*

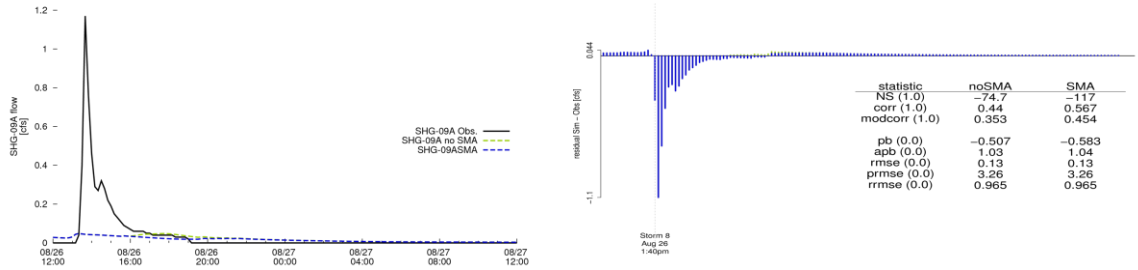


Figure D.2.49: Stray Horse Gulch—SHG-09A gauge from August 26–27, 2006.

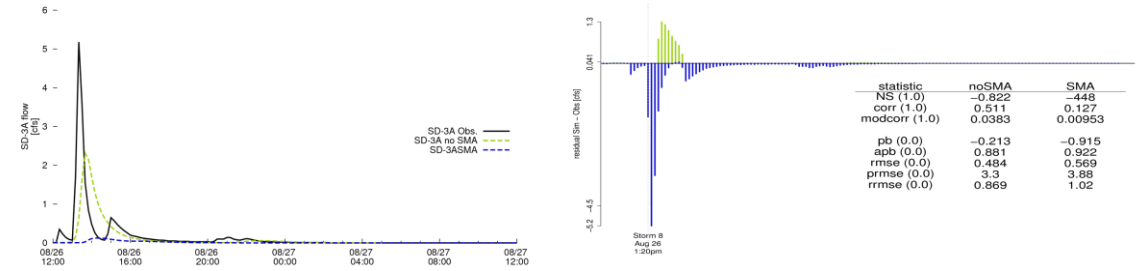


Figure D.2.50: Starr Ditch—SD-3A gauge from August 26–27, 2006.

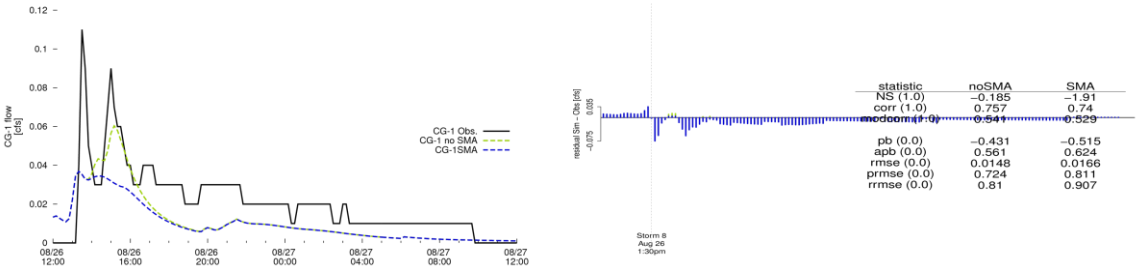


Figure D.2.51: Upper California Gulch—CG-1 gauge from August 26–27, 2006.

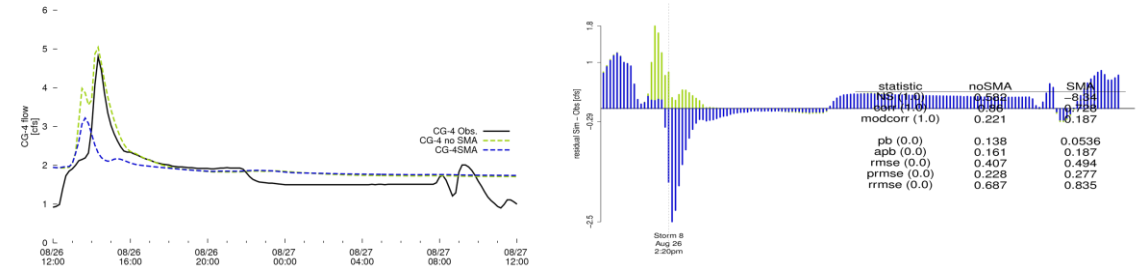


Figure D.2.52: California Gulch below Starr Ditch—CG-4 gauge from August 26–27, 2006.

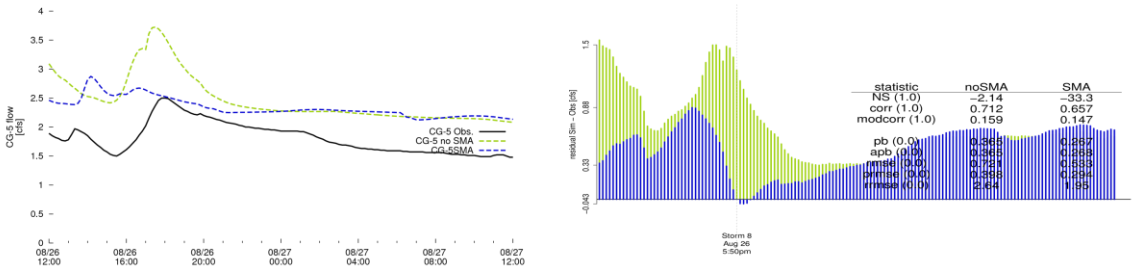


Figure D.2.53: California Gulch above WWTP—CG-5 gauge from August 26–27, 2006.

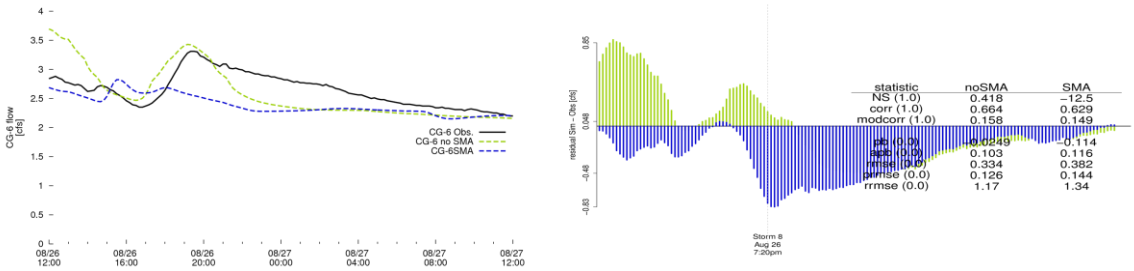


Figure D.2.54: California Gulch at Arkansas—CG-6 gauge from August 26–27, 2006.

## D.3 STATISTICAL PARAMETERS

Table D.3.1.a: All computed statistical parameters arranged by statistic.

| | | cg-1 | | cg-4 | | cg-5 | | cg-6 | | sd-3A | | shg-09A | |
|---|---|---|---|---|---|---|---|---|---|---|---|---|---|
| **Storm #** | **Statistic** | **No SMA** | **SMA** | **No SMA** | **SMA** | **No SMA** | **SMA** | **No SMA** | **SMA** | **No SMA** | **SMA** | **No SMA** | **SMA** |
| Overall | NS (1.0) | 0.12 | 0.16 | 0.17 | 0.19 | 0.27 | 0.04 | 0.44 | 0.46 | 0.29 | 0.25 | 0.28 | 0.31 |
| Storm1 | NS (1.0) | 0.02 | 0.07 | 0.01 | 0.03 | 0.14 | 0.06 | 0 | -0.1 | 0.16 | 0.18 | 0.22 | 0.26 |
| Storm2 | NS (1.0) | 0.05 | 0.08 | 0.18 | 0.3 | 0.09 | -0.04 | 0.42 | 0.28 | 0.61 | -0.22 | 0.34 | 0.39 |
| Storm3 | NS (1.0) | 0.07 | 0.19 | 0.5 | -0.36 | 0.7 | -6.15 | 0.37 | -8.68 | -0.23 | -132 | -4.72 | -15.6 |
| Storm4 | NS (1.0) | -0.08 | -0.04 | 0.19 | 0.44 | 0.21 | 0.53 | 0.36 | 0.73 | 0.66 | 0.58 | 0.27 | 0.38 |
| Storm5 | NS (1.0) | -0.45 | -0.45 | 0.45 | 0.77 | 0.05 | -1.35 | 0.61 | -4.95 | 0.72 | -0.94 | -43.9 | -43.9 |
| Storm5b | NS (1.0) | -384 | -920 | -1.17 | -4.82 | -29.3 | -97 | -8.72 | -8.33 | NaN | NaN | -2.41 | -2.41 |
| Storm6 | NS (1.0) | 0.01 | 0.39 | 0.2 | 0.54 | 0.33 | 0.57 | 0.42 | 0.34 | 0.69 | 0.78 | 0.93 | 0.66 |
| Storm7 | NS (1.0) | -0.94 | -7.19 | 0.47 | 0.62 | 0.28 | 0.56 | 0.59 | -0.38 | 0.69 | -6.03 | -24.9 | -64.6 |
| Storm8 | NS (1.0) | -0.19 | -1.91 | 0.58 | -8.34 | -2.14 | -33.3 | 0.42 | -12.5 | -0.82 | -448 | -74.7 | -117 |
| Overall | corr (1.0) | 0.65 | 0.66 | 0.6 | 0.56 | 0.74 | 0.71 | 0.67 | 0.7 | 0.67 | 0.57 | 0.81 | 0.82 |
| Storm1 | corr (1.0) | 0.9 | 0.89 | 0.71 | 0.72 | 0.63 | 0.58 | 0.36 | 0.27 | 0.84 | 0.83 | 0.93 | 0.95 |
| Storm2 | corr (1.0) | 0.9 | 0.84 | 0.92 | 0.89 | 0.79 | 0.85 | 0.69 | 0.8 | 0.79 | 0.69 | 0.82 | 0.82 |
| Storm3 | corr (1.0) | 0.76 | 0.81 | 0.91 | 0.83 | 0.94 | 0.84 | 0.86 | 0.82 | 0.79 | 0.43 | 0.7 | 0.8 |
| Storm4 | corr (1.0) | 0.9 | 0.89 | 0.98 | 0.95 | 0.81 | 0.89 | 0.65 | 0.87 | 0.92 | 0.77 | 0.92 | 0.96 |
| Storm5 | corr (1.0) | NaN | NaN | 0.88 | 0.9 | 0.9 | 0.93 | 0.89 | 0.92 | 0.87 | 0.7 | 0.86 | 0.86 |
| Storm5b | corr (1.0) | 0.51 | 0.6 | 0.42 | 0.47 | 0.55 | 0.18 | 0.54 | 0.14 | NaN | NaN | NaN | NaN |
| Storm6 | corr (1.0) | 0.3 | 0.68 | 0.81 | 0.86 | 0.88 | 0.94 | 0.67 | 0.91 | 0.97 | 0.89 | 0.99 | 0.95 |
| Storm7 | corr (1.0) | 0.86 | 0.89 | 0.91 | 0.88 | 0.96 | 0.92 | 0.89 | 0.9 | 0.87 | 0.59 | 0.37 | 0.53 |
| Storm8 | corr (1.0) | 0.76 | 0.74 | 0.86 | 0.73 | 0.71 | 0.66 | 0.66 | 0.63 | 0.51 | 0.13 | 0.44 | 0.57 |
| Overall | modcorr (1.0) | 0.45 | 0.46 | 0.48 | 0.46 | 0.54 | 0.52 | 0.49 | 0.52 | 0.6 | 0.51 | 0.74 | 0.75 |
| Storm1 | modcorr (1.0) | 0.64 | 0.64 | 0.62 | 0.63 | 0.49 | 0.45 | 0.23 | 0.17 | 0.79 | 0.78 | 0.85 | 0.87 |
| Storm2 | modcorr (1.0) | 0.66 | 0.62 | 0.56 | 0.55 | 0.42 | 0.45 | 0.35 | 0.4 | 0.47 | 0.41 | 0.72 | 0.72 |
| Storm3 | modcorr (1.0) | 0.39 | 0.42 | 0.21 | 0.19 | 0.23 | 0.2 | 0.31 | 0.3 | 0.12 | 0.06 | 0.44 | 0.5 |
| Storm4 | modcorr (1.0) | 0.37 | 0.36 | 0.47 | 0.45 | 0.38 | 0.42 | 0.37 | 0.49 | 0.59 | 0.49 | 0.74 | 0.77 |
| Storm5 | modcorr (1.0) | NaN | NaN | 0.38 | 0.39 | 0.33 | 0.34 | 0.34 | 0.35 | 0.53 | 0.42 | 0.86 | 0.86 |
| Storm5b | modcorr (1.0) | 0.33 | 0.39 | 0.28 | 0.31 | 0.36 | 0.12 | 0.36 | 0.09 | NaN | NaN | NaN | NaN |
| Storm6 | modcorr (1.0) | 0.09 | 0.2 | 0.35 | 0.37 | 0.38 | 0.41 | 0.34 | 0.46 | 0.52 | 0.48 | 0.81 | 0.79 |
| Storm7 | modcorr (1.0) | 0.5 | 0.52 | 0.26 | 0.25 | 0.31 | 0.3 | 0.34 | 0.35 | 0.31 | 0.21 | 0.24 | 0.33 |
| Storm8 | modcorr (1.0) | 0.54 | 0.53 | 0.22 | 0.19 | 0.16 | 0.15 | 0.16 | 0.15 | 0.04 | 0.01 | 0.35 | 0.45 |
| Overall | pb (0.0) | 6.6 | 4.02 | 0.31 | 0.25 | 0.44 | 0.48 | -0.03 | 0 | 0.97 | 0.42 | 1.79 | 1.35 |
| Storm1 | pb (0.0) | 15.2 | 10.8 | 3.71 | 3.18 | 1.08 | 0.96 | 0.46 | 0.29 | 5.23 | 4.6 | 6.79 | 5.85 |
| Storm2 | pb (0.0) | 18.7 | 13.7 | 1.03 | 0.66 | 0.77 | 0.56 | 0.1 | 0.02 | 0.1 | -0.29 | 1.21 | 0.96 |
| Storm3 | pb (0.0) | 4.48 | 2.55 | 0.29 | 0.06 | 0.21 | 0.07 | -0.14 | -0.21 | -0.36 | -0.84 | -0.6 | -0.72 |
| Storm4 | pb (0.0) | 282 | 95.5 | 4.26 | 1.82 | 1.68 | 0.81 | 0.27 | -0.01 | 1.06 | 0.29 | 4.66 | 3.04 |
| Storm5 | pb (0.0) | Inf | Inf | 0.26 | 0.05 | 0.39 | 0.24 | -0.1 | -0.17 | -0.22 | -0.66 | -0.74 | -0.74 |
| Storm5b | pb (0.0) | -0.9 | -0.92 | 0.14 | 0.17 | 0.41 | 0.49 | -0.13 | -0.08 | NaN | NaN | Inf | Inf |
| Storm6 | pb (0.0) | 2.12 | 0.49 | 0.75 | 0.24 | 0.54 | 0.23 | 0.07 | -0.07 | 0.77 | -0.06 | -0.36 | -0.56 |
| Storm7 | pb (0.0) | -0.44 | -0.58 | 0.96 | -0.19 | 0.91 | 0.3 | 0.02 | -0.3 | -0.4 | -0.8 | -0.66 | -0.74 |
| Storm8 | pb (0.0) | -0.43 | -0.52 | 0.14 | 0.05 | 0.37 | 0.27 | -0.02 | -0.11 | -0.21 | -0.92 | -0.51 | -0.58 |
| Overall | apb (0.0) | 7.44 | 4.93 | 0.37 | 0.31 | 0.46 | 0.5 | 0.15 | 0.13 | 1.49 | 1.36 | 2.53 | 2.24 |
| Storm1 | apb (0.0) | 15.2 | 10.8 | 3.72 | 3.2 | 1.28 | 1.19 | 0.75 | 0.53 | 5.4 | 4.83 | 6.82 | 5.89 |
| Storm2 | apb (0.0) | 18.7 | 13.7 | 1.03 | 0.67 | 0.77 | 0.57 | 0.21 | 0.13 | 0.56 | 0.5 | 1.79 | 1.55 |
| Storm3 | apb (0.0) | 4.62 | 2.7 | 0.3 | 0.18 | 0.21 | 0.25 | 0.16 | 0.21 | 0.51 | 0.84 | 0.66 | 0.75 |
| Storm4 | apb (0.0) | 282 | 95.5 | 4.32 | 1.82 | 1.68 | 0.83 | 0.57 | 0.2 | 1.19 | 0.8 | 4.67 | 3.08 |
| Storm5 | apb (0.0) | Inf | Inf | 0.28 | 0.11 | 0.39 | 0.25 | 0.12 | 0.19 | 0.4 | 0.68 | 0.86 | 0.86 |
| Storm5b | apb (0.0) | 0.91 | 0.93 | 0.14 | 0.17 | 0.41 | 0.49 | 0.13 | 0.08 | NaN | NaN | Inf | Inf |
| Storm6 | apb (0.0) | 2.72 | 1.1 | 0.77 | 0.26 | 0.54 | 0.24 | 0.22 | 0.13 | 0.85 | 0.36 | 0.42 | 0.59 |
| Storm7 | apb (0.0) | 0.6 | 0.74 | 1.18 | 0.38 | 0.92 | 0.32 | 0.39 | 0.3 | 0.59 | 0.8 | 0.78 | 0.81 |
| Storm8 | apb (0.0) | 0.56 | 0.62 | 0.16 | 0.19 | 0.37 | 0.27 | 0.1 | 0.12 | 0.88 | 0.92 | 1.03 | 1.04 |
| Overall | rmse (0.0) | 0.58 | 0.39 | 4.16 | 3.33 | 1.29 | 1.08 | 0.78 | 0.57 | 2.51 | 2.31 | 1.33 | 1.19 |
| Storm1 | rmse (0.0) | 3.89 | 2.71 | 26.8 | 23.1 | 6.39 | 5.18 | 4.48 | 3.07 | 17.5 | 16.2 | 9.34 | 8.39 |
| Storm2 | rmse (0.0) | 0.81 | 0.59 | 6.35 | 3.58 | 2.58 | 1.46 | 1.01 | 0.57 | 1.48 | 1.57 | 0.56 | 0.47 |
| Storm3 | rmse (0.0) | 0.09 | 0.05 | 1.53 | 0.57 | 0.72 | 0.84 | 0.7 | 1 | 0.94 | 1.45 | 0.22 | 0.24 |
| Storm4 | rmse (0.0) | 1.29 | 0.52 | 9.6 | 3.82 | 3.56 | 1.3 | 1.75 | 0.64 | 3.03 | 2.15 | 1.72 | 1.28 |
| Storm5 | rmse (0.0) | 0.03 | 0.03 | 1.14 | 0.32 | 1.04 | 0.6 | 0.46 | 0.7 | 0.44 | 0.7 | 0.2 | 0.2 |
| Storm5b | rmse (0.0) | 0.26 | 0.26 | 0.31 | 0.33 | 0.67 | 0.8 | 0.35 | 0.23 | 0 | 0 | 0.01 | 0.01 |
| Storm6 | rmse (0.0) | 0.09 | 0.02 | 5.27 | 1.7 | 1.96 | 0.69 | 0.92 | 0.49 | 2.18 | 0.99 | 0.25 | 0.45 |
| Storm7 | rmse (0.0) | 0.07 | 0.08 | 1.55 | 0.37 | 1.23 | 0.31 | 0.76 | 0.54 | 0.65 | 1.09 | 0.29 | 0.29 |

| | | | | | | | | | | | | | | |
|---|---|---|---|---|---|---|---|---|---|---|---|---|---|---|
| Storm8 | rmse (0.0) | | 0.01 | 0.02 | 0.41 | 0.49 | 0.72 | 0.53 | 0.33 | 0.38 | 0.48 | 0.57 | 0.13 | 0.13 |
| Overall | prmse (0.0) | | 102 | 69.2 | 2.79 | 2.24 | 0.89 | 0.75 | 0.36 | 0.26 | 22.2 | 20.5 | 44 | 39.4 |
| Storm1 | prmse (0.0) | | 43.8 | 30.5 | 10.3 | 8.93 | 2.21 | 1.79 | 1.29 | 0.88 | 18 | 16.7 | 24.7 | 22.2 |
| Storm2 | prmse (0.0) | | 82.6 | 59.4 | 2.86 | 1.61 | 1.16 | 0.66 | 0.33 | 0.19 | 1.85 | 1.96 | 4.76 | 4.02 |
| Storm3 | prmse (0.0) | | 15 | 7.22 | 0.71 | 0.27 | 0.27 | 0.32 | 0.19 | 0.27 | 1.93 | 2.98 | 1.67 | 1.79 |
| Storm4 | prmse (0.0) | | 986 | 394 | 12.6 | 5 | 3.02 | 1.1 | 0.93 | 0.34 | 3.9 | 2.77 | 16.1 | 12 |
| Storm5 | prmse (0.0) | Inf | Inf | | 0.52 | 0.15 | 0.47 | 0.27 | 0.14 | 0.22 | 0.87 | 1.37 | 1.95 | 1.95 |
| Storm5b | prmse (0.0) | | 2.83 | 2.85 | 0.18 | 0.2 | 0.41 | 0.49 | 0.13 | 0.09 | NaN | NaN | Inf | Inf |
| Storm6 | prmse (0.0) | | 9.35 | 2.18 | 2.3 | 0.74 | 0.81 | 0.28 | 0.3 | 0.16 | 3.09 | 1.4 | 0.54 | 0.97 |
| Storm7 | prmse (0.0) | | 1.76 | 2.11 | 3.26 | 0.79 | 1.53 | 0.38 | 0.46 | 0.33 | 1.04 | 1.75 | 2.84 | 2.85 |
| Storm8 | prmse (0.0) | | 0.72 | 0.81 | 0.23 | 0.28 | 0.4 | 0.29 | 0.13 | 0.14 | 3.3 | 3.88 | 3.26 | 3.26 |
| Overall | rrmse (0.0) | | 9.45 | 6.39 | 4.93 | 3.96 | 1.69 | 1.42 | 1.14 | 0.83 | 3.19 | 2.93 | 4.26 | 3.81 |
| Storm1 | rrmse (0.0) | | 12.4 | 8.61 | 9.52 | 8.22 | 2.37 | 1.92 | 3.14 | 2.15 | 6.14 | 5.68 | 5.24 | 4.71 |
| Storm2 | rrmse (0.0) | | 17 | 12.2 | 5.3 | 2.99 | 2.25 | 1.27 | 1.09 | 0.61 | 0.69 | 0.73 | 2.89 | 2.44 |
| Storm3 | rrmse (0.0) | | 9 | 4.33 | 1.7 | 0.64 | 0.67 | 0.78 | 0.77 | 1.11 | 0.65 | 1 | 0.85 | 0.91 |
| Storm4 | rrmse (0.0) | | 238 | 94.9 | 5.66 | 2.26 | 2.45 | 0.9 | 1.42 | 0.52 | 1.1 | 0.78 | 4.16 | 3.09 |
| Storm5 | rrmse (0.0) | Inf | Inf | | 1.68 | 0.48 | 1.66 | 0.96 | 0.67 | 1 | 0.52 | 0.82 | 0.95 | 0.95 |
| Storm5b | rrmse (0.0) | | 1.02 | 1.03 | 1.75 | 1.89 | 10.3 | 12.3 | 4.21 | 2.78 | NaN | NaN | Inf | Inf |
| Storm6 | rrmse (0.0) | | 7.02 | 1.64 | 4.4 | 1.42 | 1.63 | 0.57 | 1.01 | 0.54 | 1.11 | 0.5 | 0.25 | 0.45 |
| Storm7 | rrmse (0.0) | | 0.66 | 0.79 | 2.05 | 0.49 | 2.52 | 0.63 | 1.43 | 1.02 | 0.56 | 0.94 | 0.97 | 0.97 |
| Storm8 | rrmse (0.0) | | 0.81 | 0.91 | 0.69 | 0.84 | 2.64 | 1.95 | 1.17 | 1.34 | 0.87 | 1.02 | 0.97 | 0.97 |

Table D.3.2.b: All computed statistical parameters arranged by storm.

| | | cg-1 | | cg-4 | | cg-5 | | cg-6 | | sd-3A | | shg-09A |
|---|---|---|---|---|---|---|---|---|---|---|---|---|
| **Storm #** | **Statistic** | **No SMA** | **SMA** | **No SMA** | **SMA** | **No SMA** | **SMA** | **No SMA** | **SMA** | **No SMA** | **SMA** | **No SMA** |
| ALL | NS (1.0) | 0.12 | 0.16 | 0.17 | 0.19 | 0.27 | 0.04 | 0.44 | 0.46 | 0.29 | 0.25 | 0.28 |
| ALL | corr (1.0) | 0.65 | 0.66 | 0.6 | 0.56 | 0.74 | 0.71 | 0.67 | 0.7 | 0.67 | 0.57 | 0.81 |
| ALL | modcorr (1.0) | 0.45 | 0.46 | 0.48 | 0.46 | 0.54 | 0.52 | 0.49 | 0.52 | 0.6 | 0.51 | 0.74 |
| ALL | pb (0.0) | 6.6 | 4.02 | 0.31 | 0.25 | 0.44 | 0.48 | -0.03 | 0 | 0.97 | 0.42 | 1.79 |
| ALL | apb (0.0) | 7.44 | 4.93 | 0.37 | 0.31 | 0.46 | 0.5 | 0.15 | 0.13 | 1.49 | 1.36 | 2.53 |
| ALL | rmse (0.0) | 0.58 | 0.39 | 4.16 | 3.33 | 1.29 | 1.08 | 0.78 | 0.57 | 2.51 | 2.31 | 1.33 |
| ALL | prmse (0.0) | 102 | 69.2 | 2.79 | 2.24 | 0.89 | 0.75 | 0.36 | 0.26 | 22.2 | 20.5 | 44 |
| ALL | rrmse (0.0) | 9.45 | 6.39 | 4.93 | 3.96 | 1.69 | 1.42 | 1.14 | 0.83 | 3.19 | 2.93 | 4.26 |
| Storm1 | NS (1.0) | 0.02 | 0.07 | 0.01 | 0.03 | 0.14 | 0.06 | 0 | -0.1 | 0.16 | 0.18 | 0.22 |
| Storm1 | corr (1.0) | 0.9 | 0.89 | 0.71 | 0.72 | 0.63 | 0.58 | 0.36 | 0.27 | 0.84 | 0.83 | 0.93 |
| Storm1 | modcorr (1.0) | 0.64 | 0.64 | 0.62 | 0.63 | 0.49 | 0.45 | 0.23 | 0.17 | 0.79 | 0.78 | 0.85 |
| Storm1 | pb (0.0) | 15.2 | 10.8 | 3.71 | 3.18 | 1.08 | 0.96 | 0.46 | 0.29 | 5.23 | 4.6 | 6.79 |
| Storm1 | apb (0.0) | 15.2 | 10.8 | 3.72 | 3.2 | 1.28 | 1.19 | 0.75 | 0.53 | 5.4 | 4.83 | 6.82 |
| Storm1 | rmse (0.0) | 3.89 | 2.71 | 26.8 | 23.1 | 6.39 | 5.18 | 4.48 | 3.07 | 17.5 | 16.2 | 9.34 |
| Storm1 | prmse (0.0) | 43.8 | 30.5 | 10.3 | 8.93 | 2.21 | 1.79 | 1.29 | 0.88 | 18 | 16.7 | 24.7 |
| Storm1 | rrmse (0.0) | 12.4 | 8.61 | 9.52 | 8.22 | 2.37 | 1.92 | 3.14 | 2.15 | 6.14 | 5.68 | 5.24 |
| Storm2 | NS (1.0) | 0.05 | 0.08 | 0.18 | 0.3 | 0.09 | -0.04 | 0.42 | 0.28 | 0.61 | -0.22 | 0.34 |
| Storm2 | corr (1.0) | 0.9 | 0.84 | 0.92 | 0.89 | 0.79 | 0.85 | 0.69 | 0.8 | 0.79 | 0.69 | 0.82 |
| Storm2 | modcorr (1.0) | 0.66 | 0.62 | 0.56 | 0.55 | 0.42 | 0.45 | 0.35 | 0.4 | 0.47 | 0.41 | 0.72 |
| Storm2 | pb (0.0) | 18.7 | 13.7 | 1.03 | 0.66 | 0.77 | 0.56 | 0.1 | 0.02 | 0.1 | -0.29 | 1.21 |
| Storm2 | apb (0.0) | 18.7 | 13.7 | 1.03 | 0.67 | 0.77 | 0.57 | 0.21 | 0.13 | 0.56 | 0.5 | 1.79 |
| Storm2 | rmse (0.0) | 0.81 | 0.59 | 6.35 | 3.58 | 2.58 | 1.46 | 1.01 | 0.57 | 1.48 | 1.57 | 0.56 |
| Storm2 | prmse (0.0) | 82.6 | 59.4 | 2.86 | 1.61 | 1.16 | 0.66 | 0.33 | 0.19 | 1.85 | 1.96 | 4.76 |
| Storm2 | rrmse (0.0) | 17 | 12.2 | 5.3 | 2.99 | 2.25 | 1.27 | 1.09 | 0.61 | 0.69 | 0.73 | 2.89 |
| Storm3 | NS (1.0) | 0.07 | 0.19 | 0.5 | -0.36 | 0.7 | -6.15 | 0.37 | -8.68 | -0.23 | -132 | -4.72 |
| Storm3 | corr (1.0) | 0.76 | 0.81 | 0.91 | 0.83 | 0.94 | 0.84 | 0.86 | 0.82 | 0.79 | 0.43 | 0.7 |
| Storm3 | modcorr (1.0) | 0.39 | 0.42 | 0.21 | 0.19 | 0.23 | 0.2 | 0.31 | 0.3 | 0.12 | 0.06 | 0.44 |
| Storm3 | pb (0.0) | 4.48 | 2.55 | 0.29 | 0.06 | 0.21 | 0.07 | -0.14 | -0.21 | -0.36 | -0.84 | -0.6 |
| Storm3 | apb (0.0) | 4.62 | 2.7 | 0.3 | 0.18 | 0.21 | 0.25 | 0.16 | 0.21 | 0.51 | 0.84 | 0.66 |
| Storm3 | rmse (0.0) | 0.09 | 0.05 | 1.53 | 0.57 | 0.72 | 0.84 | 0.7 | 1 | 0.94 | 1.45 | 0.22 |
| Storm3 | prmse (0.0) | 15 | 7.22 | 0.71 | 0.27 | 0.27 | 0.32 | 0.19 | 0.27 | 1.93 | 2.98 | 1.67 |
| Storm3 | rrmse (0.0) | 9 | 4.33 | 1.7 | 0.64 | 0.67 | 0.78 | 0.77 | 1.11 | 0.65 | 1 | 0.85 |
| Storm4 | NS (1.0) | -0.08 | -0.04 | 0.19 | 0.44 | 0.21 | 0.53 | 0.36 | 0.73 | 0.66 | 0.58 | 0.27 |
| Storm4 | corr (1.0) | 0.9 | 0.89 | 0.98 | 0.95 | 0.81 | 0.89 | 0.65 | 0.87 | 0.92 | 0.77 | 0.92 |
| Storm4 | modcorr (1.0) | 0.37 | 0.36 | 0.47 | 0.45 | 0.38 | 0.42 | 0.37 | 0.49 | 0.59 | 0.49 | 0.74 |
| Storm4 | pb (0.0) | 282 | 95.5 | 4.26 | 1.82 | 1.68 | 0.81 | 0.27 | -0.01 | 1.06 | 0.29 | 4.66 |
| Storm4 | apb (0.0) | 282 | 95.5 | 4.32 | 1.82 | 1.68 | 0.83 | 0.57 | 0.2 | 1.19 | 0.8 | 4.67 |
| Storm4 | rmse (0.0) | 1.29 | 0.52 | 9.6 | 3.82 | 3.56 | 1.3 | 1.75 | 0.64 | 3.03 | 2.15 | 1.72 |
| Storm4 | prmse (0.0) | 986 | 394 | 12.6 | 5 | 3.02 | 1.1 | 0.93 | 0.34 | 3.9 | 2.77 | 16.1 |
| Storm4 | rrmse (0.0) | 238 | 94.9 | 5.66 | 2.26 | 2.45 | 0.9 | 1.42 | 0.52 | 1.1 | 0.78 | 4.16 |
| Storm5 | NS (1.0) | -0.45 | -0.45 | 0.45 | 0.77 | 0.05 | -1.35 | 0.61 | -4.95 | 0.72 | -0.94 | -43.9 |
| Storm5 | corr (1.0) | NaN | NaN | 0.88 | 0.9 | 0.9 | 0.93 | 0.89 | 0.92 | 0.87 | 0.7 | 0.86 |
| Storm5 | modcorr (1.0) | NaN | NaN | 0.38 | 0.39 | 0.33 | 0.34 | 0.34 | 0.35 | 0.53 | 0.42 | 0.86 |
| Storm5 | pb (0.0) | Inf | Inf | 0.26 | 0.05 | 0.39 | 0.24 | -0.1 | -0.17 | -0.22 | -0.66 | -0.74 |
| Storm5 | apb (0.0) | Inf | Inf | 0.28 | 0.11 | 0.39 | 0.25 | 0.12 | 0.19 | 0.4 | 0.68 | 0.86 |
| Storm5 | rmse (0.0) | 0.03 | 0.03 | 1.14 | 0.32 | 1.04 | 0.6 | 0.46 | 0.7 | 0.44 | 0.7 | 0.2 |
| Storm5 | prmse (0.0) | Inf | Inf | 0.52 | 0.15 | 0.47 | 0.27 | 0.14 | 0.22 | 0.87 | 1.37 | 1.95 |
| Storm5 | rrmse (0.0) | Inf | Inf | 1.68 | 0.48 | 1.66 | 0.96 | 0.67 | 1 | 0.52 | 0.82 | 0.95 |
| Storm5b | NS (1.0) | -384 | -920 | -1.17 | -4.82 | -29.3 | -97 | -8.72 | -8.33 | NaN | NaN | -2.41 |
| Storm5b | corr (1.0) | 0.51 | 0.6 | 0.42 | 0.47 | 0.55 | 0.18 | 0.54 | 0.14 | NaN | NaN | NaN |
| Storm5b | modcorr (1.0) | 0.33 | 0.39 | 0.28 | 0.31 | 0.36 | 0.12 | 0.36 | 0.09 | NaN | NaN | NaN |
| Storm5b | pb (0.0) | -0.9 | -0.92 | 0.14 | 0.17 | 0.41 | 0.49 | -0.13 | -0.08 | NaN | NaN | Inf |
| Storm5b | apb (0.0) | 0.91 | 0.93 | 0.14 | 0.17 | 0.41 | 0.49 | 0.13 | 0.08 | NaN | NaN | Inf |
| Storm5b | rmse (0.0) | 0.26 | 0.26 | 0.31 | 0.33 | 0.67 | 0.8 | 0.35 | 0.23 | 0 | 0 | 0.01 |
| Storm5b | prmse (0.0) | 2.83 | 2.85 | 0.18 | 0.2 | 0.41 | 0.49 | 0.13 | 0.09 | NaN | NaN | Inf |
| Storm5b | rrmse (0.0) | 1.02 | 1.03 | 1.75 | 1.89 | 10.3 | 12.3 | 4.21 | 2.78 | NaN | NaN | Inf |
| Storm6 | NS (1.0) | 0.01 | 0.39 | 0.2 | 0.54 | 0.33 | 0.57 | 0.42 | 0.34 | 0.69 | 0.78 | 0.93 |
| Storm6 | corr (1.0) | 0.3 | 0.68 | 0.81 | 0.86 | 0.88 | 0.94 | 0.67 | 0.91 | 0.97 | 0.89 | 0.99 |
| Storm6 | modcorr (1.0) | 0.09 | 0.2 | 0.35 | 0.37 | 0.38 | 0.41 | 0.34 | 0.46 | 0.52 | 0.48 | 0.81 |
| Storm6 | pb (0.0) | 2.12 | 0.49 | 0.75 | 0.24 | 0.54 | 0.23 | 0.07 | -0.07 | 0.77 | -0.06 | -0.36 |
| Storm6 | apb (0.0) | 2.72 | 1.1 | 0.77 | 0.26 | 0.54 | 0.24 | 0.22 | 0.13 | 0.85 | 0.36 | 0.42 |
| Storm6 | rmse (0.0) | 0.09 | 0.02 | 5.27 | 1.7 | 1.96 | 0.69 | 0.92 | 0.49 | 2.18 | 0.99 | 0.25 |

| | | | | | | | | | | | | |
|---|---|---|---|---|---|---|---|---|---|---|---|---|
| Storm6 | prmse (0.0) | 9.35 | 2.18 | 2.3 | 0.74 | 0.81 | 0.28 | 0.3 | 0.16 | 3.09 | 1.4 | 0.54 |
| Storm6 | rrmse (0.0) | 7.02 | 1.64 | 4.4 | 1.42 | 1.63 | 0.57 | 1.01 | 0.54 | 1.11 | 0.5 | 0.25 |
| Storm7 | NS (1.0) | -0.94 | -7.19 | 0.47 | 0.62 | 0.28 | 0.56 | 0.59 | -0.38 | 0.69 | -6.03 | -24.9 |
| Storm7 | corr (1.0) | 0.86 | 0.89 | 0.91 | 0.88 | 0.96 | 0.92 | 0.89 | 0.9 | 0.87 | 0.59 | 0.37 |
| Storm7 | modcorr (1.0) | 0.5 | 0.52 | 0.26 | 0.25 | 0.31 | 0.3 | 0.34 | 0.35 | 0.31 | 0.21 | 0.24 |
| Storm7 | pb (0.0) | -0.44 | -0.58 | 0.96 | -0.19 | 0.91 | 0.3 | 0.02 | -0.3 | -0.4 | -0.8 | -0.66 |
| Storm7 | apb (0.0) | 0.6 | 0.74 | 1.18 | 0.38 | 0.92 | 0.32 | 0.39 | 0.3 | 0.59 | 0.8 | 0.78 |
| Storm7 | rmse (0.0) | 0.07 | 0.08 | 1.55 | 0.37 | 1.23 | 0.31 | 0.76 | 0.54 | 0.65 | 1.09 | 0.29 |
| Storm7 | prmse (0.0) | 1.76 | 2.11 | 3.26 | 0.79 | 1.53 | 0.38 | 0.46 | 0.33 | 1.04 | 1.75 | 2.84 |
| Storm7 | rrmse (0.0) | 0.66 | 0.79 | 2.05 | 0.49 | 2.52 | 0.63 | 1.43 | 1.02 | 0.56 | 0.94 | 0.97 |
| Storm8 | NS (1.0) | -0.19 | -1.91 | 0.58 | -8.34 | -2.14 | -33.3 | 0.42 | -12.5 | -0.82 | -448 | -74.7 |
| Storm8 | corr (1.0) | 0.76 | 0.74 | 0.86 | 0.73 | 0.71 | 0.66 | 0.66 | 0.63 | 0.51 | 0.13 | 0.44 |
| Storm8 | modcorr (1.0) | 0.54 | 0.53 | 0.22 | 0.19 | 0.16 | 0.15 | 0.16 | 0.15 | 0.04 | 0.01 | 0.35 |
| Storm8 | pb (0.0) | -0.43 | -0.52 | 0.14 | 0.05 | 0.37 | 0.27 | -0.02 | -0.11 | -0.21 | -0.92 | -0.51 |
| Storm8 | apb (0.0) | 0.56 | 0.62 | 0.16 | 0.19 | 0.37 | 0.27 | 0.1 | 0.12 | 0.88 | 0.92 | 1.03 |
| Storm8 | rmse (0.0) | 0.01 | 0.02 | 0.41 | 0.49 | 0.72 | 0.53 | 0.33 | 0.38 | 0.48 | 0.57 | 0.13 |
| Storm8 | prmse (0.0) | 0.72 | 0.81 | 0.23 | 0.28 | 0.4 | 0.29 | 0.13 | 0.14 | 3.3 | 3.88 | 3.26 |
| Storm8 | rrmse (0.0) | 0.81 | 0.91 | 0.69 | 0.84 | 2.64 | 1.95 | 1.17 | 1.34 | 0.87 | 1.02 | 0.97 |

Table D.3.3: CFS error in Simulated Peak relative to observed peak flow.

| Storm # | Observed Peak Flow [cfs] | Δ SMA | Δ no SMA | Percent Error | | Absolute Error | | Improvement |
|---|---|---|---|---|---|---|---|---|
| Storm1 | 2.44 | *+13.52* | *+18.49* | *554%* | *758%* | *13.52* | *18.49* | + |
| Storm2 | 0.48 | *+3.91* | *+5.97* | *815%* | *1244%* | *3.91* | *5.97* | + |
| Storm3 | 0.06 | *+0.16* | *+0.61* | *267%* | *1017%* | *0.16* | *0.61* | + |
| Storm4 | 0.04 | *+3.16* | *+9.36* | *7888%* | *23401%* | *3.16* | *9.36* | + |
| Storm5 | 0 | *+0.08* | *+0.08* | | | *0.08* | *0.08* | - |
| Storm5b | 0.07 | *-0.04* | *-0.03* | *-62%* | *-41%* | *0.04* | *0.03* | - |
| Storm6 | 0.06 | *+0.07* | *+0.58* | *120%* | *962%* | *0.07* | *0.58* | + |
| Storm7 | 0.49 | *-0.36* | *-0.17* | *-73%* | *-34%* | *0.36* | *0.17* | - |
| Storm8 | 0.11 | *-0.07* | *-0.05* | *-64%* | *-45%* | *0.07* | *0.05* | - |
| Storm1 | 24.73 | *+87.34* | *+97.35* | *353%* | *394%* | *87.34* | *97.35* | + |
| Storm2 | 7.31 | *+15.38* | *+29.80* | *210%* | *408%* | *15.38* | *29.80* | + |
| Storm3 | 6.06 | *-2.33* | *+6.14* | *-38%* | *101%* | *2.33* | *6.14* | º |
| Storm4 | 9.41 | *+22.03* | *+49.68* | *234%* | *528%* | *22.03* | *49.68* | + |
| Storm5 | 4.45 | *+0.93* | *+3.79* | *21%* | *85%* | *0.93* | *3.79* | + |
| Storm5b | 2.2 | *-0.15* | *+0.06* | *-7%* | *3%* | *0.15* | *0.06* | - |
| Storm6 | 7 | *+9.16* | *+24.26* | *131%* | *347%* | *9.16* | *24.26* | + |
| Storm7 | 4.07 | *-0.50* | *+6.86* | *-12%* | *169%* | *0.50* | *6.86* | º |
| Storm8 | 4.8 | *-2.27* | *+0.31* | *-47%* | *7%* | *2.27* | *0.31* | - |
| Storm1 | 13.03 | *+11.98* | *+17.68* | *92%* | *136%* | *11.98* | *17.68* | + |
| Storm2 | 5.66 | *+2.21* | *+5.82* | *39%* | *103%* | *2.21* | *5.82* | + |
| Storm3 | 5.87 | *-2.43* | *+1.10* | *-41%* | *19%* | *2.43* | *1.10* | - |
| Storm4 | 5.49 | *+2.16* | *+9.14* | *39%* | *167%* | *2.16* | *9.14* | + |
| Storm5 | 3.74 | *+0.33* | *+1.84* | *9%* | *49%* | *0.33* | *1.84* | + |
| Storm5b | 1.75 | *+0.81* | *+0.90* | *46%* | *52%* | *0.81* | *0.90* | + |
| Storm6 | 5.99 | *+0.47* | *+4.16* | *8%* | *70%* | *0.47* | *4.16* | + |
| Storm7 | 2.07 | *+0.27* | *+3.64* | *13%* | *176%* | *0.27* | *3.64* | + |
| Storm8 | 2.5 | *+0.09* | *+1.42* | *4%* | *57%* | *0.09* | *1.42* | + |
| Storm1 | 8.15 | *+5.08* | *+10.04* | *62%* | *123%* | *5.08* | *10.04* | + |
| Storm2 | 5.46 | *-1.22* | *-0.70* | *-22%* | *-13%* | *1.22* | *0.70* | - |
| Storm3 | 6.02 | *-2.39* | *-1.30* | *-40%* | *-22%* | *2.39* | *1.30* | - |
| Storm4 | 5.18 | *-0.61* | *+2.13* | *-12%* | *41%* | *0.61* | *2.13* | º |
| Storm5 | 4.65 | *-1.12* | *-0.30* | *-24%* | *-7%* | *1.12* | *0.30* | - |
| Storm5b | 2.8 | *-0.24* | *-0.15* | *-9%* | *-5%* | *0.24* | *0.15* | - |
| Storm6 | 5.54 | *-1.24* | *+0.51* | *-22%* | *9%* | *1.24* | *0.51* | - |
| Storm7 | 2.92 | *-0.53* | *+1.42* | *-18%* | *49%* | *0.53* | *1.42* | º |
| Storm8 | 3.31 | *-0.70* | *+0.38* | *-21%* | *12%* | *0.70* | *0.38* | - |
| Storm1 | 15.04 | *+80.07* | *+82.42* | *532%* | *548%* | *80.07* | *82.42* | + |
| Storm2 | 14.06 | *-6.36* | *-0.05* | *-45%* | *0%* | *6.36* | *0.05* | - |
| Storm3 | 12.58 | *-12.11* | *-7.36* | *-96%* | *-58%* | *12.11* | *7.36* | - |
| Storm4 | 17.45 | *+6.18* | *+16.65* | *35%* | *95%* | *6.18* | *16.65* | + |
| Storm5 | 3.65 | *-0.88* | *+0.42* | *-24%* | *12%* | *0.88* | *0.42* | - |
| Storm5b | 1.54 | *-1.54* | *-1.28* | *-100%* | *-83%* | *1.54* | *1.28* | - |
| Storm6 | 10.04 | *+3.34* | *+12.47* | *33%* | *124%* | *3.34* | *12.47* | + |
| Storm7 | 7.8 | *-4.99* | *-0.62* | *-64%* | *-8%* | *4.99* | *0.62* | - |
| Storm8 | 5.18 | *-5.06* | *-2.83* | *-98%* | *-55%* | *5.06* | *2.83* | - |
| Storm1 | 15.31 | *+51.39* | *+53.97* | *336%* | *353%* | *51.39* | *53.97* | + |
| Storm2 | 1.26 | *+1.81* | *+1.88* | *144%* | *149%* | *1.81* | *1.88* | + |
| Storm3 | 2.05 | *-1.75* | *-1.66* | *-85%* | *-81%* | *1.75* | *1.66* | - |
| Storm4 | 3.37 | *+8.45* | *+9.29* | *251%* | *276%* | *8.45* | *9.29* | + |
| Storm5 | 1.09 | *-0.98* | *-0.98* | *-90%* | *-90%* | *0.98* | *0.98* | - |
| Storm5b | 0 | *+0.02* | *+0.02* | | | *0.02* | *0.02* | - |
| Storm6 | 7.1 | *-1.37* | *-0.84* | *-19%* | *-12%* | *1.37* | *0.84* | - |
| Storm7 | 2.12 | *-2.--* | *-1.86* | *-94%* | *-88%* | *2.00* | *1.86* | - |
| Storm8 | 1.17 | *-1.12* | *-1.12* | *-96%* | *-96%* | *1.12* | *1.12* | - |

Table D.3.4.a: CFS error in Simulated Peak relative to observed peak flow.

| Gauge | Mean/Median | Δ noSMA | Δ SMA | Improvement |
|---|---|---|---|---|
| SHG-09A | Median | -0.84 | -0.98 | - |
| | Mean | +6.52 | +6.05 | + |
| SD-3A | Median | -0.05 | -1.54 | - |
| | Mean | +11.09 | +6.52 | + |
| CG-1 | Median | +0.58 | +0.08 | + |
| | Mean | +3.87 | +2.27 | + |
| CG-4 | Median | +6.86 | +0.93 | + |
| | Mean | +24.25 | +14.40 | + |
| CG-5 | Median | +3.64 | +0.47 | + |
| | Mean | +5.08 | +1.77 | + |
| CG-6 | Median | +0.38 | -0.70 | - |
| | Mean | +1.34 | -0.33 | º |